Queen Mary
University of London

The role of metabolism during T cell senescence

Submitted in partial fulfilment of the requirements of the Degree of Doctor of Philosophy

Lauren Amy Callender

BSc (Hons), MSc, MRes

Supervisor: Dr. Siân Henson

Statement of Originality

I, Lauren Callender, confirm that the research included within this thesis is my own work or that where it has been carried out in collaboration with, or supported by others, that this is duly acknowledged. Previously published material is also acknowledged.

I attest that I have exercised reasonable care to ensure that the work is original and does not to the best of my knowledge break any UK law, infringe any third party's copyright or other Intellectual Property Right, or contain any confidential material.

I accept that the College has the right to use plagiarism detection software to check the electronic version of the thesis. I confirm that this thesis has not been previously submitted for the award of a degree by this or any other university.

Signature: Lauren Callender

Date: 06th January 2020

Abstract

The impact of T cell senescence during ageing is well established. However, T cell senescence is now recognised to play a role in a variety of age-related and metabolic diseases, such as rheumatoid arthritis and cardiovascular disease. It is therefore crucial to gain a better understanding of the mechanisms that control T cell senescence. The loss of mitochondria has been linked to both cellular senescence and ageing; however, it is still unclear whether mitochondria play a causal role in T cell senescence. Data presented here provides evidence that the differing susceptibilities to senescence that exist between $CD8^+$ and $CD4^+$ T cells is due to the inherent differences in mitochondrial content and cellular metabolism. Notably $CD4^+$ T cells displayed a higher mitochondrial mass, shown to be the result of a GATA3-PGC1a complex, which is recruited as a consequence of DNA damage.

Additionally, this thesis demonstrates the existence of a novel naïve-like senescent T cell subset, highlighting the heterogeneity of senescent T cells. This subset was found to arise because of inflammation; therefore, senescent T cells isolated from people living with type 2 diabetes (T2D) were used as a model to examine the characteristics of this subset further. Inflammatory-derived senescent T cells were phenotypically distinct to those examined from healthy age-matched control donors. With T2D senescent T cells expressing fewer of the traditional senescent-associated T cell markers and retaining more proliferative capacity, indicating they were derived from a less differentiated T cell subset. Despite this, inflammatory-derived senescent T

cells exhibited more severe mitochondrial dysfunction and dysregulated nutrient uptake and usage.

Collectively, this thesis highlights the heterogeneity of senescent T cells and supports the ever-growing appreciation that cellular metabolism and senescence are intimately linked. Going forward, mitochondrial health and cellular metabolism should be included to better define the senescence phenotype.

Acknowledgments

First and foremost, I would like to express my sincere gratitude to Dr. Siân Henson for her continuous guidance and support during my PhD. It has been a great honour to be the first member of her team and I am immensely proud of what we have achieved together over the last four years. I am also thankful for the excellent example she has provided as a successful woman in science. I could not have wished for a better mentor.

Secondly, I would like to thank all of the Translational Medicine and Therapeutics team for welcoming us into their department. In particular, I would like to thank all of the TMT girls for making my PhD experience so enjoyable. The endless hours of office chats have been a great distraction and helped keep me sane during the more stressful times of my PhD. A very special thank you goes to Dr. Elizabeth Caroll, as her encouragement and optimism played a huge role in helping motivate me during the two years we spent together in the lab.

I would also like to thank my parents (Lee and Sam), brothers (Connor and Alfie), boyfriend (Ben) and all of my friends for being so supportive - I hope I've done you all proud!

Lastly, I would like to thank the British Heart Foundation for providing me with the funding necessary to undertake my PhD research.

Publications

Callender, L.A., Carroll, E.C. Romano, E.L., Chapple, J.P., Akbar, A.N., and Henson, S.M. (Completing revisions – Nature Metabolism). GATA3 controls mitochondrial biogenesis in $CD4^+$ T cells during DNA damage. Pre-print available on bioRvix: https://doi.org/10.1101/727479

Callender, L.A., Carroll, E.C., Bober, E.A., Akbar, A.N., Solito, E., and Henson, S.M. (2019). Mitochondrial mass governs the extent of T cell senescence. *Aging Cell. 00:e13067. https://doi.org/10.1111/acel.13067*

Ø. Gadsbøll, A.-S., Jee, M.H., Funch, A.B., Alhede, M., Mraz, V., Weber, J.F., **Callender, L.A.,** et al. (2019), "Pathogenic $CD8^+$ epidermis-resident memory T cells displace dendritic epidermal T cells in allergic dermatitis", *Journal of Investigative Dermatology,* available at: https://doi.org/10.1016/j.jid.2019.07.722.

Lau, E.Y.M, Carroll, E.C., **Callender, L.A**., Hood, G.A., Berryman, V., Pattrick, M., Finer, S., Hitman, G.A., Ackland, G.L and Henson, S.M. (2019) Type 2 diabetes is associated with the accumulation of senescent T cells. *Clin. Exp. Immunol. Vol. 197 No. 2, pp. 205-213.*

Callender, L.A., Carroll, E.C., Bober, E.A., Henson, S.M. (2018). Divergent mechanisms of metabolic dysfunction drive fibroblast and T cell senescence. *Ageing Research Reviews.* Vol. 47, pp. 24-30.

Callender, L.A., Carroll, E.C., Beal, R.W.J., Chambers, E.S., Nourshargh, S., Akbar, A.N., and Henson, S.M. (2018). Human $CD8^+$ EMRA T cells display a senescence-associated secretory phenotype regulated by p38 MAPK. *Aging Cell*. Vol. 17 No. 1, pp. e12675.

Table of Contents

List of Figures

List of Tables

List of Abbreviations

APC	Antigen presenting cell
ATM	Ataxia telangiectasia mutated
ATR	Ataxia telangiectasia and Rad3-related
BV	Brilliant violet
Cav-1	Caveolin-1
CDK	Cyclin dependent kinase
CDKI	Cyclin dependent kinase inhibitor
CHEK1	Checkpoint kinase 1
CHEK2	Checkpoint kinase 2
CM	Central memory
CMV	Cytomegalovirus
DAPI	4',6-diamidino-2-phenylindole
DARE	Diabetes Alliance for Research in England
DC	Dendritic cell
DDR	DNA damage response
DMSO	Dimethyl sulfoxide
DN	Double negative
DP	Double positive
EDTA	Ethylenediaminetetraacetic acid
EM	Effector memory
EM-like	EM-like
EMRA	Effector memory that re-express CD45RA
ETC	Electron transport chain
FA	Fatty acid
FAO	Fatty acid oxidation
FAS	Fatty acid synthesis
FCCP	Carbonyl cyanide 4-(trifluoromethoxy) phenylhydrazone
FCS	Fetal calf serum
FISH	Fluorescence *in situ* hybridization

FSC	Forward scatter
GATA3	GATA binding protein 3
HIV	Human immunodeficiency virus
HSC	Haematopoietic stem cell
i-EMRA	Inflammatory-derived EMRA
IFN-γ	Interferon gamma
IL	Interleukin
IP	Immunoprecipitation
KLRG1	Killer cell lectin-like receptor G1
LCMV	Lymphocytic choriomeningitis virus
LPC	Lymphoid progenitor cell
MAPK	Mitogen-activated protein kinase
MFI	Mean fluorescence intensity
MHC	Major histocompatibility complex
MMP	Mitochondrial membrane potential
mtROS	Mitochondrial ROS
NK	Natural killer
N-like	Naïve-like
NOX4	NADPH oxidases 4
OCR	Oxygen consumption rate
OXPHOS	Oxidative phosphorylation
pAMPK	Phosphorylated AMP-activated protein kinase
PBMC	Peripheral blood mononuclear cell
PBS	Phosphate buffered saline
PDH	Pyruvate dehydrogenase
PFA	Paraformaldehyde
PGC1α	Peroxisome proliferator activated receptor gamma coactivator 1 alpha
p-p53	Phosphorylated-p53
pRB	Retinoblastoma
ROS	Reactive oxygen species

SASP	Senescence associated secretory phenotype
siRNA	Small interfering RNA
SOD2	Superoxide dismutase 2
SRC	Spare respiratory capacity
SSC	Side scatter
TCA	Tricarboxylic acid cycle
TCR	T cell receptor
TelCy5	Telomeric probe conjugated to Cy5
T2D	Type 2 diabetes
TERT	Telomerase reverse transcriptase
Th	Helper T cell
TMRE	Tetramethylrhodamine
TNF-α	Tumour necrosis factor alpha
VAT	Visceral adipose tissue
VM	Virtual memory

Chapter one: Introduction

1.1. What is cellular senescence?

Cellular senescence is a process in which cells enter a state of stable cell cycle arrest. However, despite being unable to proliferate, senescent cells remain metabolically active. The term cellular senescence was first introduced over five decades ago when Hayflick and Moorhead discovered that human fibroblasts have a finite proliferative capacity in culture (Hayflick and Moorhead, 1961). This phenomenon was described as the Hayflick limit and found to reflect a particular type of cellular senescence known as replicative senescence. It was later revealed that replicative senescence is causally linked to telomere erosion due to extensive proliferation in the absence of telomerase activity (Bodnar et al., 1998). In the early 1970s, Olovnikov (Olovnikov, 1971) and Watson (Watson, 1972) independently described this as the end-replication problem. As a result, telomeres are thought to represent a molecular clock that reflects the replicative age of a cell (Harley et al., 1990). Historically cellular senescence was viewed as an irreversible mechanism that acted to prevent cancer; however, recent discoveries have implicated senescence in many physiological roles such as embryonic development (Muñoz-Espín et al., 2013; Storer et al., 2013), tissue repair (Krizhanovsky et al., 2008), wound healing (Jun and Lau, 2010), organismal ageing (Baker et al., 2008, 2011) and paradoxically, tumorigenesis (Muñoz-Espín and Serrano, 2014; Pérez-Mancera et al., 2014).

1.1.1. The senescence phenotype

Phenotypically senescent cells are very distinctive. Senescent fibroblasts have been shown to exhibit a flat, enlarged morphology and accumulate senescence associated β-galactosidase activity (Dimri et al., 1995). Some senescent cells can also be identified by the cytological markers of senescence-associated heterochromatin foci, which are specialised domains of heterochromatin that contribute to the silencing of genes that promote proliferation (Narita et al., 2003, 2006). Furthermore, senescent cells secrete a complex pool of senescence associated secretory phenotype (SASP) factors that are comprised of pro-inflammatory cytokines, chemokines, growth factors and proteases (Coppe et al., 2006; Kuilman and Peeper, 2009). SASP factors are highly pleiotropic and can impact numerous biological processes. For instance, the SASP is able to reinforce senescence in a cell-autonomous manner as well as transmit senescence to neighbouring cells in a paracrine manner (Figure 1.1).

The response of neighbouring cells to SASP components depends on the cell type and cell context. For example, the SASP can stimulate angiogenesis (Coppe et al., 2006), increase proliferation of nearby cells potentially resulting in tumorigenesis (Krtolica et al., 2001), promote the invasion of neoplastic cells via an epithelial to mesenchymal transition (Bavik et al., 2006; Laberge et al., 2012), and disrupt normal tissue structures and function. Interestingly, one of the functions of the SASP is to attract immune cells such as natural killer (NK) cells, $CD4^+$ Th1 cells, $CD8^+$ and M1 macrophages, which in turn orchestrate the clearance of senescent cells by phagocytosis (Hoenicke and Zender, 2012; Pereira et al., 2019).

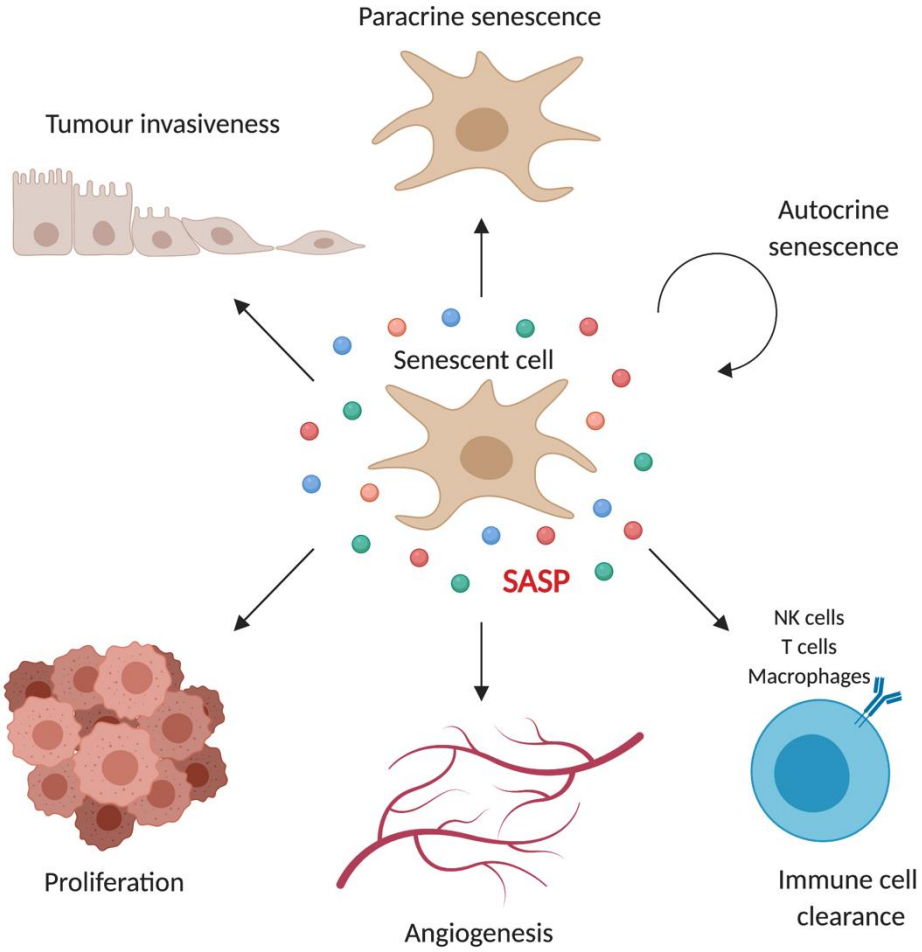

Figure 1.1: The effect of SASP factors on tissue homeostasis

SASP factors are highly pleiotropic and can impact many biological processes. The response of neighbouring cells depends on both the cell type and cell context. In addition to being able to transmit senescence in an autocrine and paracrine manner, it is now recognised that senescence can play a role in tumorigenesis as many SASP factors are able to stimulate angiogenesis, increase proliferation of nearby cells and promote invasion of nearby neoplastic cells [Adapted from (Freund et al., 2010)].

1.1.2. Replicative senescence

Replicative senescence is the process of cell cycle arrest attributed to telomere erosion. Telomeres are stretches of repetitive DNA sequences at the terminal regions of chromosomes. As a cell divides it loses between 50-200 base pairs of telomeric DNA during each S phase (Harley et al., 1990). Telomere length can be maintained by the ribonucleoprotein enzyme telomerase, which contains telomerase reverse transcriptase (TERT), a catalytic protein component that uses an RNA template sequence to add TTAGGG repeats to the chromosome ends (Collins and Mitchell, 2002). TERT is expressed in cells with high proliferation rates such as germ-line cells and cancer cells. However, most normal somatic cells express levels of TERT that are too low to prevent telomere erosion, or no TERT at all (Masutomi et al., 2003).

Critically short telomeres trigger a DNA damage response (DDR), which involves tumour suppressor pathways governed by the transcriptional regulators p53 and retinoblastoma (pRB) (Figure 1.2). These establish and maintain cell cycle arrest through the activation of cyclin dependent kinase inhibitor (CDKI) p21, which is directly induced by p53 and results in the inhibition of the cyclin E and cyclin dependent kinase (CDK) 2 complex. The regulation of p53 and pRB is also linked to the INK4a/ARF locus, which encodes two important tumour suppressor genes: p14 (Arf) and p16 (Ink4a) (Sherr, 2001). Ultimately, these pathways halt cell cycle progression by preventing the inactivation of pRB, therefore resulting in continued repression of E2F target genes required for G1 phase to S phase transition (Figure 1.2).

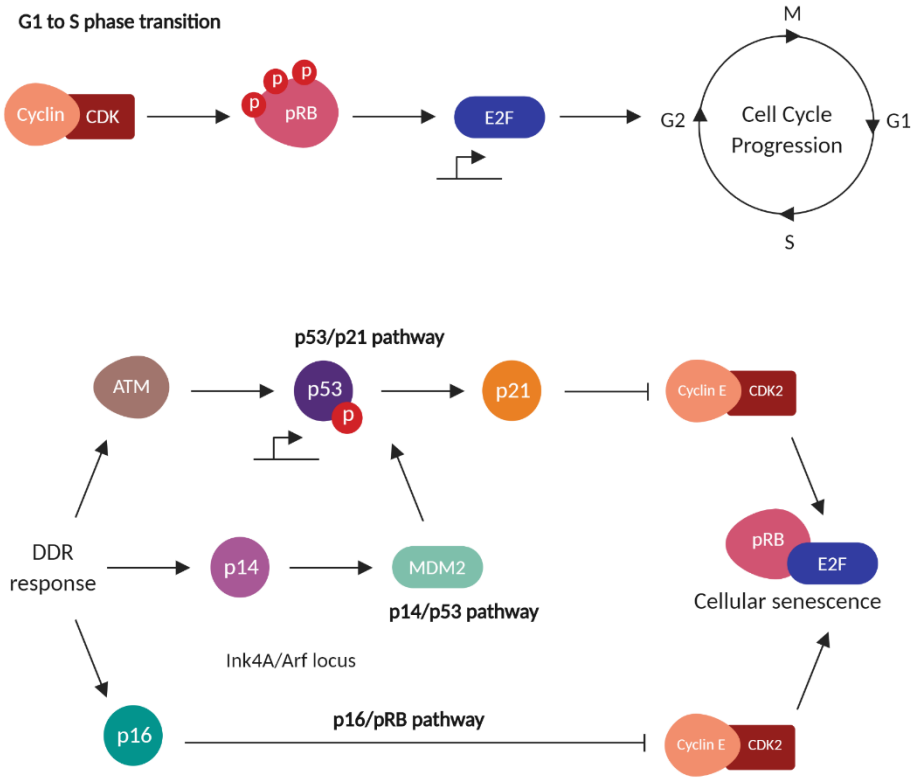

Figure 1.2: Molecular mechanisms of cellular senescence

During normal cell cycle progression, CDK-cyclin complexes phosphorylate pRB. Phosphorylation allows pRB to disassociate from the transcription factor E2F, liberating E2F from the cytoplasm and allowing it to enter the nucleus where it is able to activate the transcription of target genes that are crucial for transition from G1 phase to S phase. Senescence stimuli such as DNA damage is initially detected by key DDR protein kinases ataxia telangiectasia mutated (ATM) and/or ataxia telangiectasia and Rad3-related (ATR), resulting in activation p53. This results in the upregulation of p21, leading to the inhibition of cyclin E-CDK2, which in turn inhibits the repression of pRB, causing cell cycle arrest. The Ink4a/Arf locus is also linked to replicative senescence. p14 regulates p53 stability through inactivation of the p53 degrading E3 ubiquitin protein ligase MDM2. Whereas p16, halts cell cycle progression through binding to cyclin D-CDK4/6.

1.1.3. Premature senescence

Senescence can also be induced by various different stimuli in the absence of any detectable telomere erosion. This type of senescence is known as premature senescence. Prolonged cellular stresses such as non-telomeric DNA damage, hypoxia and increased reactive oxygen species (ROS) production have all been shown to induce premature senescence (Chen et al., 1995). Similar to telomere erosion these stresses can drive cell cycle arrest through either p53 or p16 (Lin et al., 1998; Serrano et al., 1997). For example, mechanistically increased intracellular levels of ROS have been shown to activate the p38 mitogen-activated protein kinase (MAPK), which in turn activates the p53 pathway (Passos et al., 2010).

1.1.4. Oncogene induced senescence

Despite the traditional view that activated oncogenes promote uncontrollable proliferation, oncogenes are also prominent inducers of senescence. This discovery came when an oncogenic form of RAS (H-ras-V12) generated fibroblasts that phenotypically resembled that of replicative senescent fibroblasts (Serrano et al., 1997). The list of oncogenes that are able to induce senescence has since risen to above 50 and includes oncogenes such as E2F1 (Dimri et al., 2009), Raf (Zhu et al., 1998), Mos, Cdc6 and Cyclin E (Bartkova et al., 2006). Interestingly, oncogenes are able to induce senescence through a variety of different mechanisms. For example, BRAFV600E can induce senescence through both p16 activation and through a metabolic effector pathway involving the upregulation of the mitochondrial enzyme pyruvate dehydrogenase (PDH) (Kaplon et al., 2013). PDH upregulation results in a

metabolic shift from glycolysis towards oxidative phosphorylation (OXPHOS), which in turn results in high levels of ROS production and the induction of senescence (Kaplon et al., 2013).

1.2. Immunosenescence and ageing

In the context of the immune system, senescence is known as immunosenescence and refers to the gradual deterioration of immune function that occurs with age (Dorshkind et al., 2009). For the first time in history, older individuals constitute the fastest growing population in the world, with world health organisation projections indicating that between 2015 and 2050 the proportion of the world's population over 60 years will double from 12% to 22% (World Health Organization, 2015). Immunosenescence can result in reduced adaptive immunity, leaving older individuals unable to respond to new vaccinations. Furthermore, this deterioration leaves older individuals more susceptible to infectious diseases. And an imbalance in the innate immune system, which is also associated with immunosenescence, can lead to chronic inflammation and trigger autoimmune and other age-related diseases (Bruunsgaard, 2006; Larbi et al., 2008; Licastro et al., 2005). Consequently, a better understanding of the biological mechanisms responsible for immunosenescence is required in order to match the medical and health related needs of the increasing older population.

1.2.1. The immune system

The immune system refers to a combination of specialised organs, cells and proteins that work together in order to protect against foreign organisms and pathogens. There are two arms of the immune system: innate immunity and adaptive immunity. The innate system is comprised of physical and chemical barriers such as epithelial barriers and gastric acid, which act as a first line of defence against pathogens. In addition to this, the innate system also comprises a second line of defence, which includes complement factors and many immune cells from the myeloid lineage such as neutrophils, macrophages, mast cells, basophils, eosinophils, NK cells and dendritic cells (DC). This arm of the immune system is rapid and antigen independent. By contrast, the adaptive system, consisting of T and B cells from the lymphocyte lineage, is an antigen-dependent and antigen-specific response. Consequently, the adaptive system requires more time to mount a biological response. Importantly, the adaptive immune response is able to build an immunologic memory, which enables the host to mount a much more rapid and efficient immune response following repeat exposure to an antigen. Whilst the role of each arm of the immune system is different, innate and adaptive immunity are not mutually exclusive. Instead, the two systems compliment and communicate with one another in order to orchestrate an effective immune response and as a result, defects in either system can result in host vulnerability (Bonilla and Oettgen, 2010; Turvey and David H. Broide, 2010).

1.2.2. Innate immune cell senescence and inflammageing

Immunosenescence in the innate immune system is considerably complex. The total number of myeloid progenitors does not decrease as we age. In fact some studies have documented that aged haematopoietic stem cells (HSCs) become biased towards myeloid differentiation and therefore age could result in an increase in myeloid cells (Beerman et al., 2010; Cho et al., 2008). Furthermore, as innate immune cells tend to be short lived, they are less likely to senesce. Instead immunosenescence in the innate immune system is thought to reflect cellular dysfunction (Shaw et al., 2013). This dysfunction is characterised by persistent systemic inflammation that occurs in the absence of any infections (sterile inflammation). As the levels of cytokines are far lower than the levels released in response to an acute inflammatory response, this age-associated dysfunction instead results in chronic low–grade inflammation and has consequently been termed inflammageing (Franceschi et al., 2000; Shaw et al., 2010).

1.2.3. Adaptive immune cell senescence

Ageing affects both the quantity and the quality of humoral and T cell immunity (Naylor et al., 2005; Weksler, 2000). Unlike myeloid cells, there is a gradual decrease in the total number of lymphoid progenitors as we age (Johnson, 2002). Due to the long-lived nature of memory lymphocytes, the adaptive immune system is particularly sensitive to senescence. The percentage of late memory B cells are increased in older individuals. Furthermore, these cells exhibit many hallmarks of senescence such as short telomeres, reduced cell proliferation and increased p16

expression (Frasca et al., 2017). Functionally senescent B cells have been shown to secrete less antibodies, which also have a decreased affinity for antigen (Frasca et al., 2008). Similarly, the percentage of terminally differentiated T cells, which exhibit both phenotypic and functional senescent properties, also increases with age (Henson et al., 2012, 2014). Moreover, both senescent B cells and senescent T cells have recently been shown to secrete a SASP (Callender, Carroll, Beal, et al., 2018; Frasca et al., 2017), however the main SASP components are distinct from that secreted by senescent fibroblasts (Table 1.1).

	Fibroblast SASP			
Cytokines & chemokines	Replicative	OIS	MiDAS	T cell SASP
IL-1α	+ + +	+ + +	−	+
IL-1β	+	+ +	−	+
IL-6	+ +	+ + +	−	+
IL-8	+ + +	+ + +	−	+
IL-18	+	?	−	+ + +
TNFα	+	+	+	+
IFN-γ	+	+	−	+
CCL5	+	+	−	+
CCL27	−	−	+	−
Proteases				
MMP-1, -3, -10	+	+	−	+
ADAM8	+	?	?	+
ADAMTS1	+	?	?	+
ADAM28	?	?	?	+ + +
Growth factors				
VEGF	+ + +	+ + +	−	−

Table 1.1: Comparison of fibroblast SASP with $CD8^+$ EMRA T cell SASP [Adapted from (Callender, Carroll, Bober, et al., 2018)].

1.2.4. T cell maturation

All immune cells, including T cells, develop from HSCs in the bone marrow in a process called haematopoiesis. During T cell development, committed lymphoid progenitor cells (LPCs) migrate out of the bone marrow and into the thymus where they lose the potential for B cell (Pui et al., 1999; Radtke et al., 1999) and NK cell (Michie et al., 2000) development. At this stage T cells lack a T cell receptor (TCR), as well as a CD4 and/or CD8 receptor and are therefore termed double negative (DN) thymocytes (Figure 1.3). Effective T cell immunity is dependent on a diverse TCR repertoire. This diversity is generated through a series of recombination events in the thymus which allows 10^8 specificities to be generated from just a finite number of genes. Following successful gene recombination, cells become double positive (DP) $CD4^+CD8^+$ T cells, which interact with cortical epithelial cells and undergo stringent negative selection tests to remove any self-recognising or inadequate thymocytes. Positive selection then allows a small fraction of DP cells to mature into single positive $CD4^+$ or $CD8^+$ naïve T cells, which migrate out of the thymus and into peripheral tissue where they circulate through secondary lymphoid organs awaiting an encounter with an antigen (Germain, 2002) (Figure 1.3).

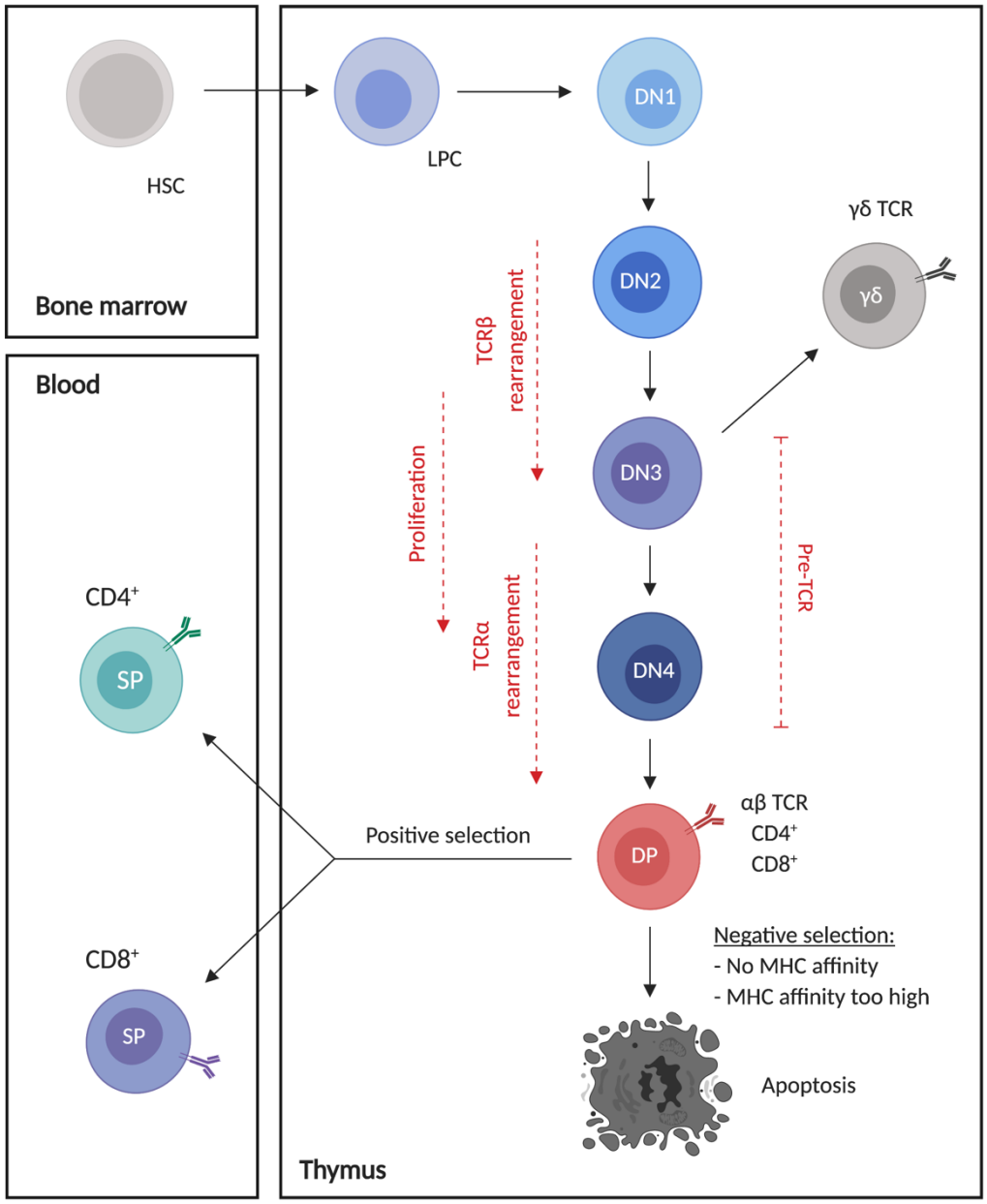

Figure 1.3: T cell development

T cells develop from HSCs. Committed LPCs migrate to the thymus where they begin as DN thymocytes. DN thymocytes can be subdivided into four stages of differentiation; DN1, DN2, DN3 and DN4. Through genetic recombination events, DN T cells can give rise to either αβ or less frequently, γδ TCR expressing cells. With regards to the αβ TCR, during DN3 to DN4 stages, T cells express the pre-TCR, composed of a rearranged TCR β-chain and a non-rearranged α-chain. Successful pre-TCR expression causes cell proliferation and leads to the

replacement of the pre TCR α-chain with a rearranged TCR α-chain, yielding a complete αβ TCR. At this stage T cells are termed DP as they express both $CD4^+$ and $CD8^+$. The fate of the DP thymocytes is then decided through interactions with cortical epithelial cells that express MHC class I and class II molecules associated with self-peptide. Too weak or too strong a signal results in apoptosis. The appropriate level of TCR signalling initiates positive selection, allowing maturation into either $CD4^+$ or $CD8^+$ single positive T cells that migrate out of the thymus and into the circulation [Adapted from (Engel and Murre, 2001; Germain, 2002)].

1.2.4.1. $CD4^+$ helper T cells

As the name suggests, $CD4^+$ helper T (Th) cells help to regulate or assist other white blood cells such as B cells, macrophages or $CD8^+$ T cells in immunological processes. Depending on the type of infection, an effective $CD4^+$ helper T cell response requires differentiation into one of the different $CD4^+$ helper T cell subsets (Iwasaki and Medzhitov, 2010), which are characterised by different cytokines signatures (Figure 1.4).

1.2.4.2. $CD8^+$ cytotoxic T cells

In contrast to $CD4^+$ helper T cells, the role of $CD8^+$ cytotoxic T cells is to directly eliminate any cells infected with invading pathogens, such as viruses, bacteria or protozoal parasites. In addition, $CD8^+$ T cells are also implicated in the removal of cancer cells, allografts from transplants and the clearance of senescent cells. After activation, $CD8^+$ T cells undergo much more extensive proliferation than $CD4^+$ cells (Foulds et al., 2002). Following activation, $CD8^+$ T cells upregulate the inflammatory cytokine receptor CXCR3, which allows them to enter peripheral tissue and migrate

to the site of infection (Groom and Luster, 2011; Hancock et al., 2002; Hokeness et al., 2007). Upon antigen recognition on the surface of a target cell, $CD8^+$ T cells act by the calcium dependent release of specialised preformed cytolytic granules containing the pore-forming perforin and granzymes. Perforin polymerises to form transmembrane pores in the target cell membrane, allowing the entry of granzymes into the cytoplasm of the target cell, which trigger the caspase cascade and subsequent cell apoptosis (Berke, 1995). To a lesser extent, apoptosis can be induced via a second mechanism that involves the binding of Fas on the surface of target cells and Fas ligand, which is present on the membrane of activated $CD8^+$ T cells. This Fas cell-surface interaction results in caspase activation, which consequently induces apoptosis in the target cells (Holler et al., 2003; Krammer, 2000; Rouvier et al., 1993). In addition to their apoptotic effects, $CD8^+$ T cells also release pro-inflammatory cytokines such as IFN-γ and TNF-α, which contribute to host defence (Martin et al., 1996; Shresta et al., 1998). For example, viral replication can be directly inhibited by IFN-γ (Kang et al., 2018).

1.2.5. T cell activation

T cells only recognise foreign antigens that are presented to them on the surface of antigen presenting cells (APCs), such as DCs, from the innate immune system. TCR signalling alone results in anergy, a non-responsive state in which T cells are unable to respond (Alberts et al., 2002). Therefore, in order to become activated, T cells require three kinds of signals. Signal 1 is provided when the antigen-MHC complex being presented is specific to a T cells unique TCR (Goldrath and Bevan, 1999). Signal

1 is also associated with a complex of invariant transmembrane proteins known as CD3 and the CD4 or CD8 co-receptors, which also bind to parts of the same class II or class I MHC, respectively (Alberts et al., 2002). Signal 2 is provided by co-stimulation of other cell surface receptors such as CD28, which recognise co-stimulatory proteins known as B7 proteins on the surface of the presenting cell. Finally, signal 3 is provided by the secretion of inflammatory cytokines (Figure 1.5). Successful activation stimulates the T cell to undergo mass proliferation, a process known as clonal expansion, and differentiate into an effector cell.

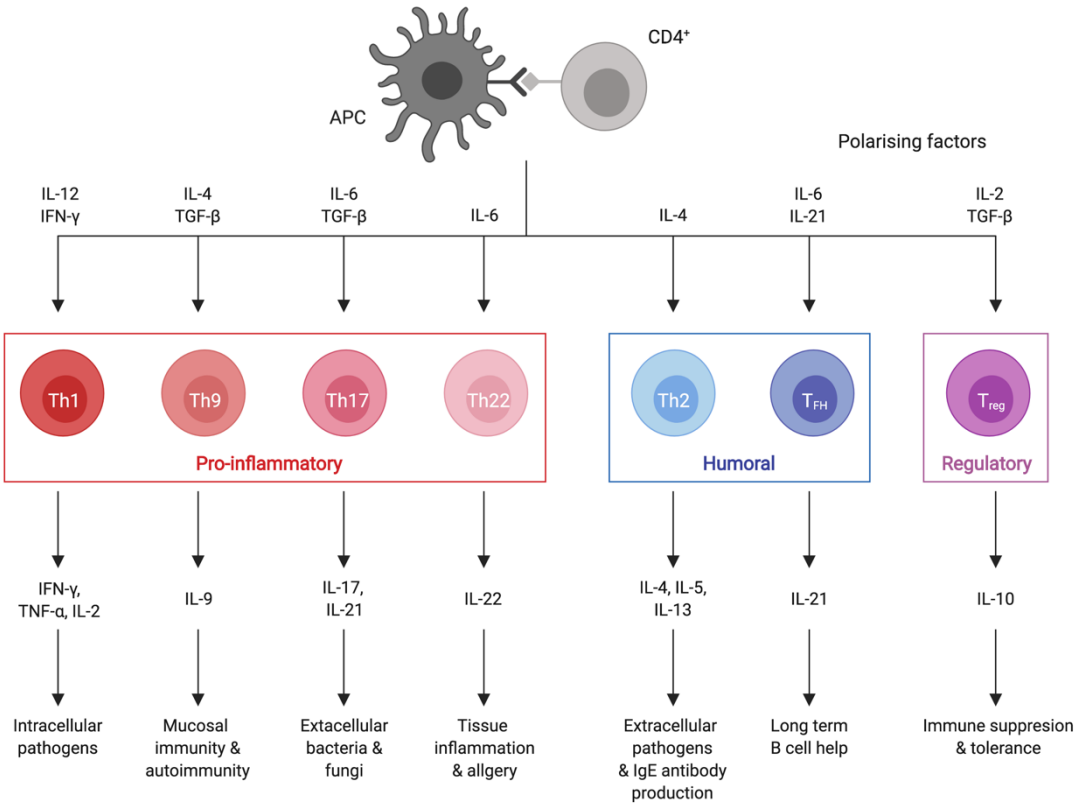

Figure 1.4: CD4⁺ Helper T cell subsets

Differentiation of helper T cell subsets is mediated by cytokines and co-stimulatory molecules produced by APCs [Adapted from (Kaplan et al., 2015; Raphael et al., 2015)].

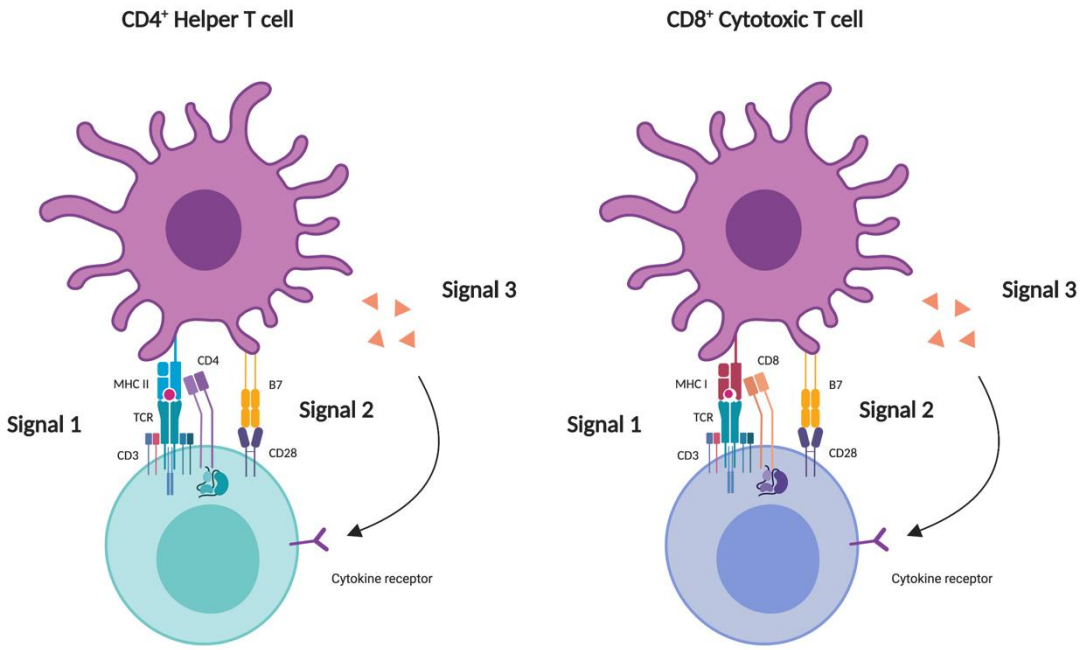

Figure 1.5: T cell activation

T cell activation requires three signals from APCs. Signal 1 is generated via TCR signalling, which involves the antigen-MHC Class I/II complex, CD3 and CD4 or CD8 depending on MHC Class. Alone, signal 1 is not sufficient to activate a T cell response. T cell activation also requires signal 2, a co-stimulatory signal involving other cell surface receptors such as CD28 which recognise B7 proteins (CD80 and CD86) on the surface of APCs. Signal 3 is produced by the secretion of cytokines such as IL-2, IL-12 and IFN-γ.

1.2.6. T cell contraction and memory formation

Despite serving different immune functions, following successful elimination of an infection, both $CD4^+$ and $CD8^+$ T cells undergo contraction of the majority of the T cell population (>90%), leaving the remaining small percentage to mature into memory T cells (Ahmed and Gray, 1996; Badovinac et al., 2002). This contraction/memory cell

selection process is not entirely random as memory cell potential is not inherited equally by all effector cells. Instead, some T cells are intrinsically more able than others to persist and populate the memory T cell pool. Although not exclusive criteria for memory formation, increased expression of CD27 and IL7-Rα and decreased expression of killer cell lectin-like receptor in the well characterised model systems of lymphocytic choriomeningitis virus (LCMV) or Listeria monocytogenes infection, have been shown to predispose for memory precursor cells in $CD8^+$ T cells (Joshi et al., 2007). Both $CD4^+$ and $CD8^+$ memory T cells are maintained for long-term survival in an antigen independent manner mainly through the actions of IL-7 and IL-15 (Surh and Sprent, 2008). This ability to generate immunological memory is invaluable as it provides the host with a set of cells that can mount a much faster and stronger immune response upon secondary infection.

Two broad subsets of memory T cell exist: central memory T cells (CM) and effector memory T cells (EM) (Sallusto et al., 1999). Functionally, CM cells produce IL-2 and tend to mount a much more robust response upon second encounter, whereas $CD4^+$ and $CD8^+$ EM cells are immediate producers of IFN-γ and TNF-α or cytotoxic proteins. Although the exact path of differentiation remains under debate, the general assumption is that T cells progress from naïve T cells through to CM, then EM, before finally becoming terminally differentiated effector memory T cells. Expression of various surface markers are used to identify human T cells in these different differentiation states (Table 1). For example, naïve T cells express CD45RA, however, as memory T cells develop they lose the expression CD45RA. Terminally

differentiated T cells regain expression of CD45RA, therefore these are known as effector memory T cells that re-express CD45RA (EMRA) (Hamann et al., 1997, 1999) (Table 1).

Surface Marker	Naïve	CM	EM	EMRA
CD45RA	+	-	-	+
CD45RO	-	+	+	-
CCR7	+	+	-	-
CD27	+	+	-	-
CD28	+	+	+	-
CD62L	+	+	-	-
CD95	-	+	+	+
KLRG1	-	-	+	+
CD57	-	-	-	+

Table 1.2: The phenotype of T cell subsets [Adapted from (Akbar et al., 2004; Kaech and Cui, 2012)].

1.2.7. T cell senescence and ageing

Immunosenescence affects all aspects of our immune system, however, much of the deterioration in the protective immune response has been attributed to defective T cell immunity (Nikolich-Zugich, 2005). This is the result of a decline in naïve T cell output due to thymic involution and the accumulation of EMRA T cells, which display many characteristics of senescent cells.

1.2.7.1. Thymic involution

The thymus is a vital primary lymphoid organ that provides a continuous, steady supply of naïve T cells, which is essential for preserving the diverse repertoire of naïve T cells responsible for tackling the broad range of new pathogens we encounter throughout life. Despite having such an important role, in humans the thymic epithelial space is replaced by fat as we age, a process known as thymic involution (Henry, 1967). Consequently, thymic output of new naïve T cells declines dramatically until it eventually reaches a point, usually around the age of 60, where there is no longer an effective naïve T cells output (Lynch et al., 2009; Taub and Longo, 2005). Consequently, new T cells must either be generated at extra thymic sites or be clonally expanded from pre-existing T cells. This depleted pool of naïve T cells means that older individuals are less equipped to fight off any new infections they may encounter.

1.2.7.2. EMRA accumulation

During primary infection, $CD8^+$ T cells upregulate the expression of telomerase, resulting in an increase in telomere length (Hathcock et al., 2003; Maini et al., 1999; Plunkett et al., 2001). This upregulation ensures that antigen specific T cells that go on to form the memory pool retain their proliferative capacity. Throughout life subsequent re-encounter with antigen induces further rounds of clonal expansion and contraction of the specific memory T cell populations (Akbar et al., 1993). The ability to upregulate telomerase decreases after repeated stimulation, consequently over time telomeres become considerably shorter. This is particularly evident in

chronic viral infections such as cytomegalovirus (CMV) and human immunodeficiency virus (HIV), which is known to cause large clonal populations of T cells with significantly reduced telomeres (Effros et al., 1996; Hodes et al., 2002; Monteiro et al., 1996). However, unlike in somatic cells, the role of telomere erosion in T cells is more complex, as it has been shown that although both $CD8^+$ and $CD4^+$ EMRA T cells have shorter telomeres than naïve T cells, they do not have the shortest telomeres when compared to other memory subsets (Di Mitri et al., 2011; Riddell et al., 2015), suggesting that non-telomeric senescent drivers are at play.

EMRA T cells lose the expression of the co-stimulatory molecule CD28, which is essential for the activation of the NF-κB pathway (Schmitz et al., 2003), IL-2 transcription and glucose metabolism (Thompson et al., 1986). Furthermore, EMRA T cells display many characteristics of cellular senescence such as a reduction in proliferative capacity (Erickson et al., 1998), defective mitochondrial function and elevated levels of ROS and p38 MAPK (Henson et al., 2014). Despite these senescent characteristics, EMRA T cells remain functionally active as they can secrete high levels of TNF-α and IFN-γ (Henson et al., 2014) and express high levels of perforin and granzyme B, indicating that they maintain potent cytotoxic activity (Plunkett et al., 2014). Moreover, $CD8^+$ EMRA T cells begin to express a variety of NK receptors suggesting a possible repurposing of these cells (Pereira et al., 2019; Tarazona et al., 2001). Consequently, they are distinct from functionally exhausted $CD8^+$ T cells, which have proliferative defects but also have lost the ability to secrete cytokines and mediate cytotoxicity (Akbar and Henson, 2011; Schurich and Henson, 2014).

1.3. Metabolic regulation of T cells

Cell metabolism is a vital regulator of T cell function and fate. As cells are stimulated to grow, proliferate or even die, their metabolic requirements change in order for cell metabolism to match these demands. In fact, pathways that regulate T cell function and metabolism are closely linked. For example, during activation of effector T cells, signals from CD28 and IL-2 induce the PI3K-dependent activation of AKT (Frauwirth et al., 2002; Wieman et al., 2007; van der Windt and Pearce, 2012). Activated AKT promotes the mTOR pathway and ultimately results in a shift toward glycolysis as the primary metabolic program even in the presence of sufficient oxygen (Edinger, 2002; Elstrom et al., 2004; Rathmell et al., 2003) - a process known as aerobic glycolysis or Warburg metabolism (Figure 1.6). This is not surprising as a metabolic program such as glycolysis, which prioritises rapid biosynthesis over efficient energy/ATP production, is much more likely to meet the metabolic needs of activated T cells that are rapidly proliferating.

Unlike their effector counterparts, memory T cells do not primarily use aerobic glycolysis. Instead they rely more on OXPHOS and mitochondrial fatty acid oxidation (FAO) for their development and persistence (Figure 1.6). Memory T cells also have increased mitochondrial mass, allowing them to use a diverse range of substrates for energy generation, hence facilitating cell survival (van der Windt and Pearce, 2012).

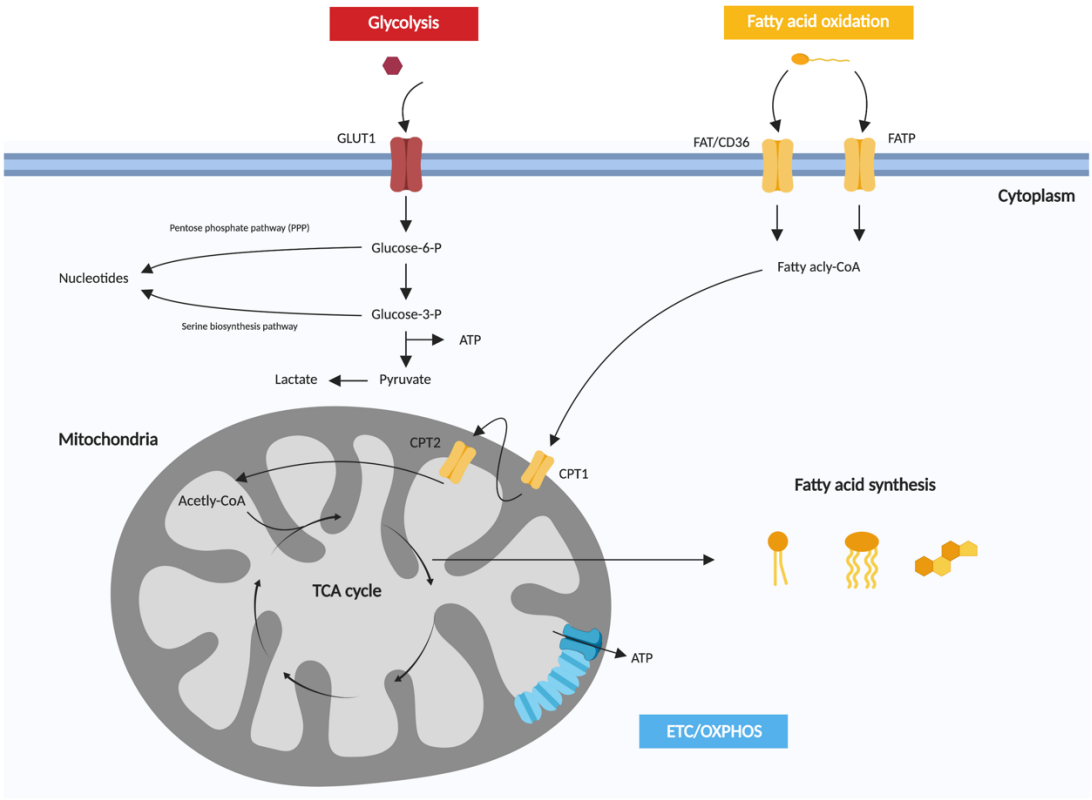

Figure 1.6: Metabolic pathways that support T cells

During OXPHOS electrons generated from the TCA cycle (blue) are transferred along the electron transport chain (ETC) in redox reactions. These reactions release energy, which is used to generate ATP. Glycolysis involves the enzymatic breakdown of glucose (red). In anaerobic conditions, glycolysis produces lactate, whereas in aerobic conditions it produces pyruvate, which is then converted to acetyl-CoA. Other substrates such as glutamine via glutaminolysis or fatty acids (FA) via fatty acid oxidation (FAO, yellow) can be metabolised in the TCA cycle to fuel OXPHOS. Furthermore, these biochemical pathways can also provide metabolic precursors for biosynthesis. For example, intermediates from glucose catabolism during glycolysis can enter the pentose phosphate pathway and the serine biosynthesis pathway to fuel the production of nucleotides and amino acids. Finally, citrate from the TCA cycle can be shuttled from the mitochondria and converted to acetyl-CoA for fatty acid synthesis (FAS) [Adapted from (Buck et al., 2015)].

1.3.1. Alterations in T cell metabolism with senescence

Senescent T cells also display a unique metabolic signature. Unlike other memory subsets, *ex vivo* derived $CD8^+$ EMRA T cells utilise anaerobic glycolysis instead of OXPHOS (Henson et al., 2014). Interestingly, this is similar to what has been shown in senescent fibroblast cells generated by replicative senescent and radiation, which shift their energy production to glycolysis (James et al., 2015). Despite a lack of proliferation, senescent T cells are highly active cells that display effector functions and secrete large amounts of cytokines and maintain potent cytotoxic activity (Henson et al., 2012). Consequently, their reliance on glycolysis ensures rapid biosynthesis to meet the high metabolic demands of these cells. Senescent $CD8^+$ T cells also exhibit mitochondrial dysfunction, which is characterised by a reduced mitochondrial content. Moreover, the remaining mitochondria are large and dysfunctional resulting in a substantially decreased mitochondrial spare respiratory capacity (SRC). These mitochondrial alterations may provide an explanation for their dependence on anaerobic glycolysis (Henson et al., 2014) and their lack of mitochondrial biogenesis is likely due to the failure of senescent $CD8^+$ T cells to activate mTORC1 – a central integrator of immune signalling and cell metabolism (Henson et al., 2014).

1.4. The relationship between senescent T cells and inflammatory diseases

In addition to their role in ageing, there is an ever growing appreciation that senescent T cells also play a role in many chronic inflammatory and metabolic diseases such as cancer (Zelle-Rieser et al., 2016), obesity (Shirakawa et al., 2016) and

rheumatoid arthritis (RA) (Weyand et al., 2014). This is not surprising as senescent T cells produce high levels of IFN-γ and TNF-α (Henson et al., 2014) and secrete a SASP meaning they are highly pro-inflammatory (Callender, Carroll, Beal, et al., 2018).

1.4.1. Senescence and Type 2 diabetes

Diabetes, in particular type 2 diabetes (T2D), is an increasing risk to human health. Globally, diabetes affects 422 million people, which equates to 8.5% of the adult population and is almost double the 4.7% of adults that were affected in 1980 (World Health Organization, 2016). Around 90% of these diabetes cases are due to T2D (World Health Organization, 2016). This rise in prevalence reflects an increase in associated risk factors of T2D, such as obesity and an ageing population. T2D is a multifactorial disease caused by insulin resistance and characterised by a combination of metabolic imbalances and chronic low-grade inflammation. Consequently, T2D was chosen as a model to investigate the relationship between inflammation, metabolism and T cell senescence. Senescence has previously been implicated in the pathogenesis of T2D. With senescent cell burden being shown to increase in tissues that undergo diabetes induced damage, such as the kidneys (Verzola et al., 2008) and pancreas (Sone and Kagawa, 2005). Interestingly, $CD4^+CD28^-$ T cells, which are a late stage differentiated population, have already been reported to accumulate in T2D (Giubilato et al., 2011). A similar finding was observed in obese mice, where senescent $CD4^+$ T cells were found to accumulate in the visceral adipose tissue (VAT) and cause the induction of chronic VAT inflammation (Shirakawa et al., 2016). More recently, $CD8^+CD28^-CD57^+$ T cells have also been

shown to increase the risk of hyperglycaemia in humans, highlighting a potential role for this subset in the pathogenesis of T2D (Lee et al., 2019). Collectively, these studies show an association between T2D and terminally differentiated T cells; however, a full assessment of T cell senescence in T2D has not been conducted.

1.5. Rationale and aims

The role of senescent T cells in ageing is well established (Chou and Effros, 2013). However, the heterogeneity that exists within the EMRA T cell population and the reason behind why the $CD8^+$ and $CD4^+$ lineages have different susceptibilities to senescence is still not understood. Furthermore, the generation of senescent T cells during inflammation and metabolic overload has not been properly investigated.

1.5.1. Specific aims

- To characterise the senescent properties of $CD8^+$ and $CD4^+$ T cells with a particular focus on the heterogeneity that lies within these senescent populations.
- To investigate the metabolic properties of senescent T cells in the $CD8^+$ and $CD4^+$ T lineages.
- To compare the senescent properties of $CD8^+$ T cells isolated from people living with T2D and healthy age-matched control donors.
- To explore the drivers of premature senescence in T2D.

Chapter two: Materials and Methods

2.1. Ethics and blood donor recruitment

Ethics for blood collection were approved by the NRES Committee North East (REC reference: 16/NE/0073) and all subjects provided written informed consent. Healthy volunteers (Age range: 20 – 75 years, median: 40 years, *n* = 45) were individuals who had not had an infection or immunisation within the last month, no known immunodeficiency, and had not received any other immunosuppressive medications within the last 6 months. People living with T2D (Age range: 50 – 77 years, median: 64 years, *n* = 52) were recruited by Prof Graham Hitman, Prof Sarah Finer, and Dr Gill Hood through the Diabetes Alliance for Research in England (DARE) database.

T2D donors were individuals that were currently living with T2D and aged > 18 years (preference was given to individuals between 50 – 60 years). Donors were excluded from the study if they were unable to provide written informed consent, had suffered from an infection or immunisation in the month prior to blood collection, had any known immunodeficiencies or a history of chemotherapy/radiotherapy, had received any immunosuppressive medications within the last 6 months, had a significant co-morbidity (renal failure, heart failure etc), had a known bleeding condition or were on warfarin medication and had a history of neoplasm in the last 10 years. In addition to a blood sample, the donors age, gender, length of time since T2D diagnosis and medications were documented.

2.2. Peripheral blood mononuclear cell (PBMC) isolation and serum collection

To isolate PBMCs, blood was collected in heparinised vacutainers (BD Biosciences), diluted in phosphate buffered saline (PBS) (Sigma-Aldrich) then layered on top of 15 mL of Ficoll-paque™ Plus (GE Healthcare) in a 50 mL falcon tube. Layered samples were centrifuged at 2,000 rpm for 20 minutes without any brake. PBMCs were then carefully aspirated and transferred to a new 50 mL falcon, mixed with PBS and centrifuged at 1,800 rpm for 15 minutes. The supernatant was then removed, and the cell pellet was resuspended in PBS before being centrifuged for a final time at 1,800 rpm for 10 minutes. Following isolation, PBMCs were stained with Trypan Blue Solution (Sigma-Aldrich), counted using a haemocytometer and then either used immediately or cryopreserved at -80°C in freezing medium (fetal calf serum (FCS) with 10% dimethyl sulfoxide (DMSO) (Sigma-Aldrich)) for future use. All PBMCs were cultured in RPMI media supplemented with 10% FCS, 1 mM L-glutamine and 1 mM penicillin and streptomycin (All Sigma-Aldrich). For serum collection, blood was collected in serum blood tubes (BD Biosciences) and centrifuged at 1,800 rpm for 10 minutes. Following centrifugation, the top serum layer was carefully removed and either used immediately or cryopreserved at -80°C.

2.3. Jurkat cell culture

Jurkat cells (clone E6-1 ATCC), an immortalised cell line derived from an acute T cell leukaemia, were cultured using RPMI-1640 media supplemented with 10% FCS, 1 mM L-glutamine and 1 mM penicillin and streptomycin. Cells were split and media was refreshed every 3-4 days. Jurkat cells were used to validate certain findings.

2.4. Antibodies

Marker	Clone	Company	Conjugate	Dilution	Use
CD3	UCHT1	Biolegend	FITC	1:20	Flow cytometry
CD4	RPA-T4 -	BD Biosciences Miltenyi Biotec	PE-CF594 APC-H7 Microbeads	1:100 1:20 1:5	Flow cytometry Magnetic sorting
CD8	SK1 -	Biolegend Miltenyi Biotec	PerCP BV711 Microbeads	1:20 1:40 2:10	Flow cytometry Magnetic sorting
CD27	O323	Biolegend	BV421 FITC	1:40 1:20	Flow cytometry
CD28	CD28.2	Biolegend	PE BV785	1:25 1:25	Flow cytometry
CD45RA	HI100	Biolegend	APC BV605	1:20 1:100	Flow cytometry
CCR7	G043H7	Biolegend	PE-Cy7	1:25	Flow cytometry
KLRG1	MAFA	Miltenyi Biotec	PE	1:20	Flow cytometry
CD57	HNK-1	Biolegend	APC	1:20	Flow cytometry
Ki-67	Ki-67	Biolegend	PE	1:25	Flow cytometry
p-p53	Ser15 – 16G8	Cell Signaling	PE	1:50	Flow cytometry
GATA3	16E10A23 16E10A23	Biolegend Biolegend	FITC unconjugated	1:20 1:1000	Flow cytometry & Western blot
CD36	5-271	Biolegend	FITC	1:20	Flow cytometry
FATP2	6B3A9	Abcam	unconjugated	1:50	Flow cytometry
FATP3	HPA006935	Atlas Antibodies	unconjugated	1:50	Flow cytometry
GLUT-1	202915	R&D systems	PE	1:10	Flow cytometry
CD107a	H4A-3	Biolegend	AF647	1:25	Flow cytometry
pAMPK	T172 – 40H9	Cell Signaling	-	1:50	Flow cytometry
PGC1α	3G6	Cell Signaling	-	1:50	Flow cytometry & Western blot
CHEK1	E250	Abcam	unconjugated	1:2	Immunoprecipitation
TOM20	FL-145	Santa Cruz	-	1:100	Confocal microscopy
Goat to Rb	-	Abcam	AF488	1:1000	Flow cytometry & Confocal microscopy

Table 2.1: List of antibodies

2.5. Flow cytometry analysis

Surface staining and intracellular staining were analysed by flow cytometry. Unstained, single colour controls and fluorescence minus one samples were prepared for control purposes. All samples were acquired on an LSR Fortessa (BD Biosciences) equipped with four lasers: 488 nm blue laser, 561 nm yellow green laser, 641 nm red laser and 405 nm violet laser and data was analysed using FlowJo software.

2.5.1. Surface marker staining for flow cytometry

Flow cytometric analysis was performed on approximately 1 x 10^6 PBMCs per sample. Cells were incubated in the dark with the Zombie_NIR live/dead stain (Biolegend) and appropriate antibodies (Table 2.1) in Brilliant Violet (BV) buffer (BD Biosciences) for 15 minutes at room temperature. Cells were washed in 200 µL of BV buffer, centrifuged at 1,800 rpm for 5 minutes and then fixed in 2% paraformaldehyde (PFA) (Sigma-Aldrich) in PBS prior to analysis.

2.5.2. Intracellular staining for flow cytometry

Approximately 1 x 10^6 PBMCs per sample were surface stained with appropriate antibodies as described above. The FIX & PERM® Cell Permeablilisation Kit (Life Technologies) was used to enable intracellular staining. Immediately after surface staining, cells were incubated with 100 µL of Reagent A (Fixation Medium) for 15 minutes in the dark at room temperature. Cells were then washed in PBS, centrifuged at 1,800 rpm for 5 minutes and resuspended in 50 µL of Reagent B (Permeablisaton

Medium) plus 10% goat serum and recommended volume of primary intracellular antibody. Cells were incubated for 20 minutes in the dark at room temperature then washed in PBS at 1,800 rpm for 5 minutes before secondary antibody was added and incubated for 20-minutes in the dark at room temperature. Finally, cells were washed in PBS and centrifuged at 1,800 rpm for 5 minutes and resuspended in 100 µL 2% PFA in PBS. Samples were either analysed immediately or stored overnight at 4°C. The Foxp3 Transcription Factor Staining Buffer Kit (Biolegend) was used for staining transcription factors and nuclear proteins. Following surface staining cells were washed in PBS and then incubated with 1 mL of the FOXP3 Fix/Perm buffer (4X) for 20 minutes in the dark at room temperature. Cells were then washed in PBS and incubated with 1 mL of the FOXP3 Perm buffer (10X) for 15 minutes in the dark at room temperature. Cells were washed again and incubated with 50 µL of FOXP3 Perm buffer (10X) and appropriate amount of the antibody being used for 30 minutes in the dark and room temperature. The cells were then washed for a final time in PBS, centrifuged at 1,800 rpm for 5 minutes and resuspended in 100 µL 2% PFA in PBS. Samples were either analysed immediately or stored overnight at 4°C.

2.5.3. Assessment of cytotoxicity via flow cytometry

To assess cytotoxicity, approximately 1 x 10^6 PBMCs were stimulated with 1 µg/µL of anti-CD3 (OKT3) and incubated with CD107a in complete RPMI-1640 media for 45 minutes at 37°C. Then 100 µM of monensin (Biolegend) (Sigma-Aldrich) was added and the cells were incubated for a further 4 hours and 15 minutes at 37°C. Next, cells were washed in PBS and surface stained as described in 2.5.1. Finally, cells were

washed in PBS, centrifuged at 1,800 rpm for 5 minutes and resuspended in 100 µL 2% PFA in PBS ready to either be analysed immediately or stored overnight at 4°C.

2.6. Magnetic bead sorting of $CD4^+$ and $CD8^+$ T cells

PBMCs were isolated as described in section 2.2 and centrifuged at 1,800 rpm following cell counting and resuspended in 80 µL MACS buffer (1x PBS supplemented with 0.5% BSA and 2mM Ethylenediaminetetraacetic acid (EDTA)) per 10^7 cells and 20 µL of either anti-$CD4^+$ or anti-$CD8^+$ conjugated MicroBeads per 10^7 cells. Samples were gently mixed and incubated at 4°C for 15 minutes. Following incubation, samples were washed with 3 mL of MACS buffer and centrifuged at 1,800 rpm for 5 minutes. In preparation for magnetic separation, dependent on cell number either MS or LS columns (Miltenyi Biotec) were placed on the separator and pre-washed with either 0.5 mL or 3 mL MACS buffer respectively. Once washed, samples were resuspended in 0.5 mL or 3 mL of MACS buffer and added to the columns. Flow through was collected in 15 mL falcons below the column. Once all the sample had passed through, the columns were washed with 3 x 0.5 mL or 3 mL of MACS buffer. Following the washes, columns were then removed from the separator and placed in a new 15 mL falcon. 0.5 mL or 3 mL of MACS buffer was then added to the columns and positively labelled cells were removed using the column plunger provided. Cells were then washed with 2 mL of MACS buffer per 10^7 cells, centrifuged at 1,800 rpm for 5 minutes. A small sample from each sort was taken to check the purity by flow cytometry.

2.7 Flow cytometry cell sorting of T cell subsets

$CD4^+$ or $CD8^+$ T cells were isolated using magnetic sorting described above. T cell subsets were surface stained with CD27 and CD45RA as describe in section 2.5.1 and then sorted into naive, CM, EM and EMRA subsets on a BD FACSAria™ Fusion equipped with three lasers: 488 nm blue laser, 641 nm red laser and 405 nm violet laser. Following isolation, subsets were then used for downstream experiments such as RNA or protein extraction, siRNA electroporation and metabolic seahorse assays.

2.8. Mitochondrial measurements

For mitochondrial mass, PBMCs were incubated with 100 nM MitoTracker Green FM (Invitrogen™) for 30 minutes at 37°C, 5% CO_2. Mitochondrial membrane potential (MMP) was investigated using Tetramethylrhodamine (TMRE) (ThermoFisher Scientific) 2 µM TMRE was incubated with PBMCs for 30 minutes at 37°C, 5% CO_2. MitoSox Red (Invitrogen™) was used to assess mitochondrial ROS production; PBMCs were incubated with 5 µM MitoSox for 30 minutes at 37°C, 5% CO_2. Following mitochondrial staining, samples were surface stained as described in section 2.5.1 and then left unfixed and immediately analysed on an LSR Fortessa (BD Biosciences).

2.8.1. Confocal microscopy analysis of mitochondria

To assess mitochondrial morphology, Jurkat cells were plated onto 12 well microscope slides at a density of 0.05 x 10^6 per well. Cells were fixed and permed using the FIX & PERM® Cell Permeablilisation Kit to enable intracellular labelling. Cells were incubated with 100 µL of Reagent A (Fixation Medium) for 15 minutes at room

temperature. Cells were then washed in PBS x 3 and resuspended in 50 µL of Reagent B (Permeablisaton Medium) plus 10% goat serum and Tom20. Cells were incubated for 30 minutes at room temperature then washed in PBS before the secondary goat to Rb antibody was added and incubated for a further 20 minutes in the dark at room temperature. Next, cells were washed in PBS and incubated with 4',6-diamidino-2-phenylindole (DAPI) (ThermoFisher Scientific) for 10 minutes at room temperature in the dark. Finally, cells were washed with PBS then fixed with 100 µL 2% PFA in PBS. Samples were imaged on a Zeiss LSM 880 confocal microscope with a X 63 oil-immersion objective lens. Excitation was at 488 nm from an argon-ion laser. Fluorescence detection was in the green; and UV; 405 nm channel. Quantification of image data was performed by measuring the intensity of the 500 – 570 nm channel using ZEN-imaging. Imaris Image Analysis software was used determine mitochondrial volume through surface 3D rendering of Z-stack images.

2.9. Live cell metabolic assays

Metabolic assays were measured in whole $CD4^+/CD8^+$ T cells and/or in $CD4^+/CD8^+$ CD27/CD45RA FACS sorted subsets. Seahorse sensor cartridges were incubated at 37°C in a non-CO_2 incubator overnight with Seahorse XF Calibrant pH 7.4 (Agilent) to rehydrate the sensor probes. All metabolic assays were performed with a cell density of 0.25 x 10^6 per well, attached using of 22.4 µg/mL of Cell-Tak (Corning®) and measured using a Seahorse XFe96 Analyser (Agilent). Cells were stimulated with 1 µg/µL of anti-CD3 and 5 ng/mL IL-2 15 minutes prior to each metabolic test.

2.9.1. Cell Mito Stress Test

The Cell Mito Stress Test (Agilent) was used to assess mitochondrial function and OXPHOS. The assay was performed in RPMI-1640 buffer without phenol red and carbonate buffer (Sigma-Aldrich) containing 25 mM glucose, 2 mM L-glutamine and 1 mM pyruvate with a pH of 7.4. The stress test was performed using 1 µM Oligomycin, 1.5 µM, carbonyl cyanide 4-(trifluoromethoxy) phenylhydrazone (FCCP), 100 nM rotenone, and 1 µM antimycin A (Agilent) (Figure 2.1). Metabolic measurements were calculated using the equations shown in Table 2.2.

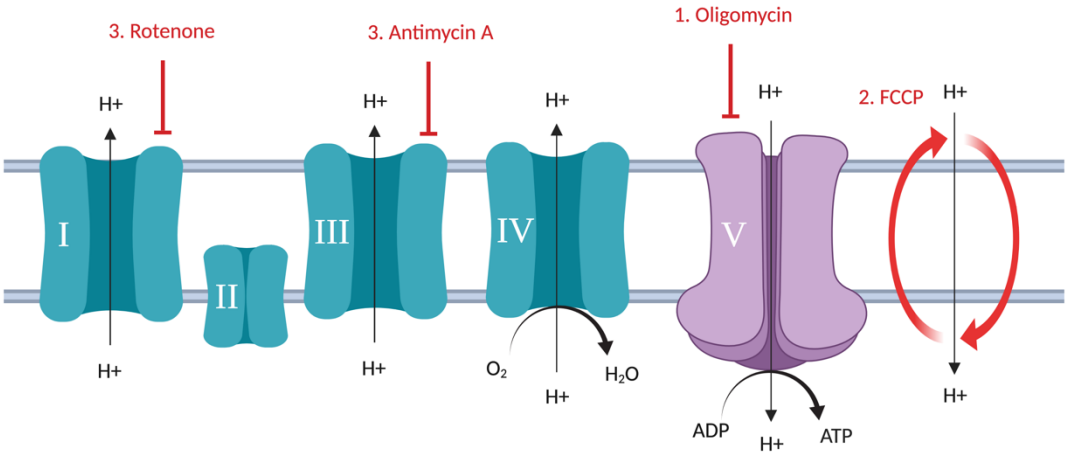

Figure 2.1: Schematic diagram of the mitochondria inhibitors used in the Cell Mito Stress Test adapted from the Agilent User Guide.

Parameter	Equation
Non-mitochondrial respiration	Measurements after Rotenone/Antimycin A injection
Basal respiration	(Measurements before first injection) – (Non-mitochondrial respiration)
Proton leak	(Measurements after Oligomycin injection) – (Non-mitochondrial respiration)
ATP production	(Measurements before Oligomycin injection) – (Measurements after Oligomycin injection)
Maximal respiration	(Measurements after FCCP injection) – (Non-mitochondrial respiration)
Spare respiratory capacity	(Maximal respiration) – (Basal respiration)

Table 2.2: Seahorse XF Cell Mito Stress Test parameter equations

2.9.2. Fatty acid oxidation

The Seahorse XF Palmitate assay (Agilent) was used to determine FAO. Cells were incubated overnight in substrate limited (DMEM (Gibco), 0.5 mM glucose, 1 mM L-glutamine, 0.5 mM carnitine, and 1% FCS). 45 minutes prior to the assay cells were transferred to warm Krebs-Henseleit KH Buffer (KHB) (111 mM NaCL, 4.7mM KCL, 1.25 mM $CaCl_2$, 2 mM $MgSO_4$, 1.2 mM NaH_2PO_4) supplemented with 2.5 mM glucose, 0.5 mM carnitine, 5 mM HEPES adjusted to pH 7.4. Then, 15 minutes prior to the assay 40 µM Etoximir was added to selected groups. Finally, the cells were provided with Palmitate:BSA (Aglient) as a substrate and a Cell Mito Stress Test as described above (Figure 2.1) was ran on the Seahorse analyser.

2.10. Nutrient uptake experiments

Approximately 1 x 10^6 PBMCs per condition were stimulated for either 1 hour or overnight at 37°C with 1 µg/µL of anti-CD3 in complete RPMI-1640 media. For glucose uptake, PBMCS were washed in PBS and centrifuged at 1,800 rpm for 5 minutes then resuspended in glucose free media for 15 to 30 minutes. 100 µM of the fluorescent glucose analogue 2-NBDG (Invitrogen™) was then added and the PBMCs were incubated in the dark for 30 minutes. Next, the cells were washed in PBS, centrifuged at 1,800 rpm for 5 minutes, and surface stained with phenotyping antibodies as described in section 2.5.1. Cells were then washed for a final time, resuspended in PBS and taken immediately to the flow cytometer for analysis. To measure lipid uptake stimulated PBMCs were incubated with the 1 nM of the fluorescent palmitate analogue BODIPY FL C_{16} (Invitrogen™) and incubated in the dark for 10 minutes. Cells were then washed in PBS, centrifuged at 1,800 rpm for 5 minutes and surface stained before being analysed by flow cytometry.

2.11. Protein extraction and western blotting

Cells were centrifuged at 1,800 rpm for 5 minutes, then the cell pellet was resuspended in approximately 200 µL of RIPA buffer plus inhibitors (protease: complete mini Roche; 11836153001, and phosphatases: cocktail set II Calbiochem; 524625). Samples were kept on ice for 15 minutes and the centrifuged at 4°C for 15 minutes at top speed before the supernatant was removed and stored as cell lysates.

Cell lysates were fractionated by SDS-polyacrylamide electrophoresis before being transferred onto nitrocellulose membranes. Membranes were then blocked with blocking buffer (5% milk power, 0.05% Tween-20 in PBS) for 1 hour at room temperature on a shaker. Primary antibody was diluted accordingly in primary antibody buffer (5% milk/BSA, 0.05% Tween-20 in PBS) and then incubated overnight at 4°C on a shaker. Membranes were then washed three times in wash buffer (PBS + 0.05% Tween-20), and secondary antibody was added in the blocking buffer then incubated for 30 minutes to 1 hour at room temperature on a shaker before being washed a further three times. The protein was detected via chemiluminescence, by means of the ECL system (GE Healthcare).

2.12. Immunoprecipitation

For immunoprecipitation experiments the Chk1 antibody was incubated with Red Protein G Affinity Gel (Sigma-Aldrich; E3403) for 1 hour at 4°C on a shaker to allow the antibody to bind to the beads. Cell lysates were prepared as described above and then incubated with the antibody-bead mix overnight at 4°C on a shaker. The following morning, samples were centrifuged, and the supernatant was discarded leaving only the proteins able to bind to Chk1. SDS-polyacrylamide electrophoresis and western blotting of GATA binding protein 3 (GATA3) and peroxisome proliferator activated receptor gamma coactivator 1-alpha (PGC1α) was then carried performed as described above.

2.13. siRNA knockdown

GATA-3 and scrambled siRNA (Table 2.3) were dissolved to a final concentration of 10 µM in electroporation buffer (15 mM NAH_2PO_4, 35 mM NA_2HPO^4, 5 mM KCl, 10 mM $MGCl_2$, 11 mM glucose, 100 mM NACl, 20 mM HEPES, 15.9 mM NaOH in Milli-Q H_2O). For each transfection cells were centrifuged at 1,800 rpm for 5 minutes and resuspended in 100 µL of the siRNA solution and transferred to an electroporation cuvette. Cells were electroporated using program T-023 on an Amaxa™ Nucleofector™ (Lonza Bioscience) and then left to recover for 24 to 48 hours in fresh RPMI-1640 media supplemented with 10% FCS, 1 mM L-glutamine and 1 mM penicillin and streptomycin ready for downstream experiments.

siRNA	Sequence	Conjugate
GATA-3	5'-/5Alex647N/UAG GCG AAU CAU UUG UUC AAA-3'	AF647
Scrambled	5' CCU GUU CUU AAA AUA GUA GGC 3'	-

Table 2.3: siRNA sequences

2.14. Cellular Senescence RT2 Profiler PCR Arrays

Unstimulated $CD8^+$ EMRA T cells from T2D and healthy age-matched control donors were isolated using MACS sorting for $CD8^+$ T cells and then FACs sorting using CD27/CD45RA for EMRA isolation as described above. RNA was extracted and pre-amplified and then ran on the Cellular Senescence RT^2 Profiler PCR Arrays (PAHS-050Z) as described below.

2.14.1. RNA extraction

Total RNA was extracted using the RNAeasy Micro Kit (217084) according to the manufacturer's protocol. First, cells were pelleted, resuspended in 350 µL of RTL buffer supplemented with 10% β-mecaptoethanol. 350 µL of 70% ethanol was added to the homogenised lysate and the total 700 µL was transferred into an RNeasy spin column placed in a 2 mL collection tube. The sample was centrifuged at 10,000 rpm for 15 seconds, and then flow through was discarded. 700 µL of RW1 buffer was loaded into the spin column, centrifuged at 10,000 rpm for 15 seconds, and then flow through was discarded. 500 µL of RPE buffer supplemented with ethanol was then added to the spin column and again centrifuged at 10,000 rpm for 15 seconds to wash the spin column membrane, afterwards flow through was discarded. An additional 500 µL of RPE buffer was added to the spin column and centrifuged at 10,000 rpm for 2 minutes. Following the second wash with RPE buffer both the flow through and 2 mL collection tube were discarded. Spin columns were placed in fresh 2 mL collection tubes and centrifuged at full speed for 1 minute to eliminate any possible carryover of RPE buffer. Finally, collection tubes were discarded, and spin

columns were placed in fresh 1.5 mL eppendorf tubes. 14 µL of RNase-free water was directly added to the spin column membrane and centrifuged at 10,000 rpm for 1 minute to elute the RNA. RNA quality and quantity were measured by spectrophotometry (Nano drop ND-1000). RNA was then frozen at -80^{o}C until ready to use for the RT^{2} profiler arrays.

2.14.2. cDNA synthesis and pre-amplication of RNA samples

Due to the low cell numbers and therefore low concentration of RNA the RT^{2} PreAMP cDNA Synthesis Kit (330451) and RT^{2} PreAMP Pathway Primer Mix (330241) were used to for preamplification of the RNA samples. First, cells were subjected to genomic DNA elimination by incubating the RNA samples with 2 µL of Buffer GE and RNase-free water in a final volume of 10 µL for 5 minutes at 42^{o}C before being placed immediately on ice for at least 1 minute. Next the samples were incubated with 10 µL of reverse transcription mix (Table 2.4) to generate a cDNA target template.

Following gentle mixing samples were incubated at 42^{o}C for exactly 20 minutes then immediately stopped by incubating at 95^{o}C for 5 minutes before being placed on ice. 5 µL of the cDNA synthesis reactions were gently mixed with 20 µL of pre-amplification mix (Table 2.5) and placed into the real-time cycler to undergo pre-amplification (Table 2.6).

Component	Volume for 1 sample
5x Buffer BC3	4 µL
Control P2	1 µL
cDNA Synthesis Enzyme Mix	1 µL
RNase Inhibitor	1 µL
RNase-free water	3 µL
Total volume	10 µL

Table 2.4: Reverse transcription mix

Component	Volume for 1 sample
RT^2 PreAMP PCR Mastermix	12.5 µL
RT^2 PreAMP Pathway Primer Mix	7.5 µL
Total volume	20 µL

Table 2.5: Pre-amplification mix

Cycles	Duration	Temperature
1	10 minutes	95°C
12	15 seconds 2 minutes	95°C 60°C
Hold		4°C

Table 2.6: Cycling conditions for pre-amplification of cDNA

After cycling 2 µL of Side Reaction Reducer was added to each sample and incubated at 37°C for 15 minutes followed by heat inactivation at 95°C for 5 minutes. Immediately after 85 µL of nuclease-free waster was added and mixed with the samples before they were either placed on ice or stored at -20°C overnight.

2.14.3. Real-Time PCR using RT2 Profiler PCR Arrays

Once the PCR components mix (Table 2.7) was prepared, 25 µL was dispensed into each well of the 96 well plate. The plate was then carefully sealed with the optical adhesive film, centrifuged for 1 minute at 1000 *g* at room temperature to remove any bubbles. The plate was then placed StepOnePlus cycler to undergo qPCR (Table 2.8).

Component	Volume for 96-well plate
2x RT2 SYBR Green MasterMix	1275 µL
Pre-amplification reaction (from previous steps)	102 µL
RNase-free water	1173 µL
Total volume	2550 µL

Table 2.7: PCR components mix

Cycles	Duration	Temperature
1	10 minutes	95°C
40	15 seconds	95°C
	1 minute	60°C

Table 2.8: Cyclin conditions for qPCR data collection

2.14.4. RT2 PCR array data analysis

Following the qPCR run C_T values for all wells were exported to a blank excel spreadsheet and imported onto the Qiagen data analysis web portal at http://dataanalysis.qiagen.com/pcr/arrayanalysis. From this the online software performed quantification using the $\Delta\Delta C_T$ method and generated fold change and fold regulation values.

2.15. Sera culture experiments

Sera isolated from T2D patients and healthy age-matched control donors was isolated from whole blood as described in sections 2.2. Sera was then incubated at 56^{o}C for 20 minutes to decomplement. PBMCs were isolated from a young donor as described in section 2.2 and cultured in either low (5mM) or high glucose (25mM) RPMI-1640 media with or without 10% sera from either T2D patients or healthy age-matched control donors. Flow cytometry staining was carried out on samples at day 0, 3 and 7 in order to phenotype the samples.

2.16. Cytokine array

Sera was collected as described in section 2.2 and cytokine levels were measured using the Proteome Profiler Human Cytokine Array (R&D Systems; ARY0058). Array membranes were first incubated with 2 mL of Array Buffer 4 for 1 hour on a rocking platform shaker to block the membranes. At the same time, the samples were prepared by adding 200 µL or each sample to 100 µL of Array Buffer 4 and then adjusted to a final volume of 1.5 mL using the Array Buffer 5. 15 µL of reconstituted Human Cytokine Array Detection Antibody Cocktail was added to each sample and left to incubate at room temperature for 1 hour. After 1 hour, Array Buffer 4 was aspirated from the membranes and the sample/antibody mixture was added. Membranes were incubated overnight at 4^{o}C on a rocking platform. The following day the membranes were washed with 20 mL 1X Wash Buffer for 10 minutes on a rocking platform shaker. This step was repeated twice more before the membranes were incubated with 2 mL of Streptavidin-HRP for 30 minutes a room temperature.

Membranes were then washed three times as described above. Finally, each membrane was covered with 1 mL of Chemi Reagent Mix, covered with a plastic sheet protector and left to incubate for 1 minute. Following incubation, the membranes were blotted to remove excess liquid and then placed in an autoradiography film cassette. Membranes were then exposed to X-ray film. Multiple exposure times were used (30 seconds – 20 minutes). Later the X-ray films were scanned and the mean pixel intensities for each cytokine (Figure 2.2) were calculated using image studio software to quantify the results.

	1	2	3	4	5	6	7	8	9	10
A	Reference spots	CCL1/ 1-309	CCL2/ MCP-1	MIP-1α/ MIP-1β	CCL5/ RANTES	CD40 Ligand/ TNFSF5	C5/C5a	CXCL1/ GROα	CXCL10/ IP-10	Reference spots
B		CXCL11/ I-TAC	CXCL19/ SDF-1	G-CSF	GM-CSF	I-CAM1/ CD54	IFN-γ	IL-1α/ IL-1F1	IL-1β/ IL-1F2	
C		IL-1ra/ IL-1F3	IL-2	IL-4	IL-5	IL-6	IL-8	IL-10	IL-12 p70	
D		IL-13	IL-16	IL-17A	!IL-17E	!L-18/ I-1F4	IL-21	IL-27	IL-32α	
E	Reference spots	MIF	Serpin E1/ PAI-1	TNF-α	TREM-1					Negative control

Figure 2.2: Human Cytokine Array coordinates

2.17. *t*-SNE analysis

Following flow cytometry acquisition, $CD8^+$ T cells were gated on healthy, live lymphocytes in FlowJo (BD) as described later in section 3.2.1. After gating on the population of interest, each sample was exported for *t*-SNE analysis. *t*-SNE was run using a custom R script.

2.18. Statistical analysis

GraphPad Prism was used to create all graphs and statistical analysis. Data are presented as mean ± standard error of mean (SEM) of n samples per group. The number of donors and when used, the statistical analysis are detailed in figure legends.

Chapter three: Characterisation of $CD8^+$ and $CD4^+$ EMRA T cells

3.1. Introduction

The majority of senescent T cell research has focused on replicative senescence (Chou and Effros, 2013); however, many types of premature senescence phenotypes have been document in fibroblasts (Kang et al., 2011; Serrano et al., 1997; Toussaint et al., 2002). It is therefore likely that other cell types, including T cells, will also be susceptible to the induction of premature senescence. Furthermore, the majority of T cell senescence has been studied in $CD8^+$ T cells, as $CD8^+$ EMRA T cells are far more abundant and undergo more dramatic phenotypic and functional changes (Henson et al., 2014). Senescent $CD4^+$ T cells are present but in fewer numbers than their $CD8^+$ counterparts. Both $CD8^+$ and $CD4^+$ EMRA T cells lose the expression of co-stimulatory molecules CD28 and CD27, although the order in which this occurs differs. $CD8^+$ EMRAs lose CD28 expression first whereas the reverse is true for $CD4^+$ EMRAs (Larbi and Fulop, 2014). Functionally, $CD4^+$ EMRAs have been shown to acquire cytolytic abilities, a quality usually reserved for $CD8^+$ T cells (Nakajima et al., 2002). Despite being able to retain some effector function both $CD8^+$ and $CD4^+$ senescent T cells have been shown to significantly contribute to T cell dysfunction and the deterioration of the immune system in older individuals (Chou and Effros, 2013).

3.1.1. Aim

The aim of this chapter was to characterise the senescent properties of both $CD8^+$ and $CD4^+$ T cells with a particular focus on the heterogeneity that lies within the senescent populations.

3.2. Utilisation of flow cytometry to identify $CD8^+$ and $CD4^+$ T cells

Flow cytometry allows in depth analysis of T cell populations. Forward scatter (FSC) and side scatter (SSC) FACS plots were used to assess both the size and granularity of cells respectively (Figure 3.1A). Lymphocytes formed a tight distinct population away from the larger monocytes, smaller red blood cells and any cellular debris (Figure 3.1A). FSC-area and FSC-height FACS plots were used to eliminate any doublets (Figure 3.1B) and gating against a live/dead stain enabled the selection of healthy, live lymphocytes (Figure 3.1C). From this either $CD8^+$ or $CD4^+$ T cells were then gated (Figure 3.1D).

3.3. $CD8^+$ and $CD4^+$ EMRA T cells increase significantly with age and are a highly heterogeneous population

3.3.1. Utilisation of CD45RA/CD27 to identify $CD8^+$ and $CD4^+$ T cell subsets

The $CD8^+$ and $CD4^+$ T cell lineages include four distinct subsets: naïve, CM, EM and EMRA. Phenotypically these subsets can be identified by flow cytometry using the cell surface markers CD45RA/CD27 (Henson et al., 2014; Koch et al., 2008); with naïve being defined as $CD45RA^+CD27^+$, CM $CD45RA^-CD27^+$, EM $CD45RA^-CD27^-$ and EMRA $CD45RA^+CD27^-$ (Figure 3.2A and B). The frequency of these four subsets were recorded for both $CD8^+$ and $CD4^+$ T cells in individuals aged 20 – 75 (Figure 3.2C). No difference was found in the percentage of naïve and EM T cells between the two lineages (Figure 3.2C); however, $CD4^+$ T cells had significantly more CM T cells whereas $CD8^+$ T cells had significantly more EMRA T cells (Figure 3.2C).

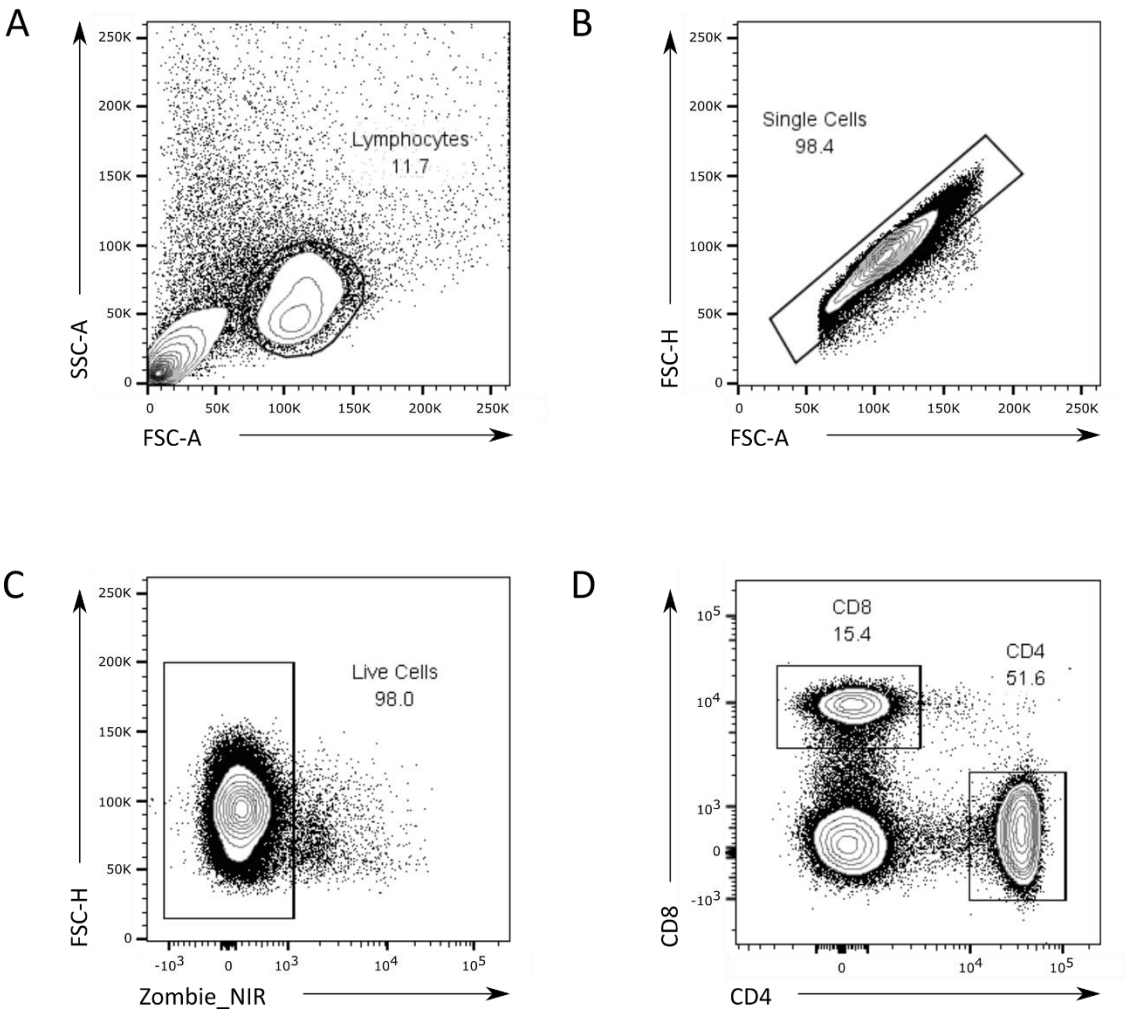

Figure 3.1: Utilisation of flow cytometry to identify $CD8^+$ and $CD4^+$ T cells

A) SSC-A/FSC-A plot: Gate around lymphocytes.

B) FSC-H/FSC-A plot: Gate around single cells.

C) FSC-H/Zombie_NIR: Gate around live cells.

D) CD8/CD4: Gate around $CD8^+$ and $CD4^+$ T cells.

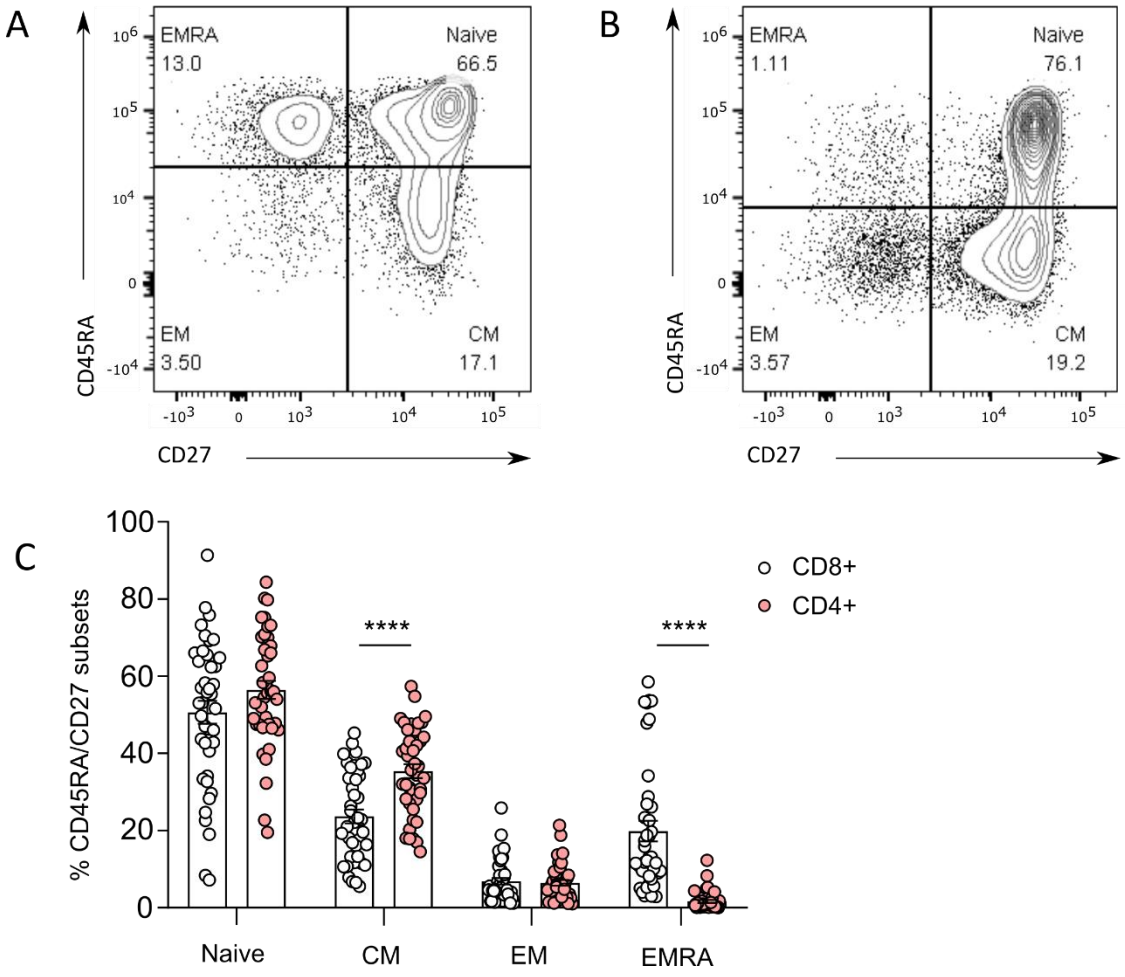

Figure 3.2: Utilisation of CD45RA/CD27 to identify $CD8^+$ and $CD4^+$ T cell subsets

A) Representative flow cytometry dot plot of $CD8^+$ CD45RA/CD27 defined subsets.

B) Representative flow cytometry dot plot of $CD4^+$ CD45RA/CD27 defined subsets.

C) Quantification of the CD45RA/CD27 defined $CD8^+$ and $CD4^+$ T cell subsets. Individuals were aged 20 – 75, with a median age of 45. Data expressed as mean ± SEM, *n* = 41. Multiple T-tests were used to determine p-values, p**** = < 0.0001.

The proportion of CD8⁺ naïve T cells decreased significantly with age (Figure 3.3A). This was accompanied by a significant increase in the CD8⁺ EMRA T cell population (Figure 3.3D). The proportions of CM and EM CD8⁺ T cells did not differ between the different age ranges (Figure 3.3B and C).

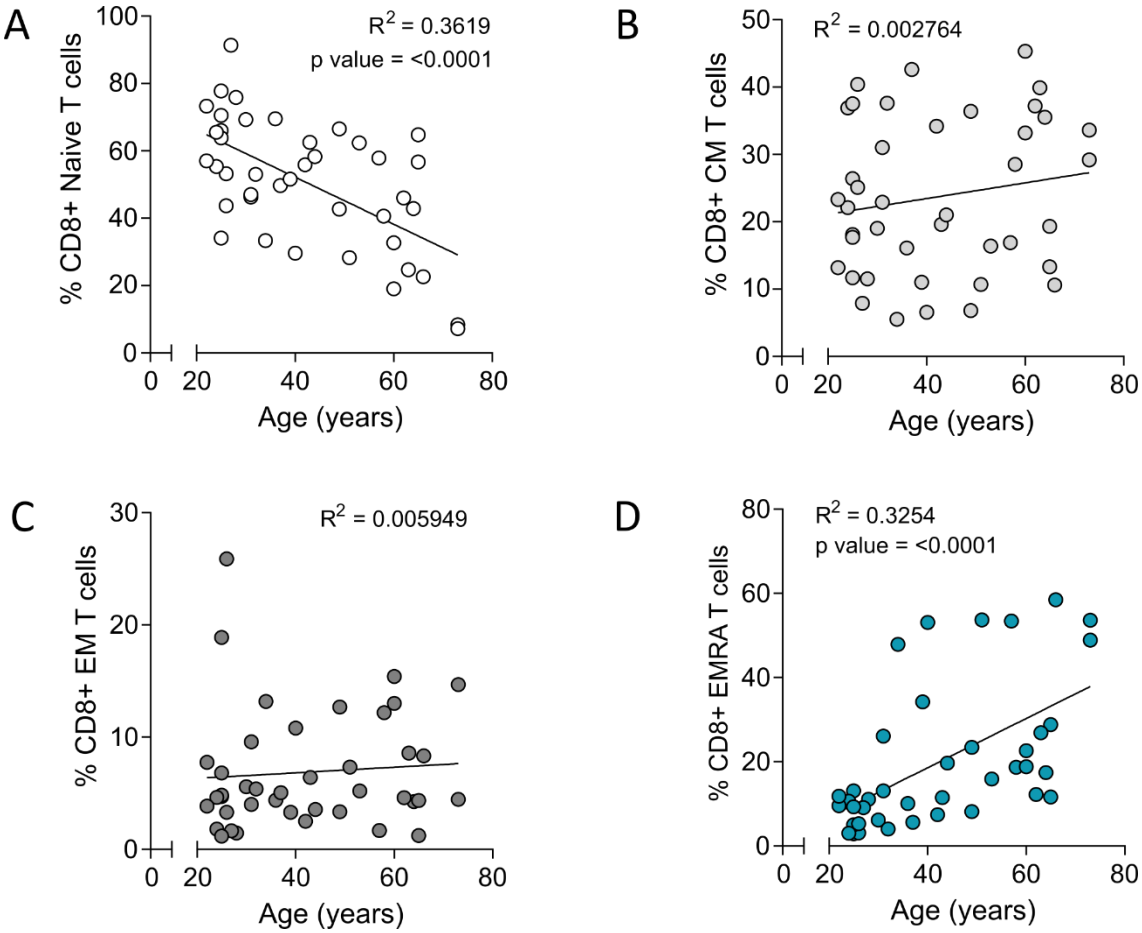

Figure 3.3: Age related changes to the frequency of CD8⁺ CD45RA/CD27 subsets

Percentage of A) Naïve, B) CM, C) EM and D) EMRA CD8⁺ T cells defined as percentage of the total CD8⁺ T cells population stratified by age. The line of best fit was generated using linear regression, *n* = 41.

The proportion of $CD4^+$ naïve T cells also decreased significantly with age (Figure 3.4A). Both the $CD4^+$ CM and EM subsets increased significantly with age (Figure 3.4B and C). Additionally, despite not being statistically significant, the $CD4^+$ EMRA subset followed the same trend as the other memory subsets (Figure 3.4D).

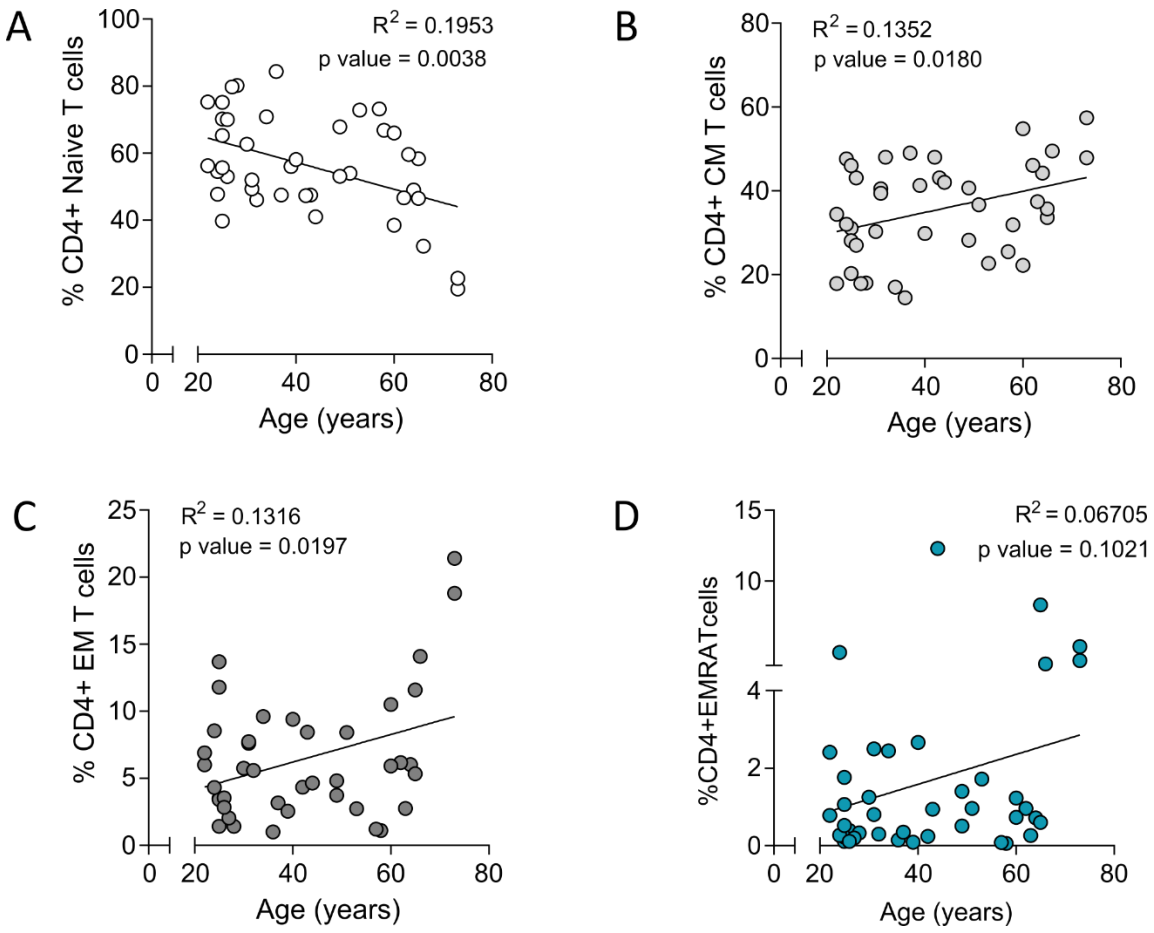

Figure 3.4: Age related changes to the frequency of $CD4^+$ CD45RA/CD27 subsets

Percentage of A) Naïve, B) CM, C) EM and D) EMRA $CD4^+$ T cells defined as percentage of the total $CD4^+$ T cells population stratified by age. The line of best fit was generated using linear regression, *n* = 41.

3.3.2. $CD8^+$ and $CD4^+$ EMRA T cells are a highly heterogeneous subset

Previously data from our lab showed that the $CD8^+$ EMRA T cell subset is highly heterogeneous (Figure 3.5), with a population that aligns to the naïve subset (N-like EMRA) and another that aligns more closely to the EM subset (EM-like EMRA) (Callender, Carroll, Beal, et al., 2018). To properly investigate the heterogeneity of the EMRA subset in both $CD8^+$ and $CD4^+$ T cells we used a phenotyping strategy that utilised the cell surface markers CD45RA, CCR7, CD27 and CD28 to define senescence (Koch et al., 2008).

The leukocyte common antigen isoform CD45RA is expressed on naïve T cells but lost during memory development. However, terminally differentiated memory T cells re-express CD45RA, therefore it can be used to define both naïve and EMRA T cells (Hamann et al., 1997, 1999). The chemokine receptor CCR7 facilitates T cell exit out of the periphery and into lymphoid tissues, making it vital for naïve T cells as it allows them to search lymphoid tissues for antigens. CM T cells also maintain high levels of CCR7 as they predominantly reside in lymph nodes (Koch et al., 2008). Conversely, EM and EMRA T cells lose CCR7 and are instead found predominantly in the blood and non-lymphoid tissues. The co-stimulatory molecules CD27 and CD28 are important for providing proliferative and survival cues to naïve T cells following antigen engagement. Both are lost during differentiation, therefore the loss of CD27 and CD28 is associated with EM and EMRA T cells (Schmitz et al., 2003; Henson et al., 2014).

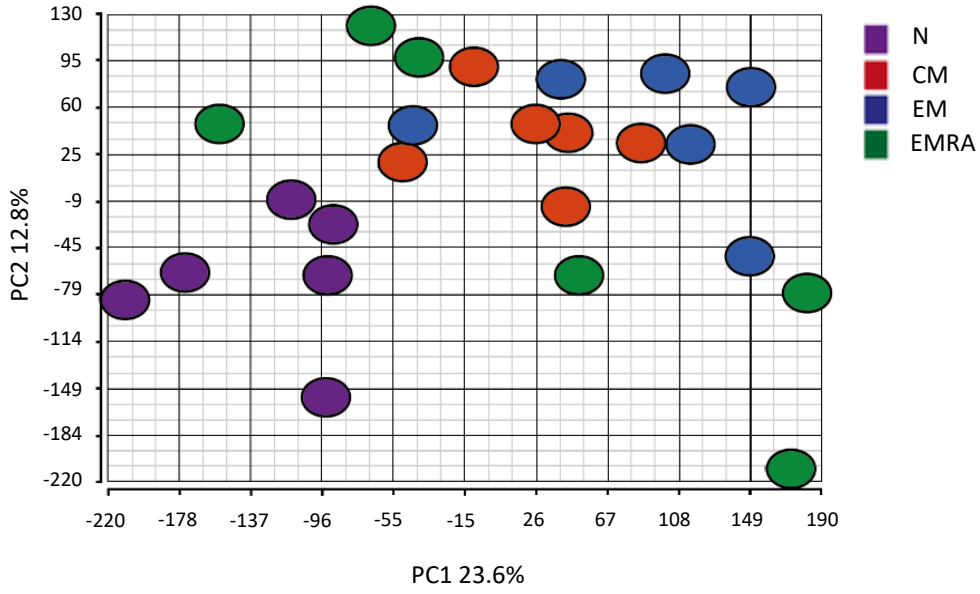

Figure 3.5: Identification of naïve-like and EM-like EMRA subsets

PCA analysis of anti-CD3 stimulated $CD8^+$ CD45RA/CD27 defined subsets ran on U113 Affymetrix human gene arrays (Data obtained from Dr. Siân Henson) (Callender, Carroll, Beal, et al., 2018).

When $CD8^+$ or $CD4^+$ T cells were gated on CD45RA/CCR7, the $CD45RA^+CCR7^-$ (EMRA) population was found to be highly heterogeneous, comprising of a N-like EMRA population expressing both CD27 and CD28 ($CD27^+CD28^+$) and a more differentiated EM-like EMRA population ($CD27^-CD28^-$) that lacked the expression of both of these markers (Figure 3.6A and C). Quantification of these two populations in individuals aged between 20 - 75 revealed that $CD8^+$ EMRA T cells were comprised predominantly of the more differentiation EM-like EMRA T cells (Figure 3.6B), whereas $CD4^+$ EMRA T cells were comprised mainly of the N-like EMRA population (Figure 3.6D).

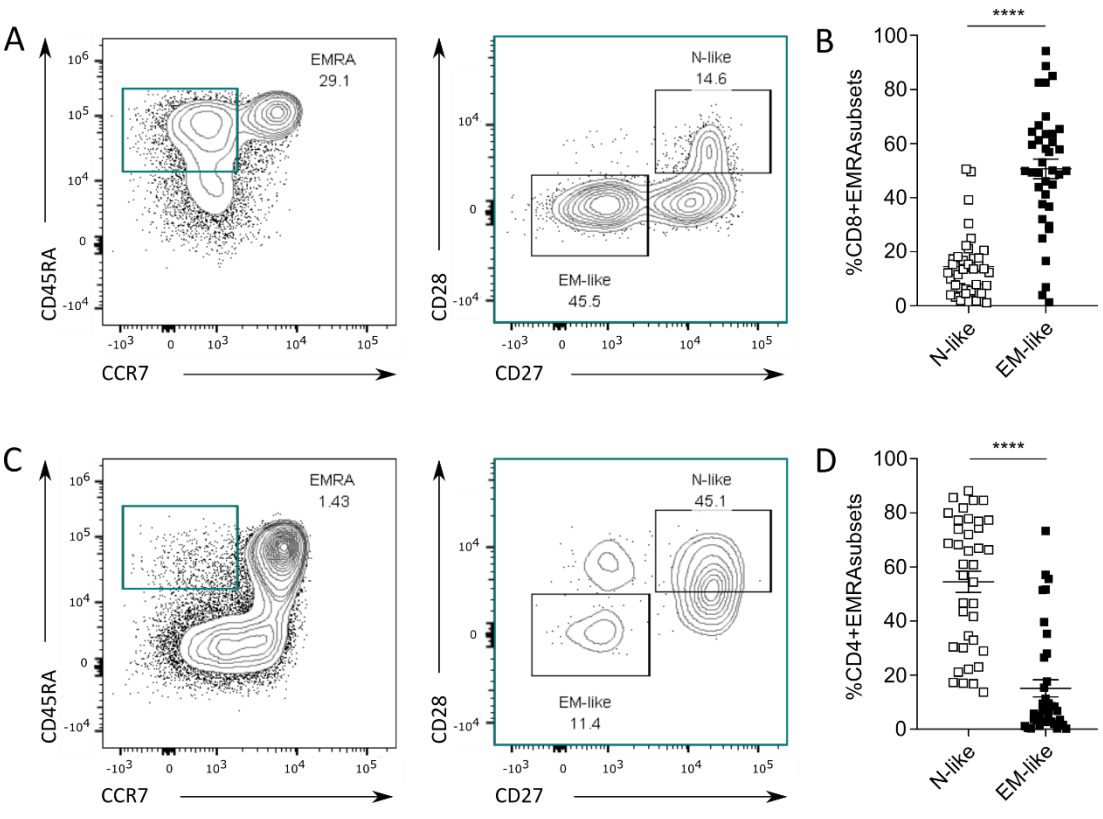

Figure 3.6: EMRA T cells are a highly heterogeneous subset

A) CD45RA/CCR7/CD27/CD28 phenotyping gating strategy on live, healthy $CD8^+$ T cells.

B) Percentage of $CD8^+$ N-like ($CD27^+CD28^+$) and EM-like ($CD27^-CD28^-$) EMRA subsets. Individuals were aged 20 – 75, with a median age of 45. Data expressed as mean ± SEM, *n* = 41. P value was determined using a paired T-test p**** = < 0.0001.

C) CD45RA/CCR7/CD27/CD28 phenotyping gating strategy on live, healthy $CD4^+$ T cells.

D) Percentage of $CD4^+$ N-like ($CD27^+CD28^+$) and EM-like ($CD27^-CD28^-$) EMRA subsets Individuals were aged 20 – 75, with a median age of 45. Data expressed as mean ± SEM, *n* = 41. P value was determined using a paired T-test p** = 0.0021.

3.4. Investigating the senescent characteristics of $CD8^+$ and $CD4^+$ T cell subsets

EMRA T cells display multiple characteristics of senescence, including high levels of DNA damage, loss of telomerase activity and low proliferative capacity (Henson et al., 2014; Di Mitri et al., 2011; Xu and Larbi, 2017). However, less is known about the senescent properties of the N-like and EM-like EMRA subsets. Therefore, various generic and T cell specific senescence markers were used to assess senescence in these subsets within both the $CD8^+$ and $CD4^+$ lineage.

3.4.1. EMRA and EM-like EMRA T cells have elevated p-p53

The transcriptional regulator p53 plays a vital role in the induction of senescence (Rufini et al., 2013). Therefore, intracellular staining of phosphorylated-p53 (p-p53) was carried out on PBMCs isolated from individuals aged 24 – 44 directly *ex-vivo*. As expected, $CD8^+$ EMRA T cells were found to have the highest levels of p-p53 (Figure 3.7A). Furthermore, the EM-like EMRA subset had significantly more p-p53 than the N-like EMRA subset (Figure 3.7B).

Naïve $CD4^+$ T cells were found to have the least amount of p-p53 (Figure 3.8A). The difference in p-p53 levels between the three memory populations followed the same trend as the $CD8^+$ T cells, with the $CD4^+$ EMRA T cells expressing the most p-p53. However, the differences were more pronounced than in the $CD8^+$ T cell lineage (Figure 3.8A). The $CD4^+$ EM-like EMRA subset also expressed high levels of p-p53; whereas, the p-p53 levels in the N-like EMRA subset were more comparable to the low levels observed in the true naïve $CD4^+$ T cells (Figure 3.8B).

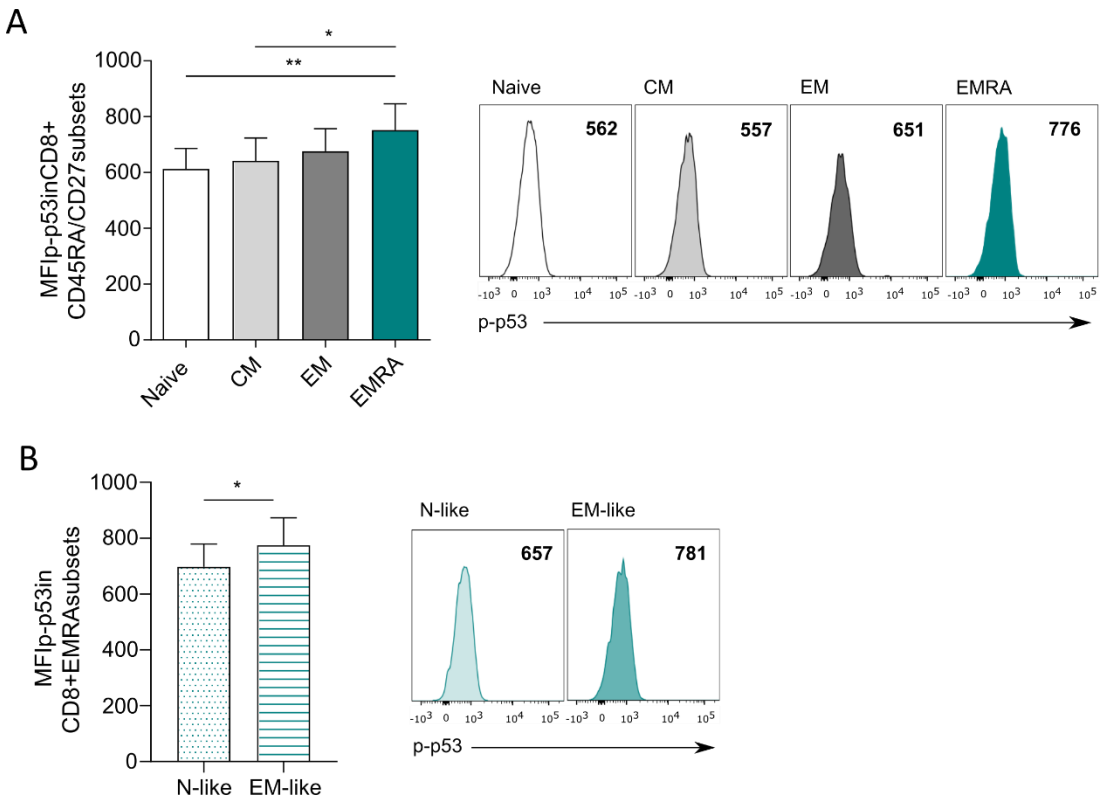

Figure 3.7: Levels of p-p53 in $CD8^+$ T cell subsets

A) MFI of p-p53 in $CD8^+$ CD45RA/CD27 defined subsets. Individuals were aged 24 – 44, with a median age of 28. Data expressed as mean ± SEM, *n* = 25. P values were determined using a repeated measures ANOVA with Tukey's multiple comparisons test p* = 0.0134 and p** = 0.0022.

B) MFI of p-p53 in $CD8^+$ N-like ($CD27^+CD28^+$) and EM-like ($CD27^-CD28^-$) EMRA subsets. Individuals were aged 24 – 44, with a median age of 28. Data expressed as mean ± SEM, *n* = 25. P value was determined using a paired T-test p* = 0.0294.

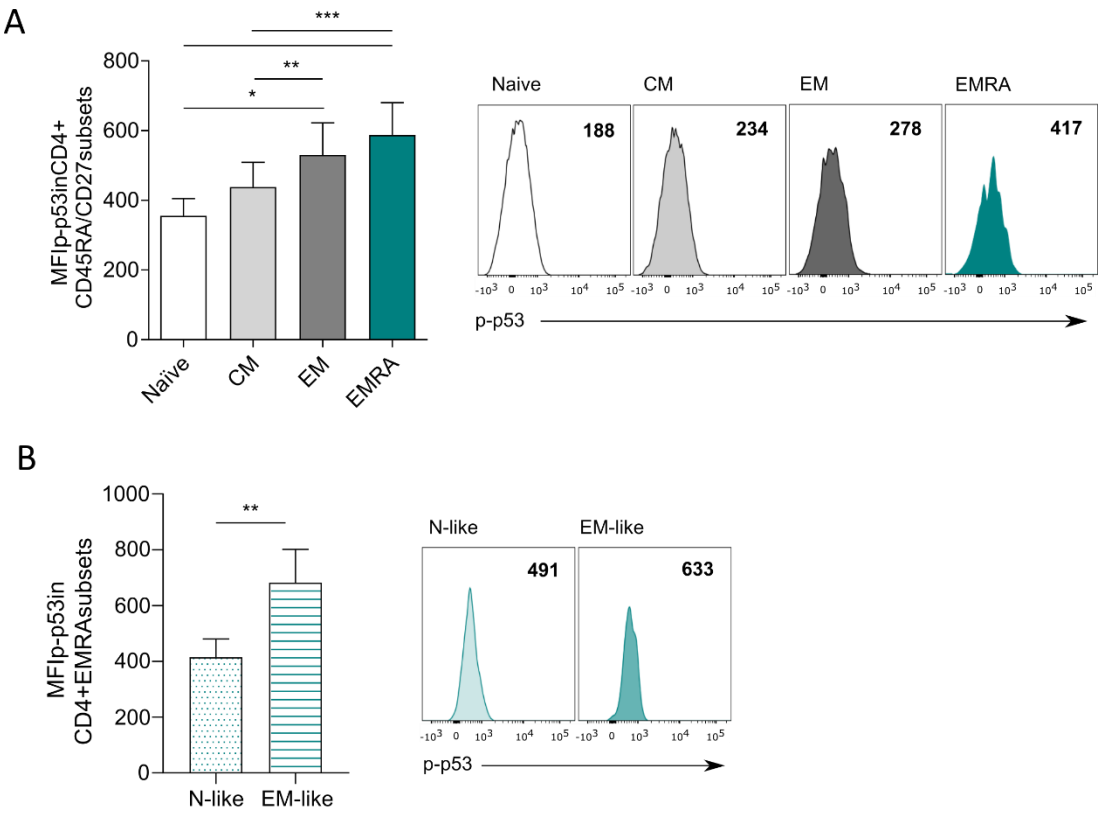

Figure 3.8: Levels of p-p53 in $CD4^+$ T cell subsets

A) MFI of p-p53 in $CD4^+$ CD45RA/CD27 defined subsets. Individuals were aged 24 – 44, with a median age of 28. Data expressed as mean ± SEM, *n* = 25. P values were determined using a repeated measures ANOVA with Tukey's multiple comparisons test p* = 0.0139, p** =0.0046 and p*** = < 0.0001.

B) MFI of p-p53 in $CD4^+$ N-like ($CD27^+CD28^+$) and EM-like ($CD27^-CD28^-$) EMRA subsets. Individuals were aged 24 – 44, with a median age of 28. Data expressed as mean ± SEM, *n* = 25. P value was determined using a paired T-test p** = 0.0058.

3.4.2. $CD8^+$ and $CD4^+$ EMRA T cells exhibit opposing proliferative capacity

Loss of proliferative capacity is another key feature of senescent cells. Ki-67 is a nuclear protein that is present during all phases of the cell cycle. Its expression is believed to be a requirement for the progression of cell division; therefore, it is an excellent marker of proliferation (Gerdes et al., 1991). Intracellular staining of Ki-67 was performed on PBMCs from individuals aged 24 – 64 directly *ex vivo*. Ki-67 levels were lowest in the $CD8^+$ naïve T cells (Figure 3.9A) and the highest in the EM T cells. The $CD8^+$ CM and EMRA subsets had similar levels of Ki-67, indicating a lower rate of proliferation in these memory subsets when compared with the EM subset. Further stratification of the $CD8^+$ EMRA cells revealed that both N-like and EM-like EMRA subsets also had relatively low Ki-67 levels (Figure 3.9B).

Intracellular Ki-67 levels were the lowest in the $CD4^+$ naïve T cell subset and $CD4^+$ CM and EM T cells had significantly higher levels of Ki-67 than the naïve subset (Figure 3.10A). In contrast to $CD8^+$ EMRA T cells, $CD4^+$ EMRA T cells had the highest levels of Ki-67, however this was not found to be statistically significantly when compared to any of the other subsets, most likely due to the large variation in the data set (Figure 3.10A) and also reflects the heterogeneity of the $CD4^+$ EMRA subset. Interestingly, Ki-67 levels found in the $CD4^+$ EM-like EMRA subset were significantly higher than the N-like EMRA subset (Figure 3.10B).

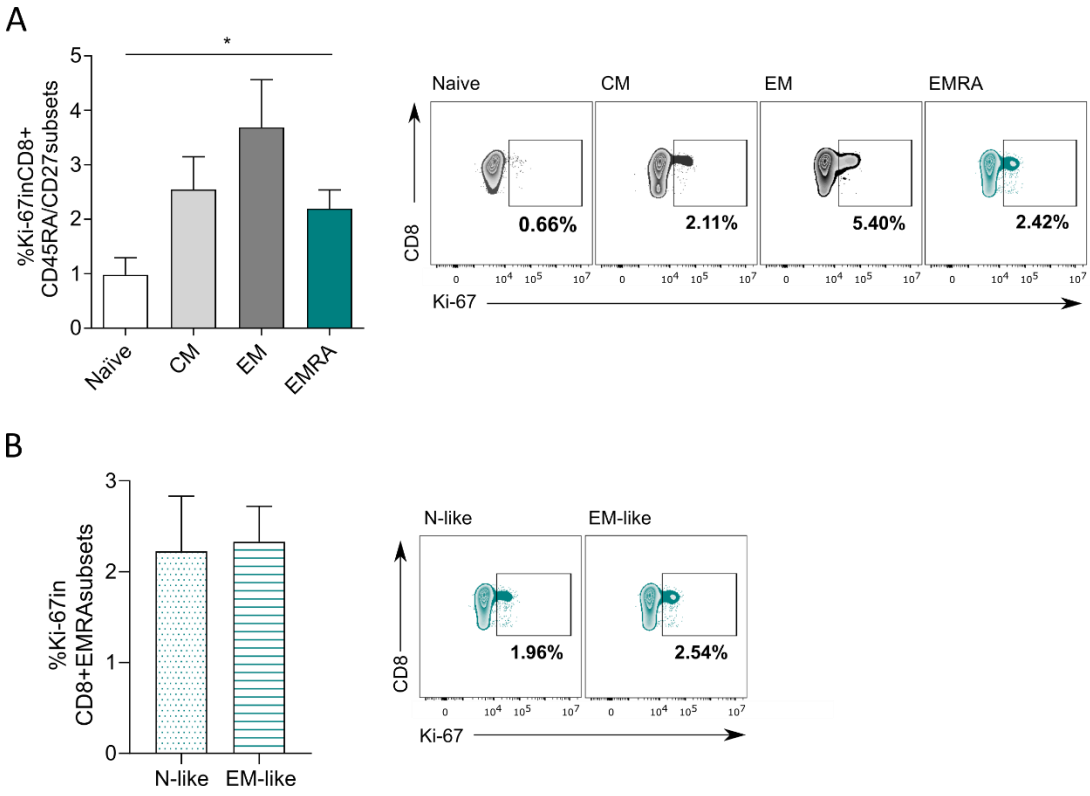

Figure 3.9: Levels of Ki-67 in $CD8^+$ T cell subsets

A) Percentage of Ki-67 in $CD8^+$ CD45RA/CD27 defined subsets. Individuals were aged 24 – 64, with a median age of 27. Data expressed as mean ± SEM, *n* = 14. P values were determined using a repeated measures ANOVA with Tukey's multiple comparisons test p* = 0.0364.

B) Percentage of Ki-67 in $CD8^+$ N-like ($CD27^+CD28^+$) and EM-like ($CD27^-CD28^-$) EMRA subsets. Individuals were aged 24 – 64, with a median age of 27. Data expressed as mean ± SEM, *n* = 14.

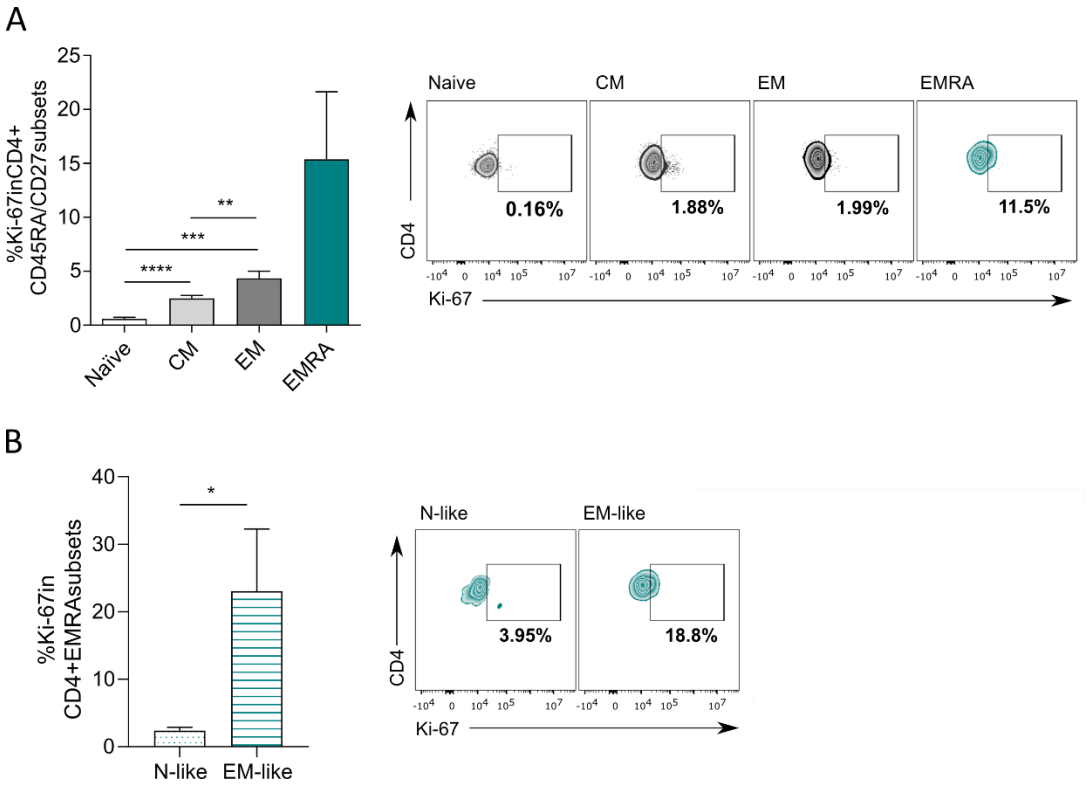

Figure 3.10: Levels of Ki-67 in CD4$^+$ T cell subsets

A) Percentage of Ki-67 in CD4$^+$ CD45RA/CD27 defined subsets. Individuals were aged 24 – 64, with a median age of 27. Data expressed as mean ± SEM, *n* = 14. P values were determined using a repeated measures ANOVA with Tukey's multiple comparisons test p** = 0.0074, p*** = 0.0003 and p**** = <0.0001.

B) Percentage of Ki-67 in CD4$^+$ N-like (CD27$^+$CD28$^+$) and EM-like (CD27$^-$CD28$^-$) EMRA subsets. Individuals were aged 24 – 64, with a median age of 27. Data expressed as mean ± SEM, *n* = 14. P value was determined using a paired T-test p* = 0.0387.

3.4.3. N-like EMRA T cells are not truly naïve

The killer cell lectin-like receptor G1 (KLRG1) is upregulated on antigen-experienced T cells (Henson et al., 2009; Voehringer et al., 2002). Consequently, KLRG1 is a good indicator of antigen experience and a widely used marker of T cell senescence. Examination of $CD8^+$ T cells from individuals aged 25 – 73 directly *ex vivo* revealed that KLRG1 levels were low on $CD8^+$ naïve T cells but dramatically increased with memory development. However, no difference between the EM and EMRA memory populations was found (Figure 3.11A). Both $CD8^+$ N-like and EM-like EMRA subsets expressed high levels of KLRG1; however, the EM-like EMRA KLRG1 levels were more comparable to that of the whole $CD8^+$ EMRA T cell subset, suggesting that this is the more differentiated subset of the two (Figure 3.11B). KLRG1 levels in the $CD8^+$ T cell compartment were significantly correlated with age (Figure 3.11C). Stratifying this correlation by subset revealed that this was due to an increase in KLRG1 in the naïve subset, as the three memory subsets showed no correlation with age (Figure 3.12).

KLRG1 levels differed significantly between all $CD4^+$ T cell subsets, with $CD4^+$ naïve T cells expressing the least and $CD4^+$ EMRA T cells expressing the most (Figure 3.13A). A significant difference was also observed between the N-like and EM-like EMRA subsets, with the EM-like EMRA cells expressing levels comparable to that of the whole $CD4^+$ EMRA T cell subset (Figure 3.13B). KLRG1 levels in the $CD4^+$ T cell compartment were significantly correlated with age (Figure 3.13C). Stratifying this correlation by subset revealed that KLRG1 levels increase with age in the naïve, EM and EMRA $CD4^+$ T cell subsets (Figure 3.14).

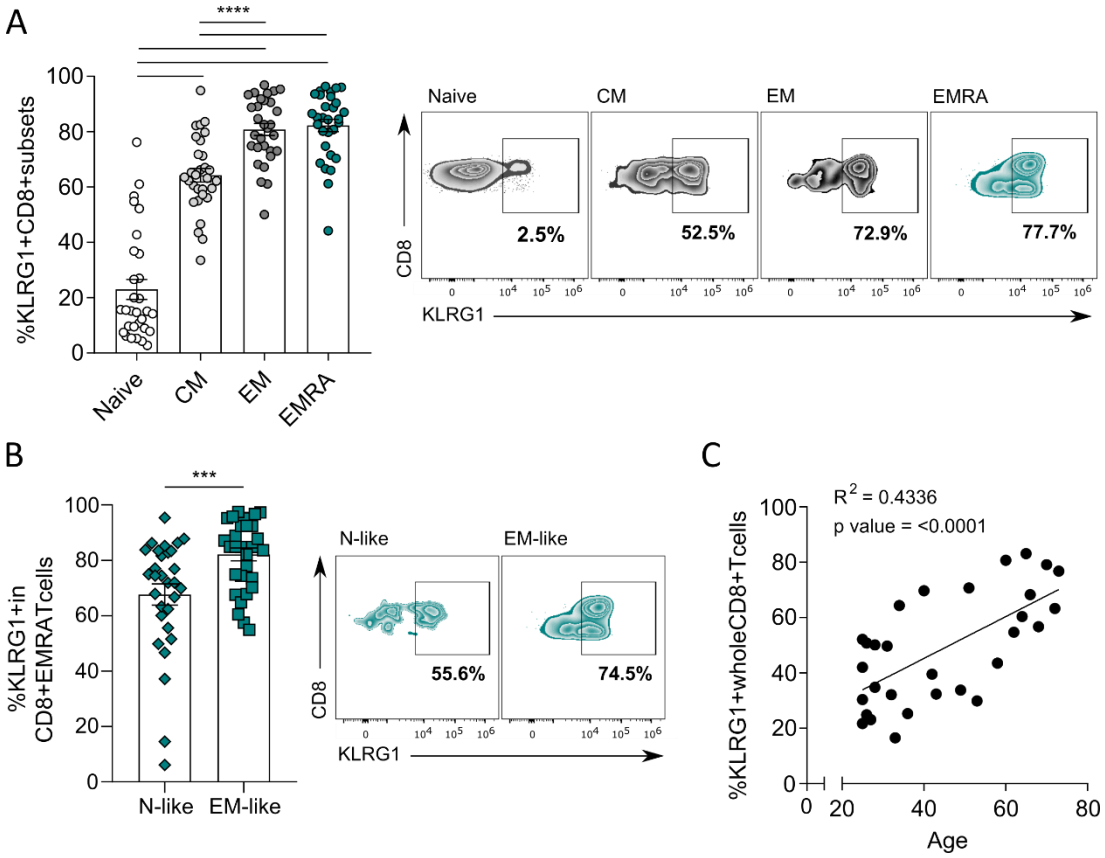

Figure 3.11: Levels of KLRG1 in CD8$^+$ T cell subsets

A) Percentage of KLRG1 in CD8$^+$ CD45RA/CD27 defined subsets with representative flow cytometry plots. Individuals were aged 25 – 73, with a median age of 32. Data expressed as mean ± SEM, *n* = 30. P values were determined using a repeated measures ANOVA with Tukey's multiple comparisons test, p**** = <0.0001.

B) Percentage of KLRG1 in CD8$^+$ N-like (CD27$^+$CD28$^+$) and EM-like (CD27$^-$CD28$^-$) EMRA subsets with representative flow cytometry plots. Individuals were aged 25 – 73, with a median age of 32. Data expressed as mean ± SEM, *n* = 30. P value was determined using a paired T-test p*** = 0.0004.

C) Age related changes to the percentage of KRLG1 in whole CD8$^+$ T cells. The line of best fit was generated using linear regression, *n* = 30.

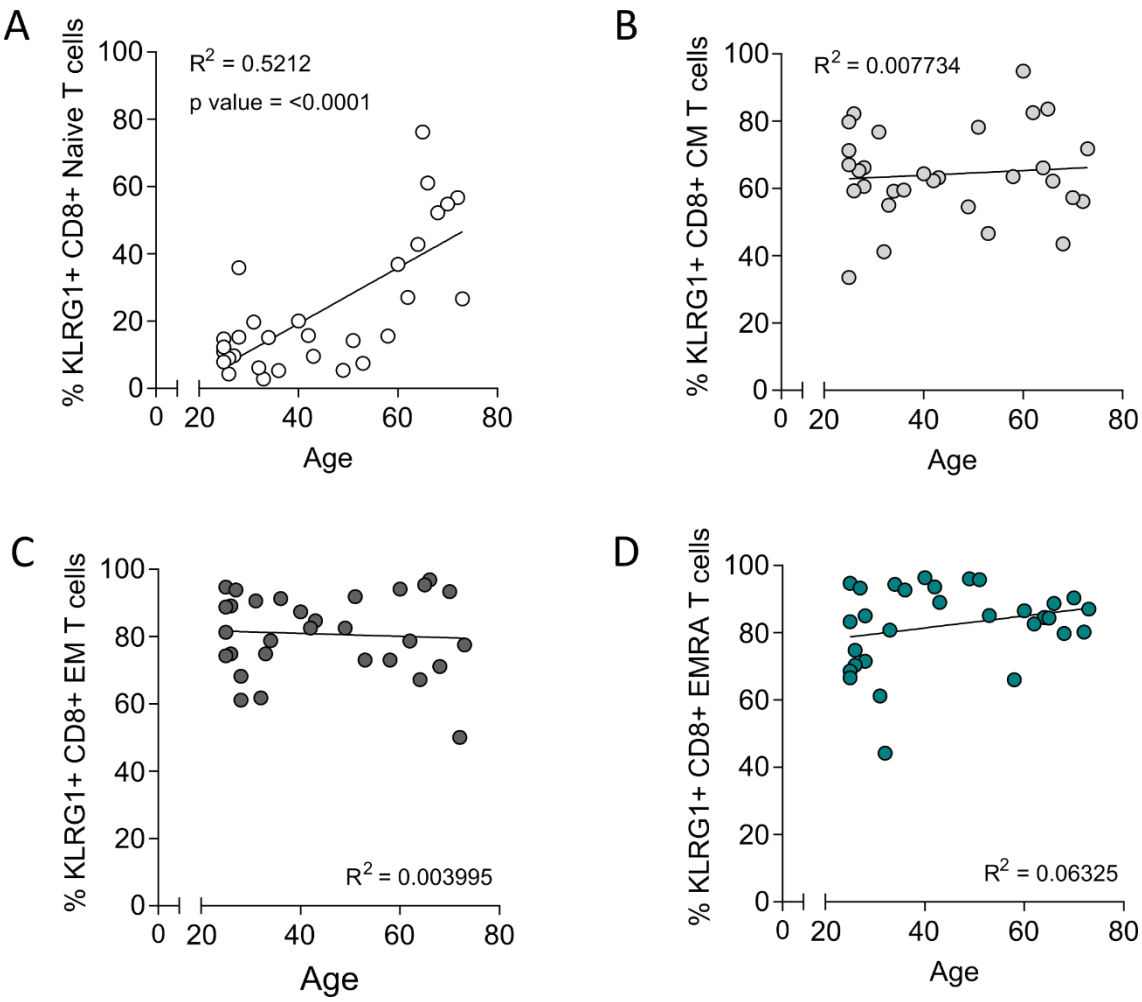

Figure 3.12: Age related changes to the percentage of KRLG1 in $CD8^+$ T cell subsets

Percentage of KLRG1 in A) Naïve, B) CM, C) EM and D) EMRA $CD8^+$ T subsets. The line of best fit generated using linear regression, *n* = 30.

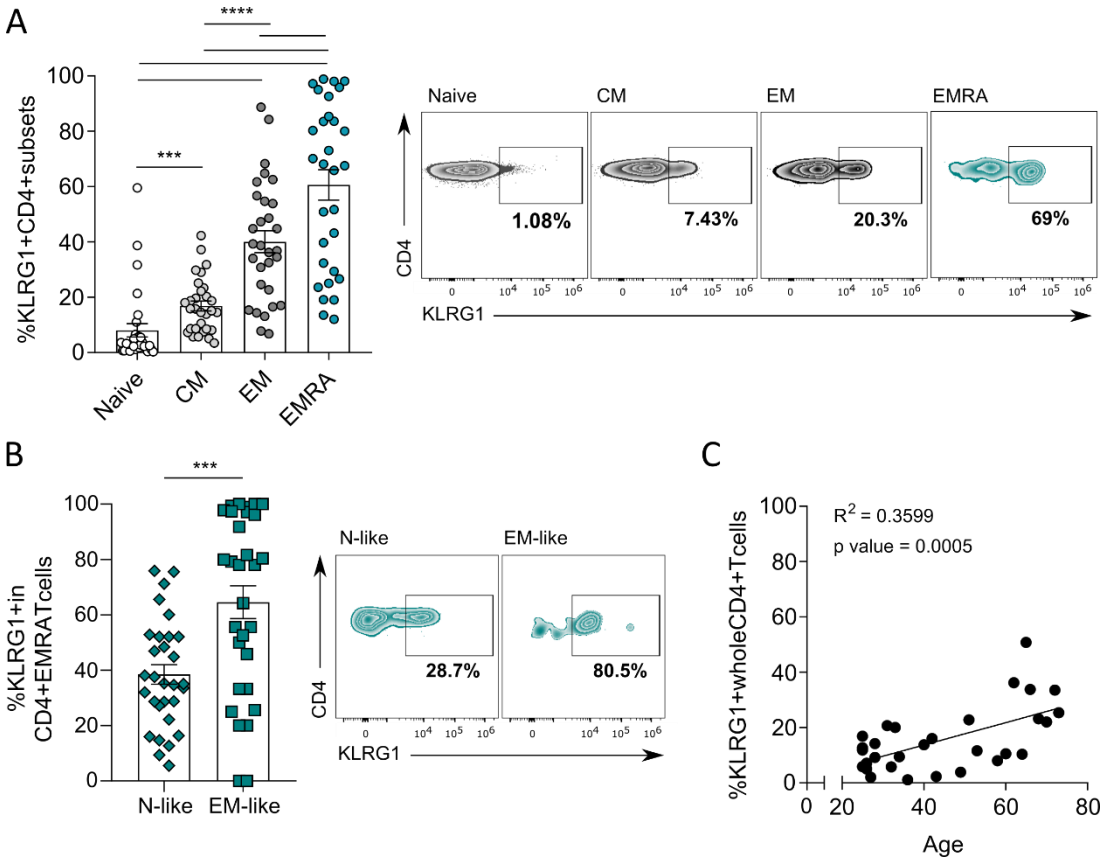

Figure 3.13: Levels of KLRG1 in CD4⁺ T cell subsets

A) Percentage of KLRG1 in CD4+ CD45RA/CD27 defined subsets with representative flow cytometry plots. Individuals were aged 25 – 73, with a median age of 32. Data expressed as mean ± SEM, *n* = 30. P values were determined using a repeated measures ANOVA with Tukey's multiple comparisons test, p*** = 0.0007, p**** = <0.0001.

B) Percentage of KLRG1 in CD4⁺ N-like ($CD27^+CD28^+$) and EM-like ($CD27^-CD28^-$) EMRA subsets with representative flow cytometry plots. Individuals were aged 25 – 73, with a median age of 32. Data expressed as mean ± SEM, *n* = 30. P value was determined using a paired T-test p*** = 0.0001.

C) Age related changes to the percentage of KRLG1 in whole CD4⁺ T cells. Line of best fit generated using linear regression, *n* = 30.

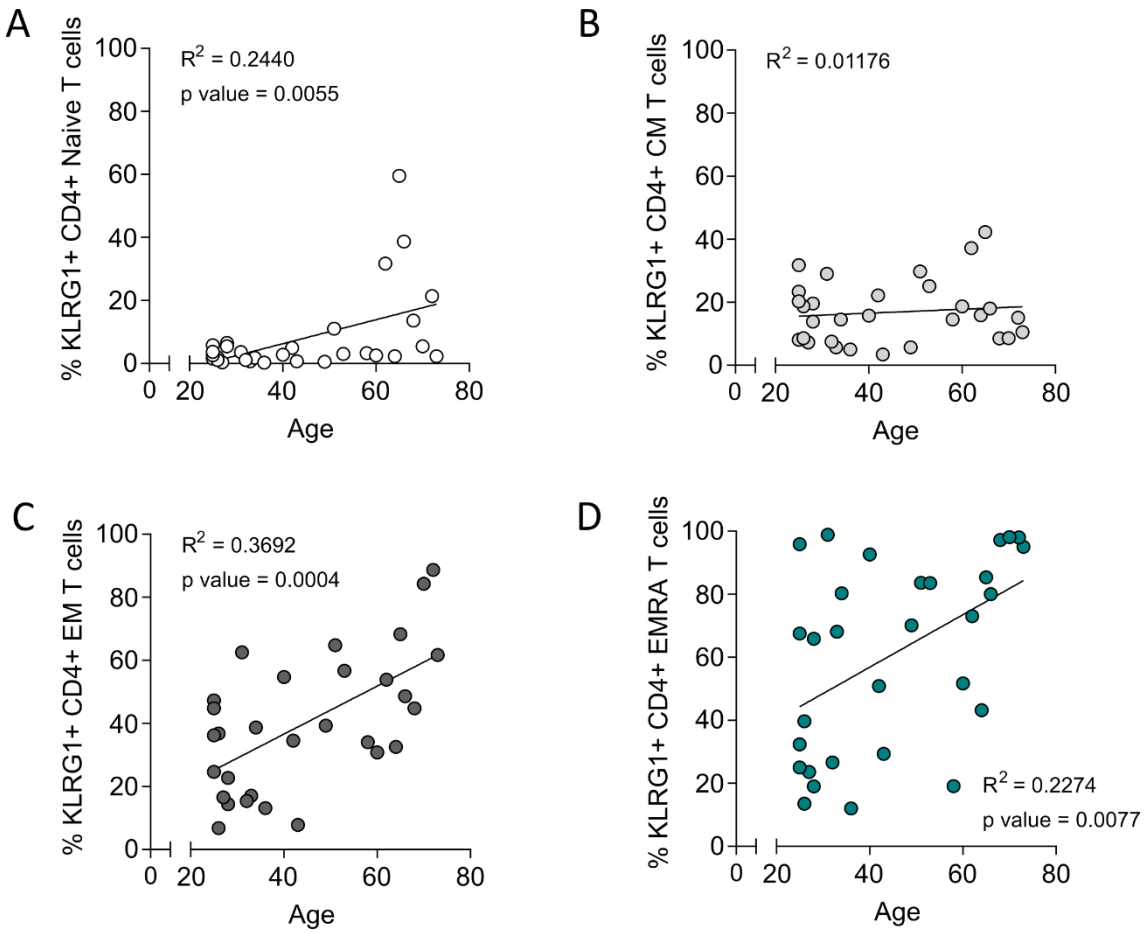

Figure 3.14: Age related changes to the percentage of KRLG1 in $CD4^+$ T cell subsets

Percentage of KLRG1 in A) Naïve, B) CM, C) EM and D) EMRA $CD4^+$ T subsets. Line of best fit generated using linear regression, *n* = 30.

3.4.4. N-like EMRA T cells are distinct from replicative T cell senescence

CD57 is another inhibitory receptor that is upregulated in response to persistent viral infections and therefore is widely associated with replicative senescence in T cells (Bandrés et al., 2000; Brenchley et al., 2003; Sze et al., 2001; Weekes et al., 1999). Examination of $CD8^+$ T cells from individuals aged 25 – 74 directly *ex vivo* revealed that naïve and CM $CD8^+$ T cells expressed very low levels of CD57 when compared with EM and EMRA T cells (Figure 3.15A). $CD8^+$ EM-like EMRA T cells had significantly higher levels of CD57 when compared with the N-like subset (Figure 3.15B). Furthermore, CD57 levels in $CD8^+$ T cells were positively correlated with age (Figure 3.15C). When these age-related changes were stratified by subset the $CD8^+$ naïve T cells were found to increase significantly with age, and although not statistically significant the $CD8^+$ EMRA T cells also showed a positive trend towards increased CD57 with age (Figure 3.16).

$CD4^+$ EMRA T cells expressed significantly more CD57 than all other subsets (Figure 3.17A). Furthermore, the $CD4^+$ EM-like EMRA T cells expressed significantly more CD57 than the N-like subset (Figure 3.17B). Similar to what was observed in the $CD8^+$ compartment, CD57 levels in whole $CD4^+$ T cells were significantly correlated with age (Figure 3.17C). Surprisingly, stratifying these changes by subset revealed no significant correlation; however, $CD4^+$ EM and EMRA T cells did show a positive trend towards increased CD57 with age (Figure 3.18).

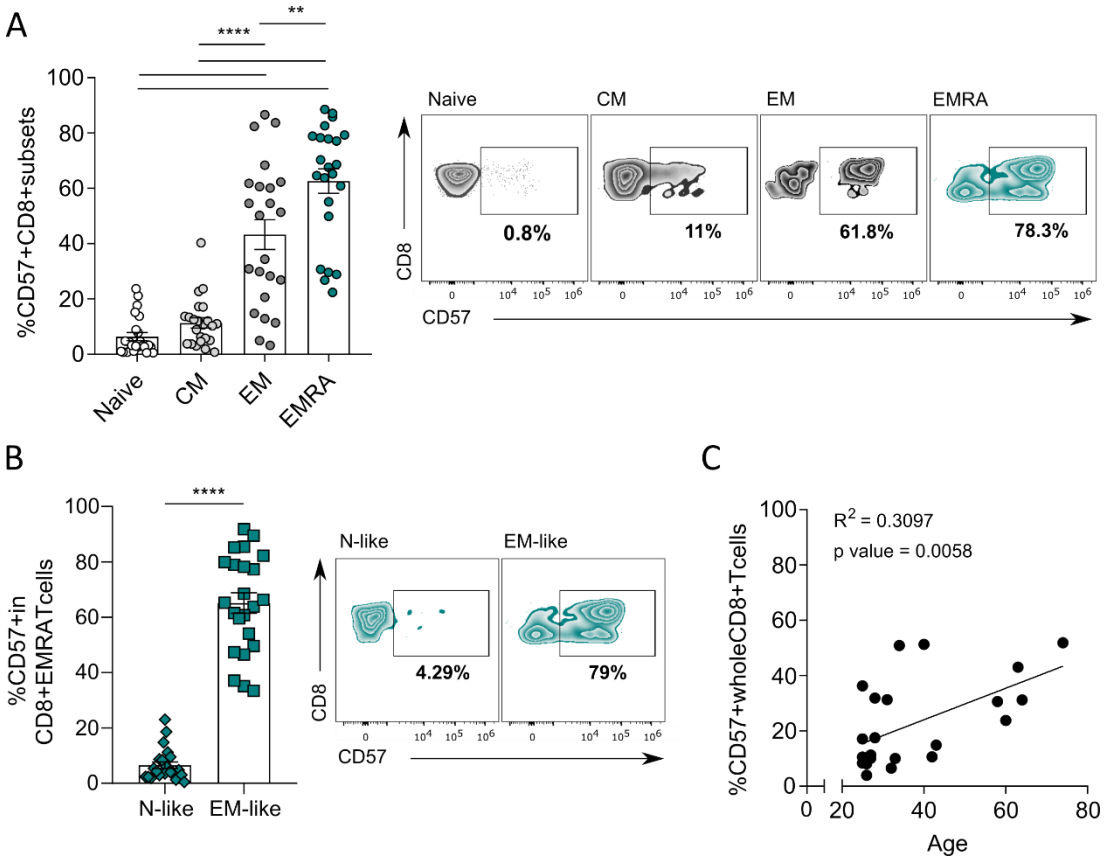

Figure 3.15: Levels of CD57 in CD8⁺ T cell subsets

A) Percentage of CD57 in CD8⁺ CD45RA/CD27 defined subsets with representative flow cytometry plots. Individuals were aged 25 – 74, with a median age of 31. Data expressed as mean ± SEM, *n* = 23. P values were determined using a repeated measures ANOVA with Tukey's multiple comparisons test, p** = 0.0016, p**** = <0.0001.

B) Percentage of CD57 in CD8⁺ N-like ($CD27^+CD28^+$) and EM-like ($CD27^-CD28^-$) EMRA subsets with representative flow cytometry plots. Individuals were aged 25 – 74, with a median age of 31. Data expressed as mean ± SEM, *n* = 23. P value was determined using a paired T-test p**** = <0.0001.

C) Age related changes to the percentage of CD57 in whole CD8⁺ T cells. Line of best fit generated using linear regression, *n* = 23.

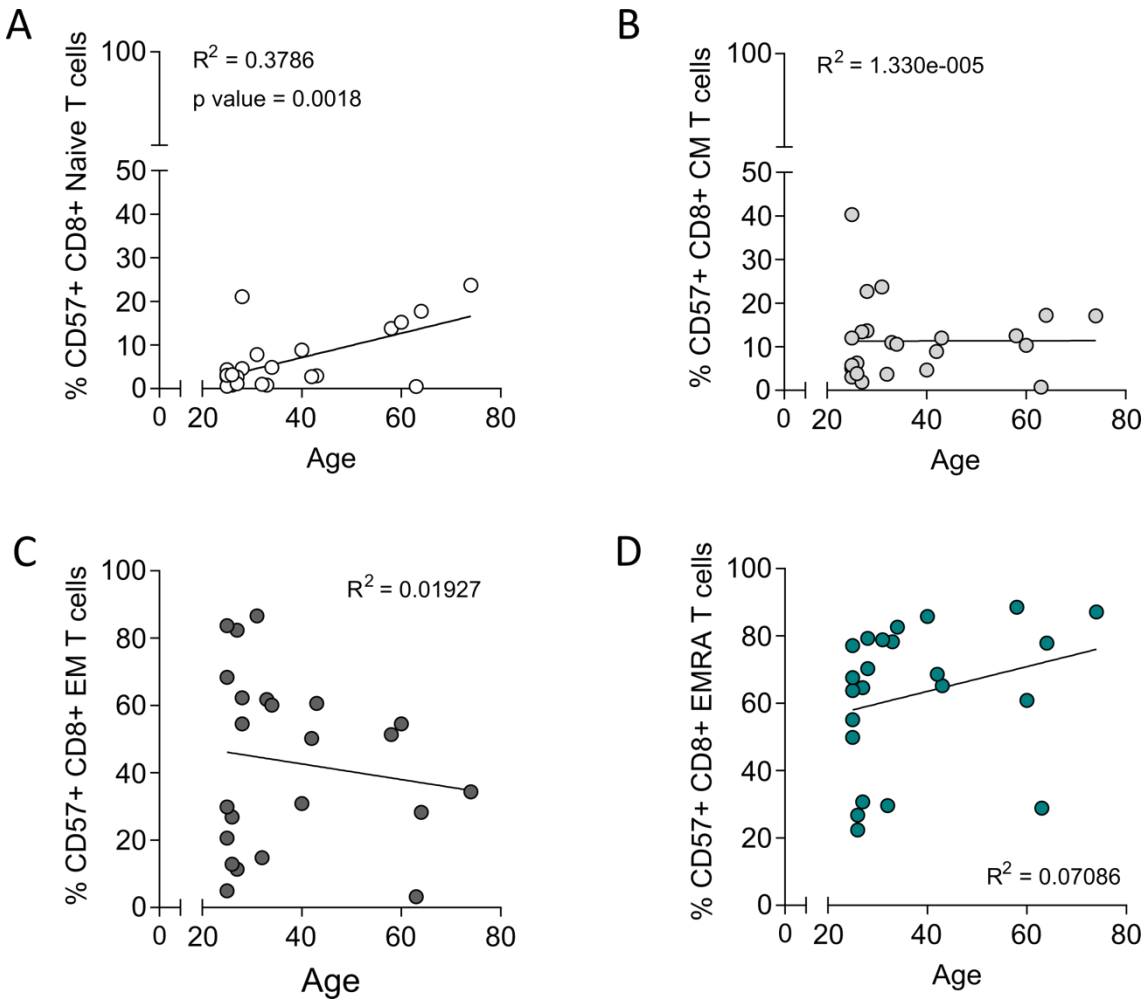

Figure 3.16: Age related changes to the percentage of CD57 in $CD8^+$ T cell subsets

Percentage of KLRG1 in A) Naïve, B) CM, C) EM and D) EMRA $CD8^+$ T subsets. Line of best fit generated using linear regression, *n* = 23.

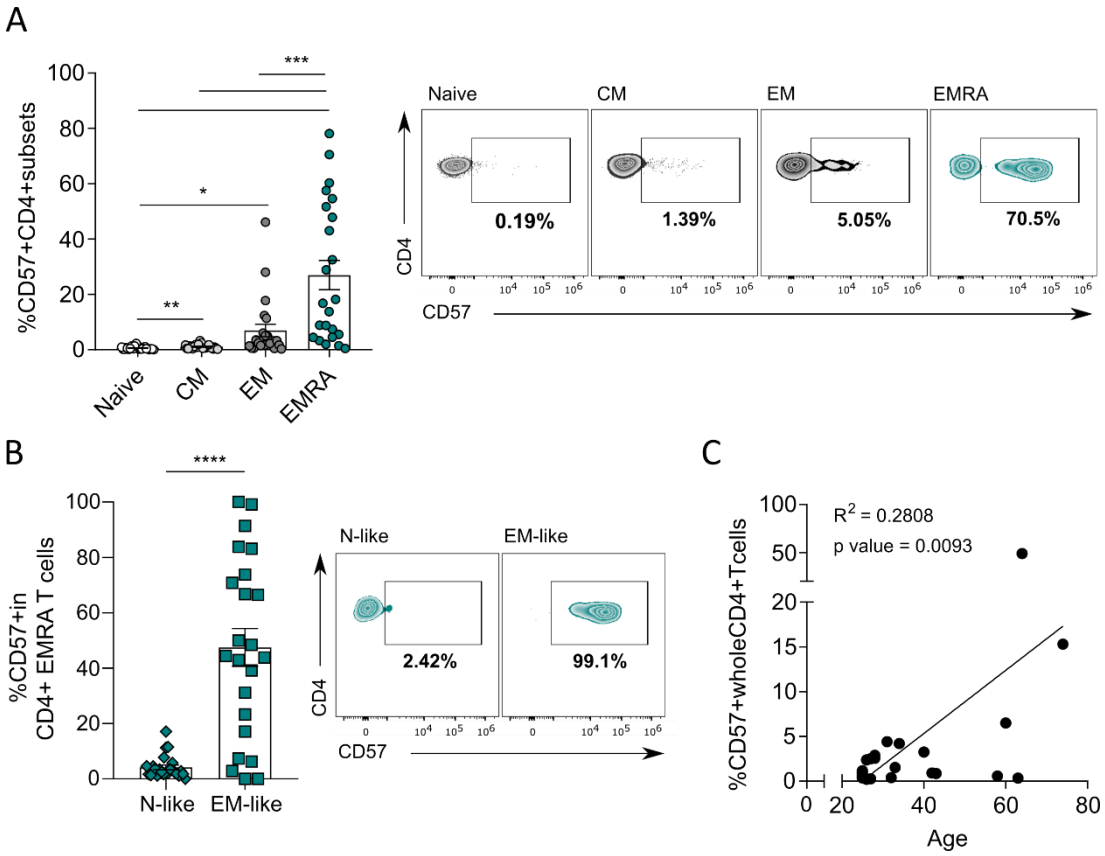

Figure 3.17: Levels of CD57 in $CD4^+$ T cell subsets

A) Percentage of CD57 in CD4+ CD45RA/CD27 defined subsets with representative flow cytometry plots. Individuals were aged 25 – 74, with a median age of 31. Data expressed as mean ± SEM, *n* = 23. P values were determined using a repeated measures ANOVA with Tukey's multiple comparisons test, p* = 0.0419, p** = 0.0041, p*** = <0.001.

B) Percentage of CD57 in $CD4^+$ N-like ($CD27^+CD28^+$) and EM-like ($CD27^-CD28^-$) EMRA subsets with representative flow cytometry plots. Individuals were aged 25 – 74, with a median age of 31. Data expressed as mean ± SEM, *n* = 23. P value was determined using a paired T-test p**** = <0.0001.

C) Age related changes to the percentage of CD57 in whole $CD4^+$ T cells. Line of best fit generated using linear regression, *n* = 23.

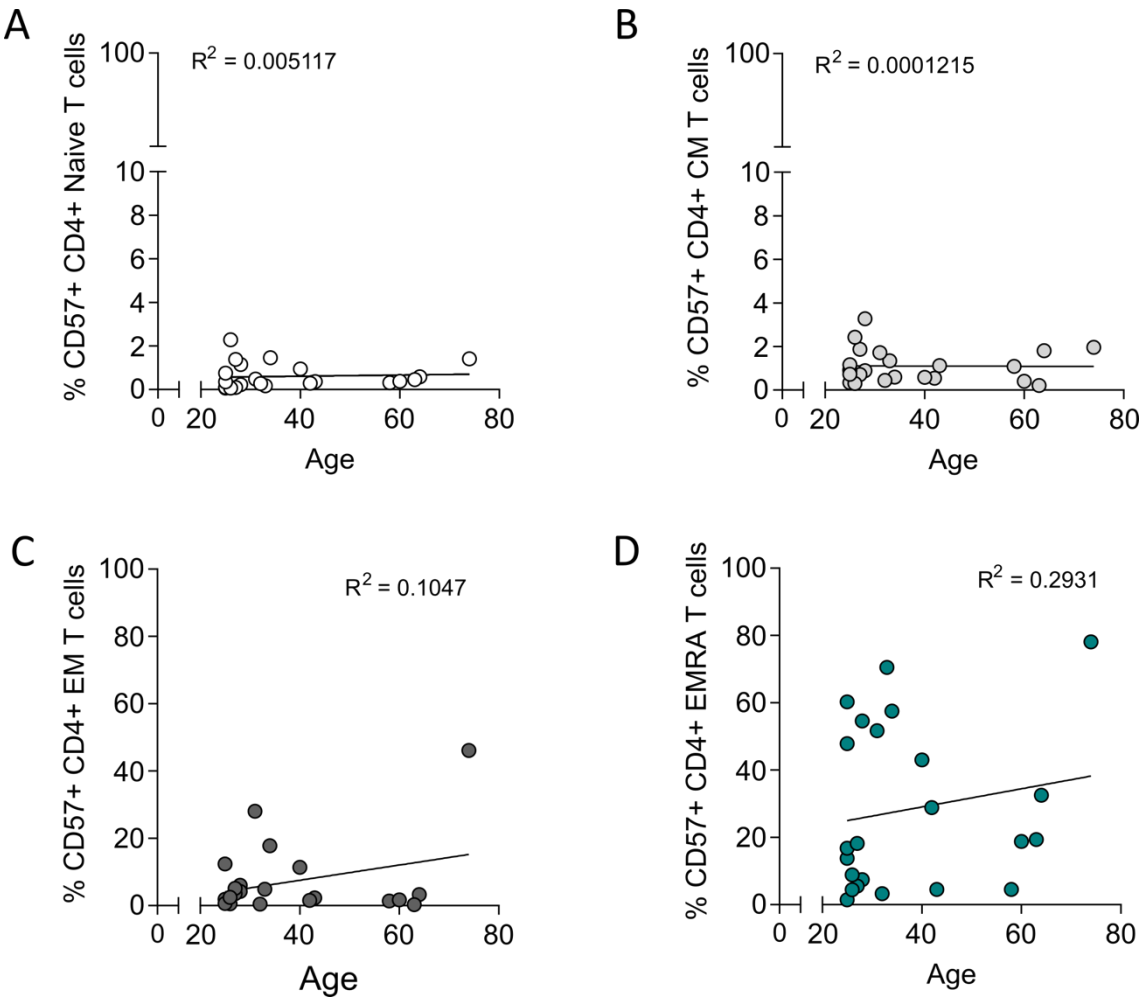

Figure 3.18: Age related changes to the percentage of CD57 in $CD4^+$ T cell subsets

Percentage of CD57 in A) Naïve, B) CM, C) EM and D) EMRA $CD4^+$ T subsets. Line of best fit generated using linear regression, *n* = 23.

3.5 Discussion

It has been well document that age significantly impacts the $CD8^+$ T cell compartment (Chou and Effros, 2013). Data presented in this chapter confirms this, as age was shown to result in both a significant decrease in naïve $CD8^+$ T cells and an increase in $CD8^+$ EMRA T cells. Although less dramatic, a similar observation was made in the $CD4^+$ lineage. This shift from naïve T cell output to the accumulation of terminally differentiated EMRA T cells significantly narrows the diversity of the TCR repertoire. Consequently this contributes to many age-related problems such as the inability to respond to new and emerging diseases (Naylor et al., 2005). What has been less documented is the existence of multiple different senescent T cell populations. Heterogeneity within memory subsets has been documented previously (Henson et al., 2015; Pulko et al., 2016). For example, a $CD8^+$ memory population with a naïve-like phenotype ($CCR7^+CD45RA^+CD28^{int}CD95^{lo}$), long telomeres, and the ability to response to persistent viral infections, has previously been found to increase during ageing (Pulko et al., 2016). Data presented in this chapter focused on the diverse nature of a more terminally differentiated population of $CCR7^-CD45RA^+$ EMRA T cells. Both the $CD8^+$ and $CD4^+$ EMRA subsets were found to be highly heterogenic populations, which displayed characteristic of either naïve or effector memory cells, and were consequently termed N-like and EM-like subsets respectively (Callender, Carroll, Beal, et al., 2018).

To become terminally differentiated it is assumed that T cells must first undergo multiple rounds of antigen stimulation. In essence, repeat stimulation of T cells

results in multiple rounds of extensive proliferation, which eventually drives T cells into a replicatively driven senescence state (Chou and Effros, 2013). However, we know from fibroblasts that senescence can be triggered via many routes, such as oxidative or oncogenic stress (Richter and Zglinicki, 2007; Serrano et al., 1997; Zhu et al., 1998), and as such, the phenotypic properties of these cells are also likely to differ.

In order to characterise the senescent properties of N-like and EM-like EMRA T cells p-p53, Ki-67, KLRG1 and CD57 were used. The phenotype of these subsets differed slightly depending on the T cell lineage; however, both $CD8^+$ and $CD4^+$ N-like EMRA T cells displayed less characteristics of senescence, as they exhibited lower p-p53, KLRG1 and CD57 than the EM-like subset. Despite having lower KLRG1 levels than the EM-EMRA, the amount of KLRG1 present on the N-like EMRAs were still high and exceeded the levels of KLRG1 present on the true naïve and CM subsets. Conversely, CD57 was virtually absent on both $CD8^+$ and $CD4^+$ N-like EMRAs. This discrepancy is interesting as both KLRG1 and CD57 are often used as markers of viral specific T cells and thought to indicate replicative senescence. However, as we have shown here, although KLRG1 and CD57 expression often correlates, the two receptors are not mutually exclusive. The simultaneous expression of KLRG1 and CD57 has been previously proposed to define truly terminally differentiated cells at a more advantaged stage of senescence (Ibegbu et al., 2006). Consequently, we conclude that EM-like EMRAs ($KLRG1^+CD57^+$) arise due to replicative senescence, whereas N-

like EMRAs ($KLRG1^{+}CD57^{-}$) are a less differentiated subset generated via premature senescence.

Both $CD8^{+}$ and $CD4^{+}$ naïve T cells began to express KLRG1 with age. This observation mirrors what has been previously shown in $CD27^{+}CD28^{+}$-defined $CD8^{+}$ naïve T cells (Henson et al., 2009). Similar phenomena have been previously documented; for example, $CD4^{+}$ naive T cells have been shown to proliferate and acquire a memory-like phenotype under lymphopenic conditions (Min et al., 2003). Interestingly, when the naïve T cell pool is significantly depleted, certain memory T cells can acquire naïve-like qualities such as responding to *de novo* infections. This has been demonstrated in influenza-naïve aged mice, where the response to a new influenza infection was largely mediated by a population of cross-reactive virtual memory (VM) $CD8^{+}$ T cells (Lanzer et al., 2018). VM T cells are distinct from true memory cells as they are generated in the absence of antigen (Cheung et al., 2009; Haluszczak et al., 2009; White et al., 2016). Although these VM populations have been observed in mice, a similar population may also be generated in humans. Collectively, these studies suggest that age can trigger naïve T cells to become memory-like even in the absence of antigen activation. However, in the event of a *de novo* infection, some memory-like naïve cells may still be able to carry out their true naïve T cell functions.

In this chapter, not only was there a reduction in the naïve T cell output in older individuals, but the naïve T cells that remained did not appear truly naïve. Over time these naïve T cells may accumulate more memory-like qualities and eventually be

pushed by additional cellular stresses into a prematurely arrested senescent phenotype such as the N-like EMRAs. Unlike their EM-like counterparts, these cells may be better able to respond to infections and carry out effector function.

Despite both being heterogenic, the proportion of N-like and EM-like EMRA T cells differed between the $CD4^+$ and $CD8^+$ T cell compartments. $CD8^+$ EMRAs showed a tendency to be more EM-like, whereas $CD4^+$ EMRAs were more N-like. These differences along with the well established observation that $CD4^+$ EMRA T cells are far rarer than their $CD8^+$ counterparts highlight the need for further investigation into the inherent differences between $CD4^+$ and $CD8^+$ T cells when it comes to the induction of senescence. This line of inquiry is continued in the next chapter.

In conclusion, this chapter revealed the existence of two distinct EMRA T cell populations – one that is generated by replicative senescence and the other by a telomere-independent mechanism. Overall, this chapter highlights the phenotypic plasticity of T cells and therefore challenges the traditional notion that T cell differentiation is a unidirectional and linear process.

Chapter four: Lineage commitment determines the extent of T cell senescence

4.1. Introduction

One of the most striking observations in the field of senescent T cell research and in the data presented in the previous chapter is how the $CD8^+$ and $CD4^+$ compartments have different susceptibilities to senescence. $CD8^+$ T cells are far more susceptible to both phenotypic and functional changes during ageing (Czesnikiewicz-Guzik et al., 2008; Goronzy et al., 2007). Furthermore, the $CD8^+$ EMRA T cell subset accumulates in higher proportions with age and are more prevalent following *in vitro* culture than $CD4^+$ EMRA T cells (Czesnikiewicz-Guzik et al., 2008). The cause of this difference has been previously attributed to the differing homeostatic mechanisms among the two lineages and to the increased gene expression instability of regulatory cell surface molecules in the $CD8^+$ EMRA subset (Czesnikiewicz-Guzik et al., 2008). However, a more robust examination into the mechanisms behind these differences has not yet been conducted.

4.1.1. Aim

The aim of this chapter was to assess the differences observed between $CD8^+$ and $CD4^+$ T cells with regards to their susceptibilities to senescence. In particular, the aim was to examine whether cell metabolism and mitochondrial health could play a protective role in preventing the onset of senescence within the $CD4^+$ T compartment.

4.2. CD4⁺ EMRA T cells develop at a slower rate than CD8⁺ EMRA T cells

Both CD8⁺ and CD4⁺ EMRA T cells exhibit characteristics of senescence (Appay et al., 2008; Henson et al., 2014; Di Mitri et al., 2011). However, the percentage of CD4⁺ EMRA T cells is small (Figure 4.1A), particularly when compared to the percentage of CD8⁺ EMRA T cells that accumulate with age (figure 4.1B). Therefore, these data suggest that CD4⁺ T cells senesce at a much slower rate than CD8⁺ T cells.

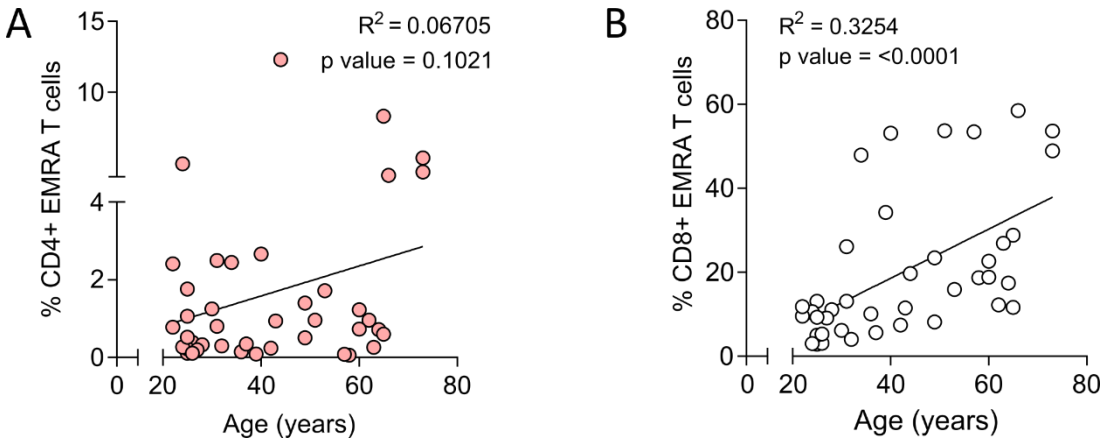

Figure 4.1: The accumulation of CD27/CD45RA-defined EMRA T cells with age

Percentage of EMRA T cells defined as percentage of the total (A) CD4⁺ or (B) CD8⁺ T cells population stratified by age. The line of best fit was generated using linear regression, *n* = 41. The data presented here was originally shown in Chapter 3 (Figures 3.3D and 3.4D) but has been repeated to enable side by side comparison.

4.3. $CD4^+$ EMRA T cells retain a high mitochondrial mass due to an increase in mitochondrial biogenesis

$CD8^+$ EMRA T cells are known to have defective mitochondria and impaired OXPHOS, which contributes to the senescent characteristics of this cell type (Henson et al., 2014). However, less is known about the health of $CD4^+$ EMRA mitochondria and subsequent respiration. To evaluate whether $CD4^+$ EMRA T cells also have mitochondria dysfunction, mitochondrial mass was assessed using Mitotracker green FM. Overall all of the $CD4^+$ CD27/CD45RA defined subsets had a higher mitochondrial mass when compared to their $CD8^+$ counterparts (Figure 4.2A). This difference was most striking between the EMRA subsets (Figure 4.2A). The data was obtained using middle aged donors with a median age of 41; however, when comparing this to a larger data set in our lab (Data not shown), this phenomenon was found to be independent of chronological age.

To further investigate this, intracellular staining of PGC1α, the key regulator of mitochondrial biogenesis, was carried out. PGC1α levels were the lowest in $CD8^+$ EMRA T cells, but the highest in $CD4^+$ EMRA T cells (Figure 4.2B). Levels amongst the two naïve and CM subsets were unchanged; however, both $CD4^+$ EM and EMRA T cells had significantly more levels of PGC1α than their $CD8^+$ counterparts (Figure 4.2B). Collectively these data showed that $CD4^+$ EM and in particular EMRA T cells had a higher mitochondrial mass due to increased mitochondrial biogenesis.

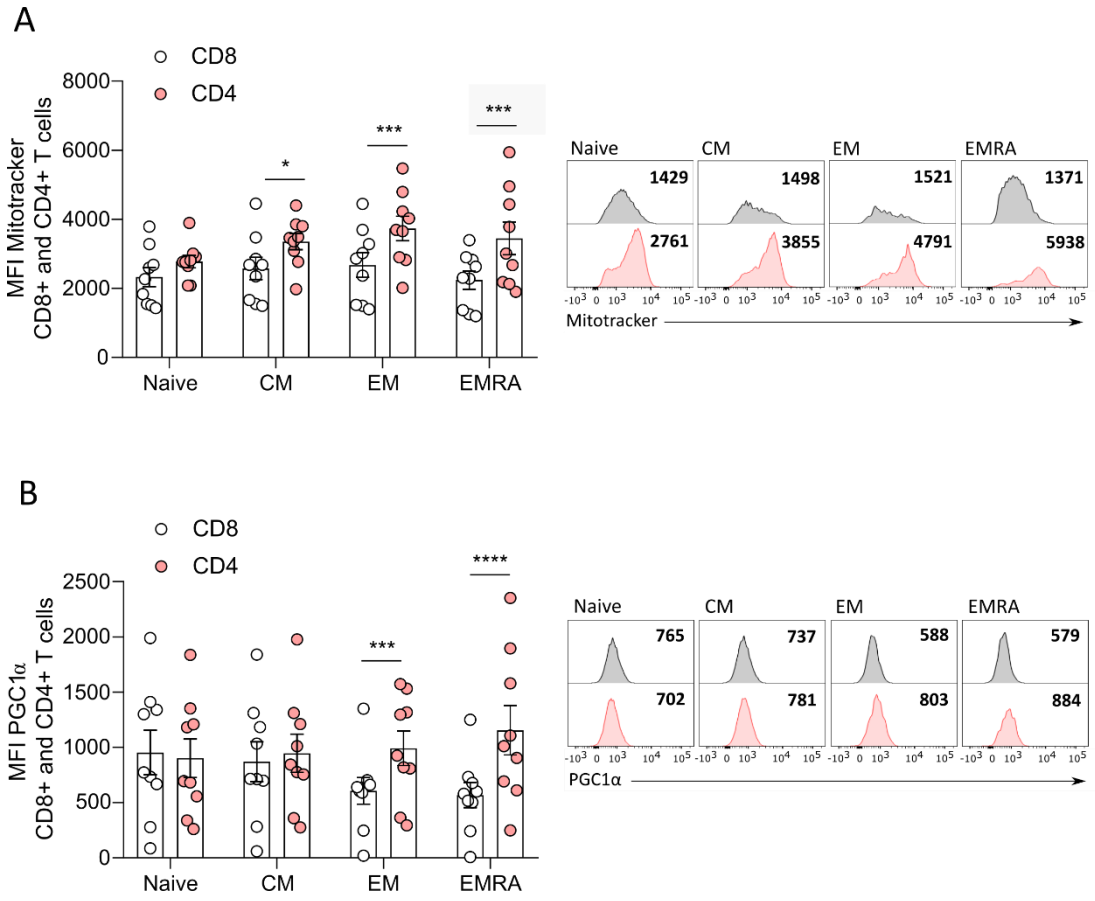

Figure 4.2: Assessment of mitochondrial mass in $CD8^+$ and $CD4^+$ T cell subsets

A) Quantification of Mitotracker green MFI in $CD8^+$ and $CD4^+$ CD45RA/CD27 defined subsets with representative flow cytometry histograms from middle aged donors. Data expressed as mean ± SEM, *n* = 9. P values were determined using a two-way repeated measure ANOVA with Bonferroni multiple comparisons test, p* = 0.0166, p*** = < 0.001.

B) Quantification of PGC1α MFI in $CD8^+$ and $CD4^+$ CD45RA/CD27 defined subsets with representative flow cytometry histograms from middle aged donors. Data expressed as mean ± SEM, *n* = 9. P values were determined using a two-way repeated measure ANOVA with Bonferroni multiple comparisons test, p*** = 0.0008 and p**** = <0.0001.

4.4. $CD4^+$ EMRA T cells have hyperpolarised mitochondria

To determine whether the increased mitochondrial mass in the $CD4^+$ EMRA subset was of functional importance TMRE, which measures MMP was used. $CD8^+$ T cell subsets had a high proportion of hypopolarised mitochondria (Figure 4.3A) whereas, $CD4^+$ Naïve, CM and EM subsets had a high proportion of healthy, intermediate MMP (Figure 4.3B). In contrast to the other $CD4^+$ subsets, $CD4^+$ EMRAs had a high proportion of hyperpolarised mitochondria (Figure 4.3B). This was also in complete contrast to the $CD8^+$ EMRAs, which predominantly displayed a hypopolarised phenotype (Figure 4.3A). The MMP provides the charge gradient required for $Ca2^+$ sequestration and the regulation of ROS production. Cell stress causes MMP dysregulation, with hyperpolaristion resulting in the production of excess ROS. However, a state of hypopolarisation is also harmful, as low amounts of ROS cause reductive stress, which can be as detrimental to homeostasis as oxidative stress (Zorova et al., 2018).

As hyperpolarised mitochondria are a source of ROS (Mills et al., 2016; Siska et al., 2017) we assessed mitochondrial ROS (mtROS) using MitoSox. Although ROS levels were the highest in $CD4^+$ EMRAs (Figure 4.4A) this increase was neutralised owing to the higher mitochondrial mass, meaning that $CD8^+$ EMRA T cells produced more ROS per mitochondria (Figure 4.4B). This data could suggest that the increased mitochondrial mass observed in $CD4^+$ EMRA T cells is a protective mechanism to ensure that $CD4^+$ EMRA T cells are able to adequately buffer the excess ROS (Zorov et al., 2014), however further work would need to be conducted to confirm this.

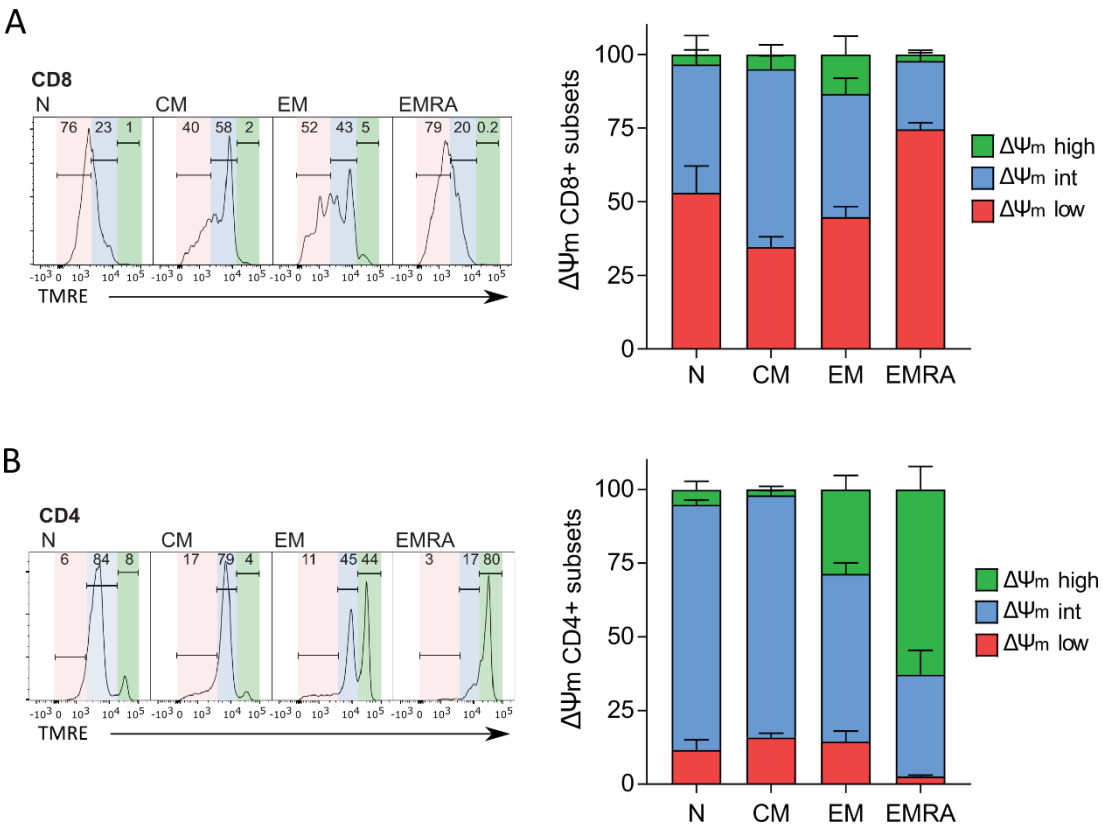

Figure 4.3: Assessment of MMP (ΔΨm) in $CD8^+$ and $CD4^+$ T cell subsets

Representative flow cytometry histograms and cumulative graphs of TMRE staining in (A) $CD8^+$ and (B) $CD4^+$ CD45RA/CD27 defined subsets from middle aged donors. Data expressed as mean ± SEM, *n* = 10.

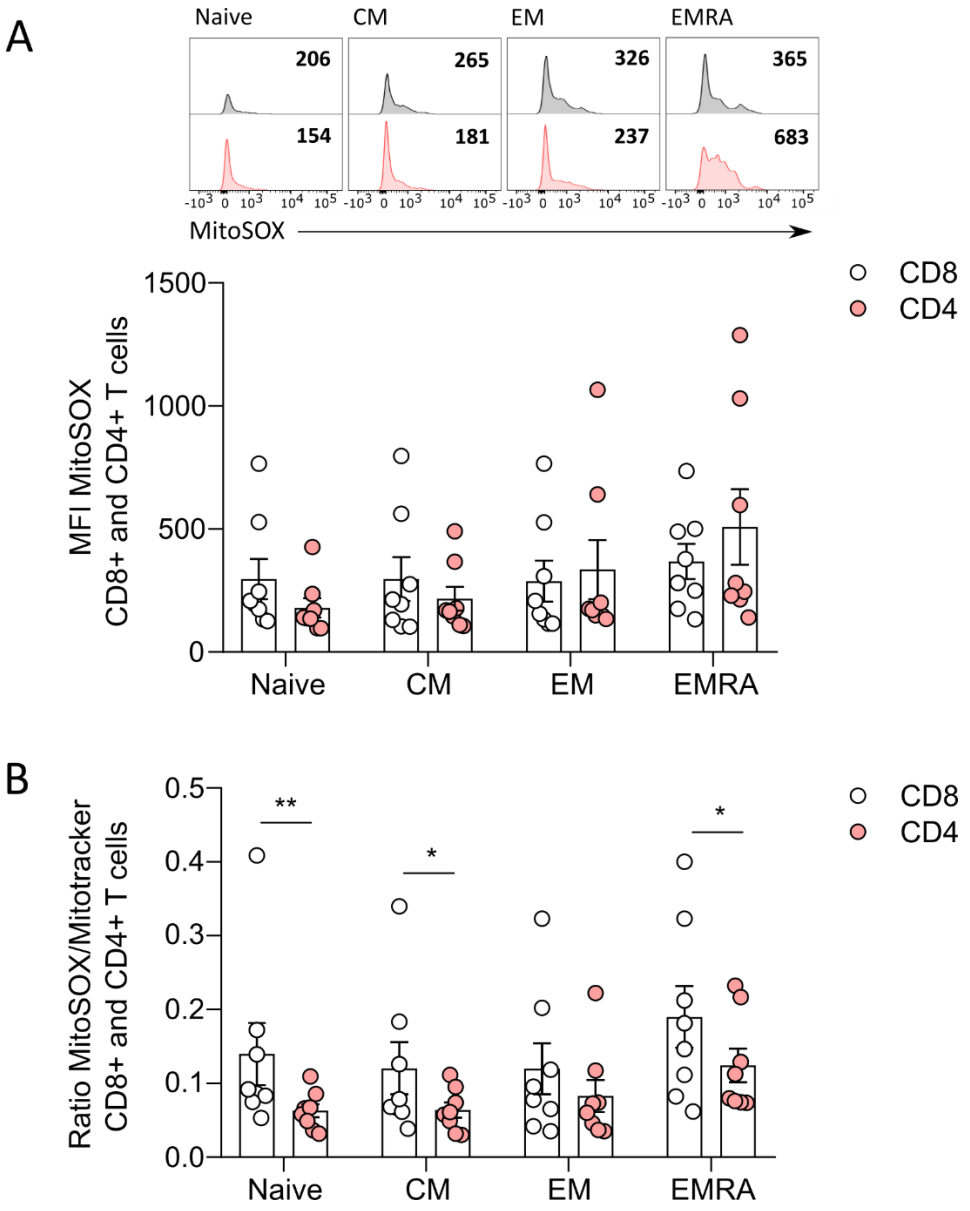

Figure 4.4: mtROS levels in $CD8^+$ and $CD4^+$ T cell subsets

A) Representative histograms and quantification of MitoSOX MFI in $CD8^+$ and $CD4^+$ CD45RA/CD27 defined subsets from middle aged donors. Data expressed as mean ± SEM, *n* = 8. P values were determined using a two-way repeated measure ANOVA with Bonferroni multiple comparisons test, p* = < 0.05, and p** = 0.0028.

B) mtROS production expressed as a ratio of mitochondrial mass in $CD8^+$ and $CD4^+$ CD45RA/CD27 defined subsets from middle aged donors. Data expressed as mean ± SEM, *n* = 8. P values were determined using a two-way repeated measure ANOVA with Bonferroni multiple comparisons test, p* = < 0.05, and p** = 0.0028.

4.5. CD4$^+$ EMRA T cells retain their oxidative capacity

To probe this further we next sought to investigate whether the increased mitochondrial mass and hyperpolarised MMP in CD4$^+$ EMRA T cells led to metabolic reprogramming. To do this we used a mitochondrial stress test to measure the bioenergetics profiles of TCR stimulated CD45RA/CD27 defined T cell subsets (Figure 4.4). The mitochondrial stress test includes the addition of four pharmacological drugs that manipulate OXPHOS. The ATP synthase inhibitor oligomycin is the first to be injected and enables the amount of oxygen used for ATP production to be calculated. Secondly, FCCP is added to uncouple the ETC from ATP synthesis. This collapses the MMP and allows the cells spare respiratory capacity (SRC) to be calculated. Lastly, rotenone and antimycin A, which are complex 1 and 3 inhibitors are added to allow for the non-mitochondrial oxygen consumption to be calculated.

Naïve CD4$^+$ T cells had significantly lower basal oxygen consumption compared to the memory T cells, however no differences were found amongst the three CD4$^+$ memory subsets (Figure 4.5A and B). Furthermore, the SRC was also significantly lower in the naïve CD4$^+$ T cells but unchanged in the three memory subsets (Figure 4.5A and C). The oxidative capacity of CD8$^+$ T cell subsets has been previously published (Henson et al., 2014); however for comparison the biogenetic profile for CD8$^+$ EMRAs have been included (Figure 4.5A). Similar results were found using unstimulated cells (Data not shown). However, as the OCR was much lower and the differences were less pronounced we chose to conduct future experiments on TCR stimulated cells.

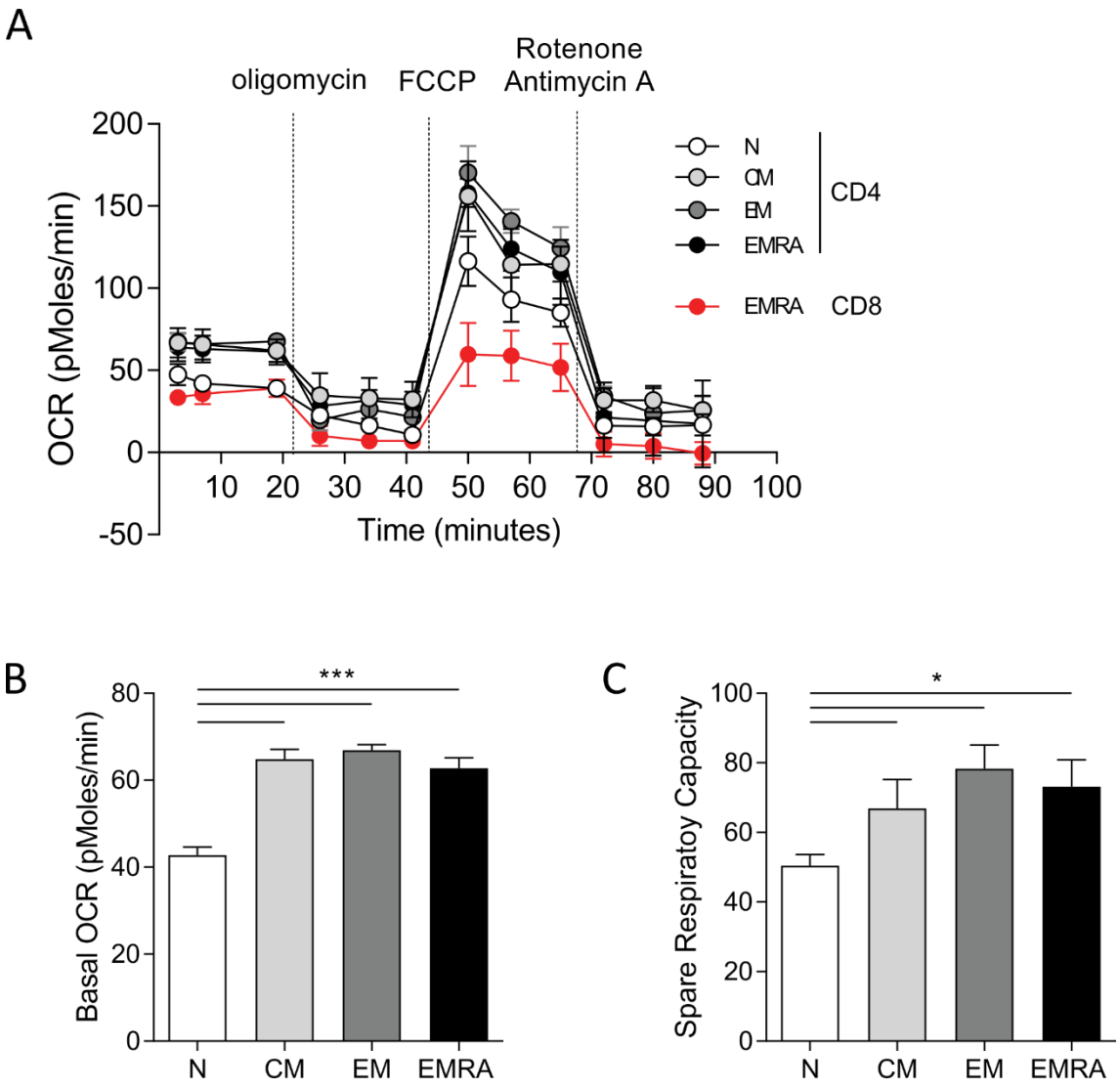

Figure 4.5: The bioenergetics profiles of CD45RA/CD27 defined T cell subsets

A) OCR of the $CD4^+$ T cell subsets and $CD8^+$ EMRA T cells from middle aged donors were measured after 15-minute stimulation with 0.5 µg/ml anti-CD3 and 5 ng/ml IL-2, cells were subjected to a mitochondrial stress test using indicated mitochondrial inhibitors. Data are representative of 4 independent experiments.

B) Basal OCR and C) the SRC after 15-minute stimulation with 0.5 µg/ml anti-CD3 and 5 ng/ml IL-2 (*n* = 4).

4.6. $CD4^+$ and $CD8^+$ EMRAs have different nutrient uptake

T cells utilise a variety of energy sources including glucose and lipids; however, their metabolic preferences are governed not only by their differentiation status but also by mitochondria fitness. Furthermore, a lack of regulatory control over nutrient usage is a recurrent theme accompanying senescence and ageing. We therefore sought to determine whether there were differences in glucose and FA uptake in the $CD8^+$ and $CD4^+$ T cell subsets. $CD8^+$ EMRAs were found to take up far less of the fluorescent glucose analogue; 2-NBDG, from their extracellular environment than their $CD4^+$ EMRA counterparts (Figure 4.6A). Glucose is internalised via GLUT1, the major glucose transporter in T cells, therefore internalisation is key for glucose uptake in T cells. The GLUT1 external/internal ratio can be used to assess internalisation. Here, $CD8^+$ EMRA T cells had the highest external/internal ratio and therefore had the least internalisation of GLUT1 and glucose (Figure 4.6B). This defect was not found in the $CD4^+$ EMRA T cells (Figure 4.6B).

The uptake of fluorescently labelled palmitate; BODIPY C16, a long chain FA was also quantified. BODIPY C16 uptake was significantly increased in $CD4^+$ EMRA T cells (Figure 4.7A). Furthermore, $CD4^+$ EMRA T cells had higher levels of the FA translocase CD36 (Figure 4.7B) and the FA transporters FATP2 and -3 (Figure 4.7C and D). Taken together these results suggest the $CD4^+$ EMRA T cells can utilise a variety of different nutrients. This could make them more adaptable, allowing them to maintain their health and fitness and potentially limit the impact of senescence. However, more work would be needed to confirm this.

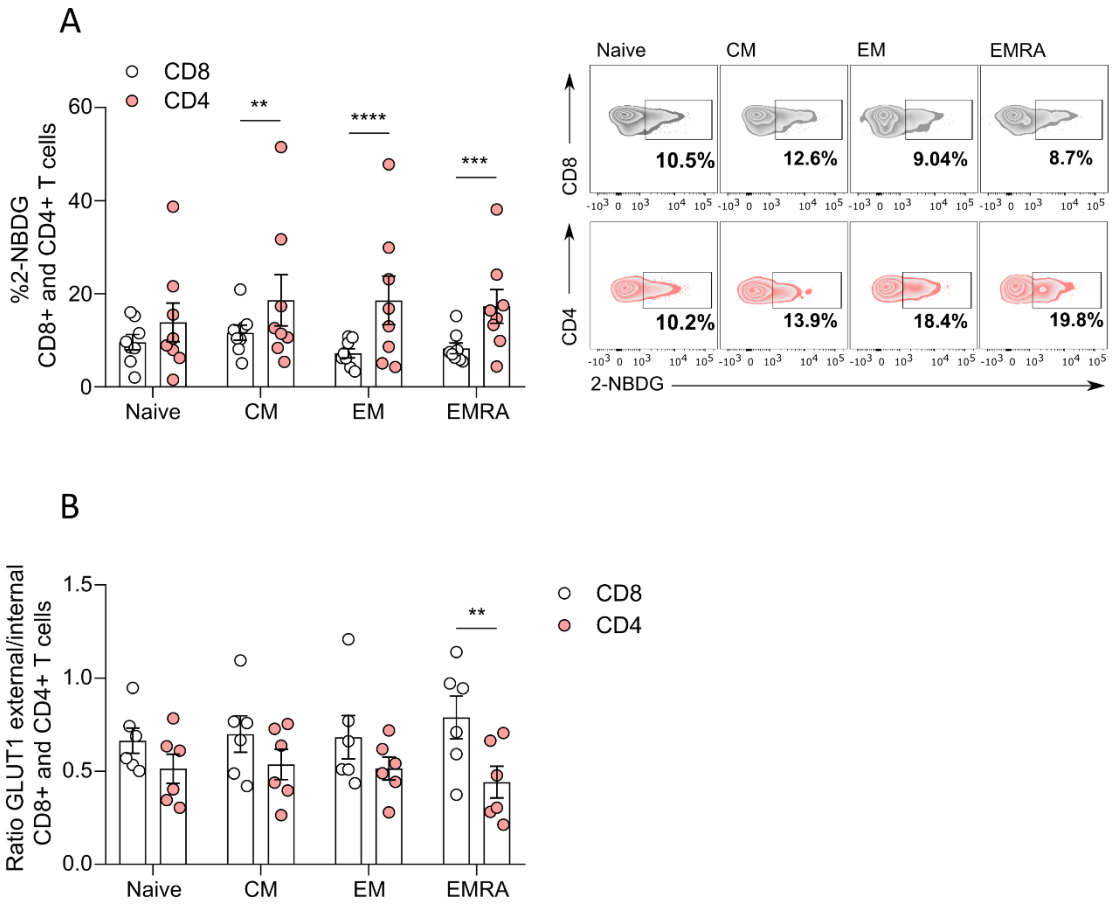

Figure 4.6: Glucose uptake in $CD8^+$ and $CD4^+$ T cell subsets

A) Glucose uptake was assessed using the fluorescent glucose analog 2-NBDG in $CD4^+$ and $CD8^+$ CD45RA/CD27 defined subsets from middle aged donors by flow cytometry following a 15-minute incubation. Data expressed as mean ± SEM, *n* = 8. P values were determined using a two-way repeated measure ANOVA with Bonferroni multiple comparisons test, p** = 0.0041, p*** = 0.0003 and p**** = <0.0001.

B) GLUT1 internalisation was determined by calculating the external/internal GLUT1 ratio of GLUT1 obtained from flow cytometry analysis of surface and intracellular staining of GLUT1. All individuals were middle aged donors. Data expressed as mean ± SEM, *n* = 6. P values were determined using a two-way repeated measure ANOVA with Bonferroni multiple comparisons test, p** = 0.0035.

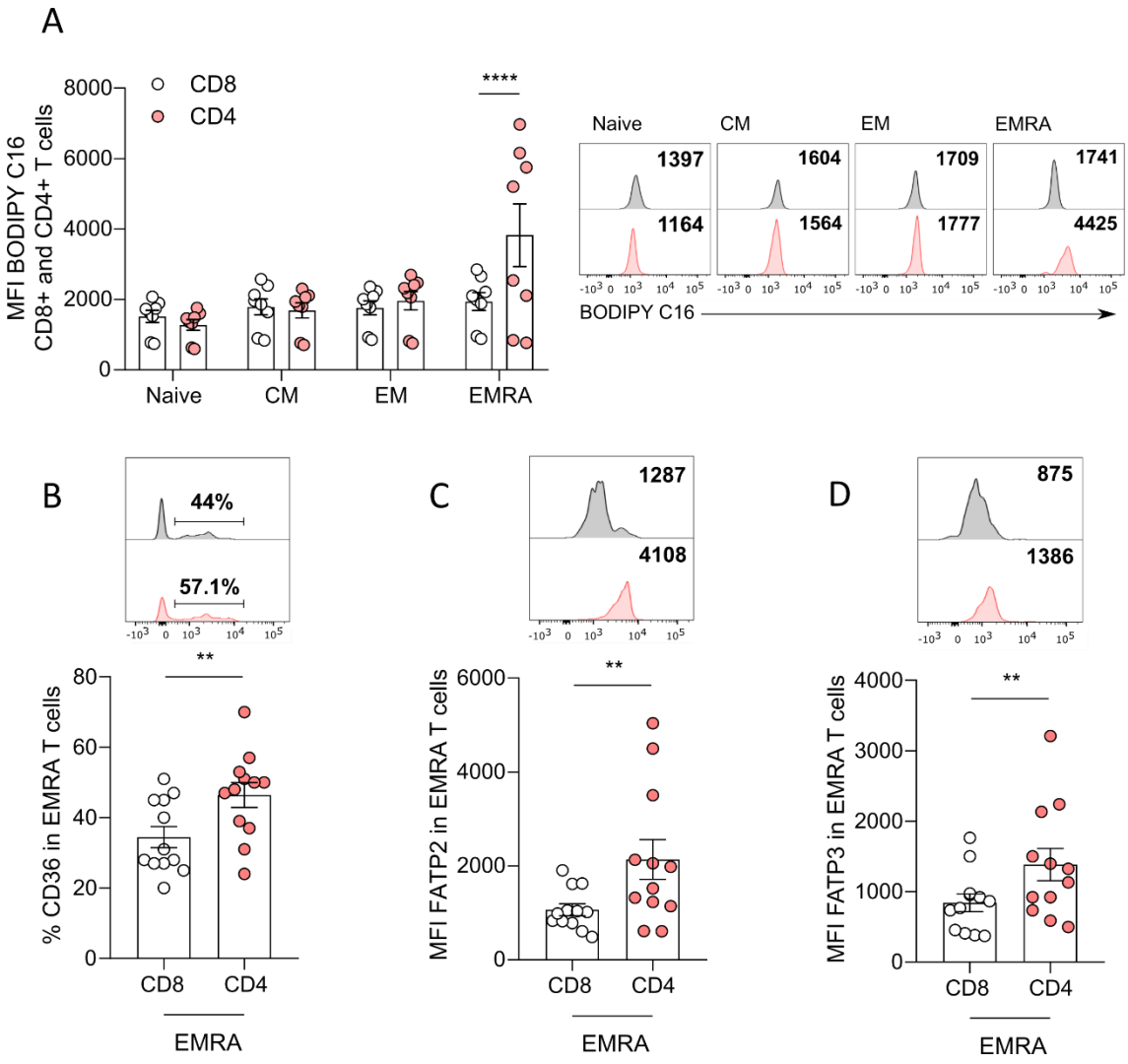

Figure 4.7: Lipid uptake in CD8⁺ and CD4⁺ T cell subsets

A) Lipid uptake was assessed using the fluorescent palmitate analog BODIPY C16 in CD4⁺ and CD8⁺ CD45RA/CD27 defined subsets by flow cytometry following a 10-minute incubation. Data expressed as mean ± SEM, *n* = 8. P values were determined using a two-way repeated measure ANOVA with Bonferroni multiple comparisons test, p**** = <0.0001.

B) Percentage of CD36⁺ cells, C) MFI of FATP2 and D) FATP3 in CD8⁺ and CD4⁺ EMRA T cells. Data expressed as mean ± SEM, *n* = 10. P values were determined using a paired T-test, p** = <0.001.

4.7. GATA3 is highly expressed in CD4$^+$ T cells

The metabolic differences observed between CD8$^+$ and CD4$^+$ EMRA led us to hypothesise that there was an inherent difference in the CD4$^+$ T cell lineage, which was offering protection against the induction of senescence through increasing mitochondrial mass and fitness. Consequently, we investigated the transcription factor GATA3, which is essential for CD4$^+$ lineage commitment during early T cell development in the thymus (Hernández-Hoyos et al., 2003). GATA3 is also required for Th2 differentiation and has therefore been regarded as a marker for Th2 cells (Zheng and Flavell, 1997). Surprisingly, we found that CD4$^+$ EMRA T cells had the highest levels of GATA3 when compared with the other three subsets (Figure 4.8), despite being more Th1 like – determined by increased IFN-γ and decreased IL-4, IL-5 and IL-13 cytokine production (Appay et al., 2008; Das et al., 2017; Sakata-Kaneko et al., 2000). In the CD8$^+$ lineage, GATA3 remained unchanged amongst the four subsets (Figure 4.8).

4.8. DNA damage recruits a GATA3-PGC1α complex

A possible connection between GATA3 and mitochondria has been previously reported. A yeast two hybrid screen showed that GATA3 is able to interact with the DNA damage proteins; ATM and ATR, as well as PGC1α (Kim et al., 2007). DNA damage can occur for a number of reasons. For instance, cells which undergo rapid proliferation tend to accumulate DNA damage, as well as many end-stage cells that have undergone replicative senescence in response to telomere dysfunction (Harley et al., 1990; Hayflick and Moorhead, 1961; Richter and Zglinicki, 2007).

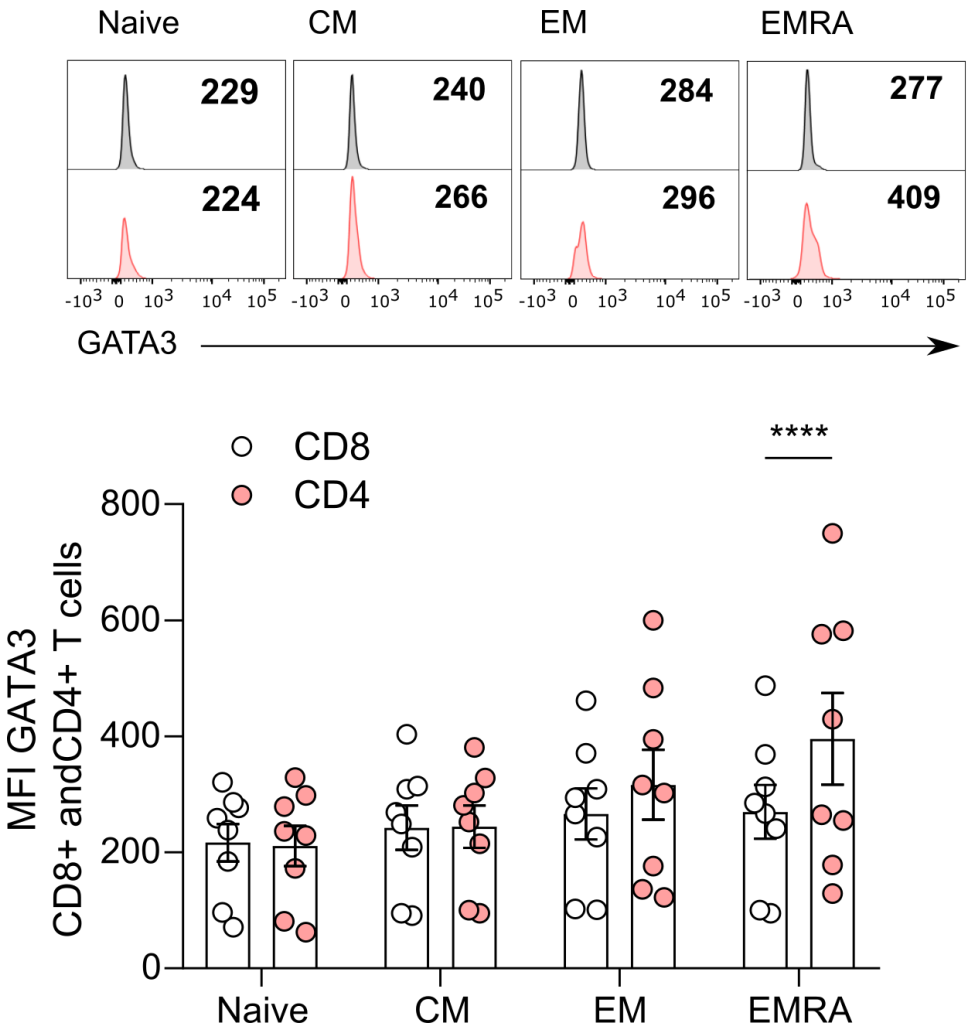

Figure 4.8: GATA3 in $CD8^+$ and $CD4^+$ T cell subsets

Representative histograms and cumulative GATA3 data in $CD4^+$ and $CD8^+$ CD45RA/CD27 defined subsets from middle aged donors. Data expressed as mean ± SEM, *n* = 8. P values were determined using a two-way repeated measure ANOVA with Bonferroni multiple comparisons test, p**** = <0.0001.

Data from the previous chapter showed that $CD4^+$ EMRA T cells have elevated levels of the downstream DNA damage response protein p53 (Figure 3.10 and 3.11). Immunoprecipitation (IP) assays showed that GATA3, PGC1α and the DNA damage protein; ATR, existed in the same complex in $CD4^+$ EMRA T cells (Figure 4.9A). GATA3 was bound to CHEK1, the downstream ATR kinase in all four $CD4^+$ T cells subsets; however, $CD4^+$ EMRA T cells had the highest levels of GATA3 bound to the ATR in all three repeats (Figure 4.9B). Little to no PGC1α was bound to the ATR in naïve and CM T cells, a small amount was bound in the EM subset; however, the EMRA T cell had a marked increase in the amount of PGC1α bound to the ATR (Figure 4.9C). To validate this additional IP experiments are being conducted in the lab using GATA3 and PGC1α pulldowns.

To mimic DNA damage, we incubated $CD4^+$ T cells with hydroxyurea; a DNA replication inhibitor known to induce DNA double strand breaks (Bianchi et al., 1986; Timson, 1975). Overnight incubation with hydroxyurea resulted in a significant increase in the amount of p-p53 (Figure 4.10A). Furthermore, IP assays showed that following treatment with hydroxyurea increased amounts of GATA3 and PGC1α were bound to the ATR (Figure 4.10B). In addition, flow cytometry analysis revealed a significant increase in PGC1α (Figure 4.11A) and an increased mitochondrial content, determined by elevated Mitotracker green staining (Figure 4.11B). Future experiments will include testing a range of different hydroxyurea concentrations to assess if a threshold exists.

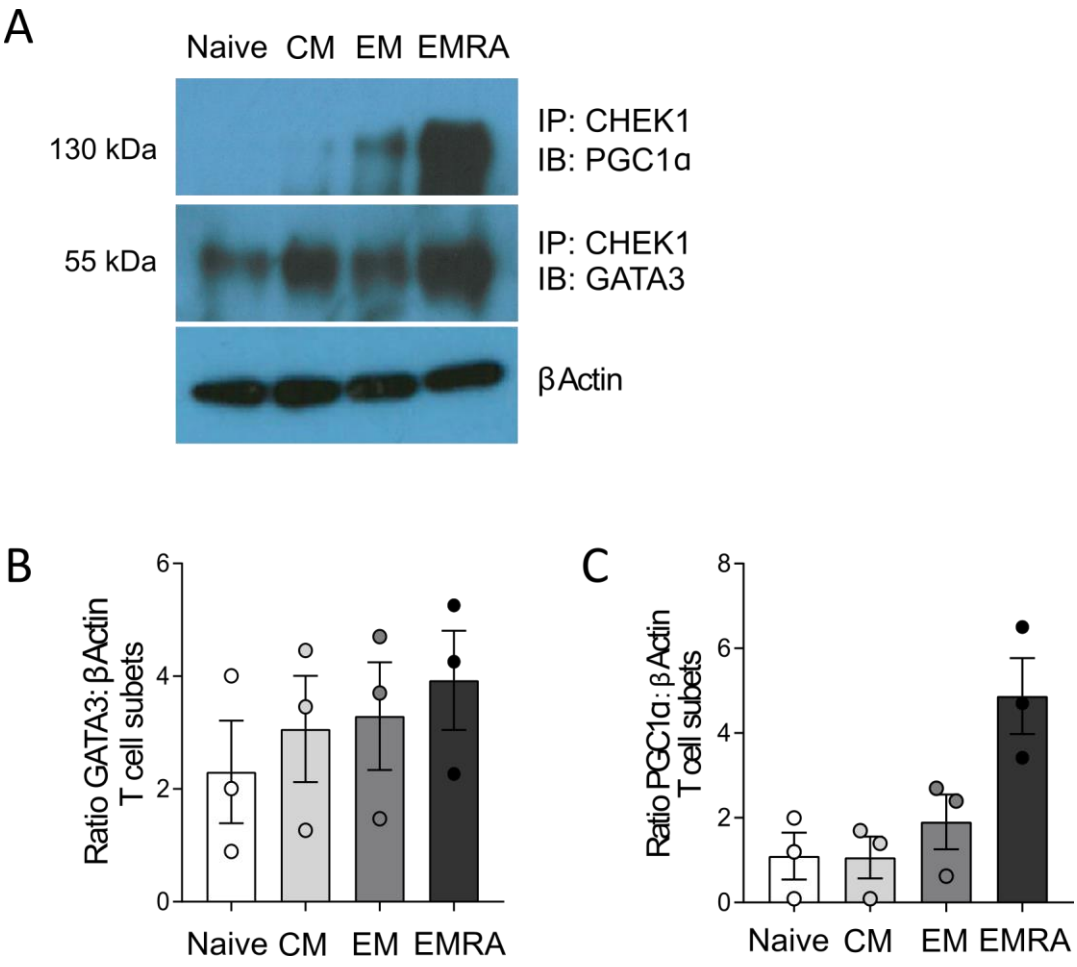

Figure 4.9: CHEK1 immunoprecipitation in $CD4^+$ T cell subsets

(A) Representative image of western blot after CHEK1 immunoprecipitation in the CD27/CD45RA defined $CD4^+$ T cell subsets and cumulative graphs to quantify the amount of (B) GATA3 and (C) PGC1α bound to the CHEK1 antibody. Data show as mean ± SEM, *n* = 3.

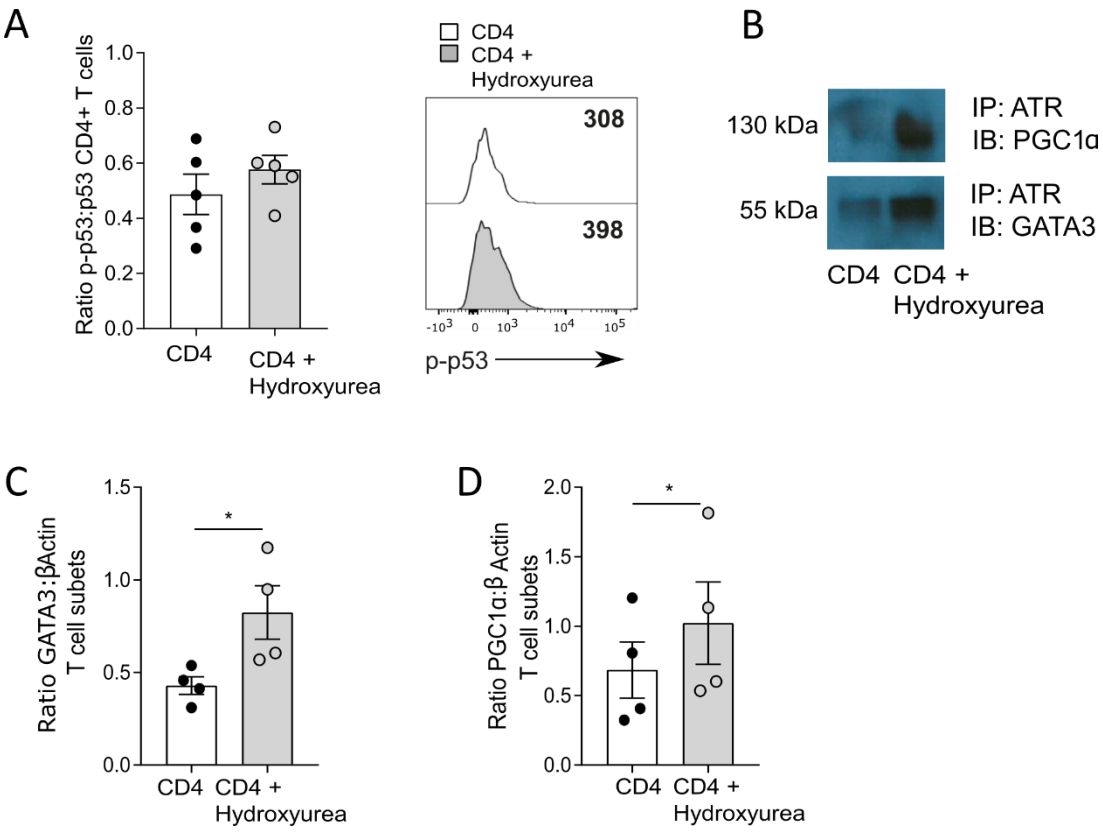

Figure 4.10: CHEK1 immunoprecipitation following hydroxyurea induced DNA damage in CD4⁺ T cells

A) Graph to show the p-p53:p53 ratio following induction of DNA damage by hydroxyurea in whole CD4⁺ T cells. Data expressed as mean ± SEM, *n* = 5.

B) Representative image of western blot after CHEK1 immunoprecipitation in CD4⁺ T cells following exposure to hydroxyurea.

C) Quantification of GATA3 and D) PGC1α bound to the CHEK1 antibody following IP. Data expressed as mean ± SEM, *n* = 3. P values were determined using a paired T-test, p* = <0.05.

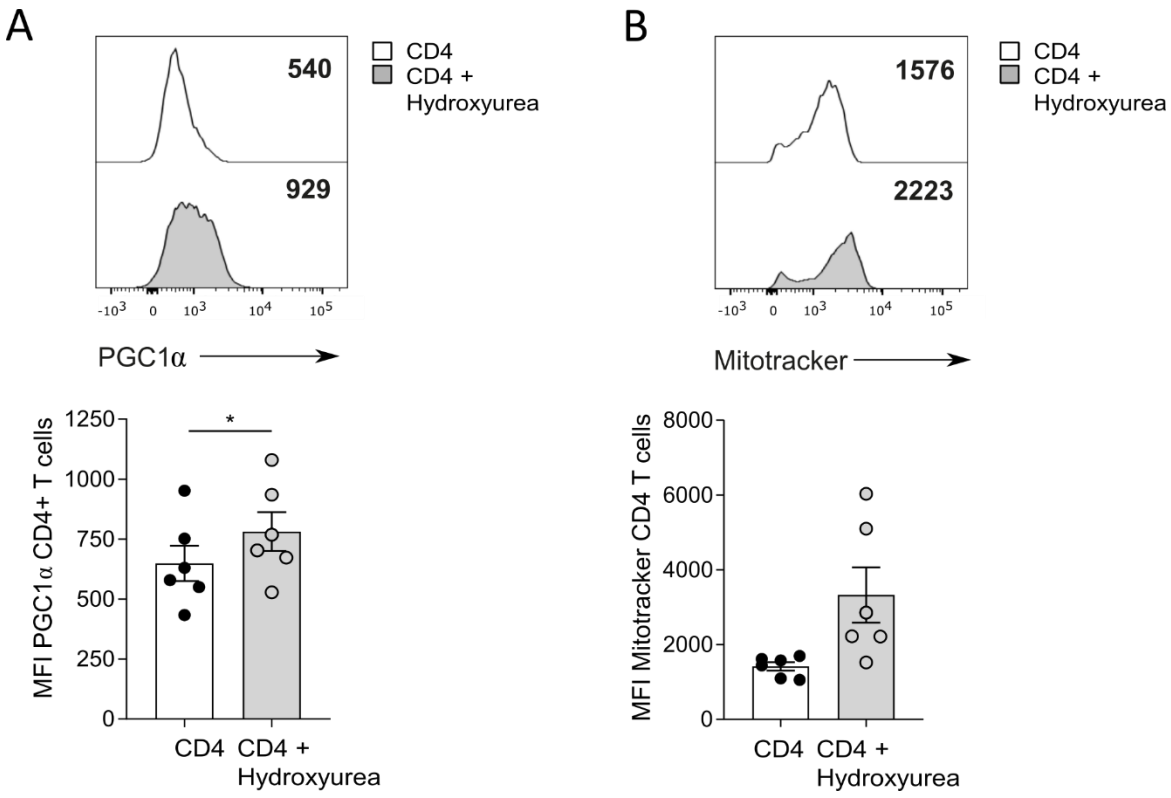

Figure 4.11: PGC1α and GATA3 following hydroxyurea induced DNA damage in $CD4^+$ T cells

A) Representative histograms and cumulative data of intracellular PGC1α levels following the induction of DNA damage by hydroxyurea in whole $CD4^+$ T cells. Data expressed as mean ± SEM, *n* = 6. P value was determined using a paired T-test, p* = <0.05.

B) Representative histograms and cumulative data of intracellular GATA3 levels following the induction of DNA damage by hydroxyurea in whole $CD4^+$ T cells. Data expressed as mean ± SEM, *n* = 6.

4.9. GATA3 directly regulates CD4$^+$ T cell metabolism and mitochondrial biogenesis

To verify that GATA3 can directly regulate mitochondria biogenesis and fitness, we used small interfering RNA (siRNA) to reduce GATA3 expression in purified human CD4$^+$ T cells following activation (Figure 4.12). Transfection with GATA3 siRNA led to a significant decrease in both the levels of PGC1α (Figure 4.13A) and Mitotracker Green staining (Figure 4.13B), signifying a marked reduction in mitochondrial mass. Confocal microscopy examination of Tom20 (Figure 4.14A), a major outer mitochondrial membrane receptor and therefore mitochondrial marker, showed a significant reduction in both mitochondrial mass (Figure 4.14B) and volume (Figure 4.14C) in Jurkat cells following transfection with GATA3 siRNA.

TMRE staining revealed a dramatic shift from hyperpolarised to hypopolarised MMP in the GATA3 siRNA transfected CD4$^+$ T cells, but not the scrambled siRNA transfected CD4$^+$ T cells (Figure 4.15A). Moreover, transfection with GATA3 siRNA dramatically inhibited the ability of CD4$^+$ T cells to perform OXPHOS when compared with CD4$^+$ T cells transfected with negative control scrambled siRNA (Figure 4.16B). Basal OCR and SRC were significantly decreased in the GATA3 siRNA transfected CD4$^+$ T cells (Figure 4.16C and D). Taken together, these data provide evidence that GATA3 is crucial for maintaining both mitochondrial mass and fitness in CD4$^+$ T cells.

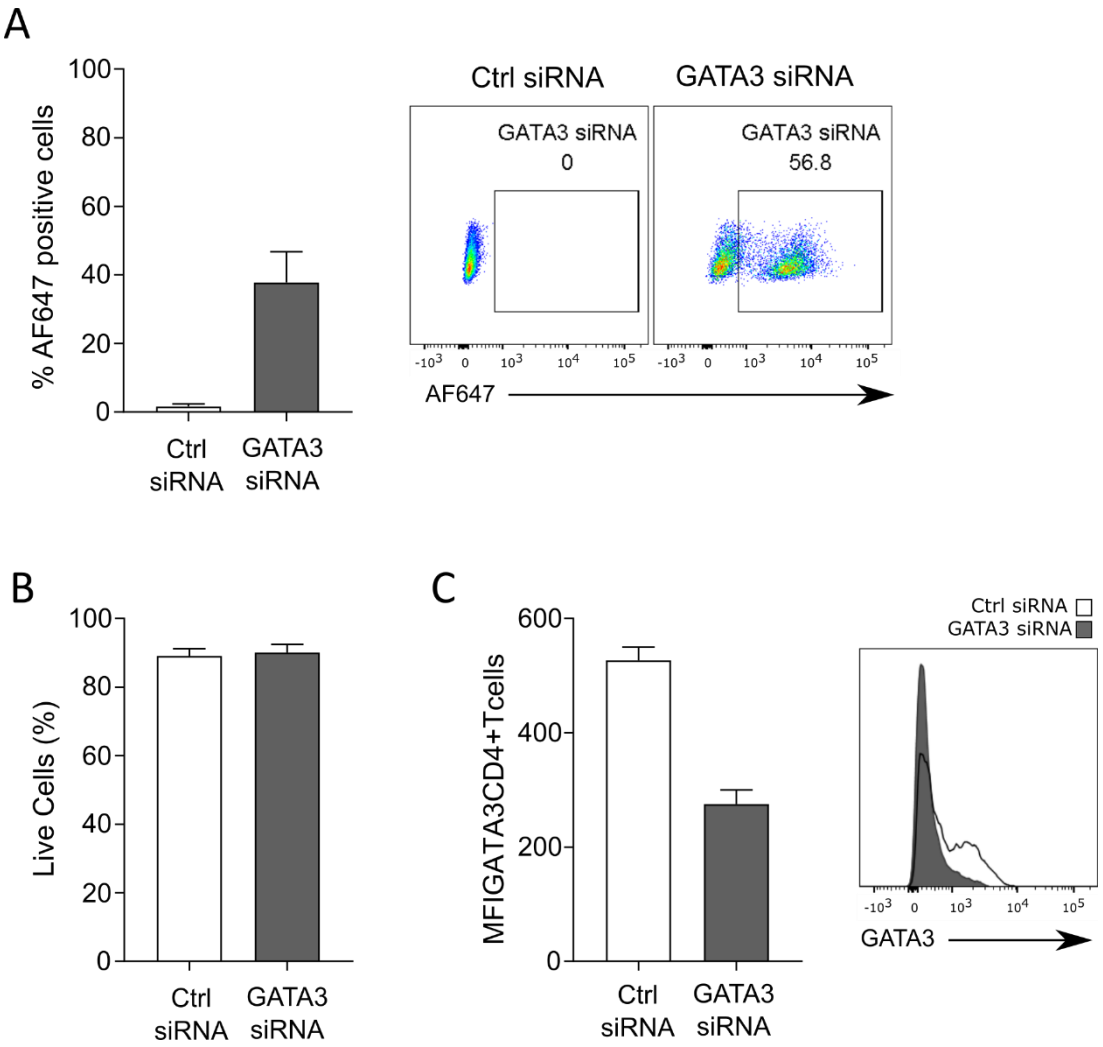

Figure 4.12: GATA3 siRNA knockdown efficacy in CD4⁺ T cells

A) Quantification of GATA3 siRNA-AF647⁺ cells in CD4⁺ T cells transfected with either scrambled control siRNA or GATA3 siRNA with representative flow cytometry plots. Data expressed as mean ± SEM, *n* = 6.

B) Percentage of live cells determined by Zombie NIR staining following GATA3 siRNA transfection. Data expressed as mean ± SEM, *n* = 6

C) GATA3 levels following siRNA knockdown in CD4⁺ T cells with representative histograms. Data expressed as mean ± SEM, *n* = 3.

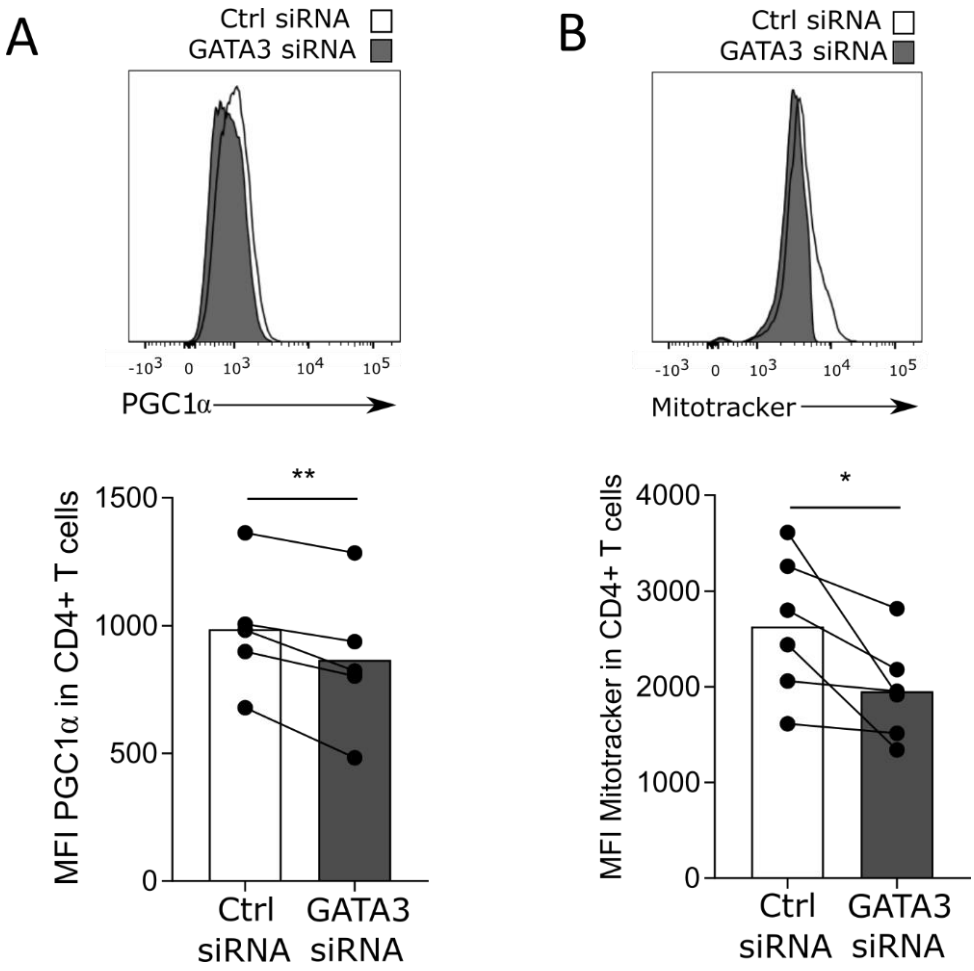

Figure 4.13: PGC1α and GATA3 following GATA3 siRNA knockdown in CD4⁺ T cells

A) Representative histograms and cumulative graph of PGC1α in CD4⁺ T cells following siRNA knockdown representative flow cytometry plots. Data expressed as mean ± SEM, *n* = 5. P value was determined using a paired T-test, p** = 0.0084.

B) Representative histograms and cumulative graph of Mitotracker in CD4⁺ T cells following siRNA knockdown representative flow cytometry plots. Data expressed as mean ± SEM, *n* = 6. P value was determined using a paired T-test, p* = 0.0442.

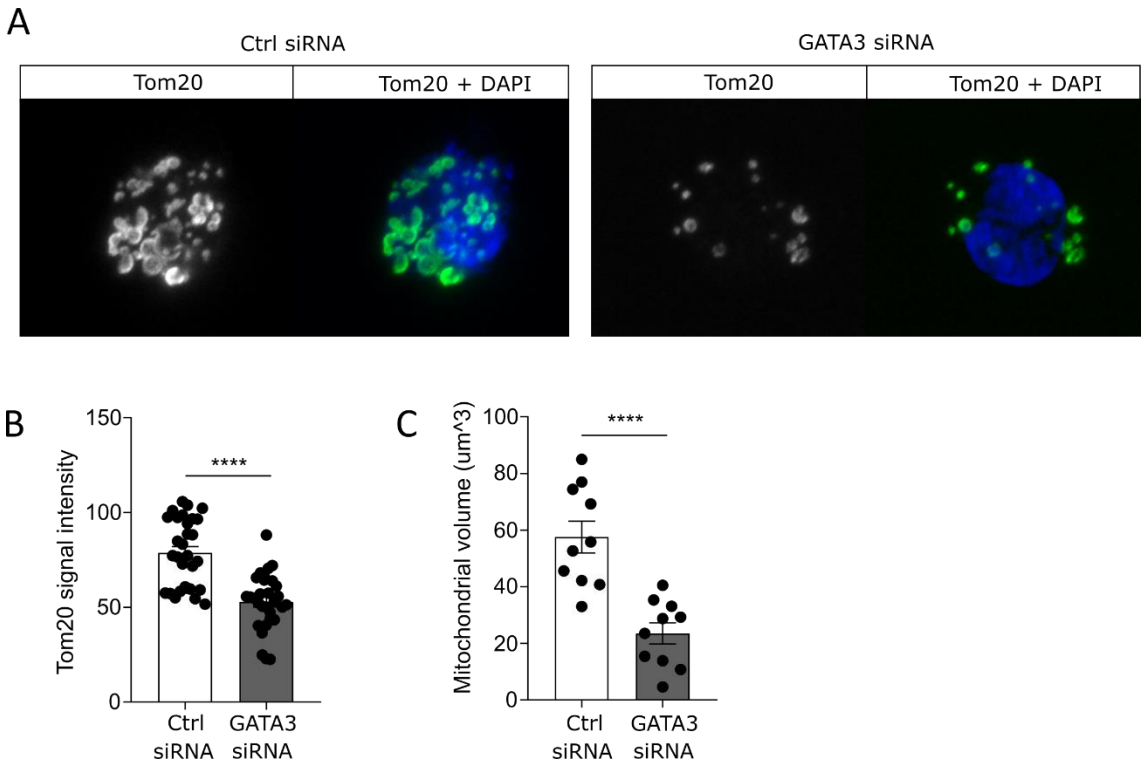

Figure 4.14: Assessment of mitochondria following GATA3 siRNA knockdown by confocal microscopy

A) Representative images of Tom20 staining in Jurkat cells transfected with either scrambled negative control siRNA or GATA3 siRNA.

B) Mitochondrial mass determined using Tom20 signal intensity. Data expressed as mean ± SEM, data from 3 individual experiments.

C) Mitochondrial volume was determined through 3D rendering of Tom20 staining Z-stack images. Data expressed as mean ± SEM, data from 3 individual experiments.

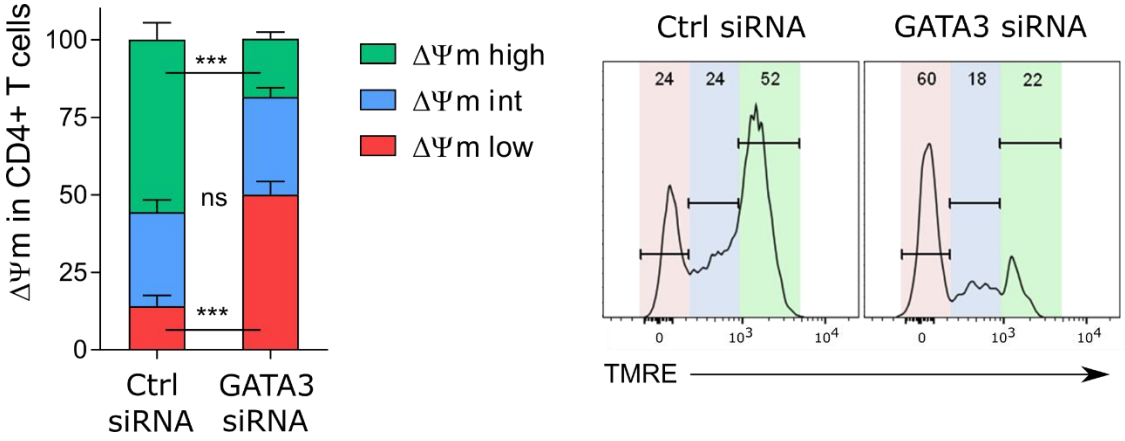

Figure 4.15: The MMP of $CD4^+$ T cells after GATA3 siRNA knockdown

Representative flow cytometry histograms and cumulative graphs of TMRE staining in $CD4^+$ T cells transfected with either scrambled negative control siRNA or GATA3 siRNA CD45RA/CD27 defined subsets. Data expressed as mean ± SEM, *n* = 6. P values were determined using a two-way repeated measure ANOVA with Bonferroni multiple comparisons test, p*** = < 0.001.

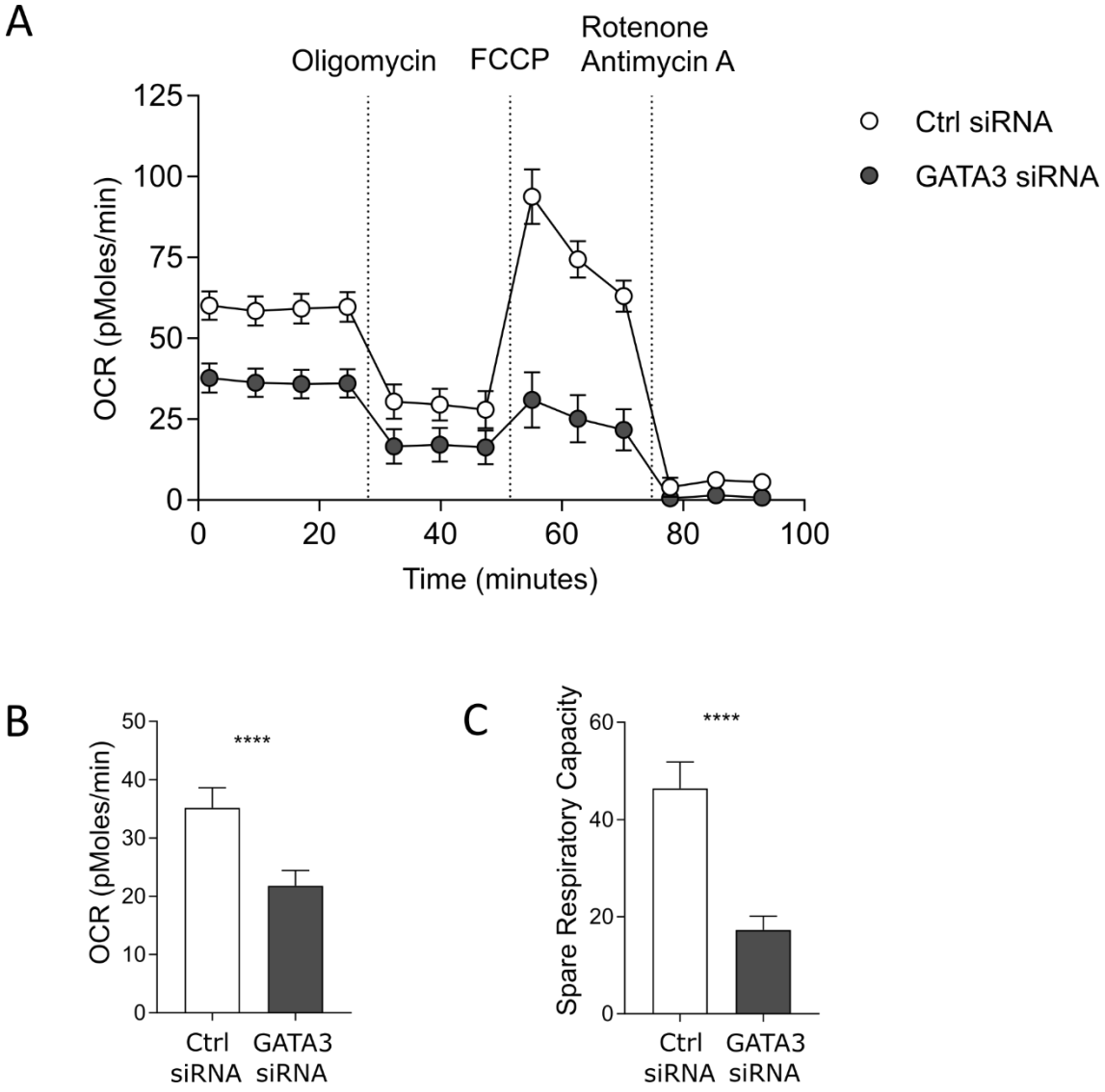

Figure 4.16: Bioenergetics profiles of CD4$^+$ T cells following GATA3 siRNA knockdown

A) OCR of CD4$^+$ T cells following siRNA knockdown with either scrambled control siRNA or GATA3 siRNA was measured after 15-minute stimulation with 0.5 µg/ml anti-CD3 and 5 ng/ml IL-2, cells were subjected to a mitochondrial stress test using indicated mitochondrial inhibitors. Data are representative of 3 independent experiments.

B) Basal OCR and C) the SRC after 15-minute stimulation with 0.5 µg/ml anti-CD3 and 5 ng/ml IL-2 (*n* = 3). P value was determined using a paired T-test, p**** = <0.0001.

4.10. Discussion

Senescent or EMRA T cells are a highly dynamic and heterogeneous subset of cells that accumulate with age (Callender, Carroll, Beal, et al., 2018), and are found in both the $CD8^+$ and $CD4^+$ T cell compartments. In addition to data presented in this thesis, others have shown that the $CD8^+$ EMRA subset accumulates more rapidly than their $CD4^+$ counterparts with age (Czesnikiewicz-Guzik et al., 2008; Koch et al., 2008). It has been suggested that the $CD4^+$ EMRA subset is more resistant to the effects of age owing to better homeostatic control compared to that of $CD8^+$ T cells. However, data in this chapter provides evidence that $CD4^+$ T cells are protected against the effects of senescence due to the induction of a GATA3-PGC1α complex in the presence of DNA damage.

Mitochondrial dysfunction is a central event in many pathologies and contributes to age-related processes. Mitochondria have been shown to participate in every aspect of ageing, such as a decline in stem cell function, cellular senescence and the development of the low grade inflammatory state (Sun et al., 2016). Alterations that occur to mitochondria with age are numerous, including reductions in mitochondrial mass (Corsetti et al., 2008), defects in mitochondrial biogenesis (Reznick et al., 2007), and impaired mitochondrial function in terms of ATP production and respiratory chain capacity (Preston et al., 2008). Indeed, here we show that the $CD8^+$ EMRA subset displayed a reduced mitochondrial mass, impaired mitochondrial biogenesis, as well as having a hypopolarised mitochondrial phenotype compared to the

$CD4^+$ EMRA subset, demonstrating that $CD8^+$ EMRA T cells had a greater degree of mitochondrial impairment compared to $CD4^+$ EMRA T cells.

Increased ROS levels have been demonstrated to be critical for the induction and maintenance of cell senescence (Davalli et al., 2016). The MMP is the central bioenergetic parameter controlling the generation of ROS (Nicholls, 2004). The $CD8^+$ EMRA subset displayed a hypopolarised phenotype; whereas, the $CD4^+$ EMRAs were in a hyperpolarised state. As expected from cells that display a high MMP, $CD4^+$ EMRAs produced more ROS than their $CD8^+$ counterparts. However, the higher mitochondrial content observed in $CD4^+$ EMRA T cells means these cells have more buffering capacity to quench the effects of ROS. Consequently, $CD4^+$ EMRA T cells are better at controlling the damaging effects of ROS and are therefore better able to control the rate of senescence (Zorov et al., 2014).

Mitochondria also play a key role in cellular metabolism, they house the ETC and the tricarboxylic acid cycle (TCA) cycle, as well as playing crucial roles in the synthesis and breakdown of lipids (Pence and Yarbro, 2018). Metabolic regulation plays an important role during cellular senescence, with dysregulated metabolism now identified as a feature of many different cell types, including T cells (Callender, Carroll, Bober, et al., 2018). There is increasing evidence that cell cultures become glycolytic as they age, depending on the senescence induction method used (Callender, Carroll, Bober, et al., 2018; James et al., 2015). $CD8^+$ EMRA T cells have been shown to lose their metabolic plasticity and become more glycolytic (Henson et

al., 2014). However, here $CD4^+$ EMRAs were able to maintain their metabolic flexibility as they retain better oxidative capacity than their $CD8^+$ counterparts. Furthermore, they also retain better glucose and lipid uptake together with increased expression of transporters.

Mechanistically, this increase in mitochondrial mass was found to be due to elevated levels of GATA3 caused by DNA damage. This led to the recruitment of a GATA3-PGC1α complex that induced mitochondrial biogenesis in $CD4^+$ T cells. Furthermore, functional analysis of $CD4^+$ T cells showed that GATA3 was crucial for T cell metabolism, as GATA3 knockdown impaired mitochondrial function and abolished the cells oxidative capacity.

Importantly, the observation that the GATA3-PGC1α complex is induced by DNA damage suggests that this mechanism may not be restricted to the lymphocyte lineage. Especially as GATA3 is expressed in a wide variety of tissues outside the haematopoietic system and has been implicated in the tumourigenesis of many cancers such as luminal breast cancer (Mehra et al., 2005), neuroblastoma (Peng et al., 2015), endometrial carcinomas (Engelsen et al., 2008), as well as in human T cell acute lymphoblastic leukaemia (Minegishi et al., 1997) and $CD4^+CD8^+$ double positive T cell lymphoma (van Hamburg et al., 2008). GATA3-positive breast cancers have been shown to be highly differentiated, with resulting tumours two-fold larger in size than control tumours (Kouros-Mehr et al., 2008). In contrast, GATA3-negative breast cancers form poorly differentiated tumours and are highly metastatic (Kouros-Mehr

et al., 2008). However, despite being associated with low metastatic potential and therefore a more favourable prognosis, GATA3-positive tumours are also associated with resistance to chemotherapy (Tominaga et al., 2012). In light of the data presented in this chapter, we hypothesise that the accumulation of DNA damage generated during chemotherapy would recruit the GATA3-PGC1α complex, allowing GATA3-positive tumours to maintain mitochondrial fitness and evade chemotherapy induced apoptosis. However, additional examination of GATA3 and its contribution to mitochondrial biogenesis in cancer is needed to confirm this.

More broadly, these data implicate that transcription factors are likely to serve additional functions after their initial roles in differentiation. This is already the case for the Th1 differentiation marker; T-bet, which is also known to be crucial for long-term memory in $CD8^+$ T cells (Intlekofer et al., 2005; Juedes et al., 2003) and maturation of NK cells (Townsend et al., 2004). More recently; STAT5, which has traditionally been associated with cytokine signalling and JAK kinases (Beyer et al., 2011), has now also been identified as a central regulator of naïve $CD4^+$ T cell metabolism (Jones et al., 2019). Furthermore, although the GATA proteins have restricted expression patterns to some extent their functions can be interchangeable. For example, GATA1, - 2, and-4 can all activate the expression of GATA3 target genes IL-4 and IL-5 and repress IFN-γ in T cells (Ranganath and Murphy, 2002). Interestingly, GATA4 has previously been shown to become activated in the presence of the ATM and ATR, resulting in the induction of senescence and a SASP in human fibroblasts

(Kang et al., 2015). These functional overlaps suggest that other GATA proteins may also be capable of influencing cell metabolism.

In summary, this chapter identified a previously unknown role for GATA3 in inducing mitochondrial biogenesis in response to DNA damage, revealing it as a key mediator cell metabolism and demonstrating that mitochondrial mass controls the senescence phenotype in T cells.

Chapter Five: T2D as a model to investigate different mechanisms for senescent T cell generation

5.1. Introduction

Senescent T cells have been implicated in a number of different chronic, inflammatory diseases, such as cancer (Zelle-Rieser et al., 2016), obesity (Shirakawa et al., 2016) and RA (Weyand et al., 2014). T2D, which is characterised by metabolic imbalances and chronic inflammation, becomes more prevalent with age (Duncan et al., 2003). Consequently, T2D was chosen as a model to investigate the relationship between inflammation, metabolism and T cell senescence. A full assessment of T cell senescence in T2D has not been conducted. However, $CD4^{+}CD28^{-}$ T cells, which are a mixture of both EM and EMRA T cells, have been found to accumulate in T2D (Giubilato et al., 2011). More recently, $CD8^{+}CD28^{-}CD57^{+}$ T cells have also been shown to increase the risk of hyperglycaemia in humans, highlighting a potential role for this subset in the pathogenesis of T2D (Lee et al., 2019). As T2D is characterised by both disrupted glucose homeostasis and chronic inflammation we hypothesised that this would result in an environment that would drive an increased rate of T cell senescence.

5.1.1. Aim:

In chapter three the existence of multiple EMRA populations were revealed. To investigate potential mechanisms responsible for premature senescence in T cells, the aim of this chapter was to compare senescent T cells from people living with T2D and healthy individuals. Due to their abundance and increased susceptibility to senescence we decided to focus solely on the $CD8^+$ T cell lineage.

5.2. Characteristics of T2D and healthy volunteers

People living with T2D were recruited from the DARE database (Table 5.1). T2D individuals had a median age of 64 years and had been living with T2D for a significant amount of time, with the mean length of time since diagnosis being 15 years. All people living with T2D were on medication, with the majority taking 3 – 6 different types of medication to control their condition (Table 5.1 and 5.2). Participation in the study was entirely voluntary and all individuals were required to travel in order for their blood to be collected meaning all T2D donors were fit enough to make this journey.

Healthy age-matched control donors were recruited internally and had a median age of 62. Healthy volunteers were individuals who had not had an infection or immunisation within the last month, no known immunodeficiency, and had not received any other immunosuppressive medications within the last 6 months.

Donor characteristics		T2D donors	Control donors
Total number of donors		52	23
Age ranges		50 - 77 years	49 – 73 years
Median age		64	62
Gender (Male / Female)		65% / 35%	48% / 52%
Mean length of time since diagnosis		15 years	N/A
Medication(s):	1 – 2	23%	N/A
	3 – 6	42%	
	7 +	35%	

Table 5.1: Donor characteristics

Category	**List of medications** (% of patients taking medication)
Diabetes	Metformin (74%), Glizcazide (20%), Canagliflozin (6%), Humalog (6%), Dulaglutide (2%), Levemir (4%), Glargine (2%), Victoza (2%), Gliptin (2%).
Statins	Atrovastatin (44%), Simvastatin (8%), Pravastatin (6%).
Other	Aspirin (22%), Rampril (20%), Candesartan (8%), Amlodipine (6%), Bendro (6%), Pregabalin (4%), Citalopram (4%), Tramadol (4%), Doxazosin (4%), Levothyroxine (4%), Solifenacin (4%), Bisoprolol (2%), Morphine (2%), Quinninesulphate (2%), Colecalciferol (2%), Taddalafil (2%), Travopost (2%), Fenofibrate (2%), Spironolactone (2%), Bendroflumethiazide (2%), Beclomethasone dipropionate (2%), Salamol (2%), Trimethoprim (2%), Paroxetine (2%), Isosorbide mononitrate (2%), Omeprazole (2%), Edoxaban (2%), Tamsulosin (2%).

Table 5.2: List of medications

5.3. People living with T2D have a prematurely aged $CD8^+$ T cell phenotype

The cell surface markers CD45RA and CD27 were used to quantify the frequency of $CD8^+$ T cell subsets in people living with T2D compared with healthy age-matched control donors (Figure 5.1A, B and C). T2D donors had a significant reduction in the number of $CD8^+$ naïve T cells, which was mirrored by a significant increase in the number of $CD8^+$ EMRA T cells (Figure 5.1C), demonstrating that people living with T2D have a prematurely aged T cell phenotype. To assess the potential impact of medications we compared the percentage of $CD8^+$ EMRA T cells with the total number of drugs, however no relationship was found (Figure 5.2).

Examination of a range of cell surface markers (CD27, CD28, CD45RA, CCR7, and KLRG1) through an unbiased *t*-SNE analysis further supported this finding (Figure 5.3A). *t*-SNE is a machine learning algorithm that clusters data based on how similar the data points are and when combined with the heatmap expression data, the properties of each cluster can be determined (Figure 5.4A).

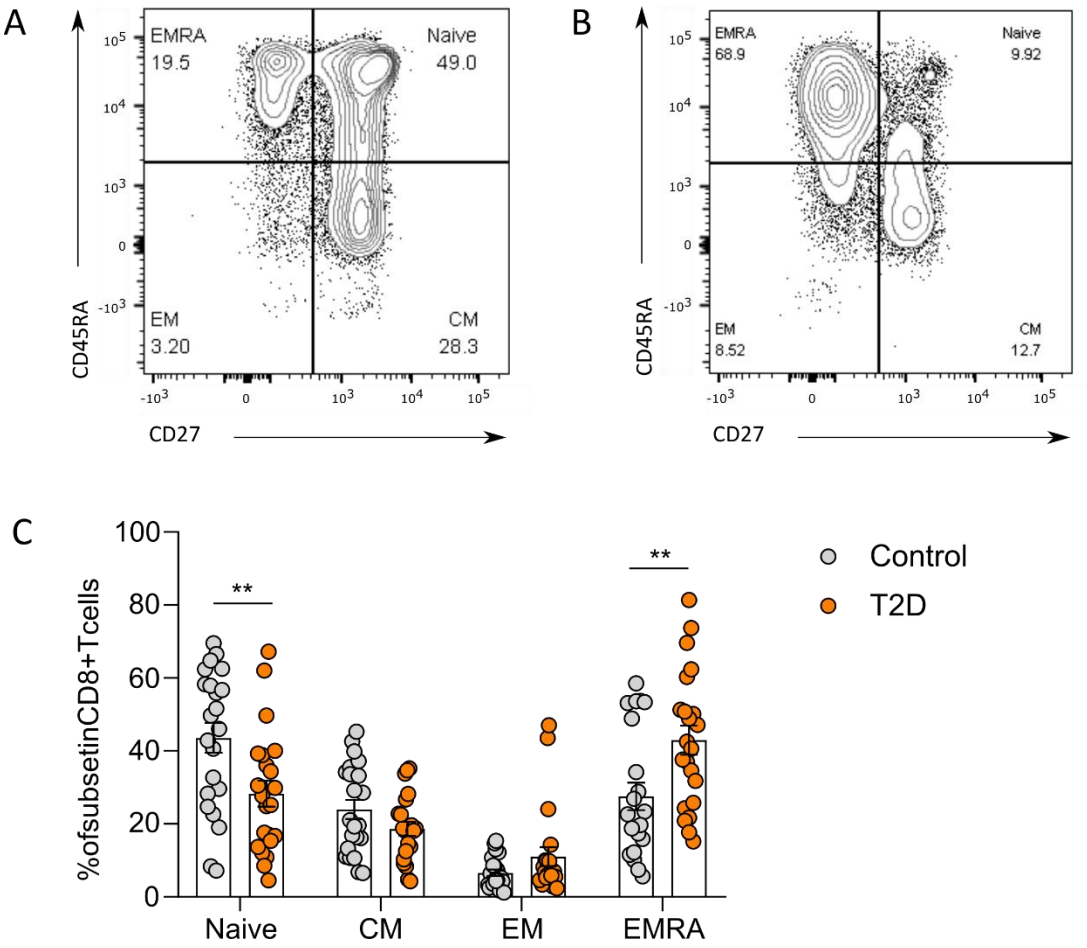

Figure 5.1: Utilisation of CD45RA/CD27 to assess $CD8^+$ subsets in people living with T2D and healthy control donors

A) Representative flow cytometry dot plot of $CD8^+$ CD45RA/CD27 defined subsets from a healthy age-matched control donor.

B) Representative flow cytometry dot plot of $CD8^+$ CD45RA/CD27 defined subsets from a T2D donor.

C) Quantification of the CD45RA/CD27 defined $CD8^+$ T cell subsets in T2D and healthy age-matched control donors. Data expressed as mean ± SEM, *n* = 22 control, 22 T2D. P values were determined using a two-way ANOVA with Bonferroni multiple comparisons test, p** = < 0.01.

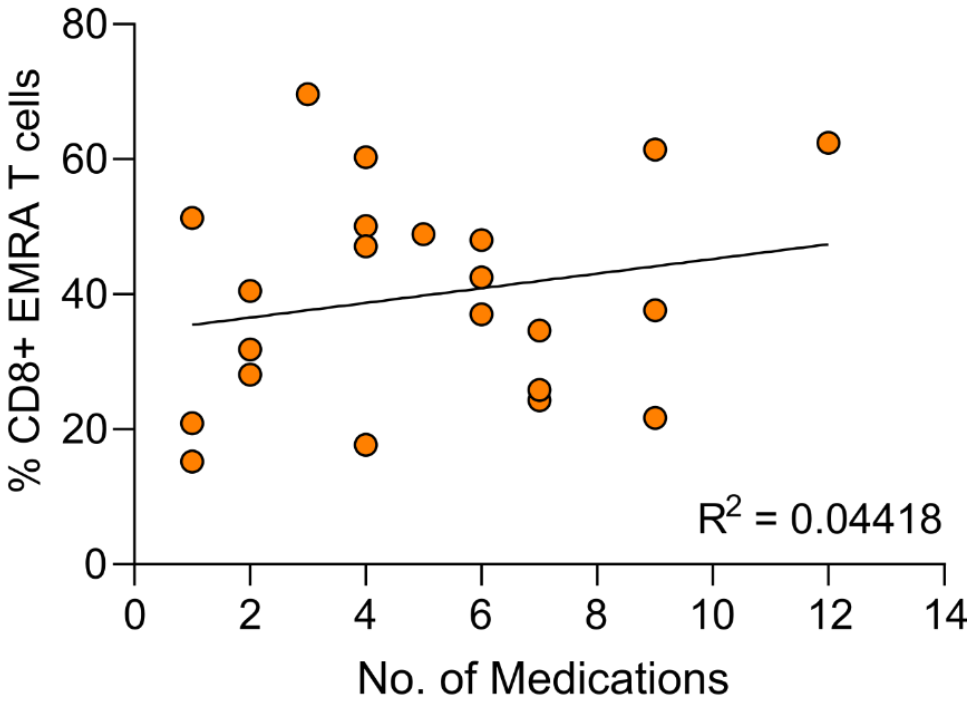

Figure 5.2: The relationship between T2D $CD8^+$ EMRA T cells and medication

Percentage of $CD8^+$ EMRA T cells defined as percentage of the total $CD8^+$ T cell population against the total number of medications, *n* = 22. Line of best fit generated using linear regression.

The *t*-SNE analysis revealed a dramatic loss in the number of true naïve $CD8^+$ T cells ($CD27^+CD28^+CCR7^+CD45RA^+KLRG1^-$) in people living with T2D (Figure 5.3A and B). Interestingly, the *t*-SNE also revealed the existence of multiple EMRA populations, further supporting the notion that EMRA T cells are highly heterogeneous (Figure 5.3A and B). EMRA 1, 2 and 3 were all $CD45RA^+CD27^-$ but expressed varying degrees of CD28 and CCR7. As expected, all 3 of these EMRA subsets also expressed high levels of KLRG1 (Figure 5.4A and B). Surprisingly, there was a dramatic loss in the number of EMRA 3 cells in the T2D donors (Figure 5.3A and B). However, an additional $CD45RA^+CD27^-$ EMRA subset, which lacked the expression of KLRG1 was identified (Figure 5.4A and B). This subset was increased greatly in T2D donors and following additional experiments, which will appear in the latter half this chapter, this subset was later termed inflammatory-derived EMRA (i-EMRA). In addition to changes to the EMRA populations, the CM 1 cluster was also dramatically increased in T2D donors (Figure 5.3A and B).

Collectively, the *t*-SNE analysis further supported the notion that EMRA T cells are highly heterogeneous and revealed the existence of a $KLRG1^-$ EMRA population.

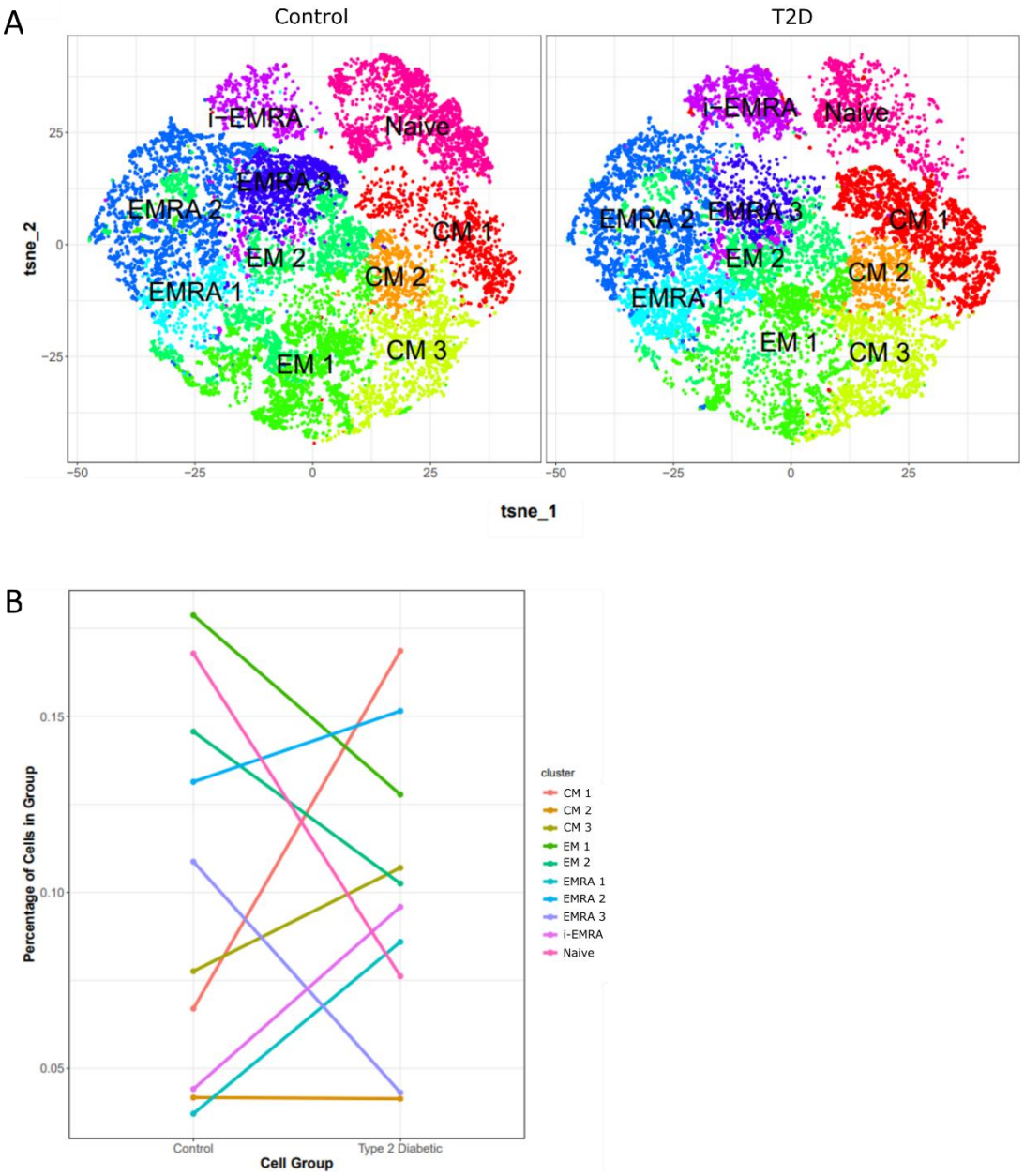

Figure 5.3: *t*-SNE cluster analysis of CD8$^+$ T cells in T2D and control donors

A) Clusterplot analysis of CD8$^+$ T cells in control and T2D donors using CD27, CD28, CD45RA, CCR7 and KLRG1, *n* = 6.

B) Rate change plot showing the change in the percentage of cells in each group between control and T2D donors, *n* = 6.

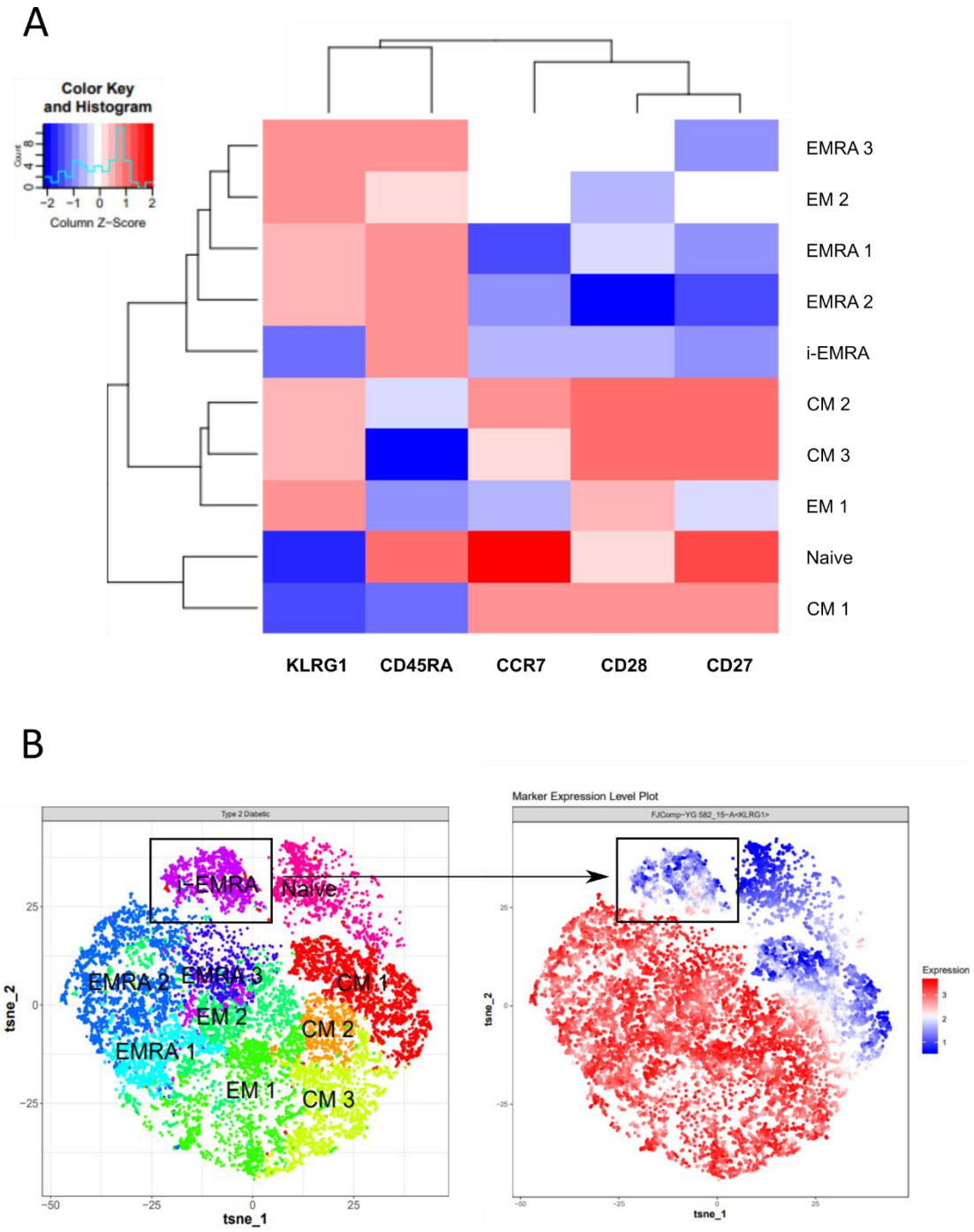

Figure 5.4: Marker expression data from *t*-SNE analysis

A) Heatmap to show protein levels of cell surface markers CD27, CD28, CD45RA, CCR7 and KLRG1 in each cluster group, *n* = 6.

B) KLRG1 expression plot to show the levels of KLRG1 throughout all of the cluster groups, *n* = 6.

5.4. T2D leads to the accumulation of KLRG1$^-$ EMRA T cells

Following the *t*-SNE analysis, examination of KLRG1 levels via traditional flow cytometry analysis revealed that healthy age-matched control donors and T2D donors had both KLRG1$^+$ and KLRG1$^-$ EMRA subsets (Figure 5.5A and B). However, T2D donors had a far greater number of the KLRG1$^-$ EMRA T cells than the control donors (Figure 5.5A and B).

5.5. T2D EMRA T cells have a distinct senescent phenotype

These changes to the composition of the EMRA population in T2D raised the question as to whether this subset was distinct from control EMRA T cells. To investigate this, Cellular Senescence RT^2 Profiler Arrays were used to assess the expression levels of 84 different senescence markers in T2D and healthy age-matched control CD8$^+$ EMRA T cells. T2D and control EMRA T cells shared numerous similarities, however there were a large proportion of genes which were altered in T2D EMRA T cells compared with control EMRAs, with 45% of genes being up-regulated and 20% down-regulated (Figure 5.6A and B).

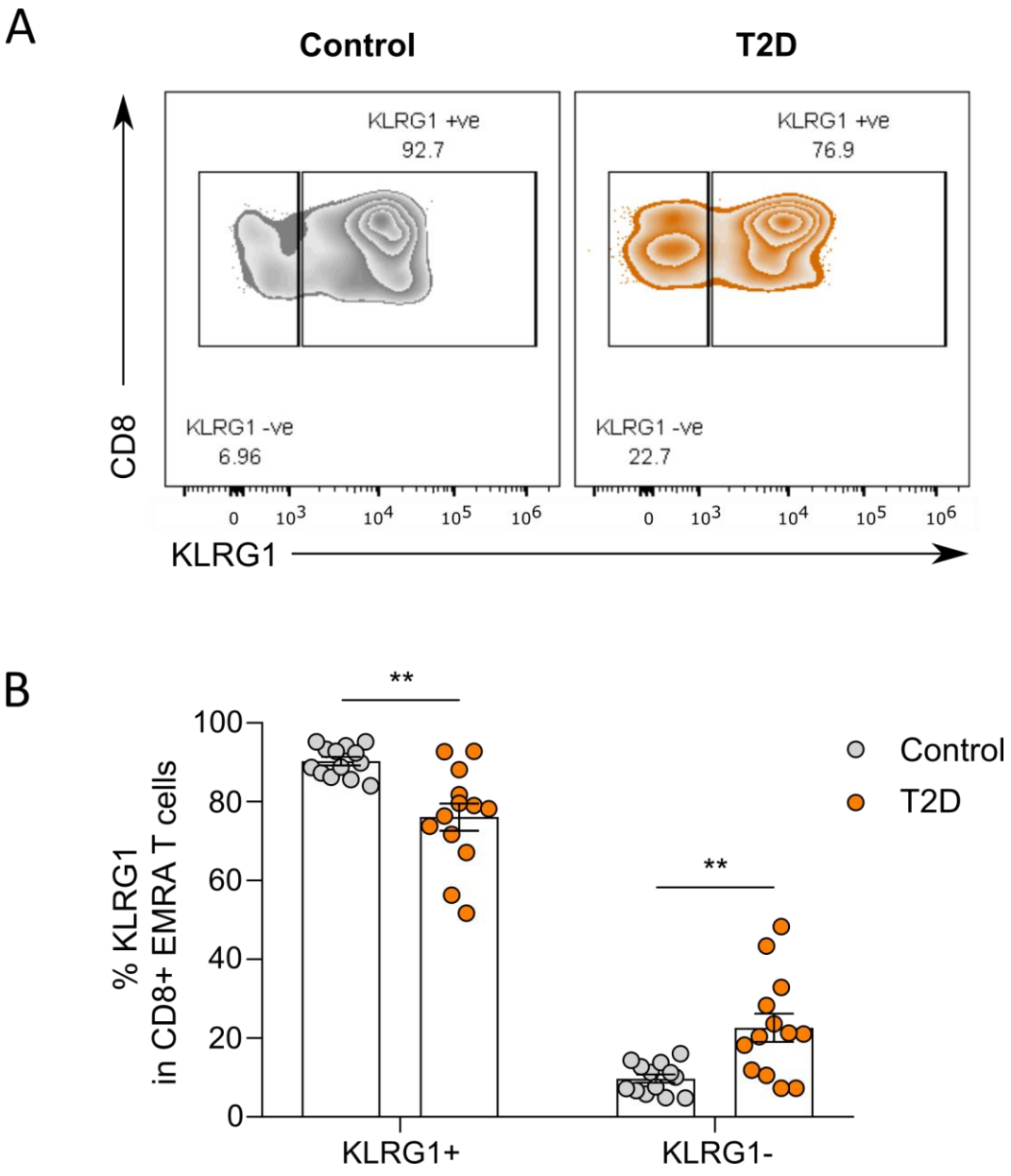

Figure 5.5: KLRG1 levels in $CD8^+$ T cell subset

A) Representative dot plots of KLRG1 + and – subsets in $CD8^+$ EMRA T cells

B) Quantification of KLRG1 + and – subsets in $CD8^+$ EMRA T cells in T2D and healthy age-matched control donors. Data expressed as mean ± SEM, *n* = 13 control, 13 T2D. P values were determined using a two-way ANOVA with Bonferroni multiple comparisons test, p** = < 0.01.

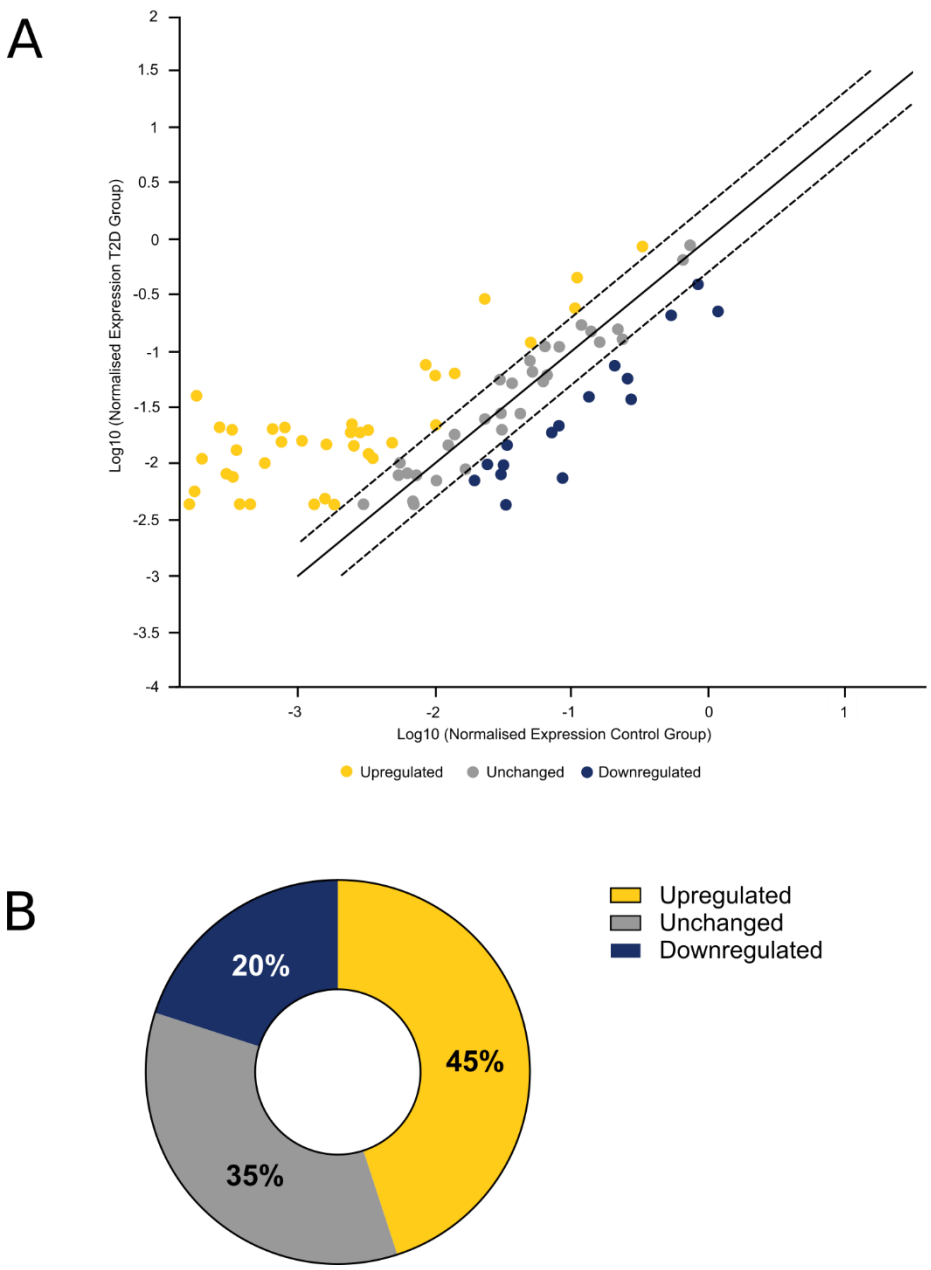

Figure 5.6: Changes in gene expression in T2D EMRAs compared with control EMRAs.

A) Scatterplot and B) pie chart illustrating the number of genes measured in the RT^2 Cellular Senescence Array that were upregulated, unchanged and downregulated in the T2D EMRAs compared to the control EMRAs. Fold change cut-off < 2, Control *n* = 3, T2D *n* = 3.

5.5.1. T2D EMRA exhibit evidence of DNA damage but not telomere erosion

Further investigating into the key genes involved in DNA damage and repair showed that p16 and p21 expression was increased in T2D EMRA cells, whereas p53 expression was unchanged (Figure 5.7). Surprisingly, ATM expression was downregulated but CHEK1 and CHEK2, which are downstream of the ATM and ATR (Awasthi et al., 2015), were increased (Figure 5.7). The most striking observation amongst these genes was the dramatic upregulation of TERT – the catalytic subunit of telomerase (Figure 5.7).

5.5.2. KLRG1$^-$ EMRAs have longer telomeres than KLRG1$^+$ EMRAs

To validate whether the increased TERT expression had any functional relevance we collaborated with Dr. Natalie Riddell at the University of Surrey to asses telomere length in CD8$^+$ EMRA T cells. This was done by combining flow cytometry with fluorescence in situ hybridization (flow-FISH). The incorporation of a nucleic acid telomeric probe $(CCCTAA)_3$ conjugated to Cy5 (TelCy5) during the flow-FISH protocol allowed for the quantification of telomeric DNA. No difference in TelCy5 was observed between control and T2D total EMRA T cells (Figure 5.8A). However, stratification using KLRG1 demonstrated that KLRG1$^-$ EMRAs have longer telomeres than conventional KLRG1$^+$ EMRA T cells (Figure 5.8B).

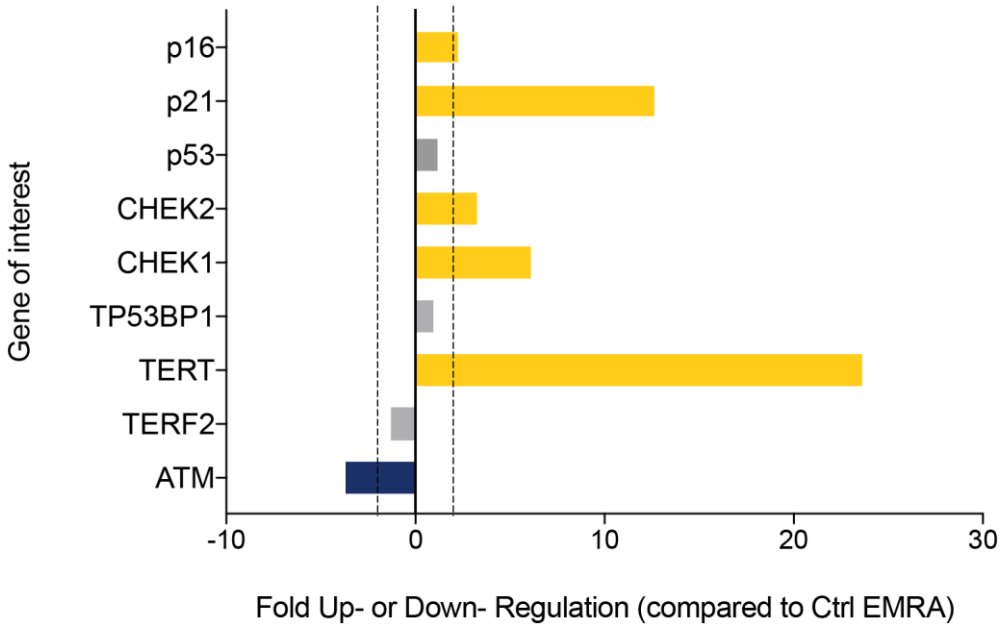

Figure 5.7: Expression of DNA damage and repair genes from the RT^2 array

Fold up- or Down-regulation of genes associated with DNA damage and repair in T2D $CD8^+$ EMRA T cells compared to control $CD8^+$ EMRAs. Fold change cut-off < 2, Control *n* = 3, T2D *n* = 3.

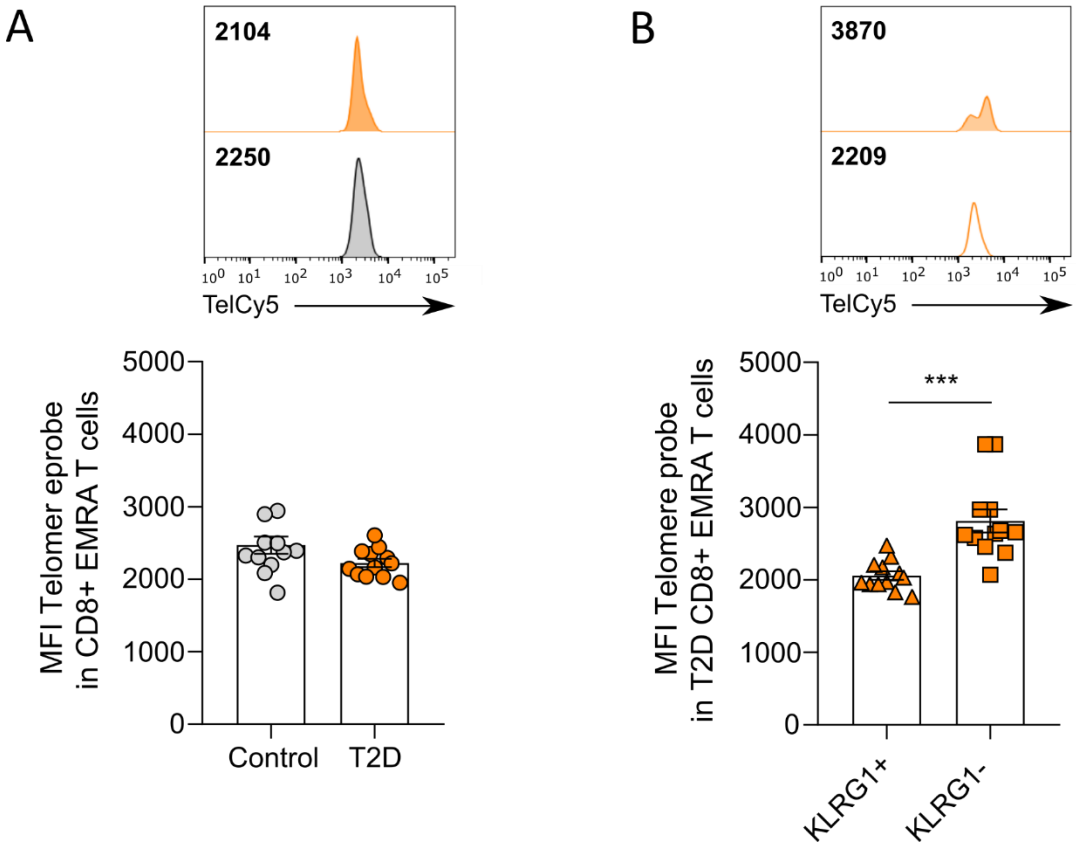

Figure 5.8: Telomere length in CD8⁺ EMRA T cells

A) Telomere length measured using Cy5 labelled telomere probe in Flow-FISH in Control CD8⁺ EMRA T cells and T2D EMRA T cells. Data expressed as mean ± SEM, control *n* = 12, T2D *n* = 12.

B) Telomere length measured using Cy5 labelled telomere probe in Flow-FISH with the KLRG1+ and – fractions of the T2D CD8⁺ EMRA T cell subset. Data expressed as mean ± SEM, *n* = 12. P value was determined using a paired T-test, p*** = 0.0004.

5.5.3. T2D EMRA T cells retain more proliferative capacity than control EMRAs

Another striking difference was the upregulation of numerous genes involved in cell cycle progression in T2D $CD8^+$ EMRA T cells compared with the healthy $CD8^+$ EMRA T cells (Figure 5.9A). This suggested that these cells might retain more proliferative capacity than age-matched control EMRA T cells. To validate this, Ki-67 was used to assess proliferative activity in $CD8^+$ EMRA T cells directly *ex vivo*. Intracellular staining did indeed reveal a significant increase in Ki-67 levels in the T2D $CD8^+$ EMRA T cells compared to age-matched $CD8^+$ EMRA T cells, which suggested that these cells have been arrested at an earlier stage prior to permanent cell cycle arrest (Figure 5.9B).

5.6. T2D EMRA T cells are less cytotoxic than control EMRAs

The role of a $CD8^+$ T cells is to efficiently kill viral infected or cancerous cells. Consequently, cytotoxicity is a vital characteristic of $CD8^+$ T cells and despite their senescent state $CD8^+$ EMRA T cells still exhibit potent cytotoxic activity (Henson et al., 2014). To investigate cytotoxicity in T2D $CD8^+$ EMRA T cells, we examined the levels of CD107a - a marker for T cell degranulation and cytotoxicity (Aktas et al., 2009). Surprisingly, CD107a levels were lower in the T2D $CD8^+$ EMRA T cells (Figure 5.10A). Furthermore, $KLRG1^-$ EMRA T cells were shown to have even lower CD107a levels, demonstrating that these cells have reduced cytotoxic ability (Figure 5.10B). Collectively, these data suggest that T2D $CD8^+$ EMRAs, in particular the $KLRG1^-$ subset, are less cytotoxic and therefore less able to carry out crucial T cell effector functions.

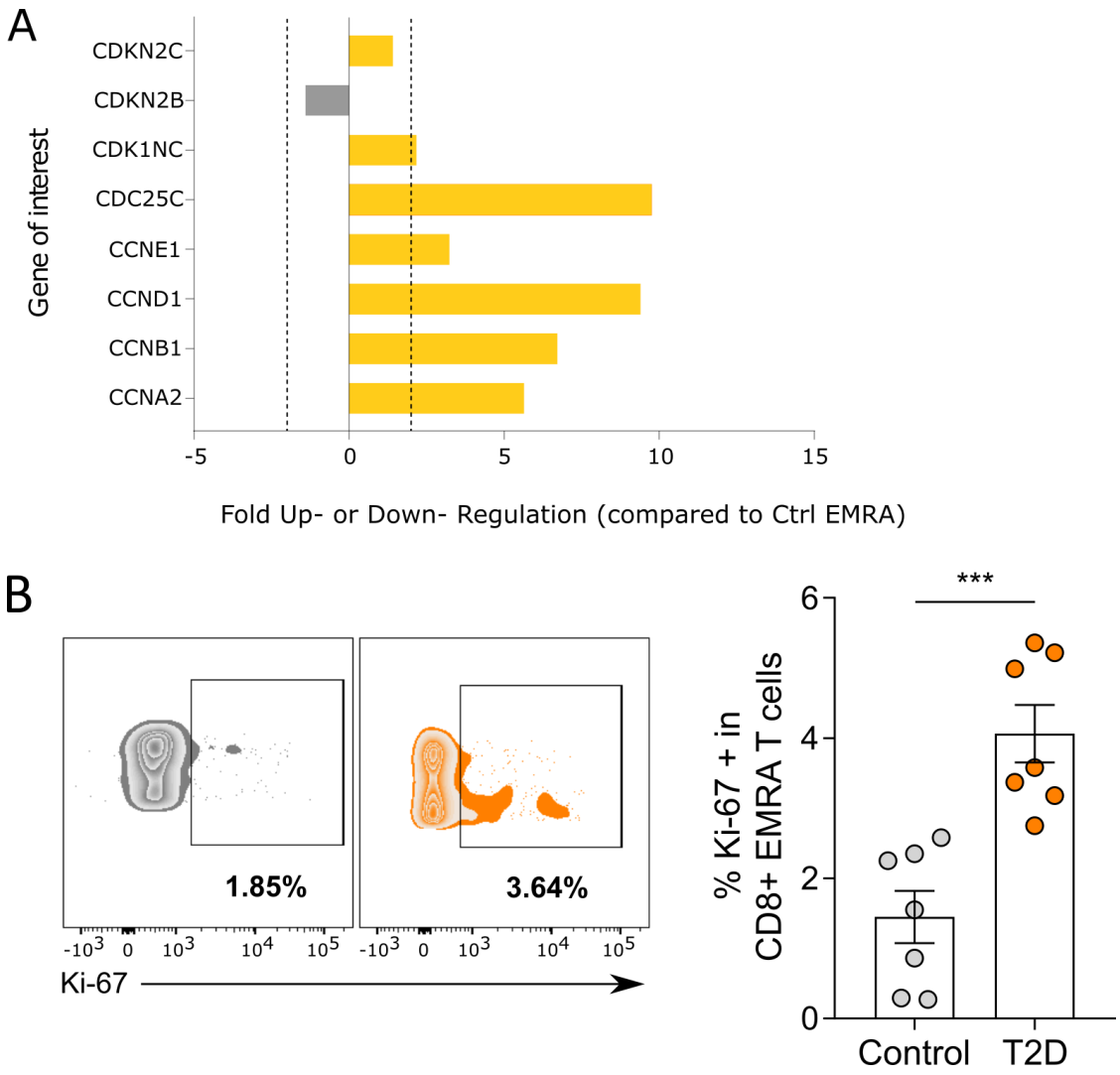

Figure 5.9: Cyclin gene expression and Ki-67 levels in CD8⁺ EMRA T cells

A) Fold up- or Down-regulation of genes associated with cell cycle progression from the RT² array in T2D CD8⁺ EMRA T cells compared to control CD8⁺ EMRAs. Fold change cut-off < 2, Control *n* = 3, T2D *n* = 3.

B) Ki-67 levels in control CD8⁺ EMRA T cells and T2D EMRA T cells. Data expressed as mean ± SEM, control *n* = 7, T2D *n* = 7. P value was determined using a paired T-test, p*** = 0.0005.

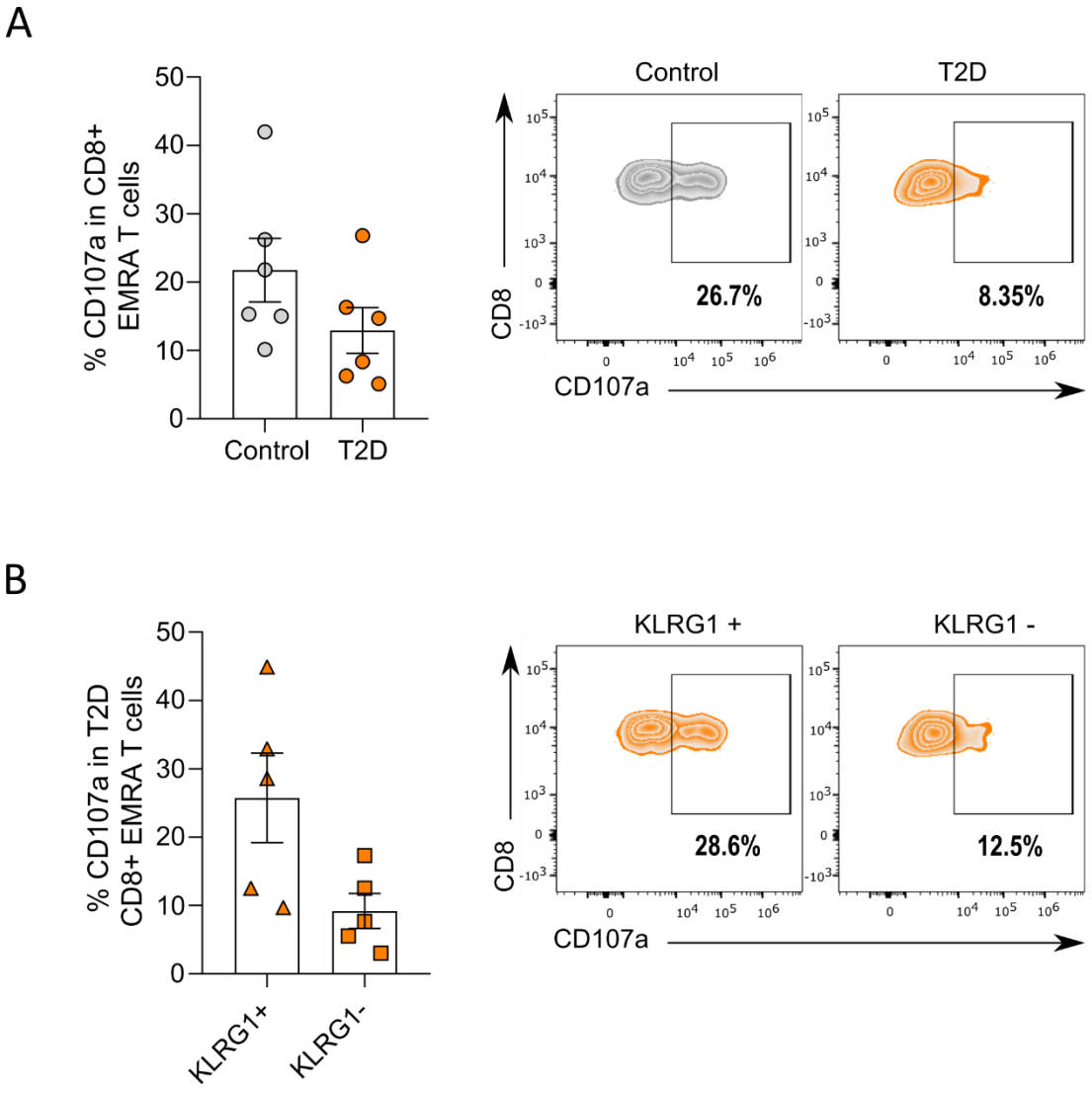

Figure 5.10: CD107a levels in CD8⁺ EMRA T cells

A) CD107a levels following 4-hour stimulation with aCD3 in the presence of monensin in control CD8⁺ EMRA T cells and T2D EMRA T cells. Data expressed as mean ± SEM, control *n* = 6, T2D *n* = 6.

B) CD107a levels following 4-hour stimulation with aCD3 in the presence of monensin in T2D CD8⁺ EMRA KLRG1⁺ and KLRG1⁻ T cells. Data expressed as mean ± SEM, control *n* = 5, T2D *n* = 5.

5.7. Premature senescence in T2D is driven by inflammation

The data so far in this chapter has highlighted the existence of a KLRG1$^-$ EMRA population in the T2D compartment. This population is likely being driven to senescence prematurely rather than reaching conventional replicative senescence as a result of repeated stimulation. This raised the question as to what was driving the premature senescence. To assess this, a series of culture experiments were conducted using the sera from T2D and healthy age-matched control donors to determine if certain factors within the sera could trigger less differentiated T cells to senesce.

5.7.1. Optimisation of sera culture experiment

In order to assess whether or not sera from T2D patients would result in an increase in senescent T cells, the culture conditions for the experiment first needed to be optimised. To do this, PBMCs from a young healthy donor were isolated and then cultured in either low (2.5mM) or high glucose (25mM) conditions with or without 10% FCS for 7 days before flow cytometry analysis. Cells cultured in both low and high glucose conditions remained viable at day 7 (Figure 5.11A). Furthermore, no difference in the percentage of CD8$^+$ EMRA T cells was observed between the low or high glucose conditions (Figure 5.11B). To mimic the environment of T2D, PBMCs from a young donor were then cultured for 7 days in high glucose media with either 10% T2D or healthy age-matched control sera.

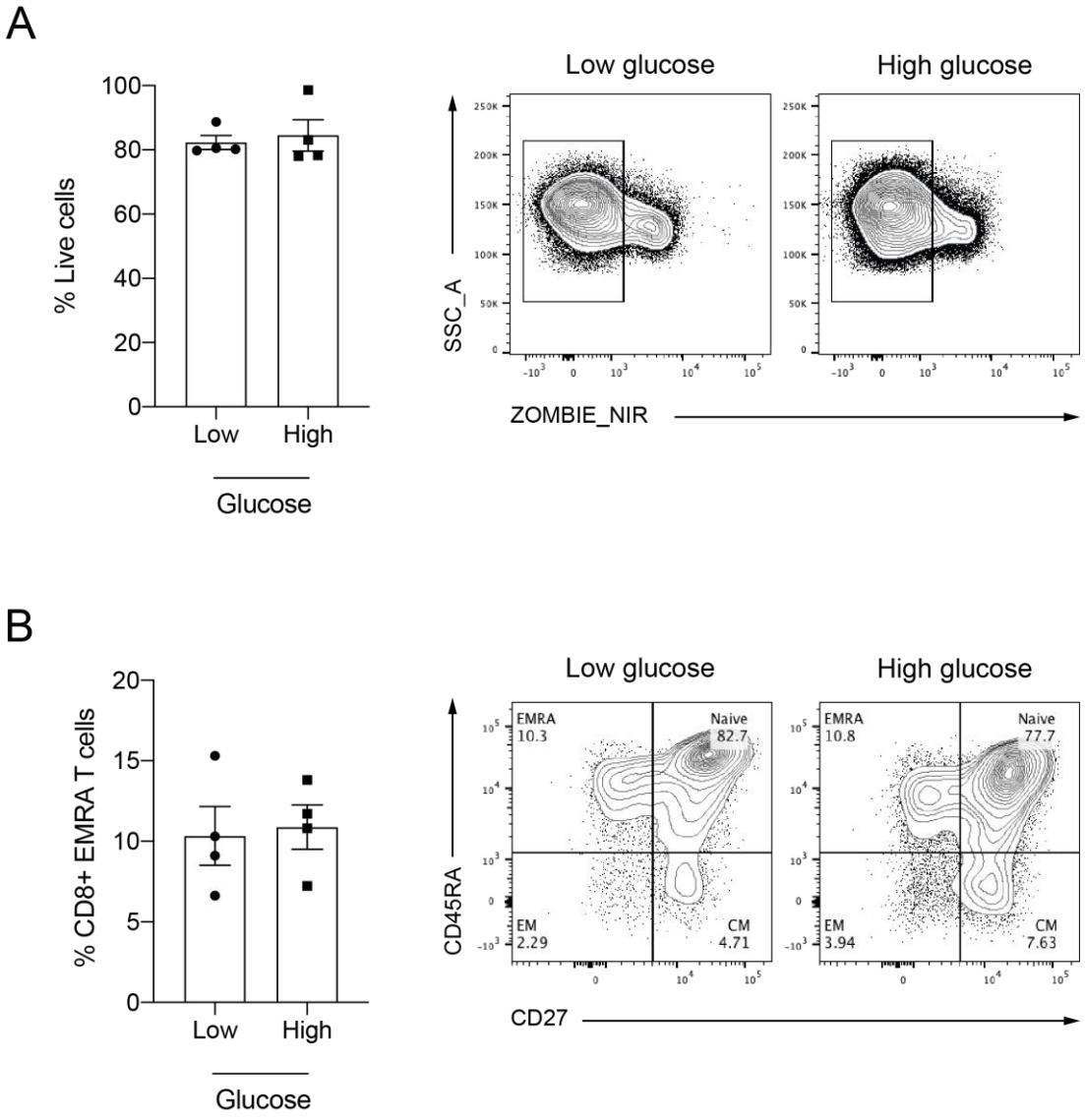

Figure 5.11: Optimisation of sera experiments

A) Percentage of live PBMCs following 7 days in culture with 10% FCS and either low (2.5mM) and high (25mM) glucose determined using ZOMBIE_NIR. Data expressed as mean ± SEM, Low *n* = 4, High *n* = 4.

B) Percentage of $CD8^+$ EMRA T cells following 7 days in culture with 10% FCS and either low (2.5mM) and high (25mM) glucose. Data expressed as mean ± SEM, Low *n* = 4, High *n* = 4.

5.7.2. T2D sera drives T cell senescence

PBMCs were phenotyped at day 0, 3 and 7 to assess whether these conditions could drive senescence. At day 3, no difference was observed between the two different conditions; however, by day 7 both the control sera and T2D sera resulted in an increase in the $CD8^+$ EMRA T cell population (Figure 5.12A and B). Despite both conditions driving an increase in EMRA T cells, the T2D sera drove this process significantly more than the control sera (Figure 5.12B). Moreover, *t*-SNE cluster analysis revealed that the type of EMRA T cells being generated in the two sera conditions were distinct (Figure 5.13 and 5.14). Incubation with control sera gave rise to an increase in EMRA 2, whereas T2D sera gave rise to both EMRA 1 and i-EMRAs (Figure 5.13 and 5.14).

5.7.3. T2D sera is highly pro-inflammatory

Following these culture experiments, the cytokine profiles of the sera was investigated. Both control and T2D sera contained numerous pro-inflammatory cytokines (Figure 5.15A and B). However, the T2D sera contained far more cytokines and the amounts of these cytokines were much greater than in the control sera (Figure 5.15B). Furthermore, a number of cytokines, such as CXCL1, IL-6, IL-8 and IL-16 were all present in the T2D sera, but completely absent in all control sera (Figure 5.15B). As a result of these sera experiments, we termed $KLRG1^-$ EMRA T cells inflammatory-derived EMRAs or i-EMRAs.

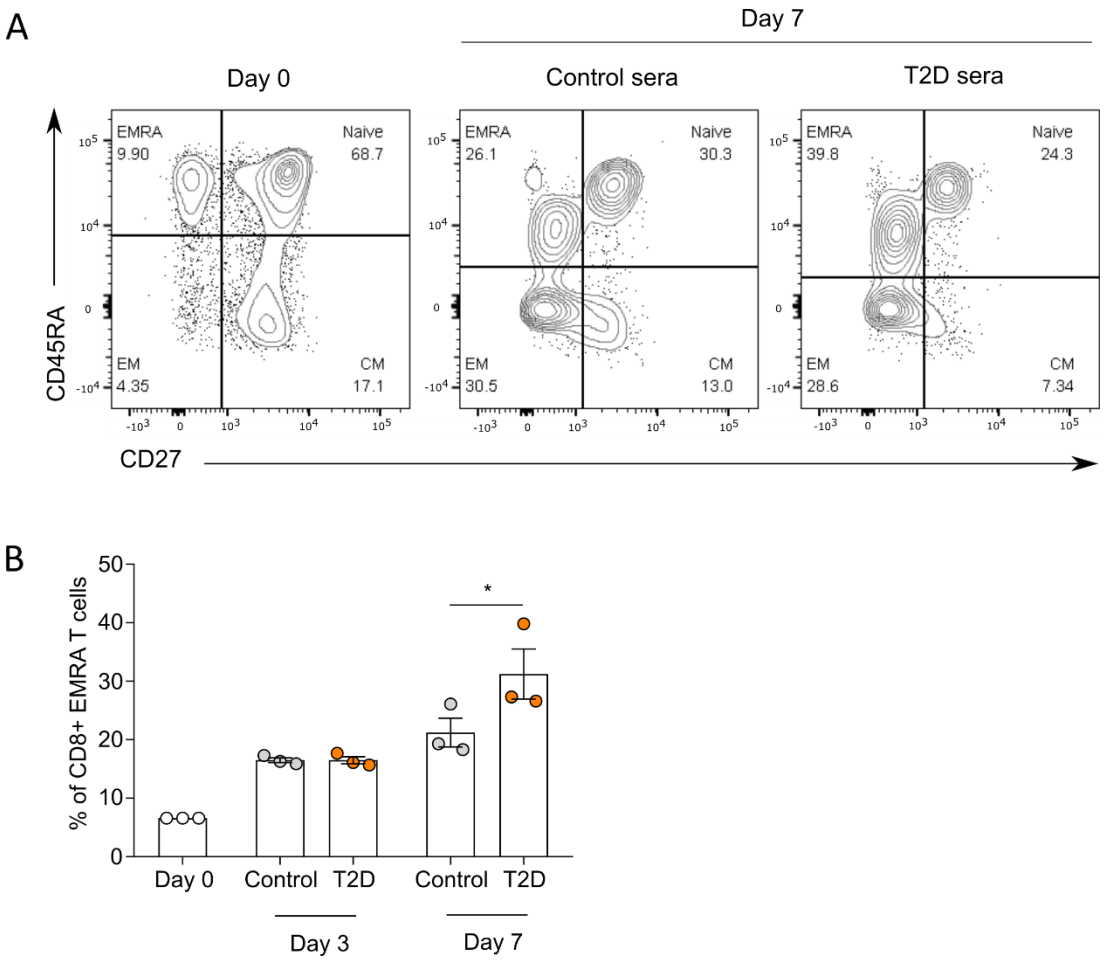

Figure 5.12: T2D sera drives CD8⁺ EMRA T cell generation

A) Representative dot plots of CD45RA/CD27 gating in CD8⁺ T cells at day 0 and 7 of culture with 10% sera from age-matched control and T2D donors.

B) Quantification of CD8⁺ EMRA T cells following incubating with 10% sera from age-matched control and T2D donors. Data expressed as mean ± SEM, *n* = 3 per condition. P value was determined using a paired T-test, p* = 0.0326.

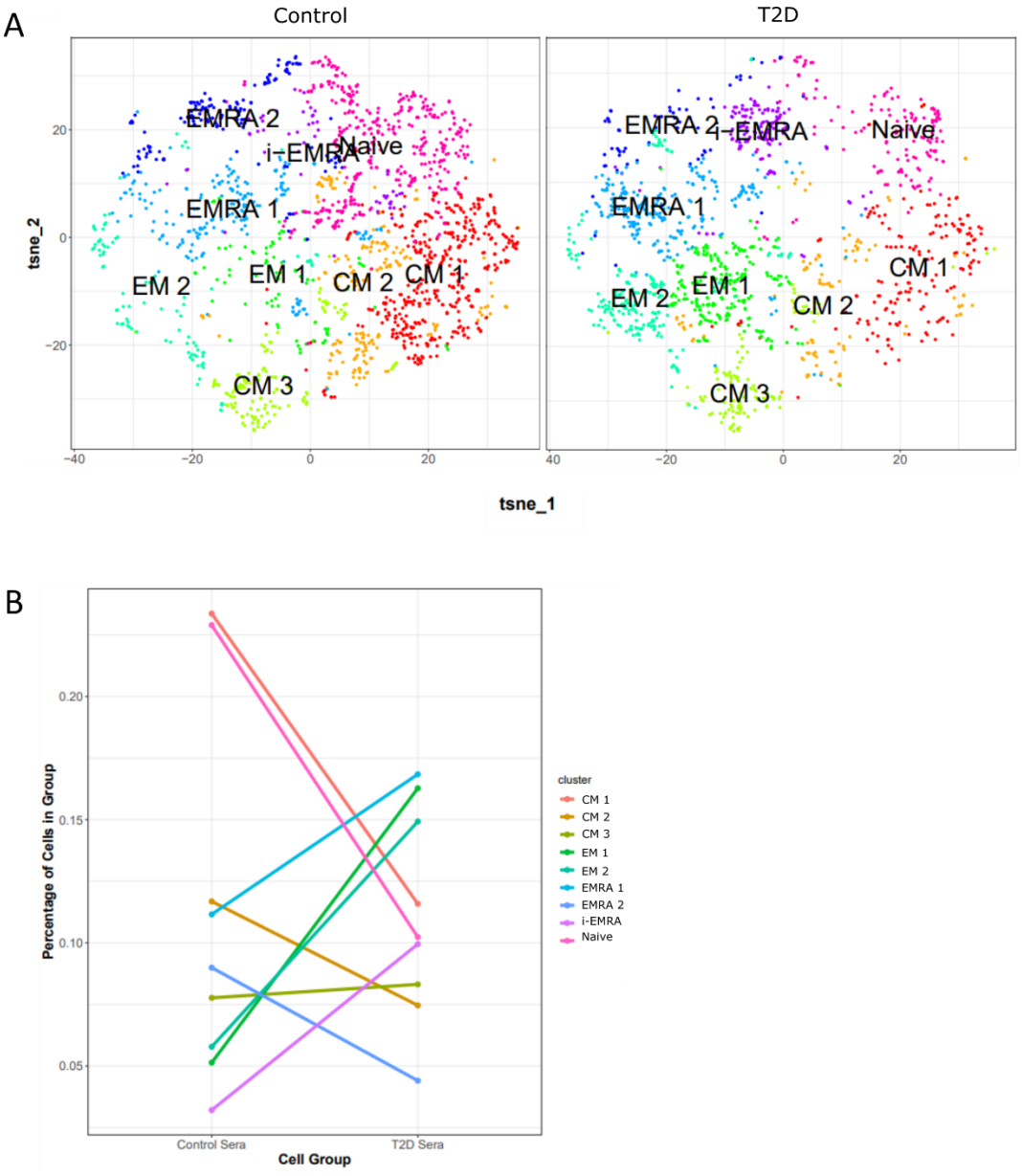

Figure 5.13: *t*-SNE cluster analysis of CD8⁺ T cells after incubation with T2D or control sera

A) Clusterplot analysis of CD8⁺ T cells following a 7-day incubation with either healthy age-matched control sera or T2D sera using CD27, CD28, CD45RA, CCR7 and KLRG1, *n* = 3.

B) Rate change plot showing the change in the percentage of cells in each group between control and T2D sera condition, *n* = 3.

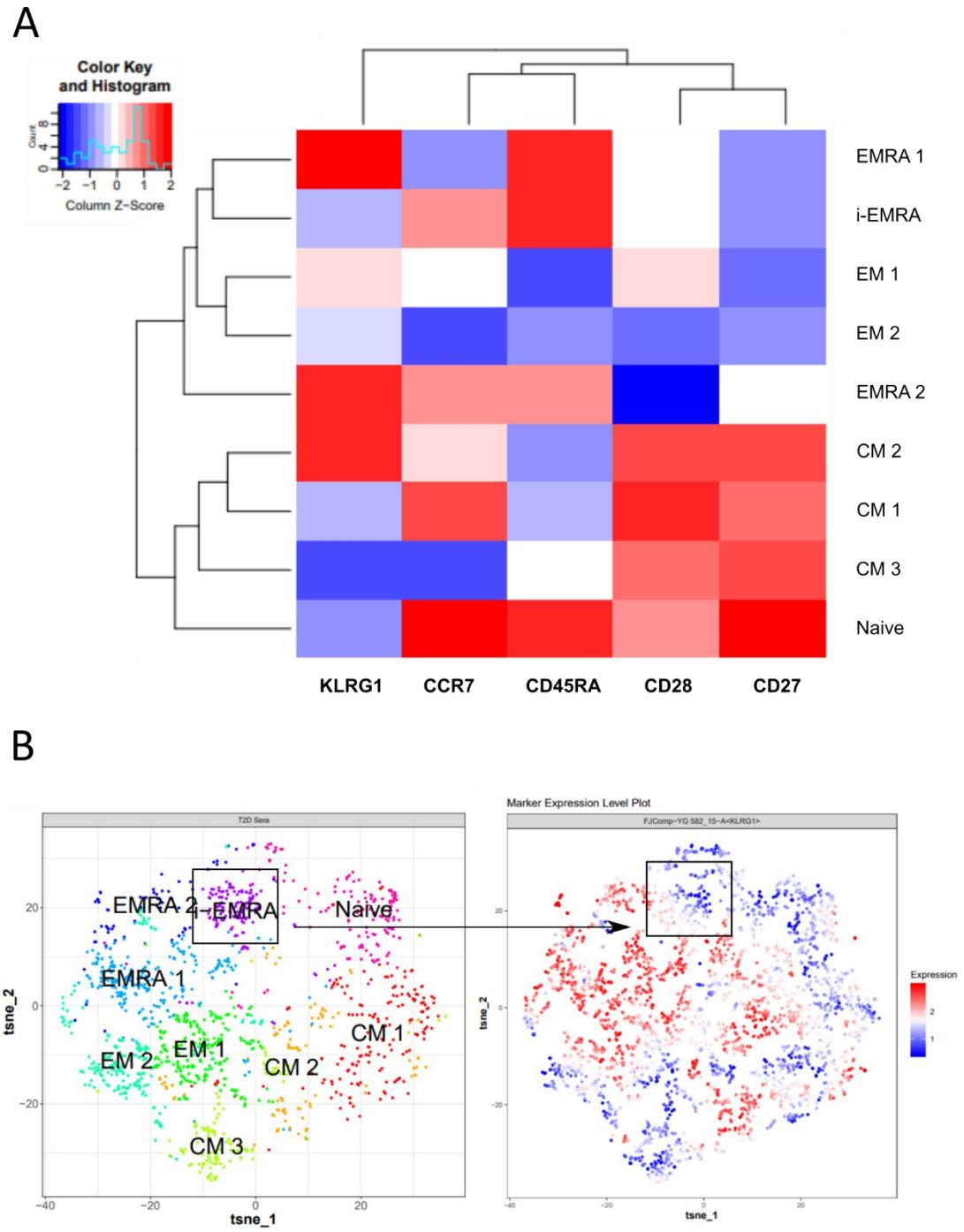

Figure 5.14: Marker expression data from *t*-SNE analysis

A) Heatmap to show protein levels of cell surface markers CD27, CD28, CD45RA, CCR7 and KLRG1 in each cluster group, *n* = 3.

B) KLRG1 expression plot to show the levels of KLRG1 throughout all of the cluster groups, *n* = 3.

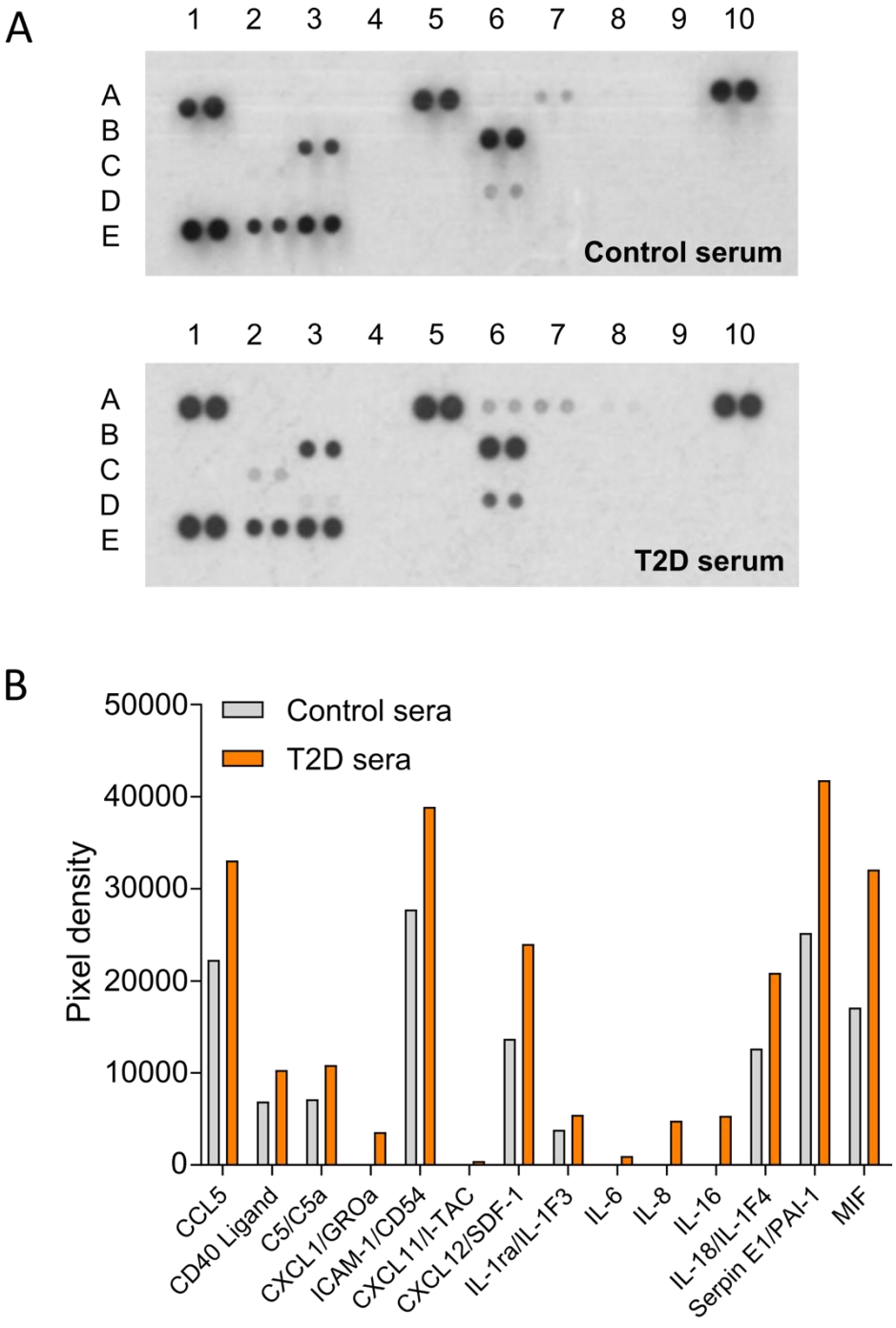

Figure 5.15: T2D sera is pro-inflammatory

A) Representative cytokine array membrane following incubation with control or T2D serum.

B) Cytokine levels quantified from the pixel densities of cytokine spots on the array membranes. Control *n* = 4, T2D *n* = 4.

5.8. T2D alters the mitochondrial and metabolic properties of $CD8^+$ EMRAs

As illustrated in chapter 4, mitochondrial health and cellular metabolism can heavily influence the onset of senescence in T cells. $CD8^+$ EMRA T cells exhibit mitochondrial dysfunction and impaired OXPHOS (Henson et al., 2014); however, the metabolic properties of $CD8^+$ EMRA T cells from people living with T2D are not known.

5.8.1. Mitochondrial ROS is elevated in T2D EMRA T cells

Mitochondrial mass, determined by Mitotracker green staining, was unchanged between the healthy age-matched control and T2D $CD8^+$ EMRA T cells (Figure 5.16A and B). However, data obtained from the RT^2 array suggested that mitochondria from T2D EMRAs may be producing more ROS than the control EMRAs. NADPH oxidases 4 (NOX4) was greatly upregulated in the T2D $CD8^+$ EMRA T cells compared with the control EMRAs (Figure 5.17A). NOX enzymes, including NOX4, are major contributors to cellular ROS (Chen et al., 2012). The mitochondrial gene; superoxide dismutase 2 (SOD2), which converts superoxide by-products of OXPHOS into hydrogen peroxide and diatomic oxygen (Velarde et al., 2012), was also elevated (Figure 5.17A). This is likely an attempt to reduce the damaging effects of elevated oxidative stress. However, despite SOD2 expression, examination of mtROS levels using the mitochondrial superoxide indicator MitoSOX revealed that mtROS levels were higher in T2D EMRA subsets compared with the control EMRAs (Figure 5.17B and C).

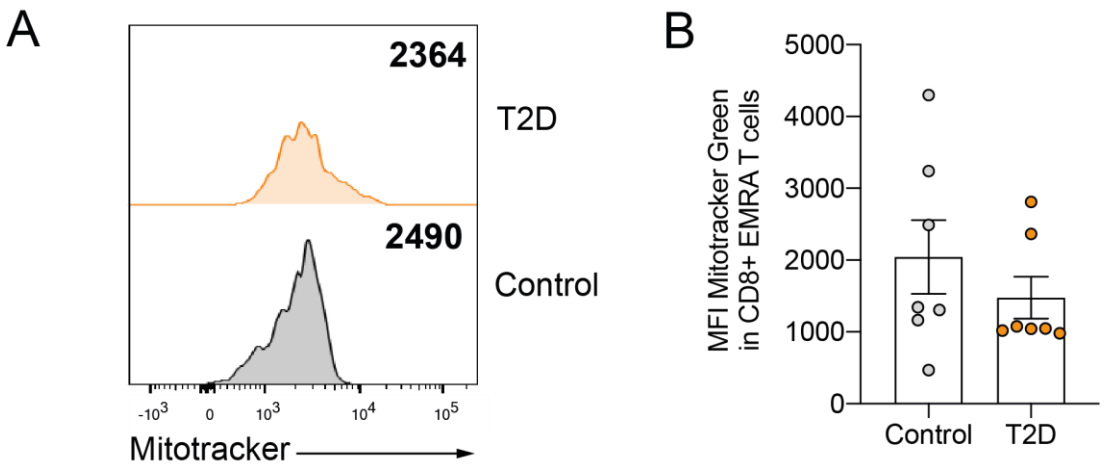

Figure 5.16: Mitochondrial mass in $CD8^+$ EMRA T cells

A) Representative histograms of Mitotracker Green in control and T2D $CD8^+$ EMRAs.

B) Quantification of mitochondrial mass using MitoTracker Green in control and T2D $CD8^+$ EMRA T cells. Data expressed as mean ± SEM, control n = 7, T2D n = 7. Difference not statistically significant.

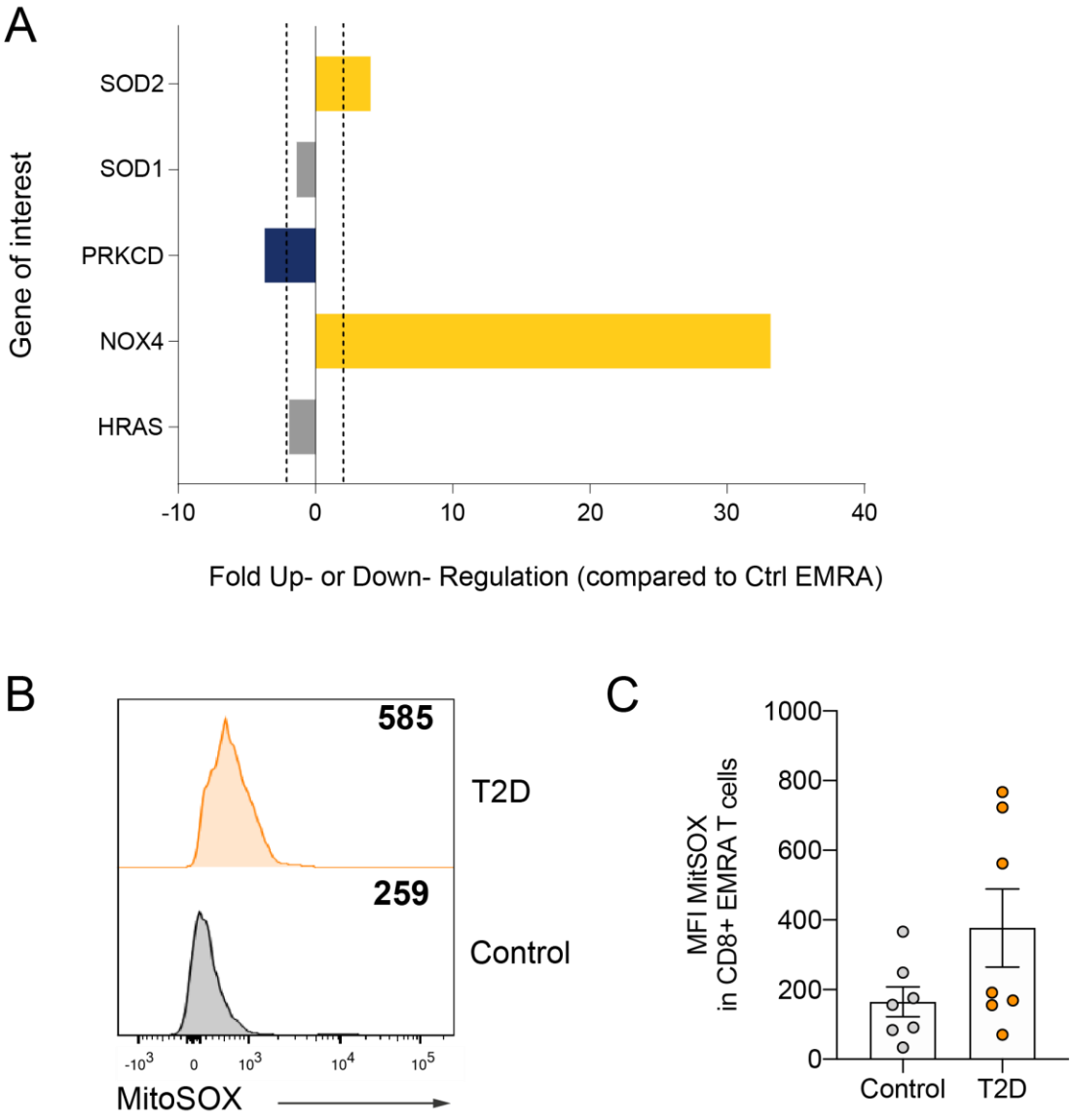

Figure 5.17: Elevated oxidative stress in T2D CD8⁺ EMRA T cells

A) Fold up- or Down-regulation of genes associated with oxidative stress from the RT^2 array in T2D CD8⁺ EMRA T cells compared to control CD8⁺ EMRAs. Fold change cut-off < 2, Control *n* = 3, T2D *n* = 3.

B) MitoSOX staining in control CD8⁺ EMRA T cells and T2D EMRA T cells. Data expressed as mean ± SEM, control *n* = 7, T2D *n* = 7.

5.8.2. CD8$^+$ T cells from T2D donors have increased oxidative respiration

Due to the limiting cell numbers obtained from T2D blood donations, it was not possible to acquire enough CD8$^+$ EMRA T cells to run a seahorse assay on this subset. Instead, the bioenergetic profiles of whole CD8$^+$ T cells from healthy age-matched control and T2D donors were compared (Figure 5.18A). Interestingly, CD8$^+$ T cells from people living with T2D had an elevated basal and maximal OCR (Figure 5.18B and C).

5.8.3. T2D CD8$^+$ EMRA T cells have altered nutrient uptake

To determine what energy source could be fuelling the increased oxidative respiration, we assessed nutrient uptake using the fluorescent glucose analogue; 2-NBDG. and fluorescent palmitate analogue; BODIPY C 16. Unsurprisingly, we found that T2D CD8$^+$ EMRA T cells displayed a lack of glucose uptake (Figure 5.19A). In contrast, CD8$^+$ EMRA T cells from T2D donors had a significant increase in palmitate uptake (Figure 5.19B). Consequently, we used the Seahorse XF Palmitate assay to investigate FAO. In this assay, cells were first conditioned in nutrient-limited media, then treated with palmitate and subjected to the sequential injection of respiration modulators (Figure 5.20A). FAO was found to be significantly decreased in T2D CD8$^+$ T cells (Figure 5.20B and C). As palmitate was not being utilised, we subsequently used Nile Red to assess the accumulation of lipid droplets. This revealed that CD8$^+$ EMRA T cells from T2D donors were indeed accumulating lipid (Figure 5.21). Unfortunately, these experiments were unable to determine what energy source was being utilised during the initial mitochondria stress test (Figure 5.20).

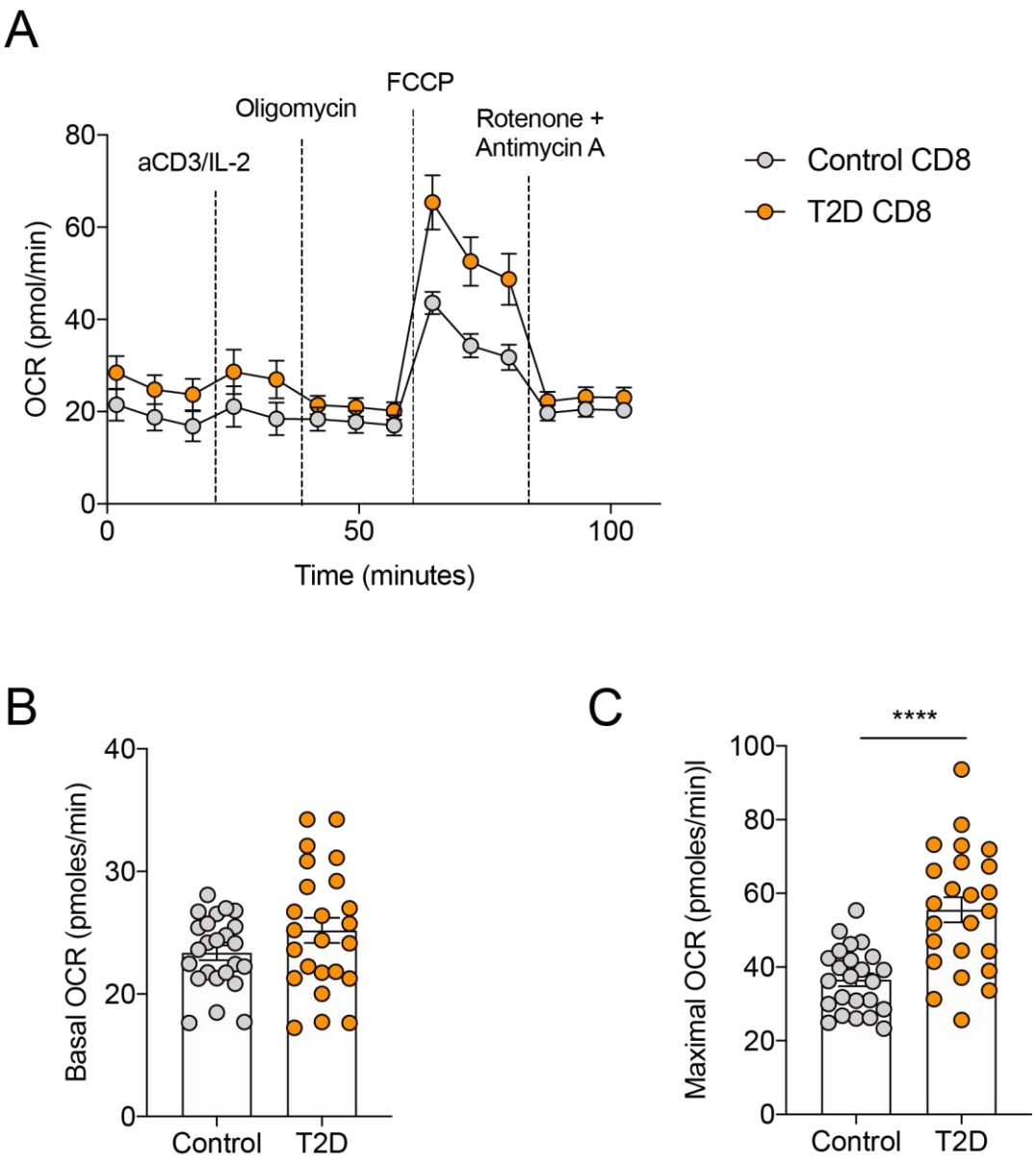

Figure 5.18: The bioenergetics profiles of T2D CD8⁺ T cells

(A) OCR of the CD8⁺ T cells was measured after 15-minute stimulation with 0.5 µg/ml anti-CD3 and 5 ng/ml IL-2, cells were subjected to a mitochondrial stress test using indicated mitochondrial inhibitors. Data are representative of 4 independent experiments. (B) Basal OCR and (C) the Maximal respiration after 15-minute stimulation with 0.5 µg/ml anti-CD3 and 5 ng/ml IL-2 (*n* = 4).

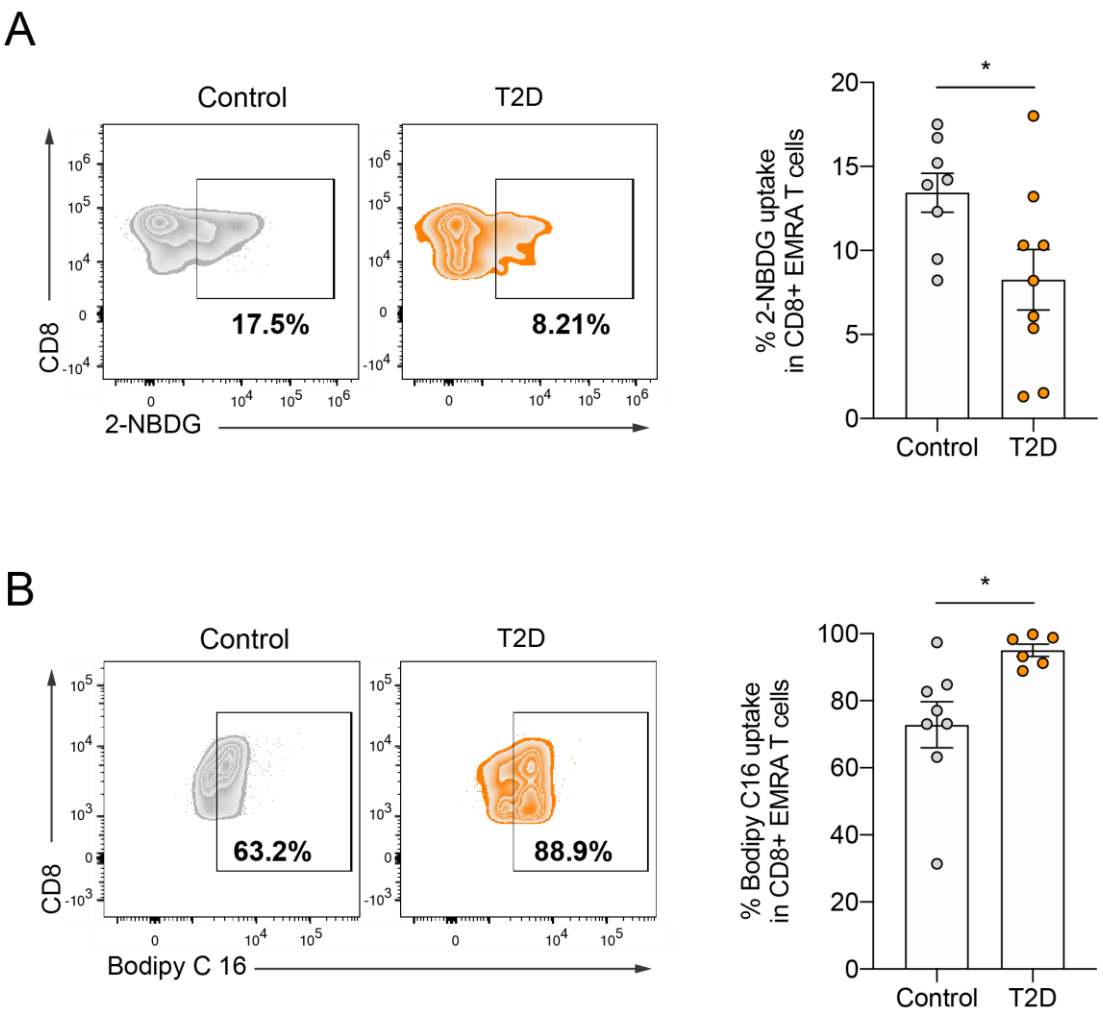

Figure 5.19: Glucose and lipid uptake in CD8⁺ EMRA T cells

A) Glucose uptake assessed using 2-NBDG in glucose free media. Representative dot plots and cumulative data. Data expressed as mean ± SEM, control *n* = 8, T2D *n* = 8. P value was determined using an unpaired T-test, p* = 0.0330.

B) Lipid uptake assessed using BODIPY C16. Representative dot plots and cumulative data. Data expressed as mean ± SEM, control *n* = 8, T2D *n* = 6. P value was determined using an unpaired T-test, p* = 0.0191.

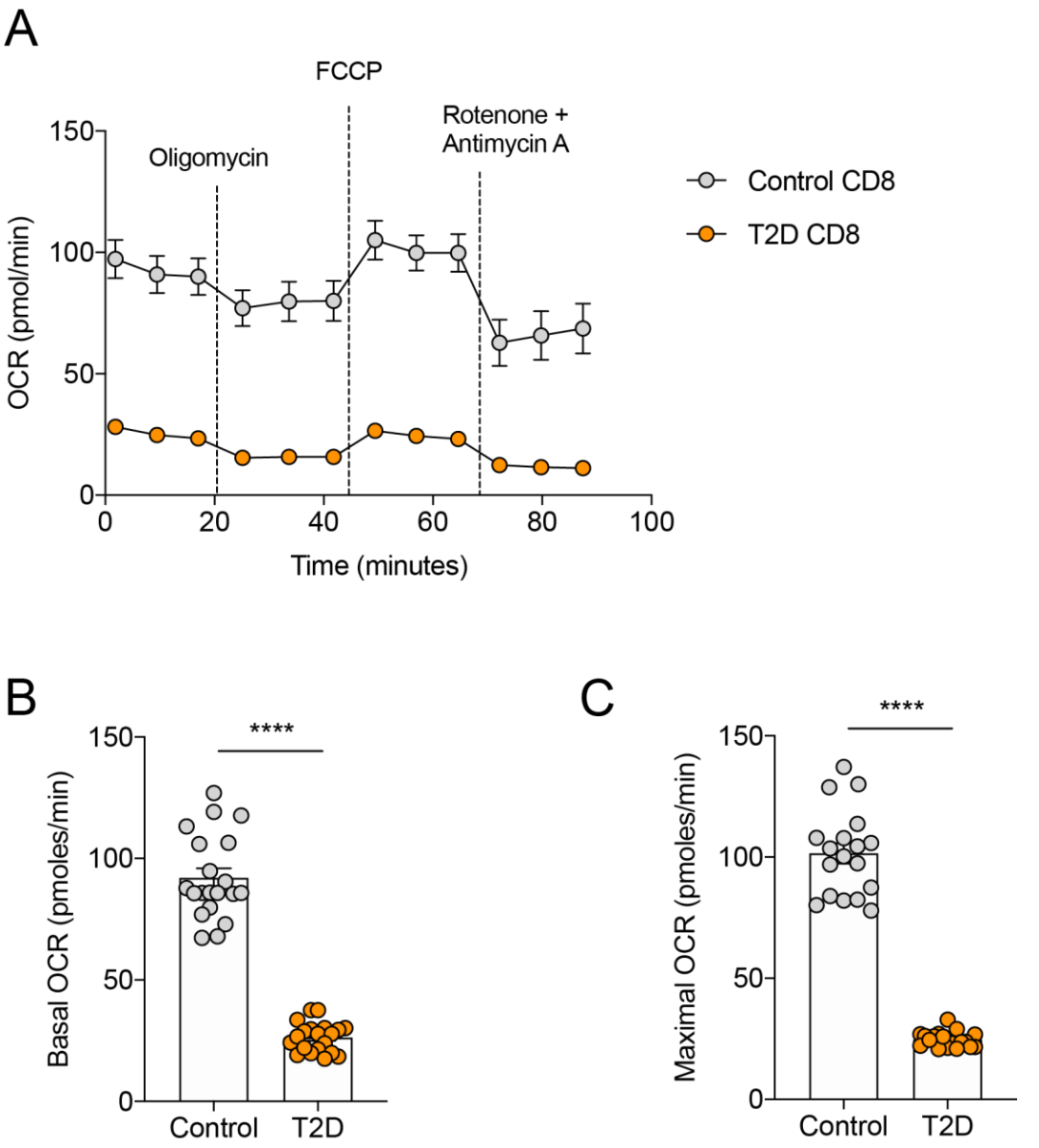

Figure 5.20: Fatty acid oxidation in CD8$^+$ T cells

A) FAO determined OCR of the CD8$^+$ T cells was measured after 15-minute stimulation with 0.5 µg/ml anti-CD3 and 5 ng/ml IL-2 and incubation with palmitate. Cells were subjected to a mitochondrial stress test using indicated mitochondrial inhibitors. Data are representative of 2 independent experiments.

B) Basal OCR and C) the Maximal respiration after 15-minute stimulation with 0.5 µg/ml anti-CD3 and 5 ng/ml IL-2 (n = 2).

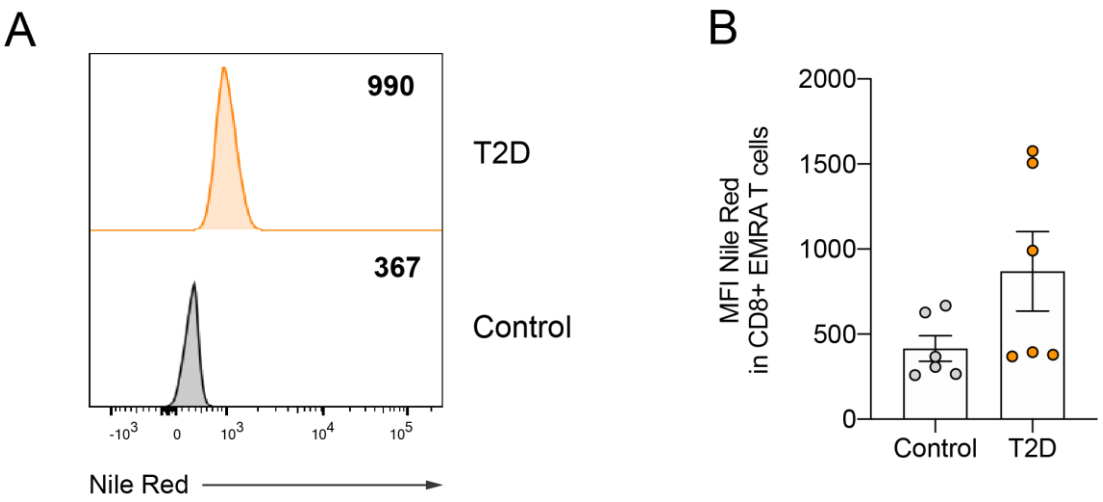

Figure 5.21: Lipid droplets in CD8⁺ EMRA T cells

A) Representative histograms of Nile Red in control and T2D CD8⁺ EMRAs.

B) Quantification of Lipid droplets using Nile Red in control and T2D CD8⁺ EMRA T cells. Data expressed as mean ± SEM, control *n* = 6, T2D *n* = 6.

5.8.4. T2D EMRA T cells have reduced AMPK levels

Following the observations of altered nutrient usage in T2D CD8⁺ EMRA T cells we examined the levels of intracellular phosphorylated AMP-activated protein kinase (pAMPK) - a master regulator of both glucose and lipid metabolism (Hardie et al., 2012). pAMPK was found to be reduced in the T2D CD8⁺ EMRA T cells compared to the healthy age-matched control EMRAs (Figure 5.22).

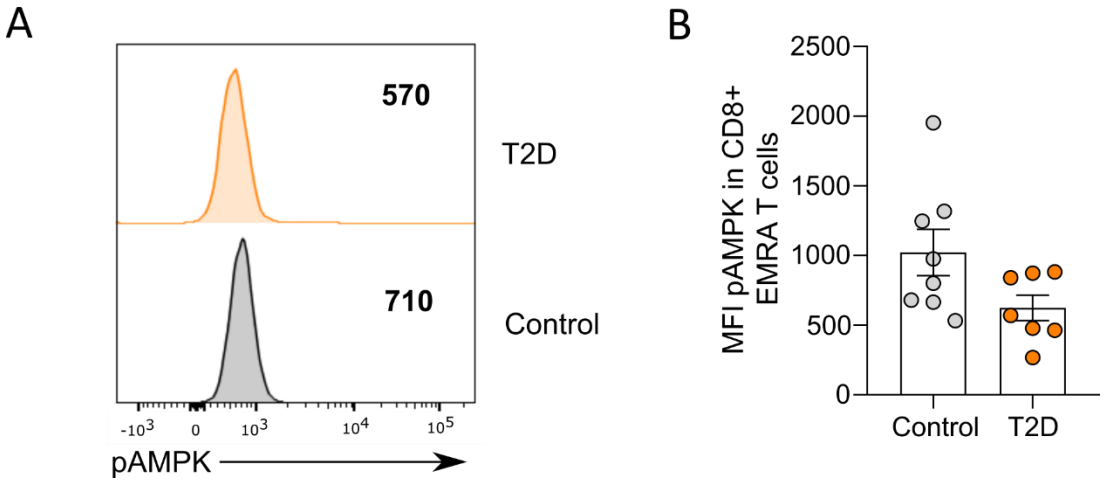

Figure 5.22: pAMPK levels in CD8⁺ EMRA T cells

A) Representative histograms of pAMPK in control and T2D CD8⁺ EMRAs.

B) Quantification of pAMPK in control and T2D CD8⁺ EMRA T cells. Data expressed as mean ± SEM, control *n* = 8, T2D *n* = 7. Difference not statistically significant.

5.9. Discussion

Many chronic viral infections, such as CMV and HIV, have been shown to drive replicative senescence in the $CD8^+$ T cell lineage (Ibegbu et al., 2006; Voehringer et al., 2001). For example, in people living with HIV, a large portion of virus specific $CD8^+$ T cells are shown to express high levels of KLRG1. In this chapter we show the accumulation of $CD8^+$ EMRA T cells in people living with T2D. Interestingly, a subgroup of these EMRA T cells had no KLRG1. Moreover, T2D $CD8^+$ EMRA T cells were found to retain some of their proliferative capacity and had longer telomeres, demonstrating that they were not generated through telomere dysfunction and replicative senescence. Surprisingly, CHEK1 and CHEK2 were upregulated despite a downregulation of the ATM. Furthermore, while p53 remained unchanged, p21 and to a lesser extent p16 were both up-regulated in T2D EMRA T cells. Interestingly, CHEK2 has been previously shown to activate p21 in a p53-independent manner in the absence of telomere dysfunction (Aliouat-Denis et al., 2005). Therefore, a similar telomere-independent mechanism involving the CHEK proteins and p21 may be responsible for the induction of premature senescence in people living with T2D.

We believe that the complete absence of KLRG1 and the positioning of the i-EMRA population next to the true naïve T cells in the *t*-SNE analysis is a big indicator as to the origin of these cells. Rather than differentiating from EM T cells as conventional EMRAs do, we propose that naïve $CD8^+$ T cells are forced into a prematurely senescent state due to the elevated inflammatory milieu these cells are subjected to in T2D. Consequently, we termed the $KLRG1^-$ EMRA population; i-EMRAs.

Inflammation plays a key role in the pathogenesis of many age-related and chronic diseases. For instance, in atherosclerosis immune cells are a key pathological player during plaque development and rupture (Libby, 2012). Numerous studies have shown a correlation between elevated levels of inflammatory markers, such as IL-6 and C-reactive protein, and the risk of cardiovascular events (Kaptoge et al., 2012; Pai et al., 2004; Ridker et al., 2000). Here we found that despite the use of medication to manage their disease, T2D donors exhibited greater levels of cytokines in their blood serum when compared to the age-matched control donors. Of course, it is hard to assess what the impact of these medications themselves are; however, it would be extremely difficult to find a large enough cohort of people living with T2D that did not manage their disease through medication to test this. Nevertheless, we found no correlation between the number of medications people were on and the number of $CD8^+$ EMRA T cells. As a result, we are confident that the increase in $CD8^+$ EMRA T cells, particularly the i-EMRA subset, is not due to the use of medication.

TNF-α plays a crucial role in insulin resistance and the onset of T2D (Moller, 2000). Moreover, *in vitro* studies have shown that incubation with TNF-α is enough to drive the onset of T cell senescence. However, no TNF-α was detected in the sera of T2D donors in our cytokine array analysis. We propose that this is due to both the short-lived nature of TNF-α and the fact that all of our study participants had been living with T2D for on average 15 years and were managing their disease through numerous medications. As a result, the chronic inflammatory cytokine signatures of these donors are likely to be different to the acute inflammatory cytokine signatures

present during the onset of disease. At this stage it is not possible to attribute the generation of i-EMRAs to a particular cytokine or combination of cytokines. In order to assess this, future experiments are be needed to fully appreciate the contribution of each cytokine to i-EMRA generation.

In addition to the inflammatory environment T cells are exposed to in T2D, senescent T cells themselves are highly pro-inflammatory and secrete a SASP (Callender, Carroll, Beal, et al., 2018), reinforcing both the senescent and inflammatory phenotype of these cells. Due to the elevated inflammatory environment that generates i-EMRA T cells in people living with T2D, we hypothesise that $CD8^+$ i-EMRA T cells will be more pro-inflammatory than conventional EMRAs. However, in order to confirm this hypothesis a robust assessment of secreted cytokines is needed. Moreover, the levels of secreted perforin and granzyme B should also be examined in order to validate that this subset has reduced cytotoxic ability. Clinically, these potential functional impairments may be responsible, at least in part, for some of the classical diabetic complications, such as increased rates of infection and impaired wound healing (Galkowska et al., 2005; Muller et al., 2005). Therefore, to confirm this we also propose conducting additional cytotoxic T cell killing assays.

Since T2D is also characterised by metabolic imbalances we began to investigate T cell metabolism in the context of T2D. Mitochondria from T2D $CD8^+$ T cells had higher oxidative capacity and T2D EMRA T cells had increased levels of mtROS compared to healthy age-matched control cells. Oxidative stress in T2D is known to contribute to

vascular complications such as atherosclerosis (Baynes and Thorpe, 1999; Dandona et al., 1996). Additionally, mtROS can also result in DNA damage and senescence (Davalli et al., 2016). Therefore, elevated mtROS levels in T2D $CD8^+$ EMRA T cells could result in damage to the extracellular environment in which they sit and may also act to reinforce the senescent phenotype of these cells.

In activated T cells, insulin stimulates glucose uptake and enhances T cells responsiveness and energy requirements necessary for appropriate T cell function (Stentz and Kitabchi, 2005). It is therefore unsurprising that $CD8^+$ EMRA T cells in the context of T2D, characterised by insulin resistance and deficiency, had impaired glucose uptake. pAMPK, which is usually activated in response to low glucose and positively regulates FAO (Hardie, 2004; Xu et al., 2012), was reduced in T2D $CD8^+$ EMRA T cells. Decreased AMPK could provide an explanation for the lack of FAO in these cells. Furthermore, if AMPK levels were increased in these cells FAO may be restored and the accumulation of FA in lipid droplets avoided.

As glucose uptake and FAO are both impaired, it remains unclear what energy source T2D $CD8^+$ T cells are metabolising. One potential candidate is glutamine. Glutamine-mediated metabolism has been shown to be important during T cell activation and proliferation (Carr et al., 2010). Furthermore, it is used in many cell types in order to fuel oxidative metabolism under stress conditions (Chendong et al., 2009; Le et al., 2012). However, as glutamine uptake is also positively regulated by pAMPK (Blagih

et al., 2015), the reduced pAMPK levels in T2D EMRAs mean this hypothesis is unclear. To be certain, specific glutamine uptake assays need to be conducted.

Due to limiting cell numbers and fluorescent markers we had available we were unable to examine mitochondrial and metabolic differences between the conventional EMRA and i-EMRA subsets. However, moving forward it would be interesting to see whether or not the differences described here are present in both EMRA subsets or not.

In summary, this chapter identified a previously undescribed subset of $CD8^+$ $KLRG1^-$ EMRA T cells, which are derived through chronic inflammation; i-EMRAs. The fact that these cells are derived from an early subset and not through replicative senescence suggests there is potential to reverse this phenotype. Furthermore, impaired nutrient uptake and usage in $CD8^+$ EMRA T cells in T2D is likely to have a profound effect on T cell function. Consequently, a better understanding of these metabolic abnormalities is crucial as metabolic manipulation of these cells may restore correct T cell function and help reduce the impact of T cell dysfunction in T2D.

Chapter six: General Discussion

The overall aim of this thesis was to examine the heterogeneous nature of senescent T cells. In particular, mechanisms of premature T cell senescence were investigated using T2D as a model system. Furthermore, the relationship between cell metabolism and the extent of T cell senescence was compared in the $CD8^+$ and $CD4^+$ T cell lineages.

6.1. T cell senescence: more than proliferative stress

It is well established that age significantly impacts the immune system, with age-related defects leading to an inability to respond to new and emerging diseases, as well as decreased vaccination efficiency (Naylor et al., 2005). Many of these problems can be attributed to alterations in the T cell compartment, manifested by a reduced pool of naïve T cells and the accumulation of senescent T cells. To date, the majority of senescent T cell research has focused on replicative senescence in response to repeated antigen stimulation or chronic viral infections such as CMV (Chou and Effros, 2013). However, as premature senescence is well document in other cell types such as fibroblasts (Kang et al., 2011; Serrano et al., 1997; Toussaint et al., 2002), it is likely that T cells are also susceptible to the induction of premature senescence.

At the molecular level p53, p16 and p21 have all been shown to play a role in replicative senescence; however, they can also act independently of telomere erosion and proliferative stress. For example, p16 has been shown many times to

accumulate in human fibroblasts that have reached their finite proliferative capacity in culture (Alcorta et al., 1996; Hara et al., 1996; Wong and Riabowol, 1996), even in the absence of p53 (Jacobs and De Lange, 2004; Mirzayans et al., 2012). Furthermore, p16 is also associated with oncogene-mediated premature senescence (Serrano et al., 1997) and in other cell types, such as human mammary epithelial cells, it has been shown that senescence is not related to replicative senescence mediated by telomere erosion but instead by p16 upregulation (Ramirez et al., 2001, 2003). This type of p16 associated premature growth arrest, which occurs independently of telomere erosion, has been referred to as a stress senescence signalling pathway. However, as these premature phenotypes occur independent of proliferative lifespan and age some have argued that the term senescence should be avoided. Instead, some researchers refer to these stress induced phenotypes as stasis (Drayton and Peters, 2002; Feijoo et al., 2016). Controversially, p16 induced stasis has sometimes been seen as an experimental artefact due to inadequate culture conditions; however, others believe that stasis is an evolutionary defence mechanism that safeguards a cell from diverse stresses (Drayton and Peters, 2002).

In T2D, we observed the accumulation of $CD8^+$ EMRA T cells; however, in comparison to healthy age-matched control EMRA T cells, they expressed lower levels of p53 and retained more proliferative capacity. Consequently, we concluded that they resembled an earlier subset that had undergone premature senescence. Although these cells did have slightly elevated p16 levels, p16 is also expressed during effector T cell differentiation and therefore not considered sufficient enough alone to indicate

T cell senescence (Goronzy and Weyand, 2019). On the other hand, p21 was highly elevated in T2D EMRA T cells. Therefore, we propose that the induction of premature senescence in these cells is through a p21 mediated mechanism independent of p53. Evidence for such mechanism has previously been shown in lung and breast carcinoma cells and immortalised human keratinocytes (Aliouat-Denis et al., 2005). The CHEK2 kinase, which was also elevated when we performed the cellular senescence array, was shown to be central in this pathway. To confirm this hypothesis, further validation that quantifies the protein levels of p21, p53 and p16 in T2D EMRA T cells compared to healthy age-matched control EMRAs should be done. Furthermore, p21 knockdown and overexpression studies would be necessary to demonstrate the importance of p21.

6.2. Inflammation and premature T cell ageing

Here we used the model system of T2D to show that inflammation acts as a stress signal and drives the generation of premature i-EMRA T cells, which are phenotypically and functionally distinct from conventional EMRAs. It is likely that $CD8^+$ i-EMRA T cells are also present in the general population; however, the elevated inflammation in T2D results in a greater accumulation of them. Conventional $CD8^+$ EMRA T cells are highly associated with ageing. However, as i-EMRA T cell generation is determined by inflammation and not replicative senescence we propose that i-EMRAs are not associated with ageing. To examine this, the frequency of $CD8^+$ i-EMRA T cells in a younger cohort of T2D individuals would be necessary.

The lack of KLRG1 on the surface of these cells make them easily detectable from conventional EMRAs. It also highlights that these cells are derived from a much earlier subset, most likely naïve T cells, rather than through the linear differentiation model that is usually associated with EMRA T cells. Interestingly, $CD8^+$ resident memory (RM) EMRA T cells, which reside in the skin, have also been shown to express significantly lower KLRG1 than peripheral blood $CD8^+$ EMRA T cells (Seidel et al., 2018). Furthermore, similar to $CD8^+$ i-EMRA T cells, $CD8^+$ RM EMRA T cells have low cytotoxic potential. (Seidel et al., 2018).

KLRG1 is not the only inhibitory receptor that accumulates on conventional $CD8^+$ EMRA T cells. Other NK receptors, such as CD57 and NKG2A, also increase (Pereira et al., 2019; Tarazona et al., 2001). The expression of NK receptors in these cells has been proposed to contribute to the regulation of their cytotoxic abilities (Tarazona et al., 2001). Consequently, we believe that $CD8^+$ i-EMRAs also lack other NK receptors, which contribute to their reduced cytotoxicity. However, further phenotypic examination of additional NK receptors should be conducted in order to confirm this.

Inflammatory-derived T cell phenotypes are not restricted to T2D, as premature T cell ageing is observed in many inflammatory diseases. For example, in RA huge expansions of $CD4^+CD28^-$ T cells occur (Martens et al., 1997). However, these cells express KLRG1, produce high levels of IFN-γ and display cytotoxic functions (Weyand et al., 2014), meaning they are more akin to conventional EMRAs than to i-EMRA T

cells. Following our work in T2D we have begun to study the generation of $CD8^+$ i-EMRA T cells in RA (Data not shown). Although this data is preliminary, it does suggest that $CD8^+$ i-EMRA T cells are a common phenomenon of inflammatory diseases and not unique to T2D.

Although we did not examine $CD4^+$ T cell senescence in the context of T2D, in light of the differences we have observed between the $CD8^+$ and $CD4^+$ T cell lineage in healthy individuals, we believe it would be interesting to also assess these differences in T2D. However, it is important to note that the broader heterogeneity of the $CD4^+$ T cell lineage mean this will require a much more extensive phenotyping panel.

6.3. Reversal of $CD8^+$ i-EMRA T cells

In recent years, the experimental elimination of senescent cells has gained a lot of attention, as these studies have shown that the clearance of senescent cells increases healthy lifespan (Baker et al., 2011, 2016). However, these studies have all been conducted in mice and do not take into account the variety of effects that senescence has on different cell types. For instance, in T cells the increase in NK receptor expression that is associated with conventional $CD8^+$ EMRAs suggests a possible re-purposing of these cells. While T cell activities, such as rapid proliferation and TCR mediated activation may be restricted in $CD8^+$ EMRAs (Cao et al., 2010), the accumulation of NK machinery allows these cells to maintain their cytotoxic abilities and conserves a level of immune protection in older individuals to compensate for the loss of T cell repertoire diversity (Vallejo et al., 2011). Therefore, removing

conventional senescent T cells is likely to result in older individuals becoming more vulnerable. Conversely, $CD8^+$ i-EMRA T cells have reduced cytotoxic ability and do not acquire NK machinery; therefore, it is currently unclear what role they play. Although, due to the elevated mtROS generation, we propose that these cells will do more harm than good, making them a pathogenic subset. Consequently, therapeutic intervention to reverse the premature senescent phenotype in these cells could be beneficial.

It would be interesting to assess whether removal of inflammation alone would be enough for these cells to revert back into their previous state or whether the inflammation causes long term damage. Experimentally, this could be assessed through a series of long-term sera cultures; whereby, the senescent phenotype of T cells is examined before, during and after sera removal. Even if the removal of inflammation allowed these cells to revert back to their original state this would still be difficult to achieve clinically, as the outcomes of using anti-inflammatory drugs to treat diseases such as T2D have so far proven inconclusive (Pollack et al., 2016). For instance, although anti-TNFα therapy has been shown to be beneficial in mouse models of insulin resistance and T2D (Hotamisligil et al., 1993), therapeutic benefits in human patients have been found to be limited (Bernstein et al., 2006; Dominguez et al., 2005; Stanley et al., 2011). Furthermore, anti-TNFα medication in RA patients is associated with an increased risk to serious infections (Atzeni et al., 2012; Bongartz et al., 2006; Galloway et al., 2011). This demonstrates that we should avoid removing inflammation entirely as it causes patients to become far more susceptible to

infections. Consequently, we believe a more targeted approach is needed to successfully manipulate $CD8^+$ i-EMRA T cells. In order to achieve this a more detailed understanding of the underlying molecular mechanisms of $CD8^+$ i-EMRA T cell generation will be needed.

6.4. Cell metabolism and T cell senescence

Metabolic regulation plays an important role during T cell senescence, with mitochondrial dysfunction and elevated aerobic glycolysis now identified as key features of $CD8^+$ senescent T cells (Henson et al., 2014). Data presented in this thesis adds to this growing body of literature as it demonstrates a link between DNA damage, the induction of mitochondrial biogenesis and protection against the onset of senescence in the $CD4^+$ compartment. Mechanistically, we were able to show that this was dependent on elevated levels of GATA3 (Figure 6.1). Although GATA3 was present in the $CD8^+$ lineage, the levels were not sufficient to recruit PGC1α and induce mitochondria biogenesis. However, GATA3 overexpression studies should be conducted to determine if this mechanism could also occur in $CD8^+$ T cells. Furthermore, assessment of GATA3 in T2D $CD4^+$ T cells would be interesting to assess whether the same level of protection is offered.

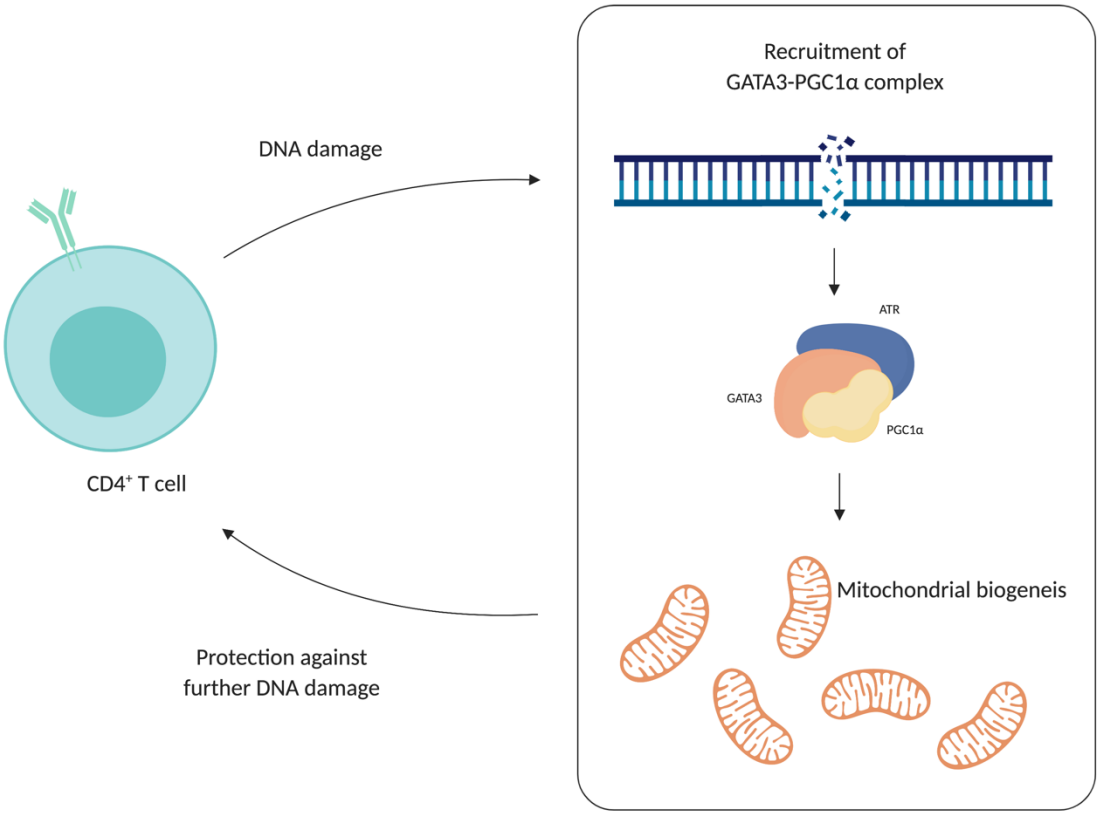

Figure 6.1: Schematic diagram illustrating the recruitment of the GATA3-PGC1α complex in response to DNA damage in $CD4^+$ T cells

As discussion in chapter 4, we believe this phenomenon extends past the lymphocyte lineage and may play an important role in many cancers. GATA3-positive breast cancers are associated with chemotherapy resistance and we believe the accumulation of DNA damage generated during chemotherapy may recruit the GATA3-PGC1α complex. Additionally, despite the traditional view that cancer cells have dysfunctional mitochondria and rely on aerobic glycolysis; the Warburg effect (Schwartz et al., 2017; Warburg et al., 1927), recent data has illustrated that this might not always be the case. For example, the breast cancer cell line MCF-7 is more dependent on mitochondrial respiration than glycolysis (Avagliano et al., 2019).

Furthermore, a previous study examining mitochondrial content and activity in human epithelial breast cancer cells demonstrated that these cells have high oxidative mitochondrial activity (Whitaker-Menezes et al., 2011). Although this study did not examine GATA3 expression, all of the breast cancer samples were selected based on the loss of stromal caveolin-1 (cav-1), a biomarker that is associated with increased oxidative stress and DNA damage (Witkiewicz et al., 2011). Consequently, it would be interesting to assess if the elevated oxidative capacity of these cells is the direct result of DNA damage induced recruitment of the GATA3-PGC1α complex.

In T cells, the recruitment of the GATA3-PGC1α complex is protective against the onset of senescence; however, the consequences of improved mitochondria health and fitness in other cell types and under different conditions may have negative impacts. For instance, additional breast cancer and pancreatic studies have examined the positive correlation between PGC1α expression and increased metastasis (Lebleu et al., 2014; Viale et al., 2014). In these studies, PGC1α induced mitochondrial biogenesis and OXPHOS, which lead to increased cell invasion and migration (Lebleu et al., 2014). Therefore, elevating mitochondrial fitness and metabolic plasticity may not always be beneficial.

To conclusively establish whether the DNA damage induced recruitment of the GATA3-PGC1α complex extends outside of the lymphocyte lineage we propose examining the relationship between mitochondria and GATA3 in other GATA3-positive cells types, particularly cancer cells.

6.5. Summary

This thesis has demonstrated the highly heterogeneous nature of senescent T cells. This heterogeneity is a direct result of the different mechanisms that drive T cells into senescence. For example, repeated antigen stimulation in response to a chronic viral infection will result in a replicative senescence phenotype; whereas, extracellular stresses such as inflammation will result in a premature senescence phenotype (Figure 6.2). Furthermore, each T cell lineage has its own distinct senescence phenotype with cell metabolism proving to be a crucial factor in determining the onset of senescence. Consequently, mitochondrial health and cellular metabolism should be included to better define the T cell senescence phenotype. These findings are important as a deeper understanding of the different drivers of senescence could help aid better and more effective drug design.

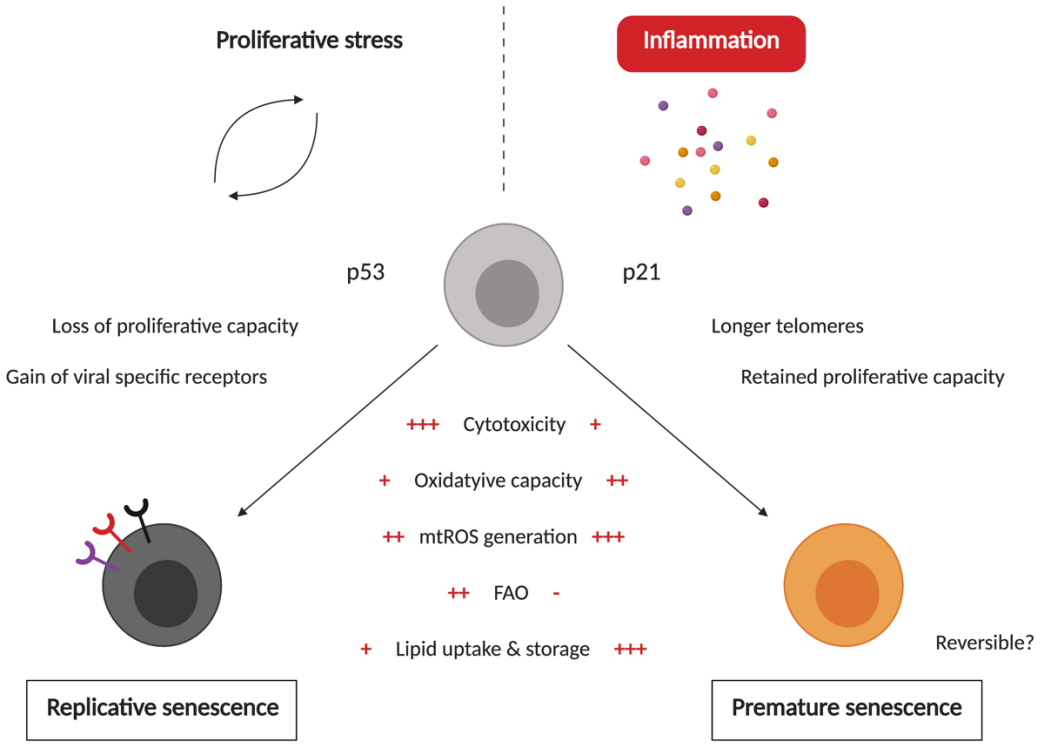

Figure 6.2: Schematic diagram illustrating the different mechanisms responsible for generating T cell senescence

References

Ahmed, R. and Gray, D. (1996), “Immunological memory and protective immunity: Understanding their relation”, Science, Vol. 272 No. 5258, pp. 54–60.

Akbar, A.N., Beverley, P.C.L. and Salmon, M. (2004), “Will telomere erosion lead to a loss of T-cell memory?”, Nature Reviews Immunology, Vol. 4 No. 9, pp. 737–43.

Akbar, A.N. and Henson, S.M. (2011), “Are senescence and exhaustion intertwined or unrelated processes that compromise immunity?”, Nature Reviews Immunology, Vol. 11 No. 4, pp. 289–95.

Akbar, A.N., Salmon, M., Savill, J. and Janossy, G. (1993), “A possible role for bcl-2 in regulating T-cell memory - a ‘balancing act’ between cell death and survival”, Immunology Today, Vol. 14 No. 11, pp. 526–32.

Aktas, E., Kucuksezer, U.C., Bilgic, S., Erten, G. and Deniz, G. (2009), “Relationship between CD107a expression and cytotoxic activity”, Cellular Immunology, Vol. 254 No. 2, pp. 149–54.

Alberts, B., Johnson, A., Lewis, J., Raff, M., Roberts, K. and Walter, P. (2002), “Helper T cells and lymphocyte activation”, Molecular Biology of the Cell.

Alcorta, D.A., Xiong, Y., Phelps, D., Hannon, G., Beach, D. and Barrett, J.C. (1996), “Involvement of the cyclin-dependent kinase inhibitor p16 (INK4a) in replicative senescence of normal human fibroblasts”, Proceedings of the National Academy of Sciences of the United States of America, Vol. 93 No. 24, pp. 13742–7.

Aliouat-Denis, C.M., Dendouga, N., Van Den Wyngaert, I., Goehlmann, H., Steller, U., Van De Weyer, I., Van Slycken, N., et al. (2005), “p53-independent regulation of

p21Waf1/Cip1 expression and senescence by Chk2", Molecular Cancer Research, Vol. 3 No. 11, pp. 627–34.

Appay, V., Van Lier, R.A.W., Sallusto, F. and Roederer, M. (2008), "Phenotype and function of human T lymphocyte subsets: Consensus and issues", Cytometry Part A, Vol. 73 No. 11, pp. 975–83.

Atzeni, F., Sarzi-Puttini, P., Botsios, C., Carletto, A., Cipriani, P., Favalli, E.G., Frati, E., et al. (2012), "Long-term anti-TNF therapy and the risk of serious infections in a cohort of patients with rheumatoid arthritis: Comparison of adalimumab, etanercept and infliximab in the GISEA registry", Autoimmunity Reviews, Vol. 12 No. 2, pp. 225–229.

Avagliano, A., Ruocco, M.R., Aliotta, F., Belviso, I., Accurso, A., Masone, S., Montagnani, S., et al. (2019), "Mitochondrial Flexibility of Breast Cancers: A Growth Advantage and a Therapeutic Opportunity", Cells, Vol. 8 No. 5, p. E401.

Awasthi, P., Foiani, M. and Kumar, A. (2015), "ATM and ATR signaling at a glance", Journal of Cell Science, Vol. 128 No. 23, pp. 4255–4262.

Badovinac, V.P., Porter, B.B. and Harty, J.T. (2002), "Programmed contraction of cd8+ t cells after infection", Nature Immunology, Vol. 3 No. 7, pp. 619–26.

Baker, D.J., Childs, B.G., Durik, M., Wijers, M.E., Sieben, C.J., Zhong, J., A. Saltness, R., et al. (2016), "Naturally occurring p16 Ink4a-positive cells shorten healthy lifespan", Nature, Nature Publishing Group, Vol. 530 No. 7589, pp. 184–9.

Baker, D.J., Perez-Terzic, C., Jin, F., Pitel, K., Niederländer, N.J., Jeganathan, K., Yamada, S., et al. (2008), "Opposing roles for p16Ink4a and p19Arf in senescence and

ageing caused by BubR1 insufficiency", Nature Cell Biology, Vol. 10 No. 7, pp. 825–36.

Baker, D.J., Wijshake, T., Tchkonia, T., Lebrasseur, N.K., Childs, B.G., Van De Sluis, B., Kirkland, J.L., et al. (2011), "Clearance of p16Ink4a-positive senescent cells delays ageing-associated disorders.", Nature, Vol. 479 No. 7372, pp. 232–6.

Bandrés, E., Merino, J., Vázquez, B., Inogés, S., Moreno, C., Subirá, M.L. and Sánchez-Ibarrola, A. (2000), "The increase of IFN-γ production through aging correlates with the expanded CD8(+high)CD28-CD57+ subpopulation", Clinical Immunology, Vol. 96 No. 3, pp. 230–5.

Bartkova, J., Rezaei, N., Liontos, M., Karakaidos, P., Kletsas, D., Issaeva, N., Vassiliou, L.V.F., et al. (2006), "Oncogene-induced senescence is part of the tumorigenesis barrier imposed by DNA damage checkpoints", Nature, Vol. 444 No. 7119, pp. 633–7.

Bavik, C., Coleman, I., Dean, J.P., Knudsen, B., Plymate, S. and Nelson, P.S. (2006), "The gene expression program of prostate fibroblast senescence modulates neoplastic epithelial cell proliferation through paracrine mechanisms", Cancer Research, available at:https://doi.org/10.1158/0008-5472.CAN-05-1716.

Baynes, J.W. and Thorpe, S.R. (1999), "Role of oxidative stress in diabetic complications: A new perspective on an old paradigm", Diabetes, Vol. 48 No. 1, pp. 1–9.

Beerman, I., Bhattacharya, D., Zandi, S., Sigvardsson, M., Weissman, I.L., Bryder, D. and Rossi, D.J. (2010), "Functionally distinct hematopoietic stem cells modulate

hematopoietic lineage potential during aging by a mechanism of clonal expansion", Proceedings of the National Academy of Sciences, Vol. 107 No. 12, pp. 5465–70.

Berke, G. (1995), "The CTL's kiss of death", Cell, Vol. 81 No. 1, pp. 9–12.

Bernstein, L.E., Berry, J., Kim, S., Canavan, B. and Grinspoon, S.K. (2006), "Effects of etanercept in patients with the metabolic syndrome", Archives of Internal Medicine, Vol. 166 No. 8, pp. 902–8.

Beyer, T., Busse, M., Hristov, K., Gurbiel, S., Smida, M., Haus, U.U., Ballerstein, K., et al. (2011), "Integrating signals from the T-cell receptor and the interleukin-2 receptor", PLoS Computational Biology, Vol. 7 No. 8, p. e1002121.

Bianchi, V., Pontis, E. and Reichard, P. (1986), "Changes of deoxyribonucleoside triphosphate pools induced by hydroxyurea and their relation to DNA synthesis", Journal of Biological Chemistry, Vol. 261 No. 34, pp. 16037–16042.

Blagih, J., Coulombe, F., Vincent, E.E., Dupuy, F., Galicia-Vázquez, G., Yurchenko, E., Raissi, T.C., et al. (2015), "The Energy Sensor AMPK Regulates T Cell Metabolic Adaptation and Effector Responses In Vivo", Immunity, Vol. 42 No. 1, pp. 41–54.

Bodnar, A.G., Ouellette, M., Frolkis, M., Holt, S.E., Chiu, C.P., Morin, G.B., Harley, C.B., et al. (1998), "Extension of life-span by introduction of telomerase into normal human cells", Science, Vol. 279 No. 5349, pp. 349–52.

Bongartz, T., Sutton, A.J., Sweeting, M.J., Buchan, I., Matteson, E.L. and Montori, V. (2006), "Anti-TNF antibody therapy in rheumatoid arthritis and the risk of serious infections and malignancies: Systematic review and meta-analysis of rare harmful effects in randomized controlled trials", Journal of the American Medical Association,

Vol. 295 No. 19, pp. 2275–85.

Bonilla, F.A. and Oettgen, H.C. (2010), “Adaptive immunity.”, The Journal of Allergy and Clinical Immunology, United States, Vol. 125 No. 2 Suppl 2, pp. S33-40.

Brenchley, J.M., Karandikar, N.J., Betts, M.R., Ambrozak, D.R., Hill, B.J., Crotty, L.E., Casazza, J.P., et al. (2003), “Expression of CD57 defines replicative senescence and antigen-induced apoptotic death of CD8+ T cells”, Blood, Vol. 101 No. 2, pp. 2711–20.

Bruunsgaard, H. (2006), “The clinical impact of systemic low-level inflammation in elderly populations. With special reference to cardiovascular disease, dementia and mortality.”, Danish Medical Bulletin, Vol. 53 No. 3, pp. 285–309.

Buck, M.D., O’Sullivan, D. and Pearce, E.L. (2015), “T cell metabolism drives immunity”, The Journal of Experimental Medicine, Vol. 212 No. 9, pp. 1345–60.

Callender, L.A., Carroll, E.C., Beal, R.W.J., Chambers, E.S., Nourshargh, S., Akbar, A.N. and Henson, S.M. (2018), “Human CD8+ EMRA T cells display a senescence-associated secretory phenotype regulated by p38 MAPK”, Aging Cell, Vol. 17 No. 1, p. e12675.

Callender, L.A., Carroll, E.C., Bober, E.A. and Henson, S.M. (2018), “Divergent mechanisms of metabolic dysfunction drive fibroblast and T-cell senescence”, Ageing Research Reviews, Vol. 47, pp. 24–30.

Cao, J.N., Gollapudi, S., Sharman, E.H., Jia, Z. and Gupta, S. (2010), “Age-related alterations of gene expression patterns in human CD8+ T cells”, Aging Cell, Vol. 9 No. 1, pp. 19–31.

Carr, E.L., Kelman, A., Wu, G.S., Gopaul, R., Senkevitch, E., Aghvanyan, A., Turay, A.M., et al. (2010), “Glutamine Uptake and Metabolism Are Coordinately Regulated by ERK/MAPK during T Lymphocyte Activation”, The Journal of Immunology, Vol. 185 No. 2, pp. 1037–44.

Chen, F., Haigh, S., Barman, S. and Fulton, D.J.R. (2012), “From form to function: The role of Nox4 in the cardiovascular system”, Frontiers in Physiology, Vol. 3, p. 412.

Chen, Q., Fischer, A., Reagan, J.D., Yan, L.J. and Ames, B.N. (1995), “Oxidative DNA damage and senescence of human diploid fibroblast cells.”, Proceedings of the National Academy of Sciences of the United States of America, Vol. 92 No. 10, pp. 4337–41.

Chendong, Y., Sudderth, J., Tuyen, D., Bachoo, R.G., McDonald, J.G. and DeBerardinis, R.J. (2009), “Glioblastoma cells require glutamate dehydrogenase to survive impairments of glucose metabolism or Akt signaling”, Cancer Research, Vol. 69 No. 20, pp. 7986–93.

Cheung, K.P., Yang, E. and Goldrath, A.W. (2009), “Memory-Like CD8 + T Cells Generated during Homeostatic Proliferation Defer to Antigen-Experienced Memory Cells”, The Journal of Immunology, Vol. 183 No. 5, pp. 3364–72.

Cho, R.H., Sieburg, H.B. and Muller-Sieburg, C.E. (2008), “A new mechanism for the aging of hematopoietic stem cells: Aging changes the clonal composition of the stem cell compartment but not individual stem cells”, Blood, Vol. 111 No. 12, pp. 5553–61.

Chou, J.P. and Effros, R.B. (2013), “T Cell Replicative Senescene in Human Aging”, Current Pharmaceutical Design, Vol. 19 No. 9, pp. 1680–98.

Collins, K. and Mitchell, J.R. (2002), “Telomerase in the human organism”, Oncogene, Vol. 21 No. 4, pp. 564–79.

Coppe, J.P., Kauser, K., Campisi, J. and Beauséjour, C.M. (2006), “Secretion of vascular endothelial growth factor by primary human fibroblasts at senescence”, Journal of Biological Chemistry, Vol. 281 No. 40, pp. 29568–74.

Corsetti, G., Pasini, E., D’Antona, G., Nisoli, E., Flati, V., Assanelli, D., Dioguardi, F.S., et al. (2008), “Morphometric Changes Induced by Amino Acid Supplementation in Skeletal and Cardiac Muscles of Old Mice”, American Journal of Cardiology, Vol. 101 No. 11A, pp. 26E-34E.

Czesnikiewicz-Guzik, M., Lee, W.W., Cui, D., Hiruma, Y., Lamar, D.L., Yang, Z.Z., Ouslander, J.G., et al. (2008), “T cell subset-specific susceptibility to aging”, Clinical Immunology, Vol. 127 No. 1, pp. 107–18.

Dandona, P., Thusu, K., Cook, S., Snyder, B., Makowski, J., Armstrong, D. and Nicotera, T. (1996), “Oxidative damage to DNA in diabetes mellitus”, Lancet, Vol. 347 No. 8999, pp. 444–5.

Das, A., Ranganathan, V., Umar, D., Thukral, S., George, A., Rath, S. and Bal, V. (2017), “Effector/memory CD4 T cells making either Th1 or Th2 cytokines commonly co-express T-bet and GATA-3”, PLoS ONE, Vol. 12 No. 10, p. e0186932.

Davalli, P., Mitic, T., Caporali, A., Lauriola, A. and D’Arca, D. (2016), “ROS, Cell Senescence, and Novel Molecular Mechanisms in Aging and Age-Related Diseases”, Oxidative Medicine and Cellular Longevity, Vol. 2016, p. 3565127.

Dimri, G.P., Itahana, K., Acosta, M. and Campisi, J. (2009), “Regulation of a

Senescence Checkpoint Response by the E2F1 Transcription Factor and p14ARF Tumor Suppressor", Molecular and Cellular Biology, Vol. 20 No. 1, pp. 273–85.

Dimri, G.P., Lee, X., Basile, G., Acosta, M., Scott, G., Roskelley, C., Medrano, E.E., et al. (1995), "A biomarker that identifies senescent human cells in culture and in aging skin in vivo.", Proceedings of the National Academy of Sciences of the United States of America, Vol. 92 No. 20, pp. 9363–7.

Dominguez, H., Storgaard, H., Rask-Madsen, C., Hermann, T.S., Ihlemann, N., Nielsen, D.B., Spohr, C., et al. (2005), "Metabolic and vascular effects of tumor necrosis factor-α blockade with etanercept in obese patients with type 2 diabetes", Journal of Vascular Research, Vol. 42 No. 6, pp. 517–25.

Dorshkind, K., Montecino-Rodriguez, E. and Signer, R.A.J. (2009), "The ageing immune system: Is it ever too old to become young again?", Nature Reviews Immunology, Vol. 9 No. 1, pp. 57–62.

Drayton, S. and Peters, G. (2002), "Immortalisation and transformation revisited", Current Opinion in Genetics and Development, Vol. 12 No. 1, pp. 98–104.

Duncan, B.B., Schmidt, M.I., Pankow, J.S., Ballantyne, C.M., Couper, D., Vigo, A., Hoogeveen, R., et al. (2003), "Low-grade systemic inflammation and the development of type 2 diabetes: The atherosclerosis risk in communities study", Diabetes, Vol. 52 No. 7, pp. 1799–805.

Edinger, A.L. (2002), "Akt Maintains Cell Size and Survival by Increasing mTOR-dependent Nutrient Uptake", Molecular Biology of the Cell, Vol. 13 No. 7, pp. 2276–88.

Effros, R.B., Allsopp, R., Chiu, C., Hausner, M.A., Hirji, K., Wang, L., Harley, C.B., et al. (1996), “Shortened telomeres in the expanded CD28-CD8+ cell subset in HIV disease implicate replicative senescence in HIV pathogenesis”, AIDS, Vol. 10 No. 8, pp. F17-22.

Elstrom, R.L., Bauer, D.E., Buzzai, M., Karnauskas, R., Harris, M.H., Plas, D.R., Zhuang, H., et al. (2004), “Akt stimulates aerobic glycolysis in cancer cells”, Cancer Research, Vol. 64 No. 11, pp. 3892–9.

Engel, I. and Murre, C. (2001), “The function of E- and ID proteins in lymphocyte development”, Nature Reviews Immunology, Vol. 1 No. 3, pp. 193–9.

Engelsen, I.B., Stefansson, I.M., Akslen, L.A. and Salvesen, H.B. (2008), “GATA3 expression in estrogen receptor α-negative endometrial carcinomas identifies aggressive tumors with high proliferation and poor patient survival”, American Journal of Obstetrics and Gynecology, Vol. 199 No. 5, pp. 543.e1–7.

Erickson, S., Sangfelt, O., Heyman, M., Castro, J., Einhorn, S. and Grandér, D. (1998), “Involvement of the Ink4 proteins p16 and p15 in T-lymphocyte senescence”, Oncogene, Vol. 17 No. 5, pp. 595–602.

Feijoo, P., Terradas, M., Soler, D., Daniel Domínguez, Tusell, L. and Genescà, A. (2016), “Breast primary epithelial cells that escape p16-dependent stasis enter a telomeredriven crisis state”, Breast Cancer Research, Vol. 18 No. 1, p. 7.

Foulds, K.E., Zenewicz, L.A., Shedlock, D.J., Jiang, J., Troy, A.E. and Shen, H. (2002), “Cutting edge: CD4 and CD8 T cells are intrinsically different in their proliferative responses.”, Journal of Immunology (Baltimore, Md. : 1950), Vol. 168 No. 4, pp.

1528–32.

Franceschi, C., Bonafè, M., Valensin, S., Olivieri, F., De Luca, M., Ottaviani, E. and De Benedictis, G. (2000), “Inflamm-aging. An evolutionary perspective on immunosenescence.”, Annals of the New York Academy of Sciences, Vol. 908, pp. 244–54.

Frasca, D., Diaz, A., Romero, M. and Blomberg, B.B. (2017), “Human peripheral late/exhausted memory B cells express a senescent-associated secretory phenotype and preferentially utilize metabolic signaling pathways”, Experimental Gerontology, Vol. 87, pp. 113–120.

Frasca, D., Landin, A.M., Lechner, S.C., Ryan, J.G., Schwartz, R., Riley, R.L. and Blomberg, B.B. (2008), “Aging Down-Regulates the Transcription Factor E2A, Activation-Induced Cytidine Deaminase, and Ig Class Switch in Human B Cells”, The Journal of Immunology, Vol. 180 No. 8, pp. 5282–90.

Frauwirth, K.A., Riley, J.L., Harris, M.H., Parry, R. V, Rathmell, J.C., Plas, D.R., Elstrom, R.L., et al. (2002), “The CD28 signaling pathway regulates glucose metabolism.”, Immunity, Vol. 16 No. 6, pp. 769–77.

Freund, A., Orjalo, A. V., Desprez, P.Y. and Campisi, J. (2010), “Inflammatory networks during cellular senescence: causes and consequences”, Trends in Molecular Medicine, Vol. 16 No. 5, pp. 238–46.

Galkowska, H., Wojewodzka, U. and Olszewski, W.L. (2005), “Low recruitment of immune cells with increased expression of endothelial adhesion molecules in margins of the chronic diabetic foot ulcers”, Wound Repair and Regeneration, Vol.

13 No. 3, pp. 248–54.

Galloway, J.B., Hyrich, K.L., Mercer, L.K., Dixon, W.G., Fu, B., Ustianowski, A.P., Watson, K.D., et al. (2011), “Anti-TNF therapy is associated with an increased risk of serious infections in patients with rheumatoid arthritis especially in the first 6 months of treatment: Updated results from the British Society for Rheumatology Biologics Register with special emph”, Rheumatology, Vol. 50 No. 2, pp. 124–31.

Gerdes, J., Li, L., Schlueter, C., Duchrow, M., Wohlenberg, C., Gerlach, C., Stahmer, I., et al. (1991), “Immunobiochemical and molecular biologic characterization of the cell proliferation-associated nuclear antigen that is defined by monoclonal antibody Ki-67.”, The American Journal of Pathology, Vol. 138 No. 4, pp. 867–73.

Germain, R.N. (2002), “T-cell development and the CD4-CD8 lineage decision”, Nature Reviews Immunology, Vol. 2 No. 5, pp. 309–22.

Giubilato, S., Liuzzo, G., Brugaletta, S., Pitocco, D., Graziani, F., Smaldone, C., Montone, R.A., et al. (2011), “Expansion of CD4+CD28null T-lymphocytes in diabetic patients: Exploring new pathogenetic mechanisms of increased cardiovascular risk in diabetes mellitus”, European Heart Journal, Vol. 32 No. 10, pp. 1214–26.

Goldrath, A.W. and Bevan, M.J. (1999), “Selecting and maintaining a diverse T-cell repertoire”, Nature, Vol. 402 No. 6759, pp. 255–62.

Goronzy, J.J., Lee, W.W. and Weyand, C.M. (2007), “Aging and T-cell diversity”, Experimental Gerontology, Vol. 42 No. 5, pp. 400–6.

Goronzy, J.J. and Weyand, C.M. (2019), “Mechanisms underlying T cell ageing”, Nature Reviews Immunology, Nature Publishing Group, Vol. 19 No. 9, pp. 573–583.

Groom, J.R. and Luster, A.D. (2011), “CXCR3 in T cell function”, Experimental Cell Research, Vol. 317 No. 5, pp. 620–631.

Haluszczak, C., Akue, A.D., Hamilton, S.E., Johnson, L.D.S., Pujanauski, L., Teodorovic, L., Jameson, S.C., et al. (2009), “The antigen-specific CD8 + T cell repertoire in unimmunized mice includes memory phenotype cells bearing markers of homeostatic expansion”, Journal of Experimental Medicine, Vol. 206 No. 2, pp. 435–48.

Hamann, D., Baars, P.A., Rep, M.H., Hooibrink, B., Kerkhof-Garde, S.R., Klein, M.R. and van Lier, R.A. (1997), “Phenotypic and functional separation of memory and effector human CD8+ T cells.”, The Journal of Experimental Medicine, Vol. 186 No. 9, pp. 1407–18.

Hamann, D., Kostense, S., Wolthers, K.C., Otto, S.A., Baars, P.A., Miedema, F. and Van Lier, R.A.W. (1999), “Evidence that human CD8+ CD45RA+ CD27- cells are induced by antigen and evolve through extensive rounds of division”, International Immunology, Vol. 11 No. 7, pp. 1027–33.

van Hamburg, J.P., de Bruijn, M.J.W., Dingjan, G.M., Beverloo, H.B., Diepstraten, H., Ling, K.W. and Hendriks, R.W. (2008), “Cooperation of Gata3, c-Myc and Notch in malignant transformation of double positive thymocytes”, Molecular Immunology, Vol. 45 No. 11, pp. 3085–95.

Hancock, W.W., Lu, B., Gao, W., Csizmadia, V., Faia, K., King, J.A., Smiley, S.T., et al. (2002), “Requirement of the Chemokine Receptor CXCR3 for Acute Allograft Rejection”, The Journal of Experimental Medicine, Vol. 192 No. 10, pp. 1515–20.

Hara, E., Smith, R., Parry, D., Tahara, H., Stone, S. and Peters, G. (1996), “Regulation of p16CDKN2 expression and its implications for cell immortalization and senescence.”, Molecular and Cellular Biology, Vol. 16 No. 3, pp. 859–67.

Hardie, D.G. (2004), “AMP-activated protein kinase: A master switch in glucose and lipid metabolism”, Reviews in Endocrine and Metabolic Disorders, Vol. 5 No. 2, pp. 119–25.

Hardie, D.G., Ross, F.A. and Hawley, S.A. (2012), “AMPK: A nutrient and energy sensor that maintains energy homeostasis”, Nature Reviews Molecular Cell Biology, Vol. 13 No. 4, pp. 251–62.

Harley, C.B., Futcher, A.B. and Greider, C.W. (1990), “Telomeres shorten during ageing of human fibroblasts”, Nature, Vol. 345 No. 6273, pp. 458–60.

Hathcock, K.S., Kaech, S.M., Ahmed, R. and Hodes, R.J. (2003), “Induction of telomerase activity and maintenance of telomere length in virus-specific effector and memory CD8+ T cells.”, Journal of Immunology, Vol. 170 No. 1, pp. 147–52.

Hayflick, L. and Moorhead, P.S. (1961), “The serial cultivation of human diploid cell strains”, Experimental Cell Research, Vol. 25, pp. 585–621.

Henry, L. (1967), “Involution of the human thymus.”, The Journal of Pathology and Bacteriology, England, Vol. 93 No. 2, pp. 661–671.

Henson, S.M., Franzese, O., Macaulay, R., Libri, V., Azevedo, R.I., Kiani-Alikhan, S., Plunkett, F.J., et al. (2009), “KLRG1 signaling induces defective Akt (ser473) phosphorylation and proliferative dysfunction of highly differentiated CD8+ T cells”, Blood, Vol. 113 No. 26, pp. 6619–28.

Henson, S.M., Lanna, A., Riddel, N.E., Franzese, O., Macaulay, R., Griffiths, S.J., Puleston, D.J., et al. (2014), “P38 signaling inhibits mTORC1-independent autophagy in senescent human CD8+ T cells”, Journal of Clinical Investigation, Vol. 124 No. 9, pp. 4004–16.

Henson, S.M., Macaulay, R., Riddell, N.E., Nunn, C.J. and Akbar, A.N. (2015), “Blockade of PD-1 or p38 MAP kinase signaling enhances senescent human CD8+ T-cell proliferation by distinct pathways”, European Journal of Immunology, Vol. 45 No. 5, pp. 1441–51.

Henson, S.M., Riddell, N.E. and Akbar, A.N. (2012), “Properties of end-stage human T cells defined by CD45RA re-expression”, Current Opinion in Immunology, Vol. 24 No. 4, pp. 476–81.

Hernández-Hoyos, G., Anderson, M.K., Wang, C., Rothenberg, E. V. and Alberola-Ila, J. (2003), “GATA-3 expression is controlled by TCR signals and regulates CD4/CD8 differentiation”, Immunity, Vol. 19 No. 1, pp. 83–94.

Hodes, R.J., Hathcock, K.S. and Weng, N.P. (2002), “Telomeres in T and B cells”, Nature Reviews Immunology, Vol. 2 No. 9, pp. 699–706.

Hoenicke, L. and Zender, L. (2012), “Immune surveillance of senescent cells-biological significance in cancer-and non-cancer pathologies”, Carcinogenesis, Vol. 33 No. 6, pp. 1123–6.

Hokeness, K.L., Deweerd, E.S., Munks, M.W., Lewis, C.A., Gladue, R.P. and Salazar-Mather, T.P. (2007), “CXCR3-Dependent Recruitment of Antigen-Specific T Lymphocytes to the Liver during Murine Cytomegalovirus Infection”, Journal of

Virology, Vol. 81 No. 3, pp. 1241–50.

Holler, N., Tardivel, A., Kovacsovics-Bankowski, M., Hertig, S., Gaide, O., Martinon, F., Tinel, A., et al. (2003), "Two Adjacent Trimeric Fas Ligands Are Required for Fas Signaling and Formation of a Death-Inducing Signaling Complex", Molecular and Cellular Biology, Vol. 23 No. 4, pp. 1428–40.

Hotamisligil, G.S., Shargill, N.S. and Spiegelman, B.M. (1993), "Adipose expression of tumor necrosis factor-α: Direct role in obesity-linked insulin resistance", Science, Vol. 259 No. 5091, pp. 87–91.

Ibegbu, C.C., Xu, Y.-X., Harris, W., Maggio, D., Miller, J.D. and Kourtis, A.P. (2006), "Expression of killer cell lectin-like receptor G1 on antigen-specific human CD8 + T lymphocytes during active, latent, and resolved infection and its relation with CD57", The Journal of Immunology, Vol. 174 No. 10, pp. 6088–94.

Intlekofer, A.M., Takemoto, N., Wherry, E.J., Longworth, S.A., Northrup, J.T., Palanivel, V.R., Mullen, A.C., et al. (2005), "Effector and memory CD8+ T cell fate coupled by T-bet and eomesodermin", Nature Immunology, Vol. 6 No. 12, pp. 1236–44.

Iwasaki, A. and Medzhitov, R. (2010), "Regulation of adaptive immunity by the innate immune system", Science, Vol. 327 No. 5963, pp. 291–5.

Jacobs, J.J.L. and De Lange, T. (2004), "Significant role for p16INK4a in p53-independent telomere-directed senescence", Current Biology, Vol. 14 No. 24, pp. 2303–8.

James, E.L., Michalek, R.D., Pitiyage, G.N., De Castro, A.M., Vignola, K.S., Jones, J.,

Mohney, R.P., et al. (2015), “Senescent human fibroblasts show increased glycolysis and redox homeostasis with extracellular metabolomes that overlap with those of irreparable DNA damage, aging, and disease”, Journal of Proteome Research, Vol. 14 No. 4, pp. 1854–71.

Johnson, K.M. (2002), “Aging and developmental transitions in the B cell lineage”, International Immunology, Vol. 14 No. 11, pp. 1313–23.

Jones, N., Vincent, E.E., Cronin, J.G., Panetti, S., Chambers, M., Holm, S.R., Owens, S.E., et al. (2019), “Akt and STAT5 mediate naïve human CD4+ T-cell early metabolic response to TCR stimulation”, Nature Communications, Vol. 10 No. 1, p. 2042.

Joshi, N.S., Cui, W., Chandele, A., Lee, H.K., Urso, D.R., Hagman, J., Gapin, L., et al. (2007), “Inflammation Directs Memory Precursor and Short-Lived Effector CD8+ T Cell Fates via the Graded Expression of T-bet Transcription Factor”, Immunity, Vol. 27 No. 2, pp. 281–95.

Juedes, A., Glimcher, L.H., Szabo, S.J., von Herrath, M. and Sullivan, B.M. (2003), “Antigen-driven effector CD8 T cell function regulated by T-bet”, Proceedings of the National Academy of Sciences, Vol. 100 No. 26, pp. 15818–23.

Jun, J. Il and Lau, L.F. (2010), “The matricellular protein CCN1 induces fibroblast senescence and restricts fibrosis in cutaneous wound healing”, Nature Cell Biology, Vol. 12 No. 7, pp. 676–85.

Kaech, S.M. and Cui, W. (2012), “Transcriptional control of effector and memory CD8+ T cell differentiation”, Nature Reviews Immunology, Vol. 12 No. 11, pp. 749–61.

Kang, C., Xu, Q., Martin, T.D., Li, M.Z., Demaria, M., Aron, L., Lu, T., et al. (2015), “The DNA damage response induces inflammation and senescence by inhibiting autophagy of GATA4”, Science, Vol. 349 No. 6255, p. aaa5612.

Kang, H.T., Lee, K.B., Kim, S.Y., Choi, H.R. and Park, S.C. (2011), “Autophagy impairment induces premature senescence in primary human fibroblasts”, PLoS ONE, Vol. 6 No. 8, p. e23367.

Kang, S., Brown, H.M. and Hwang, S. (2018), “Direct Antiviral Mechanisms of Interferon-Gamma”, Immune Network, The Korean Association of Immunologists, Vol. 18 No. 5, pp. e33–e33.

Kaplan, M.H., Hufford, M.M. and Olson, M.R. (2015), “The development and in vivo function of T helper 9 cells”, Nature Reviews Immunology, Vol. 15 No. 5, pp. 295–307.

Kaplon, J., Zheng, L., Meissl, K., Chaneton, B., Selivanov, V.A., MacKay, G., Van Der Burg, S.H., et al. (2013), “A key role for mitochondrial gatekeeper pyruvate dehydrogenase in oncogene-induced senescence”, Nature, Vol. 498 No. 7452, pp. 109–12.

Kaptoge, S., Di Angelantonio, E., Pennells, L., Wood, A.M., White, I.R., Gao, P., Walker, M., et al. (2012), “C-reactive protein, fibrinogen, and cardiovascular disease prediction”, New England Journal of Medicine, Vol. 367 No. 14, pp. 1310–20.

Kim, M.A., Kim, H.J., Brown, A.L., Lee, M.Y., Bae, Y.S., Park, J.I., Kwak, J.Y., et al. (2007), “Identification of novel substrates for human checkpoint kinase Chk1 and Chk2 through genome-wide screening using a consensus Chk phosphorylation motif”,

Experimental and Molecular Medicine, Vol. 39 No. 2, pp. 205–12.

Koch, S., Larbi, A., Derhovanessian, E., Özcelik, D., Naumova, E. and Pawelec, G. (2008), “Multiparameter flow cytometric analysis of CD4 and CD8 T cell subsets in young and old people”, Immunity and Ageing, Vol. 5, p. 6.

Kouros-Mehr, H., Bechis, S.K., Slorach, E.M., Littlepage, L.E., Egeblad, M., Ewald, A.J., Pai, S.Y., et al. (2008), “GATA-3 Links Tumor Differentiation and Dissemination in a Luminal Breast Cancer Model”, Cancer Cell, Vol. 13 No. 2, pp. 141–52.

Krammer, P.H. (2000), “CD95’s deadly mission in the immune system”, Nature, Vol. 407 No. 6805, pp. 789–95.

Krizhanovsky, V., Yon, M., Dickins, R.A., Hearn, S., Simon, J., Miething, C., Yee, H., et al. (2008), “Senescence of Activated Stellate Cells Limits Liver Fibrosis”, Cell, Vol. 134 No. 4, pp. 657–67.

Krtolica, A., Parrinello, S., Lockett, S., Desprez, P.-Y. and Campisi, J. (2001), “Senescent fibroblasts promote epithelial cell growth and tumorigenesis: A link between cancer and aging”, Proceedings of the National Academy of Sciences, Vol. 98 No. 21, pp. 12072–7.

Kuilman, T. and Peeper, D.S. (2009), “Senescence-messaging secretome: SMS-ing cellular stress”, Nature Reviews Cancer, Vol. 9 No. 2, pp. 81–94.

Laberge, R.M., Awad, P., Campisi, J. and Desprez, P.Y. (2012), “Epithelial-mesenchymal transition induced by senescent fibroblasts”, Cancer Microenvironment, Vol. 5 No. 1, pp. 30–44.

Lanzer, K.G., Cookenham, T., Reiley, W.W. and Blackman, M.A. (2018), “Virtual

memory cells make a major contribution to the response of aged influenza-naïve mice to influenza virus infection", Immunity and Ageing, Vol. 15, p. 17.

Larbi, A., Franceschi, C., Mazzatti, D., Solana, R., Wikby, A. and Pawelec, G. (2008), "Aging of the Immune System as a Prognostic Factor for Human Longevity", Physiology, Vol. 23, pp. 64–74.

Larbi, A. and Fulop, T. (2014), "From 'truly naïve' to 'exhausted senescent' T cells: When markers predict functionality", Cytometry Part A, Vol. 85 No. 1, pp. 25–35.

Le, A., Lane, A.N., Hamaker, M., Bose, S., Gouw, A., Barbi, J., Tsukamoto, T., et al. (2012), "Glucose-independent glutamine metabolism via TCA cycling for proliferation and survival in b cells", Cell Metabolism, Vol. 15 No. 1, pp. 110–21.

Lebleu, V.S., O'Connell, J.T., Gonzalez Herrera, K.N., Wikman, H., Pantel, K., Haigis, M.C., De Carvalho, F.M., et al. (2014), "PGC-1α mediates mitochondrial biogenesis and oxidative phosphorylation in cancer cells to promote metastasis", Nature Cell Biology, Vol. 16 No. 10, pp. 992–1003.

Lee, Y. ho, Kim, S.R., Han, D.H., Yu, H.T., Han, Y.D., Kim, J.H., Kim, S.H., et al. (2019), "Senescent T cells predict the development of hyperglycemia in humans", Diabetes, Vol. 68 No. 1, pp. 156–162.

Libby, P. (2012), "Inflammation in atherosclerosis", Arteriosclerosis, Thrombosis, and Vascular Biology, Vol. 420 No. 6917, pp. 868–74.

Licastro, F., Candore, G., Lio, D., Porcellini, E., Colonna-Romano, G., Franceschi, C. and Caruso, C. (2005), "Innate immunity and inflammation in ageing: A key for understanding age-related diseases", Immunity and Ageing, Vol. 2, p. 8.

Lin, A.W., Barradas, M., Stone, J.C., Van Aelst, L., Serrano, M. and Lowe, S.W. (1998), "Premature senescence involving p53 and p16 is activated in response to constitutive MEK/MAPK mitogenic signaling", Genes and Development, Vol. 12 No. 19, pp. 3008–19.

Lynch, H.E., Goldberg, G.L., Chidgey, A., Van den Brink, M.R.M., Boyd, R. and Sempowski, G.D. (2009), "Thymic involution and immune reconstitution.", Trends in Immunology, Vol. 30 No. 7, pp. 366–73.

Maini, M.K., Soares, M. V, Zilch, C.F., Akbar, A.N. and Beverley, P.C. (1999), "Virus-induced CD8+ T cell clonal expansion is associated with telomerase up-regulation and telomere length preservation: a mechanism for rescue from replicative senescence.", Journal of Immunology (Baltimore, Md. : 1950), Vol. 162 No. 8, pp. 4521–6.

Martens, P.B., Goronzy, J.J., Schaid, D. and Weyand, C.M. (1997), "Expansion of unusual CD4+ T cells in severe rheumatoid arthritis", Arthritis and Rheumatism, Vol. 40 No. 6, pp. 1106–14.

Martin, S., Kohler, H., Weltzien, H.U. and Leipner, C. (1996), "Selective activation of CD8 T cell effector functions by epitope variants of lymphocytic choriomeningitis virus glycoprotein.", Journal of Immunology, Vol. 157 No. 6, pp. 2358–65.

Masutomi, K., Yu, E.Y., Khurts, S., Ben-Porath, I., Currier, J.L., Metz, G.B., Brooks, M.W., et al. (2003), "Telomerase maintains telomere structure in normal human cells", Cell, Vol. 114 No. 2, pp. 241–53.

Mehra, R., Varambally, S., Ding, L., Shen, R., Sabel, M.S., Ghosh, D., Chinnaiyan, A.M., et al. (2005), "Identification of GATA3 as a breast cancer prognostic marker by global

gene expression meta-analysis", Cancer Research, Vol. 65 No. 24, pp. 11259–11264.

Michie, A.M., Carlyle, J.R., Schmitt, T.M., Ljutic, B., Cho, S.K., Fong, Q. and Zúñiga-Pflücker, J.C. (2000), "Clonal Characterization of a Bipotent T Cell and NK Cell Progenitor in the Mouse Fetal Thymus", The Journal of Immunology, Vol. 164 No. 4, pp. 1730 LP – 1733.

Mills, E.L., Kelly, B., Logan, A., Costa, A.S.H., Varma, M. and Bryant, C.E. (2016), "Repurposing mitochondria from ATP production to ROS generation drives a pro-inflammatory phenotype in macrophages that depends on succinate oxidation by complex II", Cell, Vol. 167 No. 2, pp. 457–470.

Min, B., McHugh, R., Sempowski, G.D., Mackall, C., Foucras, G. and Paul, W.E. (2003), "Neonates support lymphopenia-induced proliferation", Immunity, Vol. 18 No. 1, pp. 131–40.

Minegishi, N., Morita, S., Minegishi, M., Tsuchiya, S., Konno, T., Hayashi, N. and Yamamoto, M. (1997), "Expression of GATA transcription factors in myelogenous and lymphoblastic leukemia cells.", International Journal of Hematology, Japan, Vol. 65 No. 3, pp. 239–249.

Mirzayans, R., Andrais, B., Hansen, G. and Murray, D. (2012), "Role of p16 INK4A in replicative senescence and DNA damage-induced premature senescence in p53-deficient human cells", Biochemistry Research International, Vol. 2012 No. 951574, available at:https://doi.org/10.1155/2012/951574.

Di Mitri, D., Azevedo, R.I., Henson, S.M., Libri, V., Riddell, N.E., Macaulay, R., Kipling, D., et al. (2011), "Reversible Senescence in Human CD4+CD45RA+CD27- Memory T

Cells", The Journal of Immunology, Vol. 187 No. 5, pp. 2093–100.

Moller, D.E. (2000), "Potential role of TNF-α in the pathogenesis of insulin resistance and type 2 diabetes", Trends in Endocrinology and Metabolism, Vol. 11 No. 6, pp. 212–7.

Monteiro, J., Batliwalla, F., Ostrer, H. and Gregersen, P.K. (1996), "Shortened telomeres in clonally expanded CD28-CD8+ T cells imply a replicative history that is distinct from their CD28+CD8+ counterparts.", Journal of Immunology, Vol. 156 No. 10, pp. 3587–90.

Muller, L.M.A.J., Gorter, K.J., Hak, E., Goudzwaard, W.L., Schellevis, F.G., Hoepelman, A.I.M. and Rutten, G.E.H.M. (2005), "Increased Risk of Common Infections in Patients with Type 1 and Type 2 Diabetes Mellitus", Clinical Infectious Diseases, Vol. 41 No. 3, pp. 281–8.

Muñoz-Espín, D., Cañamero, M., Maraver, A., Gómez-López, G., Contreras, J., Murillo-Cuesta, S., Rodríguez-Baeza, A., et al. (2013), "Programmed cell senescence during mammalian embryonic development", Cell, Vol. 155 No. 5, pp. 1104–18.

Muñoz-Espín, D. and Serrano, M. (2014), "Cellular senescence: From physiology to pathology", Nature Reviews Molecular Cell Biology, Vol. 15 No. 7, pp. 482–96.

Nakajima, T., Schulte, S., Warrington, K.J., Kopecky, S.L., Frye, R.L., Goronzy, J.J. and Weyand, C.M. (2002), "T-cell-mediated lysis of endothelial cells in acute coronary syndromes", Circulation, Vol. 105 No. 5, pp. 570–5.

Narita, M., Narita, M., Krizhanovsky, V., Nuñez, S., Chicas, A., Hearn, S.A., Myers, M.P., et al. (2006), "A Novel Role for High-Mobility Group A Proteins in Cellular

Senescence and Heterochromatin Formation", Cell, Vol. 126 No. 3, pp. 503–14.

Narita, M., Nũnez, S., Heard, E., Narita, M., Lin, A.W., Hearn, S.A., Spector, D.L., et al. (2003), "Rb-mediated heterochromatin formation and silencing of E2F target genes during cellular senescence.", Cell, Vol. 113 No. 6, pp. 703–16.

Naylor, K., Li, G., Vallejo, A.N., Lee, W.-W., Koetz, K., Bryl, E., Witkowski, J., et al. (2005), "The influence of age on T cell generation and TCR diversity.", Journal of Immunology (Baltimore, Md. : 1950), Vol. 174 No. 11, pp. 7446–52.

Nicholls, D.G. (2004), "Mitochondrial membrane potential and aging", Aging Cell, Vol. 3 No. 1, pp. 35–40.

Nikolich-Zugich, J. (2005), "T cell aging: naive but not young.", The Journal of Experimental Medicine, Vol. 201 No. 6, pp. 837–40.

Olovnikov, A.M. (1971), "Principle of marginotomy in template synthesis of polynucleotides.", Doklady Akademii Nauk SSSR, Vol. 201 No. 6, pp. 1496–9.

Pai, J.K., Pischon, T., Ma, J., Manson, J.A.E., Hankinson, S.E., Joshipura, K., Curhan, G.C., et al. (2004), "Inflammatory markers and the risk of coronary heart disease in men and women", New England Journal of Medicine, Vol. 351 No. 25, pp. 2599–610.

Passos, J.F., Nelson, G., Wang, C., Richter, T., Simillion, C., Proctor, C.J., Miwa, S., et al. (2010), "Feedback between p21 and reactive oxygen production is necessary for cell senescence", Molecular Systems Biology, Vol. 6, p. 347.

Pence, B.D. and Yarbro, J.R. (2018), "Aging impairs mitochondrial respiratory capacity in classical monocytes", Experimental Gerontology, Vol. 108, pp. 112–117.

Peng, H., Ke, X.X., Hu, R., Yang, L., Cui, H. and Wei, Y. (2015), “Essential role of GATA3 in regulation of differentiation and cell proliferation in SK-N-SH neuroblastoma cells”, Molecular Medicine Reports, Vol. 11 No. 2, pp. 881–886.

Pereira, B.I., Devine, O.P., Vukmanovic-Stejic, M., Chambers, E.S., Subramanian, P., Patel, N., Virasami, A., et al. (2019), “Senescent cells evade immune clearance via HLA-E-mediated NK and CD8+ T cell inhibition”, Nature Communications, Vol. 10 No. 1, p. 2387.

Pérez-Mancera, P.A., Young, A.R.J. and Narita, M. (2014), “Inside and out: The activities of senescence in cancer”, Nature Reviews Cancer, Vol. 14 No. 8, pp. 547–58.

Plunkett, F.J., Franzese, O., Finney, H.M., Fletcher, J.M., Belaramani, L.L., Salmon, M., Dokal, I., et al. (2014), “The loss of telomerase activity in highly differentiated CD8+CD28-CD27- T cells is associated with decreased Akt (Ser473) phosphorylation.”, Journal of Immunology (Baltimore, Md. : 1950), United States, Vol. 178 No. 12, pp. 7710–9.

Plunkett, F.J., Soares, M.V.D., Annels, N., Hislop, A., Ivory, K., Lowdell, M., Salmon, M., et al. (2001), “The flow cytometric analysis of telomere length in antigen-specific CD8+ T cells during acute Epstein-Barr virus infection”, Blood, Vol. 97 No. 3, pp. 700–7.

Pollack, R.M., Donath, M.Y., LeRoith, D. and Leibowitz, G. (2016), “Anti-inflammatory agents in the treatment of diabetes and its vascular complications”, Diabetes Care, Vol. 39 No. Suppl 2, pp. S244-52.

Preston, C.C., Oberlin, A.S., Holmuhamedov, E.L., Gupta, A., Sagar, S., Syed, R.H.K., Siddiqui, S.A., et al. (2008), “Aging-induced alterations in gene transcripts and functional activity of mitochondrial oxidative phosphorylation complexes in the heart”, Mechanisms of Ageing and Development, Vol. 129 No. 6, pp. 304–12.

Pui, J.C., Allman, D., Xu, L., DeRocco, S., Karnell, F.G., Bakkour, S., Lee, J.Y., et al. (1999), “Notch1 expression in early lymphopoiesis influences B versus T lineage determination”, Immunity, Vol. 11 No. 3, pp. 299–308.

Pulko, V., Davies, J.S., Martinez, C., Lanteri, M.C., Busch, M.P., Diamond, M.S., Knox, K., et al. (2016), “Human memory T cells with a naive phenotype accumulate with aging and respond to persistent viruses”, Nature Immunology, Vol. 17 No. 8, pp. 966–75.

Radtke, F., Wilson, A., Stark, G., Bauer, M., Van Meerwijk, J., MacDonald, H.R. and Aguet, M. (1999), “Deficient T cell fate specification in mice with an induced inactivation of Notch1”, Immunity, Vol. 10 No. 5, pp. 547–58.

Ramirez, R.D., Herbert, B.S., Vaughan, M.B., Zou, Y., Gandia, K., Morales, C.P., Wright, W.E., et al. (2003), “Bypass of telomere-dependent replicative senescence (M1) upon overexpression of Cdk4 in normal human epithelial cells”, Oncogene, Vol. 22 No. 3, pp. 433–44.

Ramirez, R.D., Morales, C.P., Herbert, B.S., Rohde, J.M., Passons, C., Shay, J.W. and Wright, W.E. (2001), “Putative telomere-independent mechanisms of replicative aging reflect inadequate growth conditions”, Genes and Development, Vol. 15 No. 4, pp. 398–403.

Ranganath, S. and Murphy, K.M. (2002), “Structure and Specificity of GATA Proteins in Th2 Development”, Molecular and Cellular Biology, Vol. 21 No. 8, pp. 2716–25.

Raphael, I., Nalawade, S., Eagar, T.N. and Forsthuber, T.G. (2015), “T cell subsets and their signature cytokines in autoimmune and inflammatory diseases”, Cytokine, Vol. 74 No. 1, pp. 5–17.

Rathmell, J.C., Elstrom, R.L., Cinalli, R.M. and Thompson, C.B. (2003), “Activated Akt promotes increased resting T cell size, CD28-independent T cell growth, and development of autoimmunity and lymphoma”, European Journal of Immunology, Vol. 33 No. 8, pp. 2223–32.

Reznick, R.M., Zong, H., Li, J., Morino, K., Moore, I.K., Yu, H.J., Liu, Z.X., et al. (2007), “Aging-Associated Reductions in AMP-Activated Protein Kinase Activity and Mitochondrial Biogenesis”, Cell Metabolism, Vol. 5 No. 2, pp. 151–6.

Richter, T. and Zglinicki, T. von. (2007), “A continuous correlation between oxidative stress and telomere shortening in fibroblasts”, Experimental Gerontology, Vol. 42 No. 11, pp. 1039–42.

Riddell, N.E., Griffiths, S.J., Rivino, L., King, D.C.B., Teo, G.H., Henson, S.M., Cantisan, S., et al. (2015), “Multifunctional cytomegalovirus (CMV)-specific CD8+ T cells are not restricted by telomere-related senescence in young or old adults”, Immunology, Vol. 144 No. 4, pp. 549–60.

Ridker, P.M., Hennekens, C.H., Buring, J.E. and Rifai, N. (2000), “C-reactive protein and other markers of inflammation in the prediction of cardiovascular disease in women”, New England Journal of Medicine, Vol. 342 No. 12, pp. 836–43.

Rouvier, E., Luciani, M.F. and Golstein, P. (1993), “Fas involvement in Ca(2+)-independent T cell-mediated cytotoxicity.”, The Journal of Experimental Medicine, Vol. 177 No. 1, pp. 195 LP – 200.

Rufini, A., Tucci, P., Celardo, I. and Melino, G. (2013), “Senescence and aging: The critical roles of p53”, Oncogene, Vol. 32 No. 43, pp. 5129–43.

Sakata-Kaneko, S., Wakatsuki, Y., Matsunaga, Y., Usui, T. and Kita, T. (2000), “Altered Th1/Th2 commitment in human CD4+ T cells with ageing”, Clinical and Experimental Immunology, Vol. 120 No. 2, pp. 267–73.

Sallusto, F., Lenig, D., Forster, R., Lipp, M., Lanzavecchia, A., Förster, R., Lipp, M., et al. (1999), “Two subsets of memory T lymphocytes with distinct homing potentials and effector functions”, Nature, Vol. 401 No. 6754, pp. 708–12.

Schmitz, M.L., Bacher, S. and Dienz, O. (2003), “NF-κB activation pathways induced by T cell costimulation”, The FASEB Journal, Vol. 17 No. 15, pp. 2187–93.

Schurich, A. and Henson, S.M. (2014), “The many unknowns concerning the bioenergetics of exhaustion and senescence during chronic viral infection”, Frontiers in Immunology, Vol. 5, p. 468.

Schwartz, L., Supuran, C. and Alfarouk, K. (2017), “The Warburg Effect and the Hallmarks of Cancer”, Anti-Cancer Agents in Medicinal Chemistry, Vol. 17 No. 2, pp. 164–70.

Seidel, J.A., Vukmanovic-Stejic, M., Muller-Durovic, B., Patel, N., Fuentes-Duculan, J., Henson, S.M., Krueger, J.G., et al. (2018), “Skin resident memory CD8+ T cells are phenotypically and functionally distinct from circulating populations and lack

immediate cytotoxic function", Clinical & Experimental Immunology, John Wiley & Sons, Ltd (10.1111), Vol. 194 No. 1, pp. 79–92.

Serrano, M., Lin, A.W., McCurrach, M.E., Beach, D. and Lowe, S.W. (1997), "Oncogenic ras provokes premature cell senescence associated with accumulation of p53 and p16(INK4a)", Cell, Vol. 88 No. 5, pp. 593–602.

Shaw, A.C., Goldstein, D.R. and Montgomery, R.R. (2013), "Age-dependent dysregulation of innate immunity", Nature Reviews Immunology, Vol. 13 No. 12, pp. 875–87.

Shaw, A.C., Joshi, S., Greenwood, H., Panda, A. and Lord, J.M. (2010), "Aging of the innate immune system", Current Opinion in Immunology, Vol. 22 No. 4, pp. 507–13.

Sherr, C.J. (2001), "The INK4a/ARF network in tumour suppression", Nature Reviews Molecular Cell Biology, Vol. 2 No. 10, pp. 731–7.

Shirakawa, K., Yan, X., Shinmura, K., Endo, J., Kataoka, M., Katsumata, Y., Yamamoto, T., et al. (2016), "Obesity accelerates T cell senescence in murine visceral adipose tissue", Journal of Clinical Investigation, Vol. 126 No. 12, pp. 4626–4639.

Shresta, S., Pham, C.T., Thomas, D.A., Graubert, T.A. and Ley, T.J. (1998), "How do cytotoxic lymphocytes kill their targets?", Current Opinion in Immunology, Vol. 10 No. 5, pp. 581–7.

Siska, P.J., Beckermann, K.E., Mason, F.M., Andrejeva, G., Greenplate, A.R., Sendor, A.B., Chiang, Y.J., et al. (2017), "Mitochondrial dysregulation and glycolytic insufficiency functionally impair CD8 T cells infiltrating human renal cell carcinoma", JCI Insight, Vol. 2 No. 12, p. 93411.

Sone, H. and Kagawa, Y. (2005), “Pancreatic beta cell senescence contributes to the pathogenesis of type 2 diabetes in high-fat diet-induced diabetic mice”, Diabetologia, Vol. 48 No. 1, pp. 58–67.

Stanley, T.L., Zanni, M. V., Johnsen, S., Rasheed, S., Makimura, H., Lee, H., Khor, V.K., et al. (2011), “TNF-α antagonism with etanercept decreases glucose and increases the proportion of high molecular weight adiponectin in obese subjects with features of the metabolic syndrome”, Journal of Clinical Endocrinology and Metabolism, Vol. 96 No. 2, pp. E146-50.

Stentz, F. and Kitabchi, A. (2005), “Activated T Lymphocytes in Type 2 Diabetes: Implications From in Vitro Studies”, Current Drug Targets, Vol. 4 No. 6, pp. 493–503.

Storer, M., Mas, A., Robert-Moreno, A., Pecoraro, M., Ortells, M.C., Di Giacomo, V., Yosef, R., et al. (2013), “Senescence is a developmental mechanism that contributes to embryonic growth and patterning”, Cell, Vol. 155 No. 5, pp. 1119–30.

Sun, N., Youle, R.J. and Finkel, T. (2016), “The Mitochondrial Basis of Aging”, Molecular Cell, Vol. 61 No. 5, pp. 654–666.

Surh, C.D. and Sprent, J. (2008), “Homeostasis of Naive and Memory T Cells”, Immunity, Vol. 29 No. 6, pp. 848–62.

Sze, D.M.Y., Giesajtis, G., Brown, R.D., Raitakari, M., Gibson, J., Ho, J., Baxter, A.G., et al. (2001), “Clonal cytotoxic T cells are expanded in myeloma and reside in the CD8+CD57+CD28- compartment”, Blood, Vol. 98 No. 9, pp. 2817–27.

Tarazona, R., DelaRosa, O., Alonso, C., Ostos, B., Espejo, J., Pea, J. and Solana, R. (2001), “Increased expression of NK cell markers on T lymphocytes in aging and

chronic activation of the immune system reflects the accumulation of effector/senescent T cells", Mechanisms of Ageing and Development, Vol. 121 No. 1–3, pp. 77–88.

Taub, D.D. and Longo, D.L. (2005), "Insights into thymic aging and regeneration", Immunological Reviews, Vol. 205, pp. 72–93.

Thompson, C.B., Lindsten, T., Ledbetter, J.A., Kunkel, S.L., Young, H.A., Emerson, S.G., Leiden, J.M., et al. (1986), "CD28 activation pathway regulates the production of multiple T-cell-derived lymphokines/cytokines.", Proceedings of the National Academy of Sciences of the United States of America, United States, Vol. 86 No. 4, pp. 1333–7.

Timson, J. (1975), "Hydroxyurea.", Mutation Research, Netherlands, Netherlands, Vol. 32 No. 2, pp. 115–132.

Tominaga, N., Naoi, Y., Shimazu, K., Nakayama, T., Maruyama, N., Shimomura, A., Kim, S.J., et al. (2012), "Clinicopathological analysis of GATA3-positive breast cancers with special reference to response to neoadjuvant chemotherapy", Annals of Oncology, Vol. 23 No. 12, pp. 3051–7.

Toussaint, O., Royer, V., Salmon, M. and Remacle, J. (2002), "Stress-induced premature senescence and tissue ageing", Biochemical Pharmacology, Vol. 64 No. 5–6, pp. 1007–9.

Townsend, M.J., Weinmann, A.S., Matsuda, J.L., Salomon, R., Farnham, P.J., Biron, C.A., Gapin, L., et al. (2004), "T-bet regulates the terminal maturation and homeostasis of NK and Vα14i NKT cells", Immunity, Vol. 20 No. 4, pp. 477–94.

Turvey, S.E. and David H. Broide. (2010), “Innate Immunity”, J Allergy Clin Immunol, Vol. 125 No. 2, pp. S24–S32.

Vallejo, A.N., Mueller, R.G., Hamel, D.L., Way, A., Dvergsten, J.A., Griffin, P. and Newman, A.B. (2011), “Expansions of NK-like αβT cells with chronologic aging: Novel lymphocyte effectors that compensate for functional deficits of conventional NK cells and T cells”, Ageing Research Reviews, Vol. 10 No. 3, pp. 354–61.

Velarde, M.C., Flynn, J.M., Day, N.U., Melov, S. and Campisi, J. (2012), “Mitochondrial oxidative stress caused by Sod2 deficiency promotes cellular senescence and aging phenotypes in the skin”, Aging, Vol. 4 No. 1, pp. 3–12.

Verzola, D., Gandolfo, M.T., Gaetani, G., Ferraris, A., Mangerini, R., Ferrario, F., Villaggio, B., et al. (2008), “Accelerated senescence in the kidneys of patients with type 2 diabetic nephropathy”, American Journal of Physiology-Renal Physiology, Vol. 295 No. 5, pp. F1563-73.

Viale, A., Pettazzoni, P., Lyssiotis, C.A., Ying, H., Sánchez, N., Marchesini, M., Carugo, A., et al. (2014), “Oncogene ablation-resistant pancreatic cancer cells depend on mitochondrial function”, Nature, Vol. 514 No. 7524, pp. 628–32.

Voehringer, D., Blaser, C., Brawand, P., Raulet, D.H., Hanke, T. and Pircher, H. (2001), “Viral Infections Induce Abundant Numbers of Senescent CD8 T Cells”, The Journal of Immunology, Vol. 167 No. 9, pp. 4838–43.

Voehringer, D., Koschella, M. and Pircher, H. (2002), “Lack of proliferative capacity of human effector and memory T cells expressing killer cell lectinlike receptor G1 (KLRG1)”, Blood, Vol. 100 No. 10, pp. 3698–702.

Warburg, O., Wind, F. and Negelein, E. (1927), “The metabolism of tumors in the body”, Journal of General Physiology, Vol. 8 No. 6, pp. 519–530.

Watson, J.D. (1972), “Origin of concatemeric T7 DNA”, Nature New Biology, Vol. 239 No. 94, pp. 197–201.

Weekes, M.P., Wills, M.R., Mynard, K., Hicks, R., Sissons, J.G.P. and Carmichael, A.J. (1999), “Large clonal expansions of human virus-specific memory cytotoxic T lymphocytes within the CD57+ CD28- CD8+ T-cell population”, Immunology, Vol. 98 No. 3, pp. 443–9.

Weksler, M.E. (2000), “Changes in the B-cell repertoire with age”, Vaccine, Vol. 18 No. 16, pp. 1624–8.

Weyand, C.M., Yang, Z. and Goronzy, J.J. (2014), “T-cell aging in rheumatoid arthritis”, Current Opinion in Rheumatology, Vol. 26 No. 1, pp. 93–100.

Whitaker-Menezes, D., Martinez-Outschoorn, U.E., Flomenberg, N., Birbe, R.C., Witkiewicz, A.K., Howell, A., Pavlides, S., et al. (2011), “Hyperactivation of oxidative mitochondrial metabolism in epithelial cancer cells in situ: Visualizing the therapeutic effects of metformin in tumor tissue”, Cell Cycle, Vol. 10 No. 23, pp. 4047–64.

White, J.T., Cross, E.W., Burchill, M.A., Danhorn, T., McCarter, M.D., Rosen, H.R., O’Connor, B., et al. (2016), “Virtual memory T cells develop and mediate bystander protective immunity in an IL-15-dependent manner”, Nature Communications, Vol. 7, p. 11291.

Wieman, H.L., Wofford, J.A. and Rathmell, J.C. (2007), “Cytokine Stimulation Promotes Glucose Uptake via Phosphatidylinositol-3 Kinase/Akt Regulation of Glut1

Activity and Trafficking", Molecular Biology of the Cell, Vol. 18 No. 4, pp. 1437–46.

van der Windt, G.J.W. and Pearce, E.L. (2012), "Metabolic switching and fuel choice during T-cell differentiation and memory development", Immunological Reviews, Vol. 249 No. 1, pp. 27–42.

Witkiewicz, A.K., Kline, J., Queenan, M., Brody, J.R., Tsirigos, A., Bilal, E., Pavlides, S., et al. (2011), "Molecular profiling of a lethal tumor microenvironment, as defined by stromal caveolin-1 status in breast cancers", Cell Cycle, Vol. 10 No. 11, pp. 1794–809.

Wong, H. and Riabowol, K. (1996), "Differential CDK-inhibitor gene expression in aging human diploid fibroblasts", Experimental Gerontology, Vol. 31 No. 1–2, pp. 311–25.

World Health Organization. (2015), WHO | World Report on Ageing and Health 2015, World Health Organisation, available at: https://doi.org/10.1016/j.jmgm.2016.10.012.

World Health Organization. (2016), WHO | Global Report on Diabetes 2016, World Health Organisation, available at: https://www.who.int/diabetes/global-report/en/

Xu, J., Ji, J. and Yan, X.H. (2012), "Cross-Talk between AMPK and mTOR in Regulating Energy Balance", Critical Reviews in Food Science and Nutrition, Vol. 52 No. 5, pp. 373–81.

Xu, W. and Larbi, A. (2017), "Markers of T cell senescence in humans", International Journal of Molecular Sciences, Vol. 18 No. 8, p. 1742.

Zelle-Rieser, C., Thangavadivel, S., Biedermann, R., Brunner, A., Stoitzner, P., Willenbacher, E., Greil, R., et al. (2016), "T cells in multiple myeloma display features

of exhaustion and senescence at the tumor site", Journal of Hematology and Oncology, Vol. 9 No. 1, p. 116.

Zheng, W.P. and Flavell, R.A. (1997), "The transcription factor GATA-3 is necessary and sufficient for Th2 cytokine gene expression in CD4 T cells", Cell, Vol. 89 No. 4, pp. 587–96.

Zhu, J., Woods, D., McMahon, M. and Bishop, J.M. (1998), "Senescence of human fibroblasts induced by oncogenic Raf", Genes and Development, Vol. 12 No. 19, pp. 2997–2007.

Zorov, D.B., Juhaszova, M. and Sollott, S.J. (2014), "Mitochondrial reactive oxygen species (ROS) and ROS-induced ROS release", Physiological Reviews, Vol. 94 No. 3, pp. 909–950.

Zorova, L.D., Popkov, V.A., Plotnikov, E.Y., Silachev, D.N., Pevzner, I.B., Jankauskas, S.S., Babenko, V.A., et al. (2018), "Mitochondrial membrane potential", Analytical Biochemistry, Vol. 552, pp. 50–59.